The microtubule cytoskeleton of the corn smut fungus *Ustilago maydis*.

Submitted by Anna Iwona Shiel

to the University of Exeter as a thesis for the degree of
Doctor of Philosophy in Biological Sciences

December 2014

I certify that all material in this thesis which is not my own work has been identified and that no material has previously been submitted and approved for the award of a degree by this or any other University.

Signature: ……..

Anna Shiel

Abstract

Microtubules in the fungal pathogen *Ustilago maydis* have important roles, which include polar budding, morphogenesis and nuclear migration. They also serve as tracks for molecular motors, responsible for intracellular transport of organelles and membrane trafficking. Moreover, microtubules are indispensable during both interphase and cell division, and they play a crucial role in long-distance microtubule-based transport, which occurs in neurons or fungal hypha. Therefore, in order to carry out their functions correctly they need to be well organised and stabilised, which is achieved mainly by various microtubule-associated proteins. In this thesis, different aspects of microtubule (MT) cytoskeleton organisation in *U. maydis* were investigated, using bioinformatics and experimental approaches. In the first part of the thesis I studied the microtubule-associated protein (MAP) repertoire in *U. maydis*, which has never been done before in a comprehensive way. For this purpose, searches across five eukaryotic model organisms were conducted to identify all of their known MAPs, to query the *U. maydis* database. In addition, all of the proteins were checked for their domain architecture, to help decide if an orthologue had been found. As a result, 66 potential MAP orthologues were identified. The second part of this thesis focused on identifying novel factors involved in the organisation of the microtubule cytoskeleton using a specially designed genetic screen. This work involved five microtubule-organisation defect (MOD) mutants, generated by UV-mutagenesis, which were characterised by inability to produce long hyphae as well as by short, fragmented microtubules. To find which genes were responsible for this phenotype, the genomes of all mutants were sequenced and compared with a wild-type genome, and mutations in many genes were found. The analysis revealed potential candidate genes responsible for the specific phenotype of the mutants. However, most probably, UV-generated point mutations in more than one gene played a part in the defective microtubule array. In the final part of this thesis, the function of two beta-tubulin isotypes in *U. maydis* was analysed. Using conditional mutants, I demonstrated that there are subtle functional differences between the two beta tubulins.

Table of contents

Acknowledgements

First and foremost, I would like to thank Dr. Helen Dawe, who supervised a substantial chapter of this thesis as well as thesis writing up process. I cannot express how thankful I am for her amazing support and kindness, which I received during my PhD. I would also like to thank my supervisor Professor Nick Talbot for his encouragement and kind words.

I also wish to express my gratitude to the University of Exeter Annual Fund for funding this research project, without which, this thesis would not have been possible. Furthermore, I am very grateful for all the support I received from the Postgraduate Office, especially Helen, Lindsey and Laura and everyone in the School of Biosciences, who helped me in my PhD.

In addition, I would like to thank all members of Lab 211 past and present, for their assistance, support, friendship and many laughs; notably I owe huge thanks to Ewa, Catherine, Gulay, Magdalena, Kate, Stacey, Charli, Natalie, Amy and our brilliant lab manager Samantha.

I would like to give an enormous thanks to Dr Ewa Bielska for her amazing knowledge and passion, problem solving abilities, thesis help and patience in listening to me. I would not have survived this PhD without her support.

I wish to thank my wonderful parents, Iwona and Jacek, and my parents-in-law, Bridget and Norman, for their love and support as well as motivational phone conversations during experimental work and thesis writing.

Finally, I would like to thank my amazing husband George for his friendship, love and for being patient with me during the tough periods throughout writing up my thesis. I also want to thank my son David, who is my little sunshine. I did it for you boys!

List of figures

List of tables

Abbreviations

α-tubulin	alpha tubulin
aa	amino acid
Amp	ampicilin
ATP	adenosine 5’ triphosphate
bp	base pair(s)
β-tubulin	beta tubulin
cbxR	carboxin-resistance-cassette
CH	calponin homology domain
CM	complete medium
CPC	chromosome passenger complex
crg promoter	conditional arabinose induced promoter
CRISPR	clustered regularly interspaced short palindromic repeats
C-terminus	carboxy terminus
CTT	C-terminal tail
DNA	desoxyribonucleic acid
dNTP	desoxynucleotides
EBs	end-binding proteins
EE	early endosome(s)
eGFP	enhanced green fluorescent protein
ɣ-TuRC	gamma tubulin ring complex
ɣ-TuSC	gamma tubulin small complex
GFP	green fluorescent protein
eGFP	enhanced green fluorescent protein
GTP	guanosine triphosphate
HEAT	Huntington/Elongation factor3/phosphatase 2A/TOR1 repeats
hygR	hygromycin-resistance-cassette
KIF	kinesin superfamily proteins
kin1	kinesin-1
kin3	kinesin-3
MAP	microtubule-associated protein
mod	microtubule-organisation defect mutant
MT	microtubule

MtLS	microtubule tip localisation signal
MTOC	microtubule-organizing centre
N	sample size
natR	nourseothricin-resistance-cassette
nm	nitrate minimal
N-terminal	amino terminus
ori	origin of replication
P	probability
p	promoter
Pnar	conditional nitrate reductase promoter
PTM	post-translational modification
OD	optical density
ORF	open reading frame
PCR	polymerase chain reaction
P*crg*	promoter of the arabinose gene from *U. maydis*
Rab5a	small endosomal Rab5-like GTPase
RNA	ribonucleic acid
rpm	revolutions per minute
RT	room temperature
SEM	standard error of the mean
SIN	septation initiation network
SPB	spindle pole body
SPK	Spitzenkörper
+TIPS	plus-end tracking proteins
tub1	alpha tubulin gene from *U. maydis*
tub2	gamma tubulin gene from *U. maydis*
tub3	beta tubulin gene from *U. maydis*
tub4	beta tubulin gene from *U. maydis*
U	unit
WT	wild-type

Chapter 1 – Introduction

1.1 The model fungus *Ustilago maydis*

Ustilago maydis is a biotrophic pathogen that infects maize (*Zea mays*), where it causes the corn smut disease (Wahl et al., 2010). The disease results in stunted plant growth and reduces yield, leading to severe economic losses (Kamper et al., 2006; Martinez-Espinoza et al., 2002). Also, since the pioneering work of Robin Holliday, it has become an important model for molecular analyses of mating, morphogenesis, pathogenicity and DNA recombination (Feldbrugge et al., 2004). This basidiomycete fungus adopts two different morphological forms during its life cycle, a yeast-like growth habit and a filamentous form (Kahmann et al., 1995). The yeast-like cell is elongated, divides by budding, and the bud grows by tip extension, while the filamentous form divides at the apical cell and grows by tip extension (Banuett et al., 2008). The haploid sporidia are yeast-like, they grow vegetatively by budding and are nonpathogenic, but when two compatible strains fuse to form a dikaryon, this results in filamentous growth and the ability to infect maize plants (Daniels et al., 1994). Furthermore, morphological changes during the yeast to hyphal transition involve polarised growth, thought to depend on cytoskeletal reorganisation, which provides tracks for delivery of cargo proteins, essential for growth, to the hyphal tip (Fuchs et al., 2005; Geitmann and Emons, 2000). Among the transported organelles are early endosomes (EEs) required for proper cell morphogenesis (Feldbrugge et al., 2004), which are also essential for the initiation of pathogenic development, cell–cell fusion, and spore formation and germination (Fuchs et al., 2006). Moreover, it is well established that in filamentous fungi early endosome motility is supported by dynein and kinesin-3 which is thought to facilitate long-range communication between the nucleus and the growing hyphal tip (Egan et al., 2012; Lenz et al., 2006; Wedlich-Soldner et al., 2002; Zhang et al., 2011).

Previously, functional analysis of some specific processes, such as the role of motors in microtubule cytoskeleton organisation, long-range transport, or the "open" mitosis of *U. maydis* have revealed an unexpected degree of similarity between this fungus and higher eukaryotes (Steinberg and Perez-Martin, 2008).

Moreover, a study from 2007 by Munsterkotter and Steinberg revealed that the proteome of *Ustilago maydis* is, in many ways, more closely related to humans than to the fungal cousin *Saccharomyces cerevisiae*. Basically, *U. maydis* and humans share more proteins, including many disease-related ones, than *U. maydis* and *S. cerevisiae* (Munsterkotter and Steinberg, 2007). This means that *U. maydis* is an excellent system, not only for studying processes in fungi, but also in multicellular organisms. In addition, *U. maydis* can be easily cultured under laboratory conditions and is accessible to both genetic and molecular methods (Steinberg et al., 2001).

1.2 *Ustilago maydis* life cycle

The *U. maydis* dimorphic life cycle (Figure 1.1) begins when on the surface of the plant compatible cells in the form of haploid sporidia (indicated with different colour nuclei), recognise each other and switch to tip growth (Steinberg, 2007a). This recognition occurs via a pheromone-receptor system (Bolker et al., 1992), which induces a cascade of regulatory events and leads to cell cycle arrest in G2 phase (Garcia-Muse et al., 2003; Steinberg and Perez-Martin, 2008) followed by a switch from yeast-like to hyphal growth (Feldbrugge et al., 2004). Newly formed conjugation tubes fuse, resulting in a dikaryotic filament, which invades plant cells using specialised infection structure called an appressorium (Freitag et al., 2011). During penetration the host plasma membrane invaginates and completely encases the intracellular hyphae (Djamei and Kahmann, 2012). An interaction zone develops between plant and fungal membranes characterised by fungal deposits produced by exocytosis (Bauer et al., 1997; Kamper et al., 2006). Recently, new evidence has emerged, which showed that effector proteins (Pep 1, Pit 2 and Cmu 1) are secreted at the invading hyphal tip of *U. maydis* to suppress plant immunity, thereby allowing rapid fungal colonisation of plant tissue (Bielska et al., 2014a). Pep 1 acts as a potent suppressor of early plant defenses by inhibition of peroxidase activity (Hemetsberger et al., 2012), Pit 2 was shown to work as an inhibitor of apoplastic maize cysteine proteases, and is essential for *U. maydis* virulence (Mueller et al., 2013) and Cmu 1, a chorismate mutase, suppresses plant defence responses by decreasing plant salicylic acid levels (Djamei et al., 2011). Early disease symptoms of infected maize plants are chlorosis (yellowing

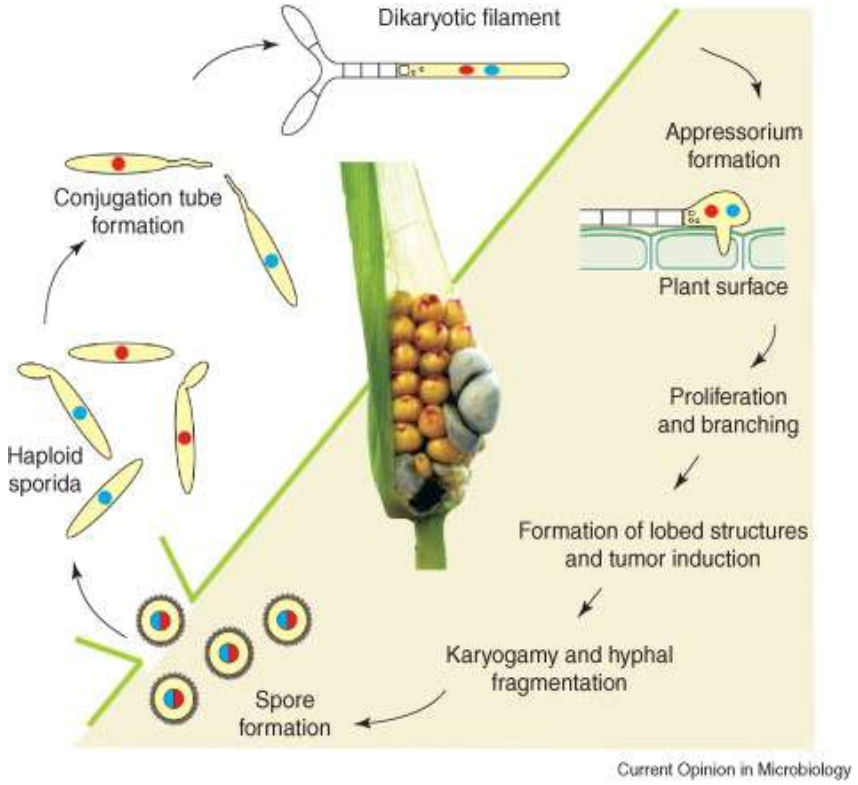

Figure 1.1 Summary of *U. maydis* life cycle.

The life cycle of *U. maydis* starts with haploid yeast-like sporidia on the surface of plant. After a pheromone exchange between the two sporidia of different mating types at the *a* and *b* locus (shown as different coloured nuclei), sexual development is initiated. As a result, conjugation hypha are formed, which fuse to form a dikaryotic filament, which is then used to invade plant tissue by forming an infection structure called an appressorium. In this way *U. maydis* filaments can penetrate and colonise the plant, manifested by formation of large tumours. After proliferation and branching inside the plant nuclear fusion occurs leading to spore formation. When diploid spores germinate they undergo meiosis and produce haploid sporidia, and a new cycle can begin again. Image taken from (Feldbrugge et al., 2004).

of tissue), the formation of anthocyanin, and stunting while signs of defense responses are not detected at in the early stages of infection.

This is based on extensive cytological and ultrastructural analysis (Banuett and Herskowitz, 1996; Basse, 2005; Snetselaar and Mims, 1993). Later, the most characteristic sign of *U. maydis* infection is formation of large plant tumours (Schilling et al., 2014). Within the tumour tissue different processes occur, such as karyogamy, hyphal fragmentation and deposition of a thick melanised wall layer, which leads to production of specialised diploid spores (García-Pedrajas et al., 2010; Snetselaar and Mims, 1994). They are called teliospores and undergo meiosis upon germination to produce the yeast-like haploid form (Banuett and Herskowitz, 1996).

1.2.1 Regulation of mating process in *U. maydis*

Pathogenic development in *U. maydis* is dependent on the transition from non-pathogenic sporidia to infective hypha through the mating process. Regulation of mating between two compatible yeast-like cells is based on two independent mating type loci, *a* and *b* (Bielska and Steinberg, 2013). They are essentially two gene complexes. One complex encodes members of the homeobox family of transcription factors, which heterodimerise on mating to generate an active transcription regulator (*b* locus), while the other complex encodes peptide pheromones and 7-transmembrane receptors that permit intercellular signalling (*a* locus) (Casselton and Olesnicky, 1998). The *a* locus is biallelic, *a1* and *a2*, and the *b* locus is multiallelic with at least 25 alleles (Puhalla, 1970), which gives 50 different mating types overall (Casselton and Olesnicky, 1998). During plant infection, the cell recognition step is mediated by the *a* locus which codes for a pheromone/receptor-based system, a lipopeptide pheromone precursor (mating factor, *mfa1* or *mfa2*) and a transmembrane pheromone receptor (pra1 or pra2) (Spellig et al., 1994), which control the fusion of haploid sporidia (Bolker et al., 1992). After cell fusion, further development depends on the *b* locus, which consists of two divergently transcribed genes encoding the unrelated homeodomain proteins bW and bE (Brachmann et al., 2001; Gillissen et al., 1992). Complex formation is genetically controlled and is restricted to bE

and bW proteins encoded by different alleles of the *b* locus, thereby guaranteeing that active heterodimers are only formed in the dikaryon and do not arise in haploid cells (Feldbrugge et al., 2004). The combination of different *b* alleles leads to the formation of a bE/bW heterodimer, which is key to pathogenic development (Kahmann and Kämper, 2004; Mahlert et al., 2009), involving transition to the filamentous dikaryotic stage and pathogenicity (Brachmann et al., 2001).

1.3 Cytoskeleton

The cytoskeleton was first observed by H. E. Huxley and J. Hanson in 1953, when they discovered a double array of filaments in cross-striated muscles using electron-microscopy techniques (Hanson and Huxley, 1953; Huxley, 1953, 1957) (Risler, 2011). It is a complex network of protein filaments, which is highly dynamic and has the ability to continuously reorganise itself as the cell changes shape, divides and responds to its environment (Alberts, 2008). Also, the cytoskeleton is found in all cells of the three domains of life, including archaea, bacteria and eukaryotes. However, the structure, function and dynamic behaviour of the cytoskeleton can be very different, depending on organism and cell type (Risler, 2009). The three main functions carried out by the cytoskeleton are: spatial organisation of the contents of the cell, physical and biochemical connection of the cell to the external environment and generation of coordinated forces that enable the cell to move and change shape (Fletcher and Mullins, 2010). In eukaryotes, the cytoskeleton is composed of three principal types of protein filaments: actin filaments, intermediate filaments, and microtubules, which are held together and linked to subcellular organelles and the plasma membrane by a variety of accessory proteins (Cooper, 2000b).

1.3.1 Microtubules

Microtubules (MTs) (Figure 1.2) are ubiquitous cytoskeletal elements built by the head-to-tail self-association of *alpha/beta*-tubulin dimers (Nogales et al., 1999). In addition to the ubiquitous alpha and beta tubulin, MTs often require the presence of an additional tubulin protein, gamma tubulin, for correct assembly as a templating protein (Erickson, 2000; Luduena, 1998; Tuszynski et al., 2006). The gamma tubulin is mainly found in the microtubule organising

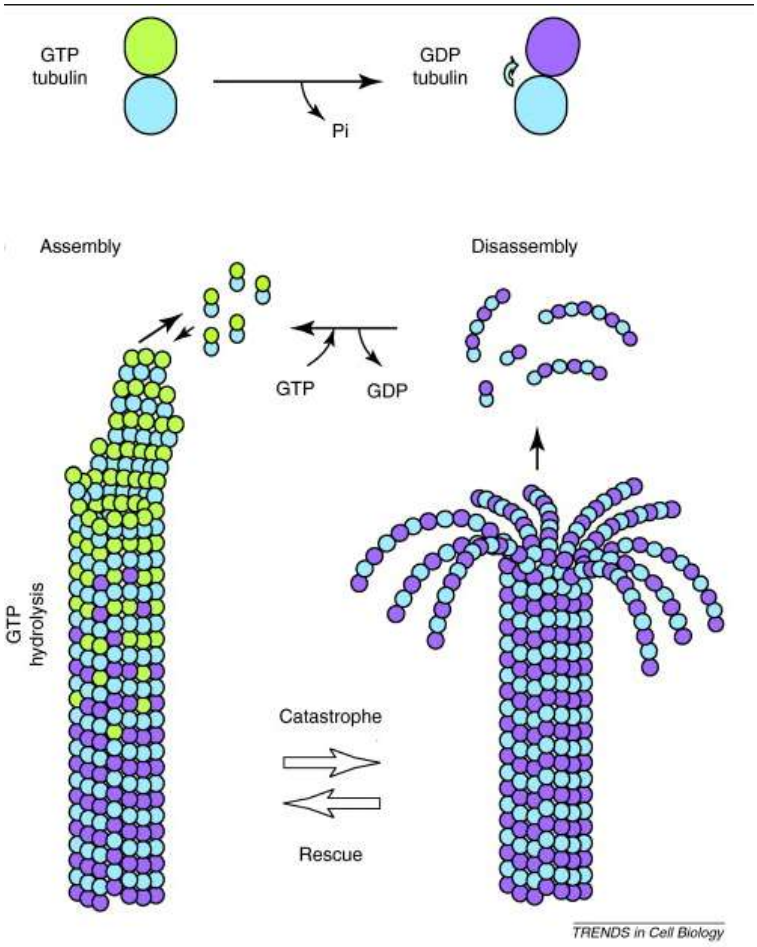

Figure 1.2 Dynamic instability of MTs

One of the main features of MTs is their ability to switch between growing and shrinking phases at their (+) ends. During microtubule assembly, α/β tubulin dimers are bound to GTP, resulting in a GTP cap, which protects it from disassembly. However, once hydrolysis reaches the MT plus-end, it begins rapid depolymerisation and shrinkage. The switch from growth to shrinkage is called catastrophe. Then, a GTP-bound tubulin can start adding to the MT plus-end again, which is known as 'rescue' (Mitchison and Kirschner, 1984). Modified image taken from (Al-Bassam and Chang, 2011).

centre and plays essential roles in the initiation of microtubule assembly (Dutcher, 2003; McKean et al., 2001; Zhao et al., 2014). The tubulin dimers are arranged longitudinally to form protofilaments, 12-15 of which are joined through lateral associations to form a 25-nm tube (Hunter and Wordeman, 2000). Microtubules are also polar structures (Amos and Klug, 1974; Desai and Mitchison, 1997) and different polymerisation rates of the two ends of the MT are a consequence of this polarity, therefore the faster growing plus end is referred to as the plus end and the slower growing end as the minus end (Allen and Borisy, 1974; Desai and Mitchison, 1997). Both microtubule ends can interact with sets of specific factors that control their dynamic status, intracellular localisation and attachment to cellular structures (Jiang and Akhmanova, 2011), also known as microtubule associated proteins (MAPs). Another important property of microtubules is their dynamic instability (Figure 1.2), which is defined as the stochastic switching between growing and shrinking at microtubule ends (Bayley et al., 1990) and this plays an important role in diverse cellular functions including cell migration and mitosis (Yenjerla et al., 2010). Microtubule assembly is accompanied by hydrolysis of GTP associated with β-tubulin, so that microtubules consist principally of 'GDP-tubulin' stabilised at the plus ends by a short 'cap' (Wade, 2009). Moreover, microtubules have different roles depending on the developmental stage of a cell. During cell division, MTs are essential for assembly and function of the mitotic spindle apparatus (a large array of MTs) (Yang et al., 2010), while in non-dividing cells, MTs organise the cytoplasm, position the nucleus and organelles (Desai and Mitchison, 1997), and serve as the main structural element of flagella and cilia (Mitchell, 2007). In fungi, microtubules serve as tracks for membrane trafficking, which is essential for fungal growth (Heath, 1995; Steinberg et al., 2001). Additionally, in filamentous fungi, microtubules are essential components of the tip growth machinery that enables continuous and rapid growth (Horio, 2007).

1.3.2 Microtubules in *U. maydis*

In *U. maydis*, microtubules are thought to be essential for extended hyphal growth and nuclear migration, but are dispensable for initial pathogenic development (Fuchs et al., 2005). Also, MT-based transport of vesicles,

organelles, RNA and protein complexes is essential for filamentous growth and therefore pathogenic development of *U. maydis* (Steinberg, 2007b). Currently, not much is known about the exact mechanisms by which hyphal microtubules are organised. However, a study by (Steinberg et al., 2001) revealed that *U. maydis* haploid cells, as well as hyphae, contained bundles of dynamic MTs, which have an anti-polar orientation and show bending and translocation, which might suggest that perhaps the hyphal MT array is polarised in a motor-dependant manner (Steinberg, 2007c). Indeed, these mechano-enzymes hydrolyze ATP for the transport of their cargo along the F-actin or the MT cytoskeleton (Schliwa and Woehlke, 2003).

1.4 Aims of the thesis

The aim of this thesis is to understand better the microtubule cytoskeleton in a filamentous fungus *Ustilago maydis* using a number of distinct approaches. Firstly, I set out to investigate the role of two beta tubulins in organising an interphase MT array. I aimed to check whether both beta tubulins are essential for building a fully functional MT cytoskeleton of *U. maydis*. In order to achieve this aim, each of the beta tubulin genes was visualised in yeast and hyphal cells and then down-regulated in specially designed mutant strains, with the effects observed in both yeast and hyphae. Secondly, the motility of early endosomes was observed, to test whether the molecular motors kinesin 3 and dynein are directly involved in this process. Thirdly, I investigated the MAPs repertoire in *U. maydis*, which has never been done before in detail. For this purpose, the AmiGO database (Carbon et al., 2009) of proteins was checked for all known MAPs. Also, publicly available databases of several model organisms were used to look for MAPs, including those of *Saccharomyces cerevisiae*, *Schizosaccharomyces pombe*, *Aspergillus nidulans*, *Drosophila melanogaster* and *Homo sapiens*. A non-redundant list of proteins was prepared and then searches in *U. maydis* database carried out. The results of these analyses have then been validated by looking at protein domains and structure. Lastly, a genetic screen was carried out to search for novel factors organising the interphase MT array. The aim was to find a gene, or genes, responsible for the defective MT cytoskeleton observed in hyphae of cytoskeletal mutants. In order to achieve that, I utilised UV-mutants generated previously, but also carried out

a new UV-mutagenesis screen to produce cytoskeletal-defective mutants using a *U. maydis* strain with GFP-tagged microtubules as a starting point, followed by epifluorescence microscopy to allow MT cytoskeleton observations of each mutant survivior of mutagenesis. For the purpose of this study, only mutants with the short hyphae and fragmented microtubules have been described. When considered together, this thesis reveals new information regarding the MT cytoskeleton of the important plant pathogenic fungus *Ustilago maydis*.

Chapter 2 - General Materials and Methods

2.1 Growth conditions

2.1.1 *Ustilago maydis*

Ustilago maydis strains were cultured on Complete Medium (CM) (Holliday, 1974) supplemented with 1 % (w/v) glucose at 28 °C, shaking at 200 rpm. Hyphal growth in all strains was induced by shifting to NM liquid medium supplemented with 1 % (w/v) glucose (Brachmann et al., 2001).

All strains of *Ustilago maydis* used and produced in this study are stored in the laboratory at University of Exeter. For long term storage, strains were grown in an overnight culture and mixed with NSY-Glycerol at a 1:1 ratio and then stored at - 80 °C.

The following media were used to cultivate *U. maydis*:

CM Medium (Holliday, 1975)
2.5 g (0.25 % w/v) casaminoacids (Melford, Ipswich, UK)
1.0 g (0.1 % w/v) yeast extract (Sigma Aldrich, Dorset, UK)
10 ml (1.0 % w/v) vitamin solution
62.5 ml (6.25 % w/v) salt solution
0.5 g (0.05 % w/v) DNA (from herring sperm) (Sigma Aldrich, Dorset, UK)
1.5 g (0.15 % w/v) ammonium nitrate (Fisher, Loughborough, UK)
Deionised H_2O added to 1 litre, pH set to 7.0 with sodium hydroxide (Fisher, Loughborough, UK)
Autoclaved for 20 min at 121 °C
Supplement with 1 % with glucose (50 % w/v stock; Fisher, Loughborough, UK) or 1 % arabinose (25 % w/v stock; Fisher, Loughborough, UK)).

YEPS light (modified from Tsukuda *et al.*, 1988)
10 g (1.0 % w/v) yeast extract (Sigma Aldrich, Dorset, UK)
4.0 g (0.4 % w/v) peptone (Fisher, Loughborough, UK)
4.0 g (0.4 % w/v) sucrose (Fisher, Loughborough, UK)
Deionised H_2O added to 1 litre
Autoclaved for 20 min at 121 °C

Vitamin Solution (Holliday, 1975)

100 mg (0.1 % w/v) thiamine hydrogen chloride (Serva Electrophoresis, Heidelberg, Germany)

50 mg (0.05 % w/v) riboflavin (Sigma Aldrich, Dorset, UK)

50 mg (0.05 % w/v) pyridoxine hydrochloride (Sigma Aldrich, Dorset, UK)

200 mg (0.2 % w/v) D-pantothenic acid hemicalcium salt (Sigma Aldrich, Dorset, UK)

50 mg (0.2 % w/v) 4-aminobenzoic acid (Sigma Aldrich, Dorset, UK)

200 mg (0.2 % w/v) nicotinic acid (Sigma Aldrich, Dorset, UK)

200 mg (0.2 % w/v) choline chloride (Sigma Aldrich, Dorset, UK)

1 g (1.0 % w/v) *myo*-inositol (Sigma Aldrich, Dorset, UK)

Deionised H_2O added to 1 litre and 40 ml aliquots frozen at -20 °C

Trace Elements (Holliday, 1975)

60 mg (0.06 % w/v) boric acid (Carl Roth, Mühlberg, Germany)

100 mg (0.01 % w/v) ferric chloride ·$6H_2O$ (Sigma Aldrich, Dorset, UK)

40 mg (0.4 % w/v) sodium molybdate·2H2O (Sigma Aldrich, Dorset, UK)

400 mg (0.04 % w/v) zinc chloride (Carl Roth, Mühlberg, Germany)

140 mg (0.14 % w/v) manganese(II) chloride·$4H_2O$ (Sigma Aldrich, Dorset, UK)

40 mg (0.04 % w/v) copper(II) sulphate·$5H_2O$ (Sigma Aldrich, Dorset, UK)

Deionised H_2O added to 1 litre and filter sterilised

Salt Solution (Holliday, 1975)

16 g (16 % w/v) monopotassium phosphate (Carl Roth, Mühlberg, Germany)

8 ml (8.0 % w/v) trace elements

1.32 g (1.32 % w/v) calcium chloride·$2H_2O$ (Sigma Aldrich, Dorset, UK)

4 g (4.08 % w/v) magnesium sulphate·$7H_2O$ (Sigma Aldrich, Dorset, UK)

8 g (8.0 % w/v) potassium chloride (Sigma Aldrich, Dorset, UK)

4 g (4.0 % w/v) sodium sulphate (Sigma Aldrich, Dorset, UK)

Deionised H_2O added to 1 litre and filter sterilised.

NSY Glycerol

5 g (0.5 % w/v) sucrose (Fisher, Loughborough, UK)

8 g (0.8 % w/v) bacto Nutrient Broth (LabM, Lancashire, UK)
1 g (0.1 % w/v) yeast Extract (Sigma Aldrich, Dorset, UK)
800 ml (80.0 % w/v) 87 % glycerol (f.c 69.6 %) (Fisher, Loughborough, UK)
Deionised H_2O added to 1 litre.
Autoclave for 20 min at 121 °C.

2.1.2 *Escherichia coli*

E .coli was grown in liquid dYT medium (Sambrook et al., 1989). Antibiotics were added, as required, at the following concentrations; ampicillin (100 µg/ml; Sigma Aldrich, Dorset, United Kingdom), kanamycin (40 µg/ml; Invitrogen Life technologies, Paisley, UK) and X-Gal (40 µg/ml; Carl Roth, Mühlberg, Germany). Liquid cultures of *E. coli* were induced at 37 °C with shaking (200 rpm). Glycerol stocks were made from exponentially growing cultures and mixed with dYT-Glycerol at a ratio of 1:1 (v/v) and stored at -80 °C. To grow cultures from glycerol stocks they were placed straight into liquid media and grown overnight.

dYT Media
12.8 g (1.6 % w/v) tryptone (Sigma Aldrich, Dorset, UK)
8.0 g (1.0 % w/v) yeast extract (Sigma Aldrich, Dorset, UK)
4.0 g (0.5 % w/v) sodium chloride (Fisher, Loughborough, UK)
10 g agar (1.3 % w/v) (LabM, Lancashire, UK)
Deionised H_2O added to 800 ml and autoclaved for 20 minutes at 121 °C

2.2 Strains and plasmids used in this study

All strains and plasmids used in this study are listed in Table 2.1. All plasmids were generated using standard techniques or *in vivo* recombination in *Saccharomyces cerevisiae,* following published protocols (Raymond et al., 2002; Sambrook et al., 1989) were followed. Methods described here were routinely used and most of the *U. maydis* strains presented in this thesis were obtained in three steps (summarised in Fig. 2.1) (Bielska and Steinberg, 2013):

1. Plasmid generation using yeast-*E. coli* shuttle vector by *in vivo* recombination in *Saccharomyces cerevisiae* ((Raymond et al., 1999); Fig. 2.1 A-F);

2. *Escherichia coli* transformation (Hanahan, 1985; Fig. 2.1 G) and plasmid DNA miniprep purification followed by digestions (Fig. 2.1 H-J);
3. *U. maydis* transformation (Schulz et al., 1990) and antibiotic selection of appropriate transformants (Fig. 2.1 K-L).

Table 2.1 List of strains and plasmids used in this study

Name	Genotype[1]	Reference
AB33	*a2 Pnar-bW2 Pnar-bE1, ble*	(Brachmann et al., 2001)
AB33_GT	*a2 Pnar-bW2 Pnar-bE1, ble / Potef--egfp-tub1*	(Fuchs et al., 2005)
MOD1	*a2 Pnar-bW2 Pnar-bE1, ble / Potef--egfp-tub1 Mut*	(Hemetsberger, 2008)
MOD2	*a2 Pnar-bW2 Pnar-bE1, ble / Potef--egfp-tub1 Mut*	(Hemetsberger, 2008)
MOD3	*a2 Pnar-bW2 Pnar-bE1, ble / Potef--egfp-tub1 Mut*	(Hemetsberger, 2008)
MOD9	*a2 Pnar-bW2 Pnar-bE1, ble / Potef--egfp-tub1 Mut*	This study
MOD4	*a2 Pnar-bW2 Pnar-bE1, ble / Potef--egfp-tub1 Mut*	(Hemetsberger, 2008)
AB33mChTub1	*a2 Pnar-bW2 Pnar-bE1, ble Potef—mCherry-tub1, hyg*	This study
AB33_Tub3-GFP	*a2 Pnar-bW2 Pnar-bE1, ble Potef—mCherry-tub1, hyg, Ptub3::tub3-egfp, nat*	This study
AB33Tub1mCherry-P-otef-Tub3-GFP	*a2 Pnar-bW2 Pnar-bE1, ble Potef—mCherry-tub1, hyg, Potef—tub3-egfp, cbx*	This study
AB33Tub1mCherry-P-otef-Tub4-GFP	*a2 Pnar-bW2 Pnar-bE1, ble Potef—mCherry-tub1, hyg, Potef—tub4-egfp, cbx*	This study
AB33_crg Tub3	*a2 Pnar-bW2 Pnar-bE1, ble / Potef--egfp-tub1, cbx, Pcrg::tub3, hyg*	This study
AB33_crg-Tub4	*a2 Pnar-bW2 Pnar-bE1, ble / Potef--egfp-tub1 cbx, Pcrg::tub4, hyg*	This study
AB33 Potef-mCherry Rab5.1	*a2 Pnar-bW2 Pnar-bE1, ble/Potef-mCherry-Rab5.1, nat*	(Bielska et al., 2014)
AB33GT_pcrg-Tub3, pOtef-mCherry-Rab5a	*a2 Pnar-bW2 Pnar-bE1, ble ipr[Potef--egfp-tub1]ips, cbx, Pcrg::tub3, hyg/Potef-mCherry-Rab5a, nat*	This study

mCherry-Rab5a	*ipr[Potef--egfp-tub1]ips, cbx, Pcrg::tub4, hyg/Potef-mCherry-Rab5a, nat*	
pkinase_um05014	p*Otef*- um05014-hyg	This study
pTub3-GFP_nat	*pTub3-Tub3::eGFP-nat, Amp*	This study
pTub4-GFP_nat	*pTub4-Tub4::eGFP-nat, Amp*	This study
pCrg-Tub3-cbx	*pTub43-Tub3::eGFP-cbx, Amp*	This study
pCrg-Tub4-cbx	*pTub4-Tub4::eGFP-cbx, Amp*	This study
pCrg-Tub3-hyg	*pCrg-Tub3::eGFP-hyg, Amp*	This study
pCrg-Tub4-hyg	*pCrg-Tub4::eGFP-hyg, Amp*	This study
pTUB3-orf_eGFP_cbx	p*Otef*_TUB3_eGFP_cbx	A. Straube, unpublished
pTUB4-orf_eGFP_cbx	p*Otef*_TUB4 _eGFP_cbx	A. Straube, unpublished

[1]*a, b*, mating type loci; P, promoter; -, fusion; *ble*^{R}, phleomycin resistance; hyg^{R}, hygromycin resistance; nat^{R}, nourseothricin resistance; cbx^{R}, carboxin resistance; /, ectopically integrated; ::, homologous replacement; *nar*, conditional nitrate reductase promoter; *otef*, constitutive promoter; *crg*, conditional arabinose induced promoter; *E1, W2*, genes of the *b* mating type locus; mCherry, monomeric red fluorescent protein; egfp, enhanced green fluorescent protein; tub1, alpha-tubulin; tub3, beta-tubulin, tub4, beta-tubulin; rab5.1, small endosomal rab5-like GTPase; Mut, UV mutant;

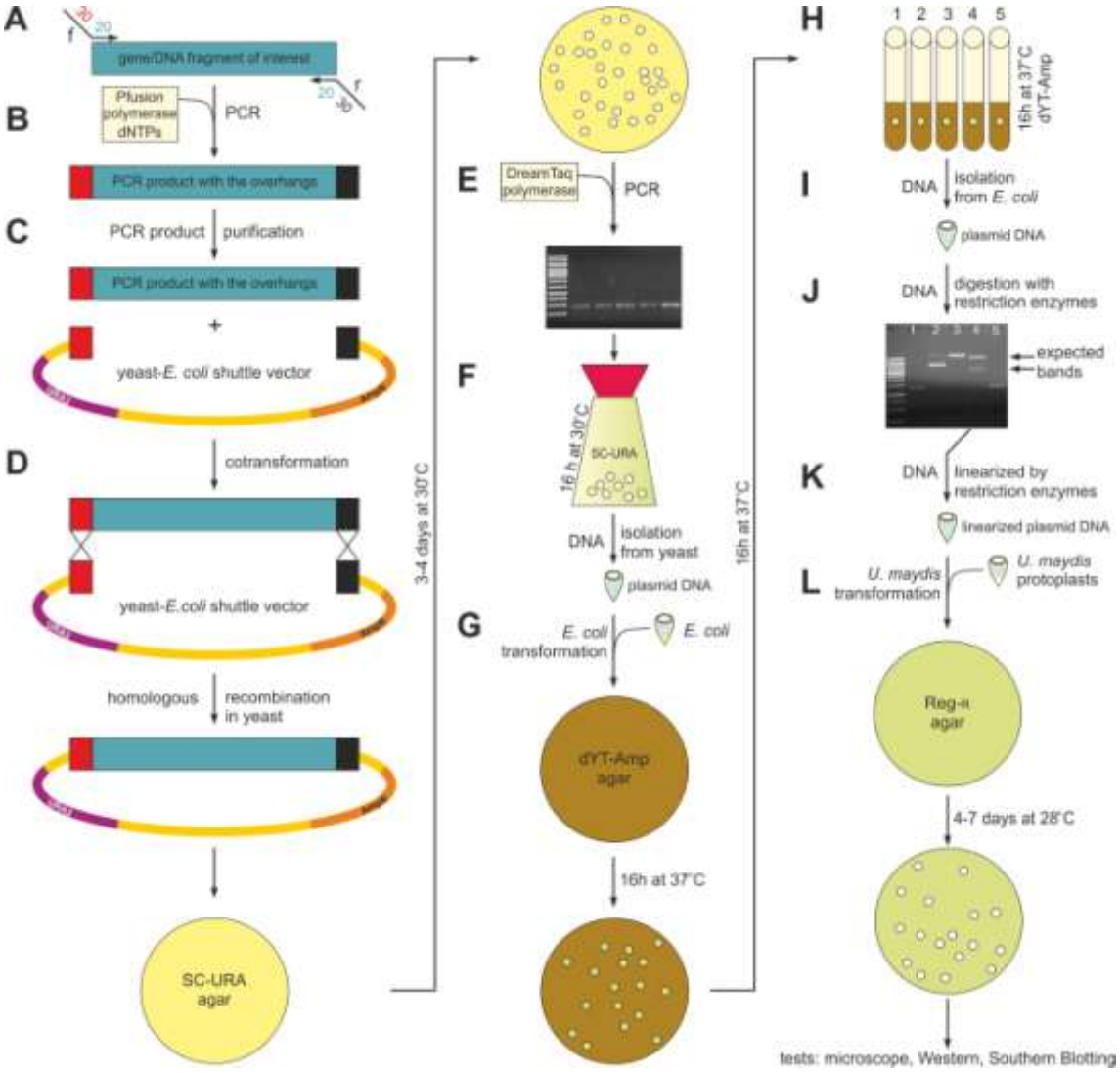

Figure 2.1 Methods used in order to obtain *U. maydis* transformants.

Abbreviations: URA3, *S. cerevisiae* selectable marker which encodes orotidine-5′phosphate decarboxylase, an enzyme which is required for *de novo* synthesis of pyrimidine ribonucleotides such as uracil; *Amp*R, *E. coli* ampicillin resistance; Reg-R agar, regeneration agar containing *U. maydis* selectable antibiotic. Figure taken from (Bielska and Steinberg, 2013). Detailed description of each method can be found in text below.

2.3 Plasmid generation

2.3.1 PCR

For construction of plasmids by *in vivo* recombination in *S. cerevisiae* (Raymond *et al.*, 1999) firstly DNA fragments were amplified by the Phusion® High-Fidelity DNA Polymerase (New England Biolabs #M0530L) in a PCR reaction (using 35 cycles) as fragments with 30 bp overhangs with a homology to the appropriate regions within the yeast-*E. coli* shuttle vector (Fig. 2.1 A-B). Standard PCR reactions were performed according to the following protocol:

Template DNA 4 µl (100 ng)
Primer 1 4 µl (f.c. 10 µM)
Primer 2 4 µl (f.c. 10 µM)
dNTPs 4 µl (f.c. 20 mM)
5x GC Buffer 20 µl
Phusion polymerase 1 µl

Deionised H_2O added to total volume of 100 µl.

Standard PCR programs were carried out under these conditions:
1. Denaturing 98 °C (30 s)
2. Denaturing 98 °C (10 s)
3. Annealing 60 °C (20 s)
4. Elongation 72 °C variable (15-30 s per kb)
5. Final Elongation 72 °C (10 min)
Steps 2. to 4. were repeated 35-40 times.

2.3.2 Gel purification of PCR products

In order to purify DNA products obtained through PCR reactions (Fig. 2.1 C), the purification was carried out according to (Boyle and Lew, 1995) protocol. PCR products were separated using an agarose gel (usually 0.8 %) and then excised. It was then followed by DNA recovery from the agarose, which involved incubation in ~1 ml of 6 M sodium iodide at 55 °C in order to allow agarose to dissolve. The solution was then mixed with 50 µl of 10 % silica glass

beads (Sigma #S-5631; in 3 M sodium iodide) and incubated at 55 °C for 5 min what allowed binding of DNA to the beads. The mixture was spun down for 1 min in a bench microcentrifuge at maximum speed (17,000 x g; Thermo Scientific Sorvall Legend Micro 17) to precipitate the silica glass beads-bound DNA. After following three steps of washes in 500 µl of DNA wash buffer, DNA was eluted from the beads by adding 10-20 µl of distilled H_2O (dH_2O) and incubating at 55 °C for 5 min. The supernatant fraction obtained after 1 min of spinning in a bench microcentrifuge at 17,000 x g was later used as purified DNA fragment for homologous recombination in yeast.

Wash Buffer
2.922 g (0.5 % w/v) sodium chloride (Fisher, Loughborough, UK)
1.211 g (0.1 % w/v) Tris-hydrogen chloride pH 7.5 (Carl Roth, Mühlberg, Germany)
730.6 mg (0.025 % w/v) EDTA (Carl Roth, Mühlberg, Germany)
Ethanol added to total volume of 500 ml (50 % w/v) (Fisher, Loughborough, UK)
Autoclave for 20 mins at 121 °C
500 ml ethanol added before use with storage at 4 °C.

2.3.3 *S. cerevisiae* transformation

S. cerevisiae cells DS94 (MATα, *ura3-52*, *trp1-1*, *leu2-3*, *his3-111*, and *lys2-801*; Raymond *et al.*, 1999) were grown in 3 ml of liquid YPD medium at 30 °C overnight with 200 rpm shaking. Next, 2 ml of overnight culture was used for inoculation of 50 ml of YPD medium (flask volume: 250 ml) and was grown at 28-30 °C with 200-230 rpm shaking. After 5 h, cells were harvested after centrifugation at 2200 rpm (centrifuge Heraeus Biofuge Stratos, using rotor Heraeus #3047) for 5 min at RT. The cell pellet was resuspended in 10 ml of dH_2O and spun down again at 2200 rpm for 5 min at RT. Cell pellet was resuspended in 300 µl of dH_2O. 50 µl of yeast cells were combined with 50 µl of denatured solution of 2 µg/µl salmon sperm DNA (w/v in dH_2O; SIGMA, Cat No: D1626), usually 2 µl of linearised shuttle vector backbone and 2-4 µl purified PCR fragments (Fig. 2.1 D). 32 µl of 1 M lithium acetate (in dH_2O; SIGMA) and

240 µl 50 % PEG 4000 (w/v in dH_2O; Prolabo) was added to the transformation reaction and mixed by pipetting. After that, the transformation mixture was incubated at 30 °C for 30 min and it was further incubated at 45 °C in a water bath for 15 min in order to generate heat shock. Cells were later spinned down in a microcentrifuge at 2000 rpm for 2 min at RT and resuspended in 200 µl dH_2O. The obtained mixture was spread onto two Sc-Ura plates in a 1:1 dilution and a 1:10 dilution and incubated at 30 °C for usually 3 days.

2.3.4 *S. cerevisiae* PCR colony screening

In order to find positive transformants, screening of yeast colonies (Fig. 2.1 E) was done using DreamTaq Green PCR Master Mix polymerase (Fermentas #K1081) and appropriate primers which bind within the gene/fragment of interest and within the shuttle vector. The components of the PCR reaction mixture and PCR steps are shown below:

yeast colony
fPrimer (f.c. 10 µM) 1 µl
rPrimer (f.c. 10 µM) 1 µl
2x DreamTaq Green PCR Master Mix 10 µl
dH_2O added to total volume of 20 µl.

Standard PCR programs were carried out under these conditions:
1. Denaturing 95 °C (3 min)
2. Denaturing 95 °C (30 s)
3. Annealing Tm-4 °C (30 s)
4. Elongation 72 °C (1 min/ 1 kb)
5. Final Elongation 72 °C (10 min)
Steps 2. to 4. were repeated 35-40 times.

2.3.5 Plasmid DNA isolation from *S. cerevisiae*

A positive colony of selected yeast strain was grown overnight in 15 ml of Sc-Ura medium at 30 °C with 200 rpm shaking. The cells were harvested the next day by centrifugation at 1500 rpm (centrifuge Heraeus Biofuge Stratos, using

rotor Heraeus #3047) for 5 min at RT and the cell pellet was resuspended in 0.5 ml sterile dH_2O. The cells were then transferred into 1.5 ml eppendorf tube and centrifuged for 5 s in a microcentrifuge at 17,000 x g. After discarding of the supernatant, the cell pellet was vortexed in the residual water and 200 µl of yeast lysis buffer and 200 µl phenol:chloroform:isoamylalcohol (25:24:1) was added. The cells were disrupted by adding 0.3 g of acid washed glass beads (size 425 – 600 µm), followed by 10 min vibration on a IKA Vibrax VXR (IKA-Werke, Staufen, Germany). Next, after addition of 200 µl of TE buffer (pH 8.0), cell debris and organelles were removed by centrifugation for 5 min at RT in a microcentrifuge at 17,000 x g. The aqueous phase was then transferred to a new tube and separated from the lower organic phase containing proteins, polysaccharides and lipids. $1/10^{th}$ volume of 3M sodium acetate (pH 5.5) and 1 ml of 96 % ethanol was added to the aqueous phase containing nucleic acids and obtained mixture was incubated at -20 °C for 15 min. Afterwards, it was centrifuged in a bench microcentrifuge at 17,000 x g for 20 min. The supernatant was discarded and the pellet was resuspended in 400 µl of TE buffer (pH 8.0) and 4 µl of RNase A (10 mg/ml). The incubation at 37 °C allowed the pellet to dissolve. To the resuspended pellet 10 µl of 4 M ammonium acetate and 1 ml of 96 % ethanol was added followed by 2 min spinning in a bench microcentrifuge at 17,000 x g. After discarding the supernatant, the pellet was washed twice with 500 µl of 70 % ethanol and air dried. Then the pellet was resuspended in 20 µl dH_2O.

2.4 *E. coli* transformation

The *E. coli* strain DH5α (Hanahan, 1985) was used, for all cloning reactions and plasmid construction purposes, 6 to 8 µl of isolated yeast DNA was used for chemically competent *E. coli* cell transformation (Fig. 2.1 G). Heat shock was performed at 42 °C for 45-60 s followed by 5 min on ice and 1 h incubation in 200 µl of dYT at 37 °C in a Thermomixer (Eppendorf; Fisher Scientific) with shaking at 1000 rpm. Cells were plated onto dYT agar plates containing 100 µg/ml ampicillin and were grown overnight at 37 °C.

2.4.1 Preparation of thermo-competent *E. coli* cells

The preparation of thermo-competent cells was carried out by standard procedures (Sambrook et al., 1989). Overnight starter culture (3 ml LB broth) was inoculated with a single colony of DH5α (Stratagene, California, USA) and grown at 37 °C. The next day, 250 ml of SOB in a 1 L flask was inoculated with 1 ml of overnight culture, and incubated at 37 °C in a rotary shaker (Thermo Scientific, Massachusetts, USA) at 200 rpm until an of OD_{600} at 0.6 was reached. The cells were transferred to culture tubes and placed on ice for 10 minutes, before centrifugation at a low speed of 2500 x g for 5 min, at 4 °C. The cells were re-suspended in 80 ml of TB and rested on ice for 10 minutes and then centrifuged again. While spinning, 1.4 mL Dimethyl Sulfoxide (DMSO; Carl Roth, Mühlberg, Germany) was added to 18.6 mL of ice-cold TB and 20 ml of the TB-DMSO (7 % DMSO in TB) was used to resuspend the pellet The cells were placed on ice for a further 10 minutes, before being aliquoted into 50 or 100 µl batches on ice (in pre-cooled tubes on ice) and frozen immediately in liquid nitrogen. The competent cells were then stored at –80 °C and defrosted when required.

Media and solutions used in this method were as follows:

SOB media

20 g (20 % w/v) tryptone (Sigma Aldrich, Dorset, UK)
5 g (5.0 % w/v) yeast extract (Sigma Aldrich, Dorset, UK)
2 ml (2.0 % w/v) 5 M sodium chloride (Fisher, Loughborough, UK)
2.5 ml (0.25 % w/v) 1 M potassium chloride (Sigma Aldrich, Dorset, UK)
10 ml (1.0 % w/v) 1 M magnesium chloride (Sigma Aldrich, Dorset, UK)
10 ml (1.0 % w/v) 1 M magnesium sulphate (Sigma Aldrich, Dorset, UK)
Deionised H_2O added to 1 litre
Autoclave for 20 mins at 121 °C

LB Broth
10 g tryptone (Sigma Aldrich, Dorset, UK)
5 g yeast extract (Sigma Aldrich, Dorset, UK)
10 g sodium chloride (Fisher, Loughborough, UK)
Deionised H_2O added to 800 ml
Autoclave for 20 mins at 121 °C

2.4.2 Digestion of DNA with restriction endonucleases

All restriction endonucleases were obtained from New England Biolabs (Ipswich, UK). DNA digestions were carried out using buffer solutions provided by the manufacturer in a total volume of 50 µl with 2 µg of plasmid DNA or 10 µg of genomic DNA and 5-10 units of enzyme. 0.1 M BSA (New England Biolabs (NEB), Ipswich, UK) was added if required, to stabilise proteins during incubation and finally deionised water was added. The digestion mixture was then incubated at 37 °C (or higher if NEB instructions for enzymes indicated so) for at least two hours or overnight. A 1 µl sample of the digestion mix was then analysed using an 0.8 % agarose gel to check if DNA bands were correct.

2.5 DNA gel electrophoresis

In order to visualise DNA from PCRs or digestion, 1 µl samples were mixed with a DNA loading buffer (bromophenol-blue and sucrose) and water and then loaded into a TAE 0.8 % agarose gel that had been stained with ethidium bromide (4 µl per 100 ml; Fisher, Loughborough, UK). Samples were also loaded with a 1 kb ladder (Fermentas, Thermo Scientific, Massachusetts, USA) to provide a reference for the sizes of the bands seen. Gels were run for up to 1 hour, depending on the size of bands required. The gel was observed with an ultraviolet (UV) transilluminator (UV solo TS imaging system; Biometra, Göettingen, Germany) and the picture taken could be used as proof of correct band sizes for cloning and PCR confirmation of transformants. The illuminated gel slice could also be cut out and dissolved, in order to recover the DNA, as described previously.

2.6 *U. maydis* transformation

Transformation of *U. maydis* strains was performed as described in (Schulz et al., 1990). For transformation, 4 µl of linearised DNA (1- 5 µg) and 1 µl of Heparin (Sigma) were mixed with the 50 µl of protoplasts and incubated for 30 min on ice. Next, 0.5 ml of STC/40 %PEG (15 ml STC buffer, 10 g PEG 4000 (Fisher) and deionized distilled water added to 25 ml) was added on top of the protoplasts and carefully pipetted up and down. The whole reaction was

incubated for 15 min on ice and then whole amount was plated on Regeneration-Agar supplemented with the antibiotic (usually 400 µg/ml hygromycin or 300 µg/ml ClonNat). Plates were then incubated at 28 °C. Colonies appeared after 4-6 days and were singled-out on CM-agar plates containing the appropriate antibiotic and glucose or arabinose. Single colonies were picked and saved on CM-plates with the appropriate antibiotic (usually 200 µg/ml hygromycin or 150 µg/ml ClonNat).

To make protoplasts, *U. maydis* cells were grown overnight in YEPS medium (modified from (Tsukuda et al., 1988)) at 28 °C to a cell density of OD_{600} 0.6 – 0.8. Then, they were collected by centrifugation (10 min, 3000 rpm, RT) into Falcon tube and washed in 25 ml SCS before re-suspension in 1 ml SCS containing 10 mg Lysing Enzyme (Sigma). Next, cells were incubated at RT for 10-15 min after which the morphology of cells was checked for the removal of the cell wall under a microscope. When ~ 30-40 % of cells turned round instead of the normal cigar-shape and the rest of them looked like they were about to protoplast, they were washed three times with pre-chilled (4 °C) SCS, and centrifuged at 2400 rpm for 10 min at 4 °C each time. The cells were then washed once with pre-chilled STC buffer before re-suspending them in 0.5 ml of this buffer. The cell suspension was aliquoted as 50 µl samples which were used immediately in a transformation or stored at -80 °C.

SCS

Solution 1:

5.9 g (0.6 % w/v) sodium citrate·2H2O (f.c 20 mM) (Carl Roth, Mühlberg, Germany)

182.2 g (18.2 % w/v) sorbitol (f.c.1M) (Melford, Ipswich, UK)

Deionised H_2O added to 1 litre

Solution 2:

4.2 g (0.4 % w/v) citric acid·H_2O (f.c. 20 mM) (Carl Roth, Mühlberg, Germany)

182 g 18.2 % w/v) sorbitol (f.c. 1 M) (Melford, Ipswich, UK)

Deionised H_2O added to 1 litre

Add solution 2 to solution 1 until pH of 5.8 was reached (ratio 1:2 is 5:1)

STC - buffer

50 ml (50 % w/v) sorbitol (Melford, Ipswich, UK)

1.0 ml (1.0 % w/v) 1 M tris-HCl pH 7.5 (Carl Roth, Mühlberg, Germany)
10.0 ml (10.0 % w/v) 1 M calcium chloride (Sigma Aldrich, Dorset, UK)
Deionised H_2O added to 100 ml
Autoclave for 20 mins at 121 °C
STC/40 % PEG
90 ml (60.0 % w/v) STC buffer
60 g (40 % w/v) PEG 4000 (Fisher, Loughborough, UK)
Deionised H_2O added to 150 ml and filter sterilised before use.

Regeneration (REG) Agar
8.0 g (1.0 % w/v) yeast extract (Sigma Aldrich, Dorset, UK)
16.0 g (2.0 % w/v) peptone (Fisher, Loughborough, UK)
16.0 g (2.0 % w/v) sucrose (Fisher, Loughborough, UK)
145.76 g 18.22 % w/v) sorbitol (Melford, Ipswich, UK)
Deionised H_2O added to 800 ml
6.0 g agar (1.5 % w/v) per 400 ml media (LabM, Lancashire, UK)
Autoclave for 20 mins at 121 °C

2.6.1 Identification of positive transformants

In order to check for the presence of the correct plasmid integration in *U. maydis* transformants, individual colonies were plated onto CM-plates containing the antibiotic, present in the inserted construct and then allowed to grow for 2-3 days. Then they were subjected to the microscopy observation.

2.7 DNA isolation from *Ustilago maydis*

The protocol was adapted from (Hoffman and Winston, 1987). 2 ml of an overnight culture, grown in YEPS at 28 °C, 200 rpm, was pelletted in a 2 ml Eppendorf tubes by centrifugation (1 min at 13,000 x g). After discarding the supernatant 0.3 g of glass beads (Sartorius), 400 µl Usti-Lysis-buffer and 500 µl of Phenol-Chloroform were added and the samples were incubated for 10 min min on a Vibrax-VXR shaker (IKA, Staufen, Germany) at full speed. Then, the samples were centrifuged for 15 min at 13,000 x g to separate the phases and

about 400 µl of the top watery phase of the supernatant was transferred into 300 µl of Chloroform and shaken again on the Vibrax for 2 min at full speed. After that, samples were centrifuged again for 15 min at 13,000 x g and 400 µl of the top supernatants' phase was transferred to a 1.5 ml Eppendorf tube and mixed with 1 ml of 98 % ethanol. Tubes were then mixed by inverting and left for 10 min in a room temperature and then centrifuged for 10 min at 13,000 x g. Supernatant was discarded and the samples were washed with 70 % ethanol for 5 min at 13,000 x g. Next, the samples were centrifuged for 1 min at 13,000 x g to remove residual alcohol with a pipette. The pellet was re-suspended in 50 µl H_2O/RNase and incubated for 15 min, 300 rpm at 55 °C. After that 1 µl of the DNA was usually run on a gel to quantify and then stored at –20 °C for further analyses.

Lysis Buffer
5.845 g (5.85 % w/v) sodium chloride (Fisher, Loughborough, UK)
10 ml (10 % w/v) 1M tris-HCl (pH 8.0) (Carl Roth, Mühlberg, Germany)
20 ml (20 % w/v) triton X (Carl Roth, Mühlberg, Germany)
50 ml (50 % w/v) 20% SDS (Fisher, Loughborough, UK)
2 ml (2 % w/v) 0.5 M EDTA (Carl Roth, Mühlberg, Germany)
Deionised H_2O added to 1 litre and filter sterilised

TE
4 ml (1.0 % w/v) 1 M tris (Melford, Ipswich, UK)
800 µl (0.8 % w/v) 0.5 M EDTA (Carl Roth, Mühlberg, Germany)
Deionised H_2O added to 400 ml
pH adjusted to 8.0 with 0.4 M sodium hydroxide

2.8 Southern blotting

Southern blots were carried out on the strains tagged *in locus* with GFP and *crg*-beta tubulin mutant strains to confirm the correct integration of GFP or *crg*-promoter replacing the native one, respectively.

Before transformation, the plasmids were digested with restriction endonucleases (New England Biolabs (NEB), Ipswich, UK) and for Southern

blotting, the restriction enzymes were chosen not to cut inside the insert, to allow binding of the probe, to confirm the homologous integration.

Genomic DNA was isolated, as previously mentioned, for *U. maydis* DNA extraction. Probes were generated using DIG probe labelling mix (Roche, West Sussex, UK) as per the manufacturer's instruction. The following parameters were used as a guide for probe amplification; initial denaturation at 98 °C for 45 s, followed by 30 cycles of 98 °C for 10 s, 60 °C for 10 s, and 72 °C for 60 s, and then a final extension at 72 °C for 60 s. The probe was then purified by gel extraction and precipitation. Following isolation and digestion of genomic DNA, DNA fragments were separated on an agarose gel with a xylene cantanol loading buffer (6x loading buffer = 0.1% xylene cyanol, 30% glycerol). The gel was then depurinated in 0.25 M hydogren chloride for 15 mins and neutralised in 0.4 M sodium hydroxide, before being transferred to an Amersham Hybond - NX membrane (GE Healthcare, Buckinghamshire, UK) for a minimum of 4 hours. The membrane was then UV cross-linked to ensure complete transfer and incubated with hybridisation buffer and probe at 68 °C overnight. The following day, the membrane was washed, blocked and then detected using streptavidin-IRDye 800CW conjugate (LiCOR; GE Healthcare, 57 Buckinghamshire, UK) as per the manufacturer's instructions. It was then developed onto X-ray film (Fisher, Loughborough, UK) using a LiCOR Odtssey scanner.

Hybridisation buffer
500 ml (50 % w/v) 1 M sodium phosphate
350 ml (35 % w/v) 20 % SDS
Deionised H_2O added to 1 litre and store at 28 °C.

2.9 Other media and buffers

dYT-glycerol	1.6 % (w/v) tryptone, 1 % (w/v) yeast extract, 0.5 % (w/v) NaCl, 69.6 % (v/v) glycerol
Neutralisation solution	0.9 M sodium acetate pH 4.8, 0.5 M NaCl
NM (nitrate minimal)	0.3 % (w/v) KNO_3, 6.25 % (v/v) salt solution

medium, pH 7.0	(Holliday, 1974)
Sc-Ura medium	0.17 % (w/v) yeast nitrogen base without amino acids, 0.5 % (w/v) ammonium sulphate, 0.5 % (w/v) casein hydrolysate, 0.002 % (w/v) adenine, 2 % (w/v) glucose
STC buffer	10 mM Tris-HCl pH 7.5, 100 mM $CaCl_2$, 1 M sorbitol
YPD medium	1 % (w/v) yeast extract, 2 % (w/v) peptone, 2 % (w/v) D-glucose

2.10 Microscopy and live cell imaging

2.10.1 Determination of optical density

The cell density of liquid *U. maydis* cultures was measured at 600 nm wavelength (OD_{600}) in a Spekol 1500 (Analytik Jena, Germany) photometer against un-inoculated medium as reference. If the density of the culture exceeded 1, the culture was diluted to allow accurate measurements. A value of OD_{600} = 1 corresponds to ~ 1-5 $\times 10^7$ cells/ml.

2.10.2 Live cell imaging

For checking strains at the microscope cells were placed on 2 % agar cushion, covered with a coverslip and immediately observed using IX81 inverted microscope (Olympus, Hamburg, Germany). Excitation of fluorescently labelled proteins was achieved by solid state lasers (488 nm/50 mW) under the control of a VS-AOTF100 System (Visitron System, Munich, Germany). Z-axis stack images were taken at 400nm step size using Piezo device (Piezosystem GmbH, Jena, Germany) and then converted to maximum projections to observe whole microtubule array using MetaMorph ® (Life Science Imaging Ltd, Buckinghamshire, UK). In order to avoid oxygen depletion in the samples, they were observed for no longer than 15 minutes.

All measurements and image processing were carried out using MetaMorph ® (Life Science Imaging Ltd, Buckinghamshire, UK), and graphs were created with Prism4 (GraphPad, Calfornia, USA).

Chapter 3 – A study of beta tubulins in *Ustilago maydis*

3.1 Introduction

Beta tubulin is one of the basic components of microtubules and its nucleotide sequences are highly conserved (Tuszynski et al., 2006). It has also been predicted that MT assembly and stability are regulated through transcription of different tubulin isotypes, folding of tubulin monomers, formation of functional dimers and through post-translational modifications (Nogales, 2000; Yoshikawa et al., 2003).

Most species express multiple isotypes of alpha and beta tubulins, the building blocks of microtubules. Those tubulins are most divergent at their C-terminal tail regions (Hashimoto, 2013), which are the putative binding sites for several microtubule-associated proteins (Sullivan et al., 1986). Although the crystal structure of an α/β heterodimer has been mostly resolved, the precise structure of the carboxy (C)-termini remains elusive, even though the C-termini play critical roles in regulating microtubule structure and function (Freedman et al., 2011). The C-termini are also the sites of most of the post-translational modifications, which in mammalian tubulin alpha-1A/1B play a major role in directing intracellular trafficking, microtubule dynamics, and mitotic events, and can vary depending on the cell and disease state, such as cancer and neurodegenerative disorders (Sahab et al., 2012).

The number of genes encoding tubulins ranges from one or two genes in fungi, to five to seven in vertebrates or to as many as six alpha and beta tubulin genes in plants (Monnat et al., 1997). Each evolutionarily conserved isotype tends to have specific negatively charged stretches of 15 or more amino acid residues at their C-terminal tail (CTT) and to a lesser extent, the N-terminal region also tends to be isotype specific (Wade, 2009). Comparison of the number of genes encoding alpha and beta tubulins in different model organisms (Table 3.1) reveals that higher plants and humans have the highest number of tubulin isotypes, while unicellular organisms have at most two alpha and two beta genes. *U. maydis* has a single alpha tubulin, two beta tubulin genes, and a single gamma tubulin gene.

Over the past few decades there have been many studies which were aimed at explaining the relationship between tubulin isotypes and their functions. For instance, a study in budding yeast showed that mutation in a crucial beta tubulin serine at position 172 (previously discovered in mammals by (Fourest-Lieuvin et al., 2006)), caused abnormal MT dynamics and impaired mitosis, as well as abnormal function of +TIPs (Caudron et al., 2010).

Moreover, in *Neurospora crassa,* which has only one beta-tubulin gene and two alpha-tubulin genes, the expression profiles of the two alpha-tubulin mRNAs and proteins, showed distinct patterns of expression during the macroconidial germination, and this together with their unusually high divergent primary structures (35% identity) suggests that the differential alpha-tubulin isoforms could be involved in specific functions during organism development (Monnat et al., 1997).

Similarly, beta-tubulins in *Aspergillus nidulans* are also unusually divergent suggesting that their products may have different functions (May et al., 1987). Although it was demonstrated that beta-tubulins are functionally interchangeable by promoter swapping experiments, it is also known that one beta tubulin (benA) is involved in both vegetative growth and asexual sporulation, while the second one (tubC) is involved mainly in asexual sporulation (May, 1989; May et al., 1987; Oakley, 2004). *A. nidulans* has also two alpha tubulin isotypes and those are even more divergent than beta tubulins, however they were discovered to be functionally interchangeable and it was suggested that there may be subtle functional differences between them (Kirk and Morris, 1993).

Interestingly, in plants such as *Arabidopsis thaliana* and *Oryza sativa*, which contain nine and eight genes encoding beta tubulins respectively (Table 3.1), the relationship between beta-tubulins was established mainly by studying their expression patterns in different organs. In addition, studies in rice (*Oryza sativa*) showed that the influence of different phytohormones can down- or upregulate beta-tubulin gene function (Yoshikawa et al., 2003). Overall, in plants, many beta-tubulin genes exhibit unique developmentally regulated patterns of

expression and respond to environmental signals in different ways (Cheng et al., 2001).

Furthermore, in mammals, there are at least six alpha and seven beta tubulin isotypes encoded by multiple genes that display differential tissue expression (Lopata and Cleveland, 1987; Luduena, 1998). For example, a study from 2011 in humans had shown the expression of eight human beta tubulin isotypes in different nontumoral (healthy) and tumoral tissues, using especially developed quantitative RT-PCR. The researchers found that the contribution of the different isotypes to the total beta tubulin content varied for each tissue and had a complex pattern, which is important, because it could contribute to the toxicity profile of the microtubule-binding drugs (Leandro-Garcia et al., 2010). In addition, the specific isotypes significantly altered in tumours might represent markers for drug response.

Here, I set out to examine the role of the two *U. maydis* beta tubulins using bioinformatics and localisation studies.

Table 3.1 Number of tubulin isotypes found in different groups of organisms

	Organism	Alpha tubulin	Beta tubulin	Gamma tubulin
Basiodiomycota	***Ustilago maydis***	**1**	**2**	**1**
	Cryptococcus neoformans	1	2	1
	Puccinia graminis	1	1	1
	Coprinopsis cinerea	2	1	1
	Schizophyllum commune	2	1	1
Ascomycota	*Saccharomyces cerevisiae*	2	1	1
	Schizosaccharomyces pombe	2	1	1
	Aspergillus nidulans	2	2	1
	Neurospora crassa	2	1	1
	Candida albicans	1	1	1
	Fusarium graminearum	2	2	1
Multicellular organisms	*Drosophila melanogaster*	4	4	2
	Oryza sativa	3	8	1
	Arabidopsis thaliana	6	9	2
	Homo sapiens	15	21	3

3.2 Materials and methods

3.2.1 Analysis of *U. maydis* β-tubulin protein sequences

The *U. maydis* β-tubulin protein sequences were retrieved from *U. maydis* MIPS genome database http://mips.helmholtz-muenchen.de/genre/proj/ustilago. To identify domains of β-tubulin proteins, their sequences were submitted to InterProScan (Zdobnov and Apweiler, 2001) online domain database program. The cartoons of the proteins were drawn using DOG 2.0 software (Ren et al., 2009a).

3.2.2 Sequence alignment of *U. maydis* beta tubulins

The protein sequences were aligned using ClustalW software (Thompson et al., 1994). Shading of the alignments was carried out using BOXSHADE version 3.21 (written by Kay Hoffmann and Michael D. Baron).

3.2.3 Construction of phylologenetic trees

Sequences were aligned in ClustalX (Thompson et al., 1997) using default parameters. An unrooted neighbour-joining tree (Saitou and Nei, 1987) was constructed from amino acid sequences of alpha, beta and gamma tubulin-encoding genes from diverse eukaryotes. The analysis involved 91 amino acid sequences and was conducted in MEGA6 (Tamura et al., 2013). Numbers on the tree represent bootstrap values as determined by MEGA6 program.

3.2.4 RT-PCR

First step was to obtain RNA, which was isolated from yeast-like and hyphal cells of *U. maydis*. It was kindly provided by Dr. Catherine Collins. RNA was isolated from yeast-like *Ustilago maydis* (strain AB33) cultures which were grown on CM-glucose media for either 8 hours (day) or overnight using protocol based on paper from (Schmitt et al., 1990). Similarly, RNA was isolated from hyphal cells of *U. maydis* which were either grown on NMG media for 8 hours (day) or overnight.

Next, all RNA were treated with DNase, to avoid any DNA contaminations. The RNA was diluted 1/10 and treated with DNase as follows with DNA-free kit from Ambion (cat# AM1906):

5 µl RNA (1/10 dilution)
5 µl DNase buffer
39 µl DNase/RNase free water
1 µl DNase

Then it was incubated at 37 °C for 1 hour, 2 µl DNase Inactivation Reagent was added and it was left at RT for 2 min with mixing. The reaction tubes were then centrifuged at 10,000 g for 1.5 min, transferred to new tube and stored at -80 °C freezer.

To check that the entire genomic DNA had been removed from the RNA, 5 µl of DNased RNA was diluted to a final volume of 20 µl with DNase/RNase free water (as this is the amount of RNA that will be used for cDNA synthesis in a final volume of 20 µl) and a PCR was performed for tub3 and tub4 genes. If the genomic DNA is removed no product will be obtained. A positive and a negative PCR were also performed with 1/100 dilution of tub3 and tub4 plasmids and no template, respectively. The expected sizes of those PCR products were 1220 bp and 1270 bp.

For tub3:

Dream Taq 2X mix	10 µl
Primer $_{f}$AL102	1 µl
Primer $_{r}$AL103	1 µl
DNased RNA	1 µl
Water	7 µl

For tub4:

Dream Taq 2X mix	10 µl
Primer $_{f}$AL104	1 µl
Primer $_{r}$AL105	1 µl

DNased RNA	1 µl
Water	7 µl

PCR program:

1. 94 °C 2 min
2. 94 °C 30 sec
3. 59 °C 30 sec
4. 72 °C 1 min 10 sec
5. Go to step 2, 34 times
6. 72 °C 10 min
7. 20 °C forever
8. end

Next step was cDNA synthesis and as no genomic DNA was detected in DNAsed RNA, it was used for cDNA synthesis. cDNA was made with superscript III first strand synthesis supermix (Invitrogen, Paisley, UK) in a 0.2 ml thin walled PCR tube:

DNased RNA	5 µl
Primer (50 µM oligo$(dT)_{20}$	1 µl
Annealing buffer	1 µl
DNase/RNase free water	1 µl

The tubes were incubated in PCR machine at 65 °C for 5 min followed by ice for at least 1 min. The following were added to the tube on ice:

2X first strand buffer	10 µl
Superscript III/RNaseOUT Enzyme mix	2 µl

Then they were vortexed briefly, centrifuged and incubated in a PCR machine at 50 °C for 50 min followed by 85 °C for 5 min to terminate reaction.

For the RT-PCR 1 µl of cDNA was used for beta tubulins as described above. If the band of the expected size was present that indicated that the RNA has been reversed transcribed as prior to cDNA synthesis no product was obtained from the DNase treated samples. A positive and a negative PCR were also performed.

3.2.5 Construction of plasmids for this study

pTub3-GFP_nat: This plasmid contains a fragment of tub3 ORF region fused C-terminally to eGFP. The construct contains nourseothicin resistance cassette (*nat*R). The plasmid was generated through *in vivo* recombination in the yeast *S. cerevisiae* by amplification of 3 fragments and cloning them into a pNEB_nat vector (New England Biolabs (NEB), Ipswitch, UK modified for yeast recombination). A fragment containing the last 1000bp of the tub3 gene without terminator (with overhangs designed for recombination with pNEB_nat yeast vector and eGFP) was amplified from the genomic *U. maydis* DNA (using promers $_{f}$AL47 and $_{r}$AL48); a fragment of 1032 bp in length encoding eGFP and 30bp of Tnos terminator (with overhangs designed for recombination with tub3 gene fragment and *nat*R) was amplified from the potef-Tub3-eGFP_cbx (provided by Dr. Anne Straube) plasmid (using primers $_{f}$AL49 and $_{r}$AL50) and a 1519 bp fragment of tub3 terminator (with overhangs designed for recombination with *nat*R cassette and pNEB_nat yeast vector) was amplified from the genomic *U. maydis* DNA (using promers $_{f}$AL51 and $_{r}$AL52). All fragments were cloned into the pNEB_nat yeast vector linearised with *Bsr*GI and *Sac*I restriction enzymes.

pcrgTub3_hyg: This plasmid contains a fragment of tub3 ORF region fused behind inducible *crg* promoter. The construct contains hygromycin resistance cassette (*hyg*R). The plasmid was generated through *in vivo* recombination in the yeast *S. cerevisiae* by amplification of 3 fragments and cloning them into a pNEB_cbx vector (New England Biolabs (NEB), Ipswitch, UK modified for yeast recombination) and then *cbx*R cassette was replaced with *hyg*R. A fragment containing a 997 bp of region just before the tub3 gene (with overhangs designed for recombination with pNEB_cbx yeast vector and *cbx*R cassette) was amplified from the genomic *U. maydis* DNA (using primers $_{f}$AL70 and $_{r}$AL71); a fragment of 3508 bp in length encoding *crg* promoter (with overhangs designed for recombination with *hyg*R) was amplified from the pcrg-eGFP_cbx (provided by Dr. Ewa Bielska) plasmid (using primers $_{f}$SK129 and $_{r}$SK130) and a 996 bp fragment of tub3 gene with 30 bp of Tnos terminator (with overhangs designed for recombination with *cbx*R cassette and pNEB_cbx yeast vector) was amplified from the genomic *U. maydis* DNA (using promers $_{f}$AL72 and

$_{r}$AL73). All fragments were cloned into the pNEB_cbx yeast vector linearised with *Pac*I and *Sac*I restriction enzymes. Finally, *cbx*R cassette was cut out using a *Not*I restriction enzyme and replaced with *hyg*R cassette obtained from pNEB-hyg-yeast (cut out with *Eco*RV and *Bam*HI restriction enzymes) vector ligated with T4 DNA ligase (New England Biolabs (NEB), Ipswich, UK).

pcrgTub4_hyg: This plasmid contains a fragment of tub4 ORF region fused behind inducible *crg* promoter. The construct contains hygromycin resistance cassette (*hyg*R). The plasmid was generated through *in vivo* recombination in the yeast *S. cerevisiae* by amplification of 3 fragments and cloning them into a pNEB_cbx vector (New England Biolabs (NEB), Ipswitch, UK modified for yeast recombination) and then *cbx*R cassette was replaced with *hyg*R. A fragment containing a 1028 bp of region just before the tub4 gene (with overhangs designed for recombination with pNEB_cbx yeast vector and *cbx*R cassette) was amplified from the genomic *U. maydis* DNA (using promers $_{f}$AL70 and $_{r}$AL71); a fragment of 3508 bp in length encoding *crg* promoter (with overhangs designed for recombination with *hyg*R) was amplified from the pcrg-eGFP_cbx (provided by Dr. Ewa Bielska) plasmid (using primers $_{f}$SK129 and $_{r}$SK130) and a 1000 bp fragment of tub4 gene with 30 bp of Tnos terminator (with overhangs designed for recombination with *cbx*R cassette and pNEB_cbx yeast vector) was amplified from the genomic *U. maydis* DNA (using promers $_{f}$AL76 and $_{r}$AL77). All fragments were cloned into the pNEB_cbx yeast vector linearised with *Pac*I and *Sac*I restriction enzymes. Finally, *cbx*R cassette was cut out using a *Not*I restriction enzyme and replaced with *hyg*R cassette obtained from pNEB-hyg-yeast (cut out with *Eco*RV and *Bam*HI restriction enzymes) vector ligated with T4 DNA ligase (New England Biolabs (NEB), Ipswich, UK).

3.2.6 Construction of strains for this study

In-locus GFP tagging

Plasmid pTub3-GFP_nat was transformed into AB33_RT strain, as described in General Materials and Methods. Positive transformants were firstly identified visually at the microscope and then confirmed by southern blotting.

Downregulation of tub3 and tub4 using arabinose inducible *crg* promoter.

Plasmids pcrgTub3_hyg and pcrgTub4_hyg, where each beta-tubulin was put under *crg* promoter, to replace the native promoter, were transformed into AB33_GT strain, as described in General Materials and Methods. Positive transformants were identified using colony PCR, then southern blotting. Following the confirmation of desired strains, the beta-tubulin mutants were grown overnight in CM-Ara, in order to induce the *crg* promoter (Mahlert et al., 2006), which controlled one of the beta-tubulin isoforms. It was followed by centrifugation at 3000 rpm and transfer to CM-Glu media, where the *crg* promoter was repressed, which caused downregulation of tub3 or tub4 gene.

Table 3.2 Primers used in this study

Primer	Sequence (5' – 3')
fAL47	ACGACGTTGTAAAACGACGGCCAGTGAATTTCCAACTCGTCCACTCGCTC
rAL48	GTGAACAGCTCCTCGCCCTTGCTCACCATGTACTGGATGGATTCTTCGTGGG
fAL49	CATGGTGAGCAAGGGCGAG
rAL50	TAGAGCGGCCGCGGCGCGCCCCCGGGTACCAGATCCCCATCGAATTCTC
fAL51	AACGTTATTTATATTTCAAATTTTTCTTTTCCATCCAGTATGCTGATGAAC
rAL52	ACAGGAAACAGCTATGACCATGATTACGCCCAACGACGACGGCACACGTA
fAL70	AAACGACGGCCAGTGAATTCGAGCTCGGTAATTGTGGACACATCGATCGC
rAL71	GAGCGAAGATCCCCGCGGCCGCGGCGCGCCTGAGCGAATATCGTGGAAGG
fAL72	GGTGAAACTCGATGAGGCCAAAAAAGATACATGCGTGAGCTCATCACGTA
rAL73	ATCATCGCAAGACCGGCAACAGGATTCAATGTGAAAAAGTGAAGACGCGG
fAL74	AAACGACGGCCAGTGAATTCGAGCTCGGTAACCTGTGGGTGTTGTGTTAG
rAL75	GAGCGAAGATCCCCGCGGCCGCGGCGCGCCCCAAACTGACACTCTGGATG
fAL76	GGTGAAACTCGATGAGGCCAAAAAAGATACATGCGTGAGATTGGTAAGTC
rAL77	ATCATCGCAAGACCGGCAACAGGATTCAATAAACGCCTGCTGCGTGATCT
fAL102	AGCAACTCTGCAAGGTCGGC
rAL103	TGGCCTTGTTCCTCGTACTC
fAL104	GTAACCAGGTCGGTACCAAG
rAL105	TCGCCCTCAATGTCCTCGTC
fSK129	CCATCAACGTGCTCGATGCGGCCGCGGCGCGATCCCGCGATACGCACCTTG
rSK130	GTATCTTTTTTGGCCTCATCGAGT

3.3 Results

Characterisation of β-tubulins using bioinformatics

As most eukaryotic organisms express multiple tubulin genes with each distinct tubulin isoform having an essential function, it has been shown that not every tubulin molecule is interchangeable (Tuszynski et al., 2006). According to the MIPS database (http://mips.gsf.de/genre/proj/ustilago/), *Ustilago maydis* has one α-tubulin, tub1 (UM01221), two separate genes encoding β-tubulins, tub3 (UM10558) and tub4 (UM05828), and one γ-tubulin, tub2 (UM03803). Whilst the α- and γ-tubulin genes have been both characterised and shown to be essential genes (Steinberg et al., 2001; Straube et al., 2003), at present, not much is known about the β-tubulins, and their significance for the biology of *U. maydis* remains opaque.

3.3.1 Domain architecture of *U. maydis* beta tubulins

As a first step in revealing the need for two separate beta tubulin genes, I analysed the domain architectures of the putative *U. maydis* beta-tubulin sequences using InterProScan (Zdobnov and Apweiler, 2001). Both sequences had a highly similar domain organisation consisting of an amino-terminal GTPase domain, followed by a central helix, 2-layer sandwich domain and carboxy-terminal domain (Fig. 3.1), but differed at the extreme C-terminus, which is longer in Tub3 protein by 24 amino acids (Fig. 3.1). This high degree of similarity in predicted domain organisation is in accordance with the literature. As the structures of tubulins are almost identical, each monomer can be divided into three functional domains: the N-terminal domain containing the nucleotide-binding region, an intermediate domain containing the Taxol- binding site, and the C-terminal domain (Nogales et al., 1998) which has MT-associated proteins binding sites (Keskin et al., 2002).

3.3.2 Amino acid alignment of *U. maydis* beta tubulins

The primary amino acid sequence of the two proteins was analysed using EMBOSS Needle online software

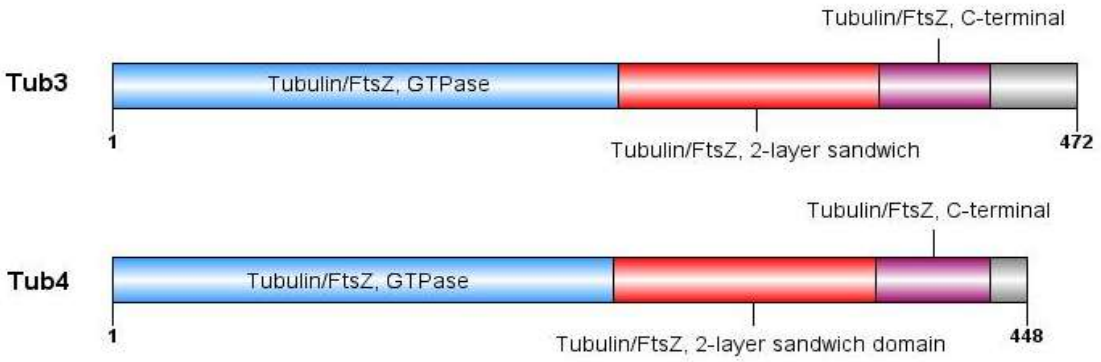

Figure 3.1 Domain architecture of beta tubulins found in *Ustilago maydis*

For each protein its domain architecture is shown, determined using the InterPro online software (Hunter et al., 2012). The cartoons were drawn using DOG 2.0 software (Ren et al., 2009a). The blue domain denotes GTPase domain, red domain marks 2-layer intermediate domain and purple-coloured domain shows C-terminal domain. All of those domains are typically present in most tubulins. The main difference between the two beta tubulins is visible at their C-terminal tails, as Tub3 has additional 24 amino acids on its tail in comparison to Tub4.

Figure 3.2 Alignment of the predicted amino acid sequences of Tub3 and Tub4

The predicted amino acid sequence of *U. maydis* Tub3 (UM10558) was aligned with Tub4 (UM05828). Sequences were aligned using ClustalW (Thompson et al., 1994). Shading of the alignments was carried out using BOXSHADE version 3.21 (written by Kay Hoffmann and Michael D. Baron). Tub3 shows 61.7 % identity and 76.9 % similarity to Tub4. Identical amino acids are highlighted with a black background and amino acids with similar side-chains, with a grey background. Red boxes mark the C-terminal tails of beta-tubulins, which have 22.7 % identity and 29.5 % similarity, which was predicted by the EMBOSS Needle online software ((Goujon et al., 2010; McWilliam et al., 2013; Rice et al., 2000).

(Goujon et al., 2010; McWilliam et al., 2013; Rice et al., 2000) a Pairwise Sequence Alignment tool (http://www.ebi.ac.uk/Tools) (Fig. 3.2). Both sequences are very highly conserved between each other, except for their C-terminal tails (CTTs) (Fig. 3.2). Comparison of the amino acid sequences revealed that the putative beta tubulin genes share 61.7 % identity and 76.9 % similarity, which was much higher than sequence similarity between other *Ustilago* tubulins. However, the beta tubulin CTTs (Fig. 3.2, red box) were much more divergent and had only 22.7 % identity and 29.5 % similarity. In comparison, the average identity/similarity between beta tubulins and alpha tubulin was 38.4 %/57.9 %, and for beta tubulins and gamma tubulin it was 34.5 %/54.6 %, which shows that these sequences are closely related, but not as much as beta tubulins.

3.3.3 Phylogenetic trees of tubulins

To confirm that these tubulins do indeed belong to the beta tubulin functional group, I constructed a phylogenetic tree using protein sequences from different fungi as well as other model organisms (Figure 3.3). The genetic relationship of beta tubulins was explored by constructing a neighbour-joining tree (Saitou, 1987) of a broad section of beta tubulin-encoding genes from diverse eukaryotes. First of all, alpha, beta and gamma tubulins formed separate clades. Second, gamma tubulins form an outgroup and comparison of the tree indicates that alpha and beta tubulins are more closely related to each other, than to gamma tubulin, which is not surprising as they are both an integral part of the whole microtubule lattice. Finally, all of *U. maydis's* tubulin genes grouped with the similar-type tubulins from other filamentous fungi. The two putative *Ustilago* beta tubulins were found in two separate basidiomycota-specific clades, with one of them, Tub3, closely related to other fungal beta tubulins and the second one, Tub4, closer to the beta tubulins of multicellular organisms (Figure 3.4). At the same time, a phylogenetic analysis of beta tubulins was carried out with the use of the same organisms as before check how those genes were grouped. It appeared that beta tubulins were divided into four separate clades, which included multicellular organisms, Ascomycota and two Basidiomycota groups. Each of the *U. maydis* beta tubulins belonged to a separate Basidiomycotian group, however both of them were closely related to

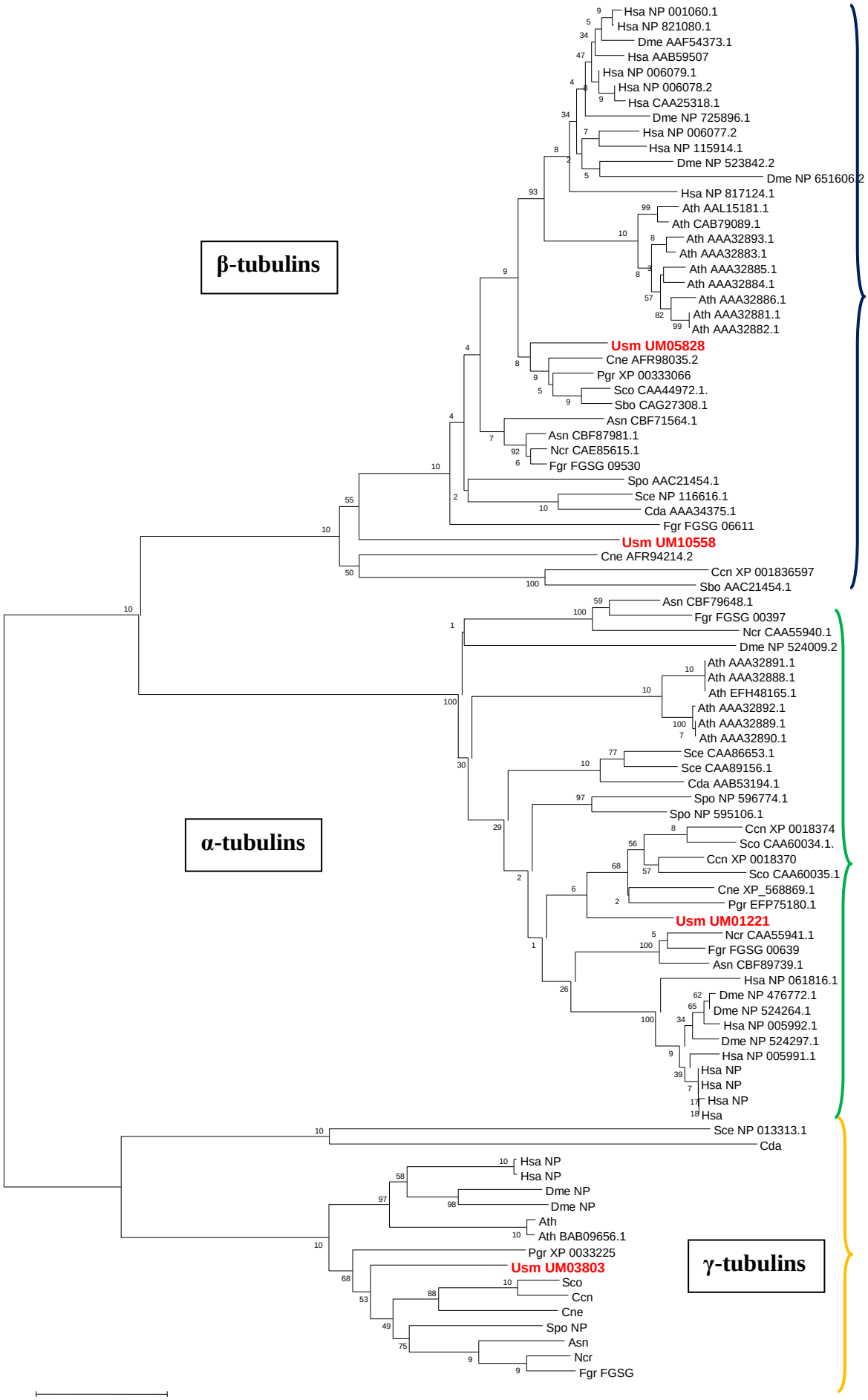
β-tubulins
Hsa NP 001060.1
Hsa NP 821080.1
Dme AAF54373.1
Hsa AAB59507
Hsa NP 006079.1
Hsa NP 006078.2
Hsa CAA25318.1
Dme NP 725896.1
Hsa NP 006077.2
Hsa NP 115914.1
Dme NP 523842.2
Dme NP 651606.2
Hsa NP 817124.1
Ath AAL15181.1
Ath CAB79089.1
Ath AAA32893.1
Ath AAA32883.1
Ath AAA32885.1
Ath AAA32884.1
Ath AAA32886.1
Ath AAA32881.1
Ath AAA32882.1
Usm UM05828
Cne AFR98035.2
Pgr XP 00333066
Sco CAA44972.1.
Sbo CAG27308.1
Asn CBF71564.1
Asn CBF87981.1
Ncr CAE85615.1
Fgr FGSG 09530
Spo AAC21454.1
Sce NP 116616.1
Cda AAA34375.1
Fgr FGSG 06611
Usm UM10558
Cne AFR94214.2
Ccn XP 001836597
Sbo AAC21454.1
α-tubulins
Asn CBF79648.1
Fgr FGSG 00397
Ncr CAA55940.1
Dme NP 524009.2
Ath AAA32891.1
Ath AAA32888.1
Ath EFH48165.1
Ath AAA32892.1
Ath AAA32889.1
Ath AAA32890.1
Sce CAA86653.1
Sce CAA89156.1
Cda AAB53194.1
Spo NP 596774.1
Spo NP 595106.1
Ccn XP 0018374
Sco CAA60034.1.
Ccn XP 0018370
Sco CAA60035.1
Cne XP_568869.1
Pgr EFP75180.1
Usm UM01221
Ncr CAA55941.1
Fgr FGSG 00639
Asn CBF89739.1
Hsa NP 061816.1
Dme NP 476772.1
Dme NP 524264.1
Hsa NP 005992.1
Dme NP 524297.1
Hsa NP 005991.1
Hsa NP
Hsa NP
Hsa NP
Hsa
γ-tubulins
Sce NP 013313.1
Cda
Hsa NP
Hsa NP
Dme NP
Dme NP
Ath
Ath BAB09656.1
Pgr XP 0033225
Usm UM03803
Sco
Ccn
Cne
Spo NP
Asn
Ncr
Fgr FGSG

Figure 3.3 Phylogenetic analysis of α, β and γ -tubulin amino acid sequences from a range of organisms.

A neighbour-joining tree (Saitou and Nei, 1987) was constructed from amino acid sequences of alpha, beta and gamma tubulin-encoding genes from diverse eukaryotes. Tree topology was tested by 500 bootstrap re-sampling of the data. *Ustilago's* beta tubulins belonged to separate basidiomycota-specific clades, with one of them, Tub3, closely related to other fungal beta tubulins and the second one closer to the metazoan beta tubulins. The analysis involved 91amino acid sequences and was conducted in MEGA6 (Tamura et al., 2013). Abbreviations: Hsa, *Homo sapiens;* Dme, *Drosophila melanogaster*; Ath*, Arabidopsis thaliana*; Usm, *Ustilago maydis*; Cne, *Cryptococcus neoformans*; Pgr, *Puccinia graminis*; Sco, *Schizophyllum commune*; Sbo, *Suillus bovinus*; Asn, *Aspergillus nidulans*; Ncr, *Neurospora crassa*; Fgr, *Fusarium graminearum*; Spo, *Schizosaccharomyces pombe*; Sce, *Saccharomyces cerevisiae*; Cda, *Candida albicans*; Ccn, *Coprinopsis cinerea*.

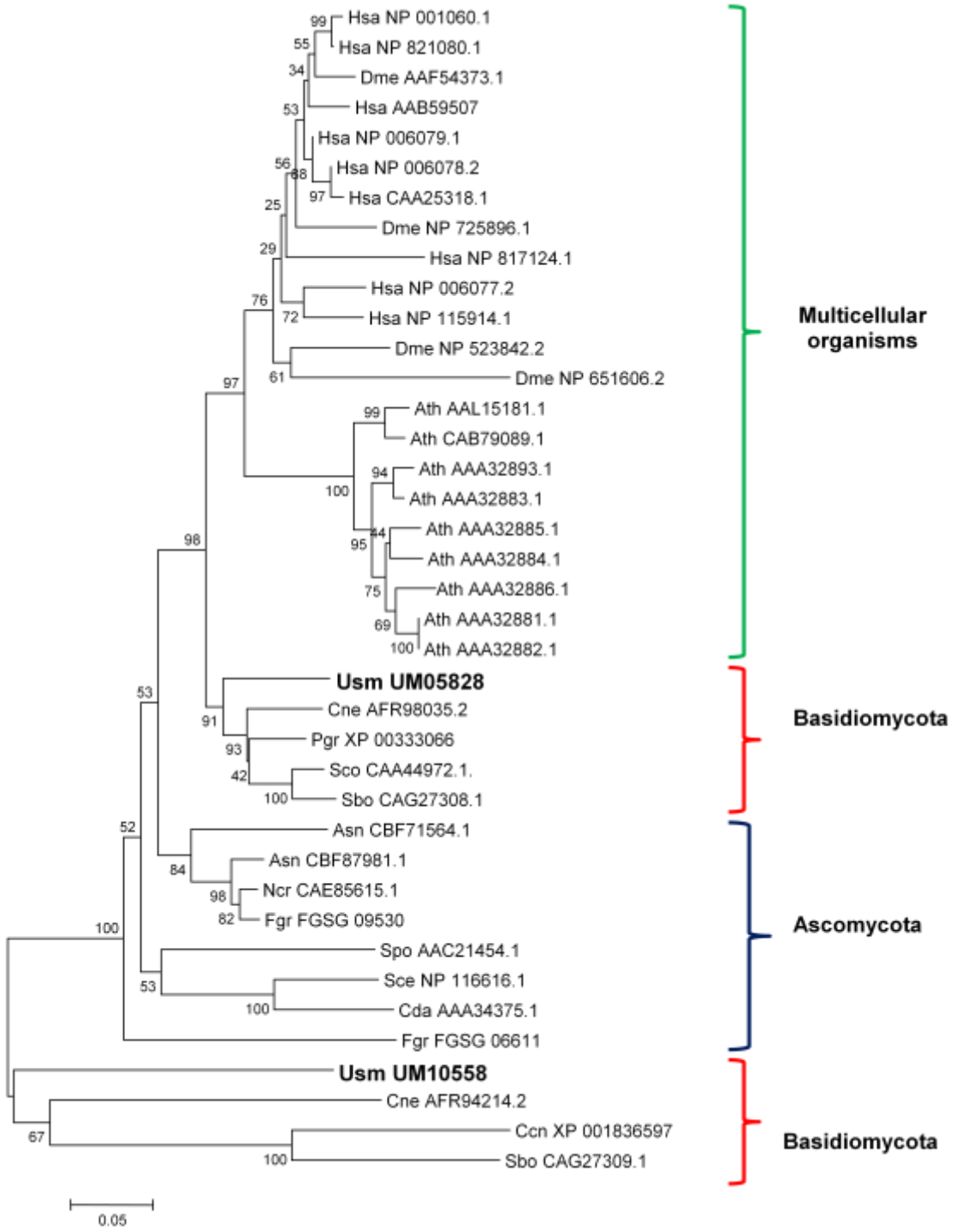

Figure 3.4 Phylogenetic analysis of β-tubulin amino acid sequences from a range of organisms.

A neighbour-joining tree (Saitou and Nei, 1987) was constructed from amino acid sequences of beta tubulin-encoding genes from diverse eukaryotes. Tree topology was tested by 500 bootstrap re-sampling of the data. *Ustilago's* beta

tubulins belonged to separate basidiomycota-specific clades and were closely related to other fungal beta tubulins. The analysis involved 39 amino acid sequences and was conducted in MEGA6 (Tamura et. al., 2013). Abbreviations: Hsa, *Homo sapiens;* Dme, *Drosophila melanogaster*; Ath*, Arabidopsis thaliana*; Usm, *Ustilago maydis*; Cne, *Cryptococcus neoformans*; Pgr, *Puccinia graminis*; Sco, *Schizophyllum commune*; Sbo, *Suillus bovinus*; Asn, *Aspergillus nidulans*; Ncr, *Neurospora crassa*; Fgr, *Fusarium graminearum*; Spo, *Schizosaccharomyces pombe*; Sce, *Saccharomyces cerevisiae*; Cda, *Candida albicans*; Ccn, *Coprinopsis cinerea*.

beta tubulins from filamentous fungi. Therefore, the Tub3 and Tub4 sequences do indeed represent members of the beta tubulin group.

3.3.4 Beta tubulin genes are expressed in yeast and hyphal forms of *Ustilago maydis*

In order to examine when and where beta tubulin genes are expressed in *U. maydis*, reverse-transcriptase PCR (RT-PCR) was performed on yeast-like and hyphal *U. maydis* cultures. PCR products of the expected size (1220 bp for tub3 and 1270 bp for tub4) were obtained for both sequences, indicating that both beta tubulins are expressed. Comparison of the results from yeast-like and hyphal cultures showed that both beta tubulins are expressed in both cell types (Figure 3.5), indicating that neither can be considered to be cell-stage-specific.

3.3.5 Visualisation of beta tubulins in *Ustilago maydis*

Since *U. maydis* has only one gene for alpha tubulin, all microtubules contain this isotype and therefore it can be used as a marker to visualise cellular microtubules alongside the two beta tubulins to see if the beta tubulins are present on different populations of MTs.

In order to visualise beta tubulins in *U. maydis* cells, I made use of two plasmids, each containing a beta tubulin with GFP on the C-terminus. Initially, I transformed each of the beta tubulin plasmid separately into a strain where alpha tubulin was tagged with mCherry to compare visually the distribution of microtubules stained by GFP-tagged beta tubulins. Microscopy analysis showed that both Tub3-GFP and Tub4-GFP stained all visible microtubules when compared with mCherry tagged microtubules in yeast-like cells (Figure 3.6) and in hyphae (not shown). However, as the beta tubulins were overexpressed in these initial experiments, we decided to tag them *in locus* with GFP, again in the strain with mCherry-alpha tubulin. Tub3::GFP was localised on all visible microtubules in yeast-like cells and hyphae (Figure 3.7), as before; however it was not possible to visualise Tub4::GFP. The reason for the failure to see Tub4 is unknown, but presumably reflects a technical issue or very low expression levels, as mRNA for the native transcript is made in both cell types (Fig. 3.5).

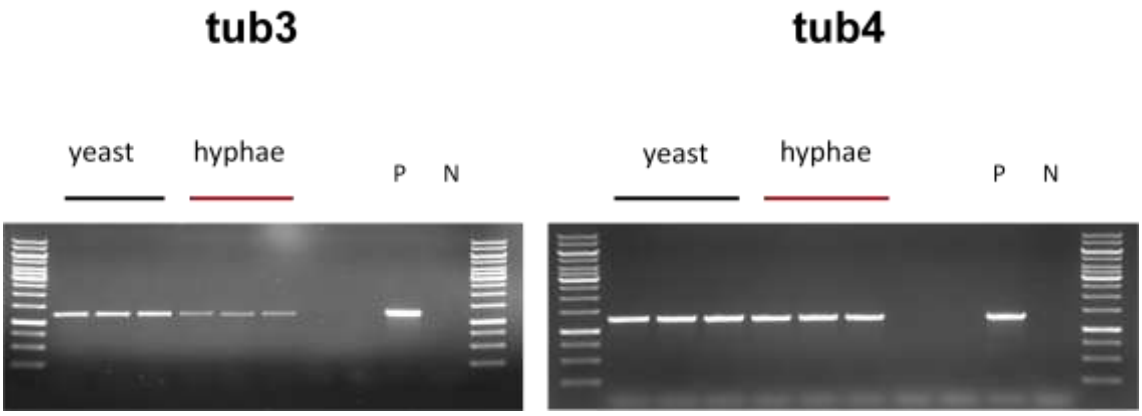

Figure 3.5 Tub3 and tub4 genes are expressed in yeast-like and hyphal forms of *Ustilago maydis*.

Reverse-transcriptase PCR (RT-PCR) was performed using three separate samples isolated from yeast and hyphae of *U. maydis*. For both beta tubulins, the results show that they are both expressed in yeast and hyphal forms of *U. maydis*. P refers to a positive control; N refers to a negative control with no DNA.

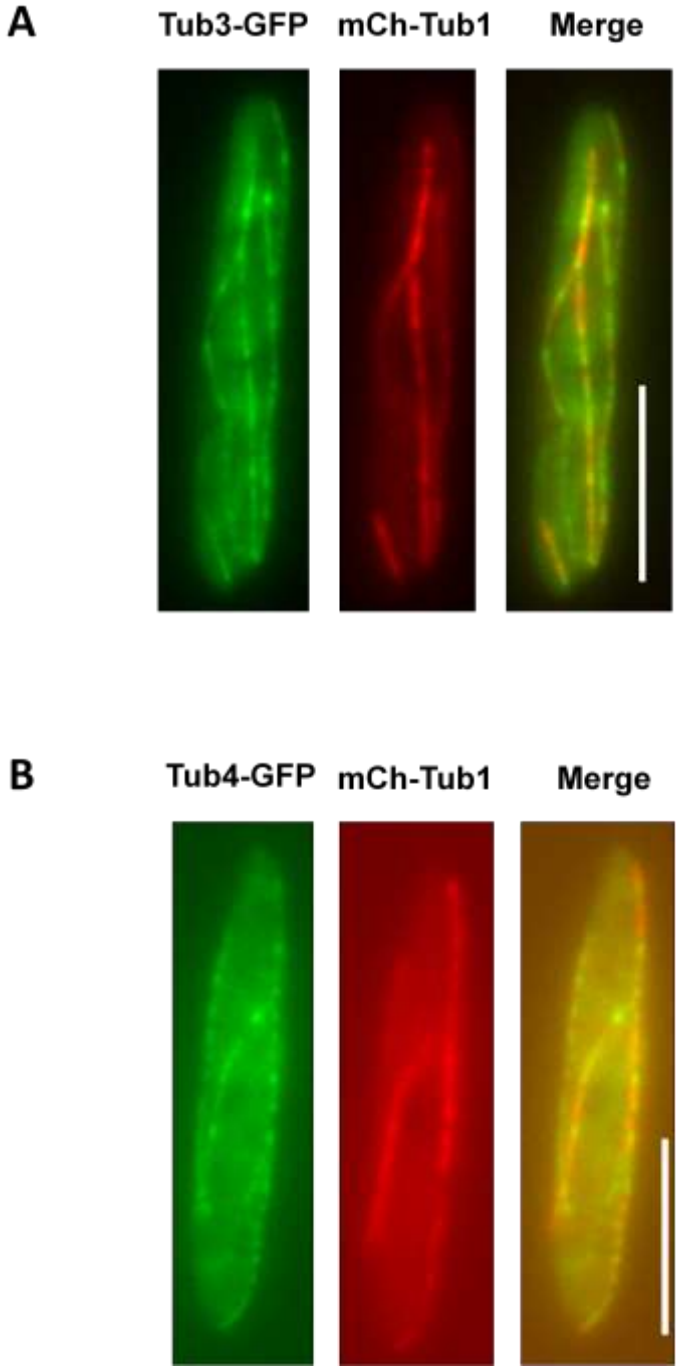

Figure 3.6 Visualisation of overexpressed beta tubulins in *Ustilago maydis.*

Both panels (A and B) show images depicting microtubules visualised in yeast-like cells.

(**A**) Left and right panels show fluorescence of the Tub3-GFP and mCherry-Tub1, respectively. The right panel shows the previous images merged together

where Tub3-GFP and mCherry-Tub1 microtubules co-localised completely. Scale bar represents 5 μm.

(**B**) Left and right panels show fluorescence of the Tub4-GFP and mCherry-Tub1, respectively. The right panel shows the previous images merged together where Tub4-GFP and mCherry-Tub1 microtubules co-localised completely. Scale bar represents 5 μm.

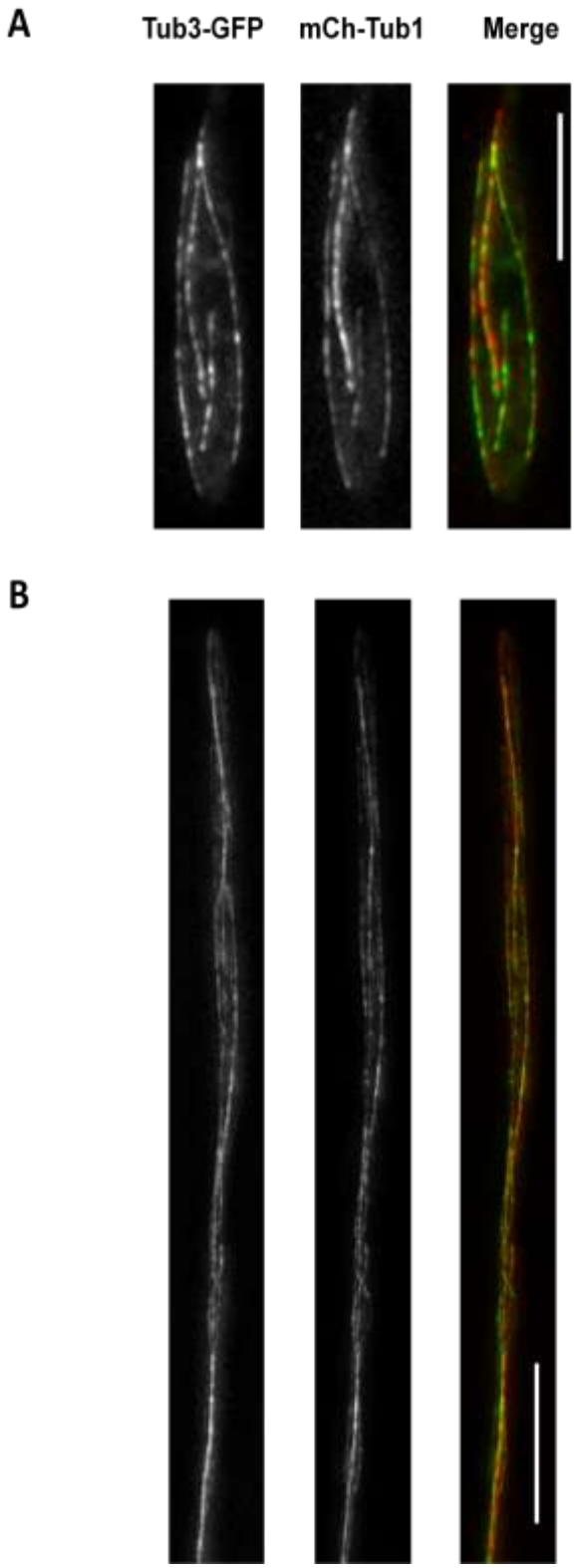

Figure 3.7 All microtubules with GFP-tagged beta tubulin Tub3 co-localised with mCherry-alpha tubulin microtubules.

(**A**) Images depicting microtubules visualised in the yeast like cell. Left and right panels show fluorescence of the Tub3-GFP and mCherry-Tub1, respectively. The right panel shows the previous images merged together where Tub3-GFP and mCherry-Tub1 microtubules co-localised completely. The images present maximum projection obtained from *z-axis* stack. Scale bar represents 5 μm.

(**B**) Images depicting microtubules visualised in a hyphal cell. Left and right panels show fluorescence of the Tub3-GFP and mCherry-Tub1, respectively. The right panel shows the previous images merged together where Tub3-GFP and mCherry-Tub1 microtubules co-localised completely. The images present maximum projection obtained from *z-axis* stack. Scale bar represents 10 μm.

3.3.6 Downregulation of beta tubulin genes causes microtubule organisation phenotypes in yeast-like cells and hyphae.

In order to check what effect a depletion of each beta tubulin would have on the microtubule behaviour, I prepared conditional mutants. Constructs were made, with each beta tubulin gene put under a strong inducible promoter (*crg* promoter, (Bottin et al., 1996)), which replaced the native one. To induce the *crg* promoter, media were supplied with arabinose as the only carbon source and to switch it off, media had to be changed into glucose-containing where the promoter was repressed. They were then transformed into the strain with GFP-alpha-tubulin and the microtubules examined using light microscopy. Conditional mutant strains were obtained for both beta tubulins and four of these were chosen for further work, two, where the native Tub3 promoter was replaced by the *crg* promoter and the other two with the *crg* promoter instead of the Tub4 promoter.

Yeast-like cells

Microscopic analysis revealed that in yeast-like cells there were no visible differences between WT and crg-beta-tubulin mutants or between *crg*-tub3 and crg-tub4, when the cultures had arabinose as a carbon source (Fig. 3.8, left column, panel A). When quantified, the results confirm no significant differences between the strains (panel B, Figure 3.8). However, when all cultures were shifted to the media containing glucose, a dramatic change in the microtubule array was visible, shown in the right column (Fig. 3.8, right column, panel A). Both *crg*-beta-tubulin mutants showed defective microtubules, which were fragmented in appearance (Fig. 3.8, yellow arrows), with a significant decrease in microtubule length compared to wild-type (Fig. 3.8 C). In addition, switching off promoters of beta tubulin conditional mutants showed that when tub3 promoter was off, tub4 alone was not able to maintain fully functional MT cytoskeleton.

Hyphal cells

Microscopic analysis of the same experiment, but carried out in hyphal cells revealed identical results in the cultures with arabinose, shown on the images in panel A, Figure 3.9. When quantified, the results confirm no significant differences between the strains (panel C, Figure 3.9). Similarly, when all

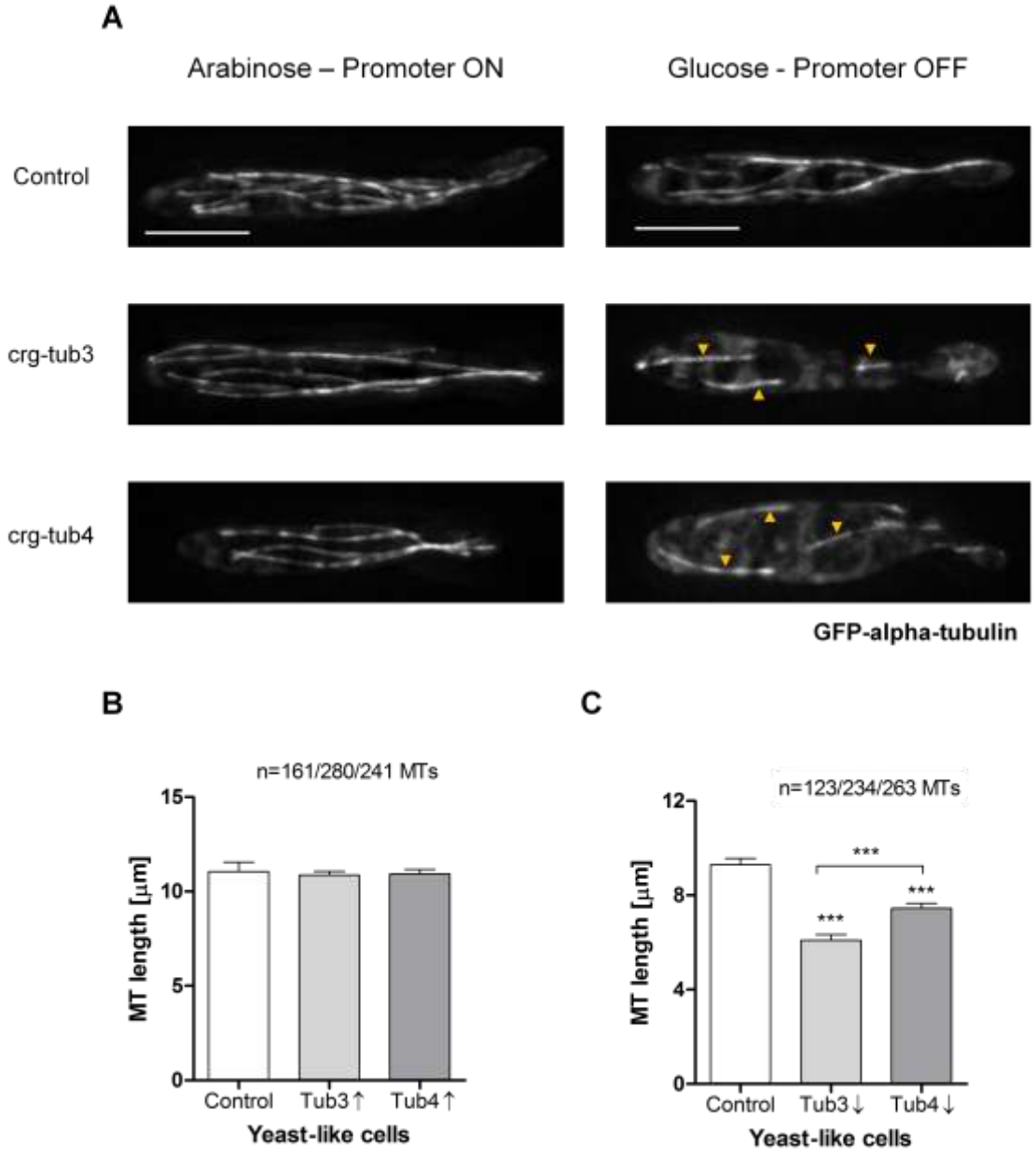

Figure 3.8 Switching off beta tubulin promoters causes phenotype in yeast-like cells of *U. maydis*

A. Images depicting fluorescently labelled GFP-alpha tubulin in yeast-like cells of *U. maydis*. The images in the left column show cells grown in a liquid culture with addition of arabinose. The images in the right column show cells grown in a liquid culture with addition of glucose. Yellow

arrows point to fragmented microtubules in the crg-mutants, when their promoters were switched off. Bars represent 5 µm.

B. Bar chart depicting microtubule length in *crg*-mutants grown in cultures with arabinose. The graph shows MT track length in the yeast-like cells of *U. maydis* when the beta tubulin promoters were on. All bars are given as mean±SEM, sample size *n* is indicated as total number of microtubules (taken from 30 cells) from three independent experiments.

C. Bar chart depicting microtubule length in *crg*-mutants grown in cultures with glucose. The graph shows MT track length in the yeast-like cells of *U. maydis* when the beta tubulin promoters were switched off. All bars are given as mean±SEM, sample size *n* is indicated as total number of microtubules (taken from 30 cells) from three independent experiments. Triple asterisk indicates statistically significant difference at $P<0.0001$, Mann-Whitney test.

All images present maximum projection obtained from *z-axis* stack.

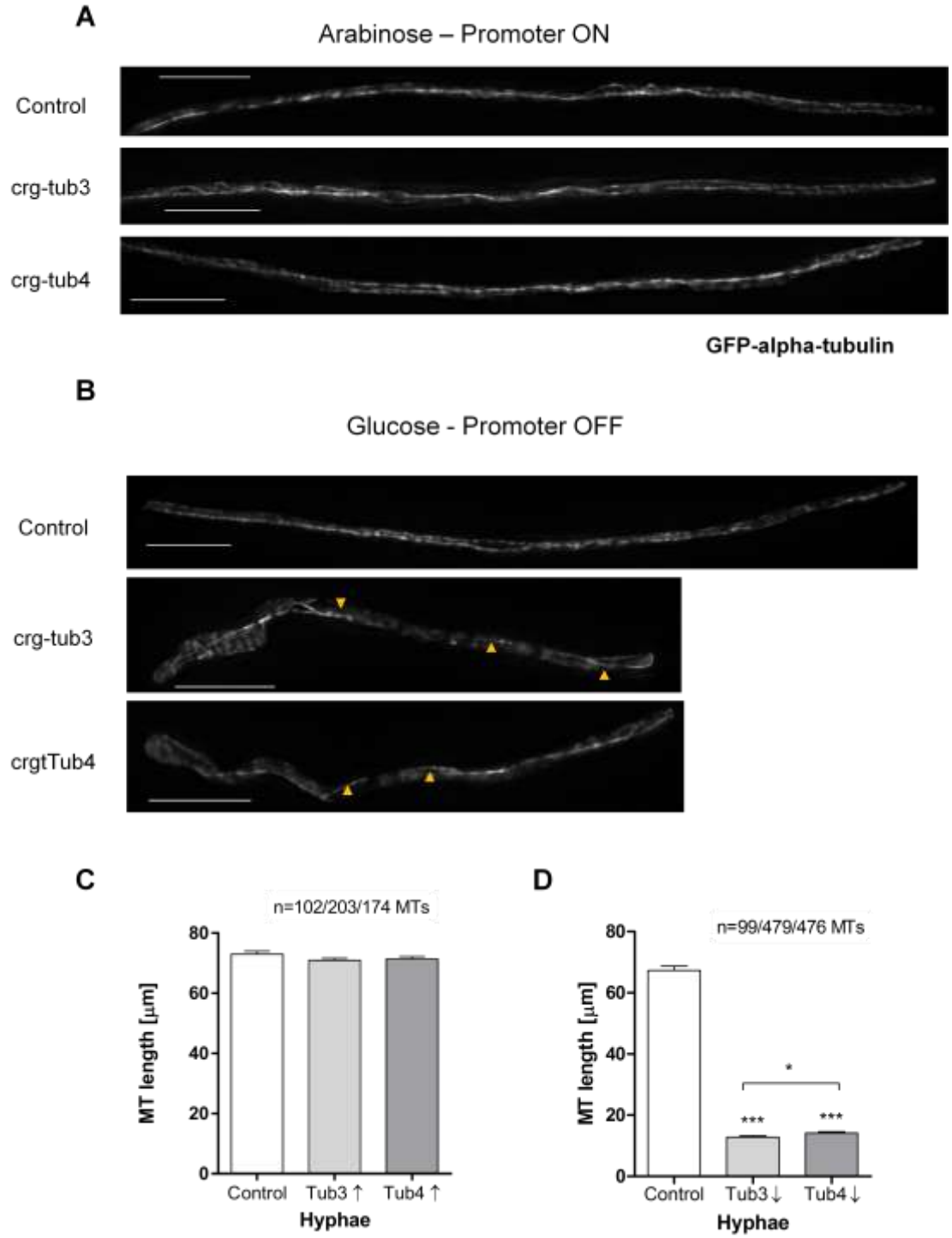

Figure 3.9 Switching off beta tubulin promoters causes phenotype in hyphal cells of *U. maydis*

A. Images depicting fluorescently labelled GFP-alpha tubulin in hyphal cells of *U. maydis*. The images show cells grown in a liquid culture with addition of arabinose. Bars represent 5 µm.

B. Images depicting fluorescently labelled GFP-alpha tubulin in hyphal cells of *U. maydis*. The images show cells grown in a liquid culture with addition of glucose. Yellow arrows point to fragmented microtubules in the *crg*-mutants, when their promoters were switched off. Bars represent 5 µm.

C. Bar chart depicting microtubule length in *crg*-mutants grown in cultures with arabinose. The graph shows MT track length in the hypha of *U. maydis* when the beta tubulin promoters were on. All bars are given as mean±SEM, sample size *n* is indicated as total number of microtubules (taken from 30 cells) from three independent experiments.

D. Bar chart depicting microtubule length in crg-mutants grown in cultures with glucose. The graph shows MT track length in the hypha of *U. maydis* when the beta tubulin promoters were switched off. All bars are given as mean±SEM, sample size *n* is indicated as total number of microtubules (taken from 30 cells) from three independent experiments. Triple asterisk indicates statistically significant difference at $P<0.0001$ to control, single asterisk indicates significant difference at $P=0.0086$ between two types of crg-beta tubulin mutants (standard t-test assuming Welch's correction).

The images present maximum projection obtained from *z-axis* stack.

cultures were shifted to the media containing glucose, a dramatic change in microtubule array and hyphae morphology occurred, as shown on panel B, Figure 3.9. Both *crg*-beta-tubulin mutants were not able to produce long filaments with long MTs and had fragmented microtubules (Fig. 3.9, yellow arrows), alongside significant drop in microtubule length, in comparison to WT (panel D, Figure 3.9). Beta tubulin conditional mutants also significantly differed from each other, with *crg*-tub3 mutants producing slightly shorter microtubules.

3.3.7 Endosome motility in the conditional β-tubulin mutants

Endosomes are small organelles, which move bi-directionally along microtubules via opposing molecular motors (Steinberg, 2007a). The endosome anterograde motility is mediated by the plus-end-directed kinesin-3 motor and retrograde endosome motility occurs via the to minus-end-directed dynein motor (Wedlich-Soldner et al., 2002). In order to examine if and how depletion of each beta tubulin influenced the velocity of the molecular motors on microtubules, we decided to assess early endosome motility using live cell imaging of mCherry-Rab5a-labelled early endosomes (EEs) in yeast-like cells (Fig. 3.10).

Kymograph analysis revealed that while EEs move bidirectionally in control cells (panel A, Figure 3.10) and in *crg*-β-tubulin mutants grown with arabinose (left column, panels B and C, Figure 3.10), there is hardly any directed motility of endosomes, when the beta tubulin promoters are switched off (right column, panels B and C, Figure 3.10). The yellow arrows point to vertical lines, which represent stationary endosomes. Both antero- and retrograde endosome motility was decreased in crg-mutants. The anterograde motility of EEs had decreased significantly in the *crg*-tub3 mutants, when tub3 promoter was depleted, in comparison to the WT and *crg*-tub4 cells, while it did not change in the *crg*-tub4 mutants (Figure 3.11). Retrograde motility of EEs was also significantly decreased in both beta tubulin mutants in comparison to the WT (Figure 3.11). In addition, in both beta tubulin mutants there were stationary endosomes present, which indicates that a number of motors were ’frozen’ on microtubules.

This work was undertaken with the help of Dr. Ewa Bielska who acquired movies, which were used for the analysis of the endosome motility in the

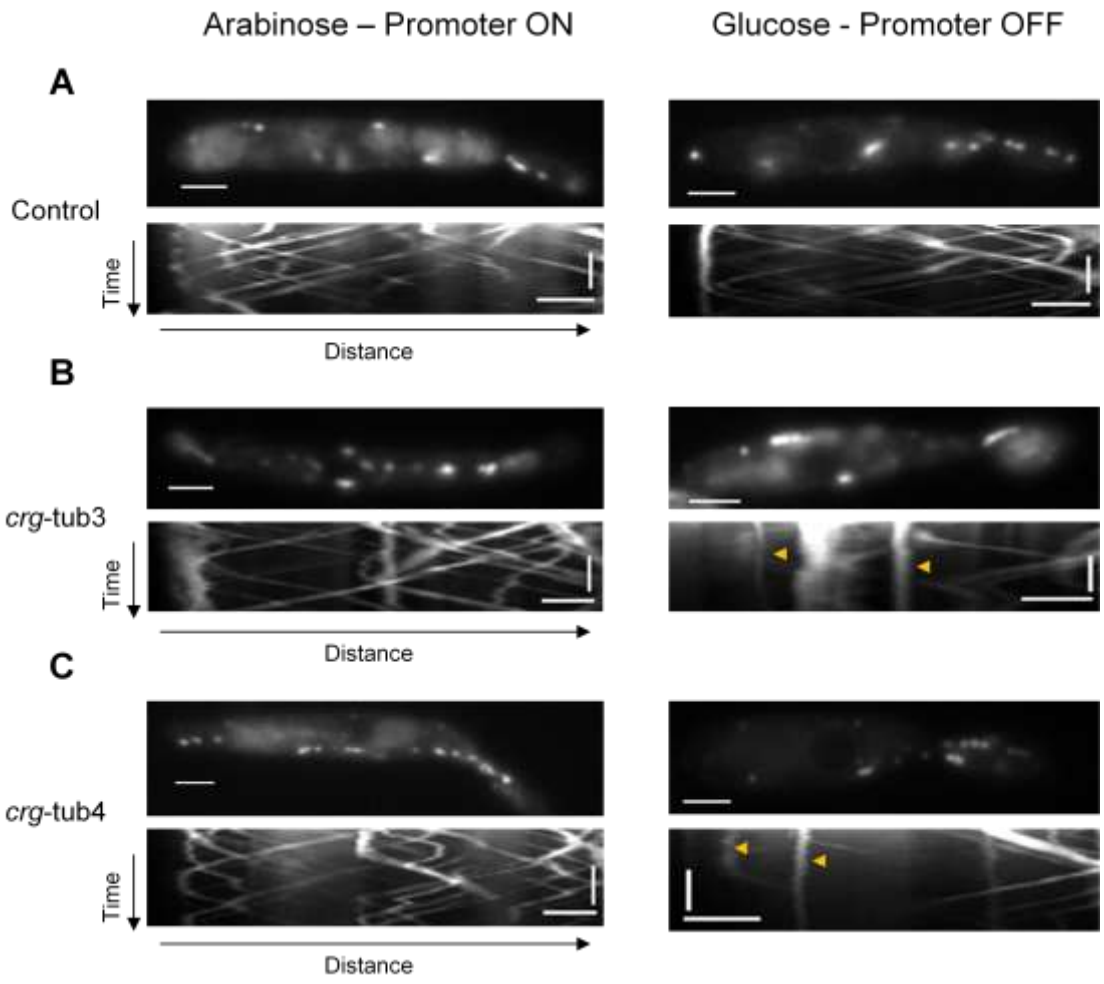

Figure 3.10 Endosome motility in conditional β-tubulin mutants is disrupted when beta tubulin promoters are turned down.

A. Images depicting fluorescently labelled mCherry-Rab5a labelled EEs in yeast-like cells of *U. maydis*. The images in the first row show cells of the control strain grown in a liquid culture with addition of arabinose (left column) or glucose (right column). The bars represent 5 µm. The images in the second row are kymographs showing motility of mCherry-Rab5a labelled EEs in the cells above. The bars on the kymograps represent seconds and micrometers.

B. Images depicting fluorescently labelled mCherry-Rab5a labelled EEs in yeast-like cells of *U. maydis*. The images in the first row show cells of the *crg*-Tub3 strain grown in a liquid culture with addition of arabinose (left

column) or glucose (right column). The bars represent 5 µm. The images in the second row are kymographs showing motility of mCherry-Rab5a labelled EEs in the cells above. Yellow arrows point to stationary endosomes in the ‘off’ conditions, which resulted in disruption of motors. The bars on the kymograps represent seconds and micrometers.

C. Images depicting fluorescently labelled mCherry-Rab5a labelled EEs in yeast-like cells of *U. maydis*. The images in the first row show cells of the *crg*-tub4 strain grown in a liquid culture with addition of arabinose (left column) or glucose (right column). The bars represent 5 µm. The images in the second row are kymographs showing motility of mCherry-Rab5a labelled EEs in the cells above. Yellow arrows point to stationary endosomes in the ‘off’ conditions, which resulted in disruption of motors. The bars on the kymograps represent seconds and micrometers.

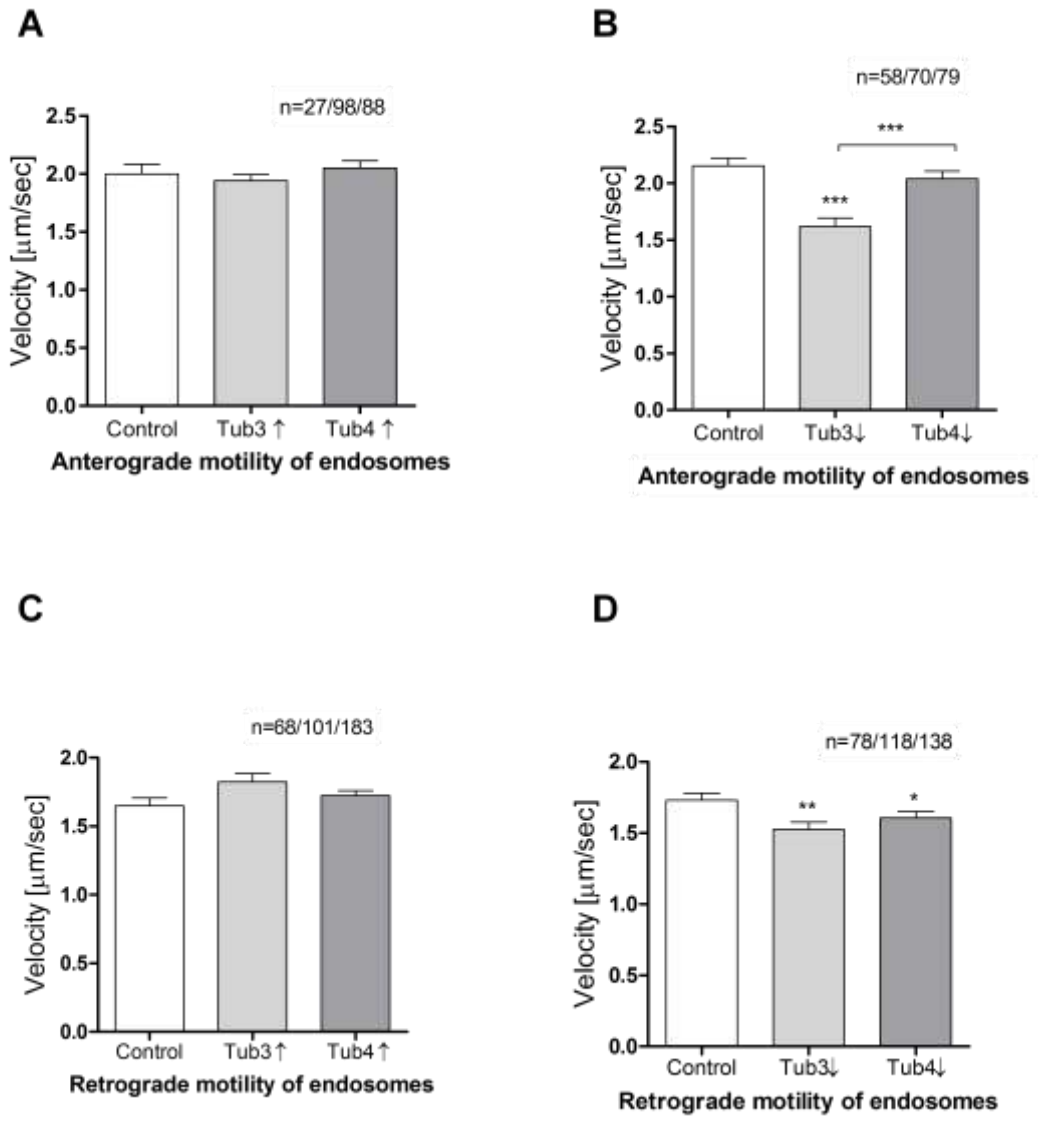

Figure 3.11 Switching off beta tubulin promoters causes phenotype in hyphal cells of *U. maydis*

A. Bar chart depicting anterograde motility of early endosomes in crg-mutants grown in cultures with arabinose. The graph shows velocity of EEs in the yeast-like cells of *U. maydis* when the beta tubulin promoters were on. All bars are given as mean±SEM, sample size *n* is indicated as total number of microtubules (taken from 30 cells) from two independent experiments.

B. Bar chart depicting anterograde motility of early endosomes in crg-mutants grown in cultures with glucose. The graph shows velocity of EEs in the yeast-like cells of *U. maydis* when the beta tubulin promoters were off. All bars are given as mean±SEM, sample size *n* is indicated as total number of microtubules (taken from 30 cells) from two independent experiments. Triple asterisk indicates statistically significant difference at P<0.0001 to control and between two types of *crg*-beta tubulin mutants (Mann-Whitney test).

C. Bar chart depicting retrograde motility of early endosomes in *crg*-mutants grown in cultures with arabinose. The graph shows velocity of EEs in the yeast-like cells of *U. maydis* when the beta tubulin promoters were on. All bars are given as mean±SEM, sample size *n* is indicated as total number of microtubules (taken from 30 cells) from two independent experiments.

D. Bar chart depicting retrograde motility of early endosomes in crg-mutants grown in cultures with glucose. The graph shows velocity of EEs in the yeast-like cells of *U. maydis* when the beta tubulin promoters were off. All bars are given as mean±SEM, sample size *n* is indicated as total number of microtubules (taken from 30 cells) from two independent experiments. Double asterisk indicates statistically significant difference at P=0.0047, single asterisk indicates statistically significant difference at P=0.03, (Mann-Whitney test).

conditional beta tubulin mutants and Dr. Catherine Collins who provided RNA samples for RT-PCR.

3.4 Discussion

The aim of the work in this chapter was to understand why there are two isotypes of beta tubulins in *U. maydis* and if they are is a functionally different. *U. maydis* beta tubulins have never been systematically investigated before, with regards to their functions.

Firstly, using bioinformatics methods I wanted to check for differences between *U. maydis* beta tubulins by looking at their protein sequences. Therefore, I checked a domain structure of beta tubulins, which revealed domains that are typically present in most tubulins. However, the amino acid alignment of beta tubulins showed that the main difference is in their C-terminal tails (CTTs). Basically, Tub3 has additional 24 amino acids in its CTT, which could be significant to its function, because there is a lot of evidence that the C-terminal tails of both α- and β-tubulin play critical roles in regulating MT assembly and function (Freedman et al., 2011).

I also discovered that *U.maydis* beta tubulins have very divergent structures with 61.7 % identity and 76.9 % similarity, which suggests their potential involvement in performing specific functions. However, they could still be interchangeable, based on the research in other fungi. For example, in *A. nidulans* which has two alpha tubulins, they can replace one another, but deletions of these two genes result in different phenotypes (Oakley, 2004). Two β-tubulin genes with different roles in hyphal growth and fungicide resistance also have been characterised in the wheat scab fungus *Fusarium graminearum* (Liu et al., 2013; Zhao et al., 2014). Based on that, perhaps promoter swapping experiments should be done on *U. maydis* beta tubulins as well as CTTs swapping to check if they are still functional. As well as that a real-time PCR should be performed in yeast-like and hyphal cells of *U. maydis* to see if there are differences in expression patterns of both beta tubulins.

In addition, analysis of the phylogenetic tress confirmed that *U. maydis* beta tubulins belong to that particular group of tubulins and they also belong to separate clades. According to a recent study of molecular evolution and functional divergence of tubulins, beta tubulins underwent complex gene

duplication and gene loss events in different fungal lineages and the two beta tubulin genes of basidiomycetes formed two distinct clades named β_1- (*U. maydis* tub4) and β_2-tubulins (*U. maydis* tub3) (Zhao et al., 2014).

Secondly, I applied experimental methods to find out if both beta tubulins are present in different morphological forms of *U. maydis* and then carried out experiments *in vivo.* The results of the reverse-transcriptase PCR showed, that both of beta tubulins are expressed in the yeast-like and hyphal cells, therefore they are most probably not specific to either of those cells. However, this method does not show the quantitative expression level of beta tubulins and that is why it would be beneficial to perform a real-time PCR in both morphological forms. The expression patterns of both beta-tubulins could show if different kinds of cells have preference towards a particular beta-tubulin. This could help in revealing specific functions of beta tubulins. For example, a high expression pattern of one beta tubulin in hypha might indicate its role in a long-distance transport or significance of plant pathogenicity. Human cells are known to have 21 β-tubulins (Dutcher, 2003) and it was shown that each tissue has a complex pattern of tubulins, and tumoral tissues exhibited altered expression in specific tumour types (Leandro-Garcia et al., 2010).

Interestingly, the two beta tubulins are not next to each other in the *U. maydis* genome, but on two different chromosomes. This probably indicates that they are not products of recent gene duplication, but they evolved to facilitate different functions. A molecular evolutionary study in fungi indicated that alpha tubulins and β_2-tubulins (*U. maydis* Tub3) have been under strong divergent selection and adaptive positive selection, where many positively selected sites are at or adjacent to important functional sites and likely contribute to functional diversification (Zhao et al., 2014).

Next, I attempted to visualise both beta tubulins in *U. maydis*. Initially, I used the available plasmids, where each beta tubulin was under a constitutive promoter and was tagged with GFP, for ectopic integration in a strain with mCherry-tagged alpha tubulin (tub1). The results showed that both GFP-tagged beta tubulins colocalised with mCherry-alpha tubulin microtubules. This was the case for yeast-like and hyphal cells and the GFP signal was quite poor, which can

happen when the proteins are overexpressed, like in this case. Then, I decided to tag each beta tubulin *in locus* under a native promoter to visualise beta tubulins and compare their colocalisation again with mCherry-alpha tubulin tagged microtubules. However, due to unknown circumstances, I was only able to achieve visualisation for tub3, and not tub4 gene. Therefore, Tub3-GFP tagged microtubules colocalised with mCherry-Tub1 in both yeast-like and hyphal cells, and also the GFP signal improved, in comparison to overexpressed beta tubulins. The next challenge here is to visualise Tub4 and check if it colocalises with mCherry-alpha tubulin tagged microtubules.

Moreover, in order to find out if depletion of beta tubulin would cause a phenotype in *Ustilago* cells, I prepared conditional beta tubulin mutants. In each type of mutant one of beta tubulin genes was controlled by an inducible promoter, *crg*, which replaced the native one. When the mutants were cultivated in the media supplied with arabinose, beta tubulins promoters were switched on, but when shifted to the media with arabinose, the promoters were switched off. To observe the microtubules during after depletion of promoters, a strain with GFP-alpha-tubulin tagged microtubules was used. The results indicated that a depletion of each beta tubulin caused a visible phenotype in yeast-like and hyphal cells. In both cases, the microtubules were appeared to be short and in fragments, in addition the hyphal cells were short and wavy in appearance. This data was quantified, which revealed that in *crg*-beta tubulin mutants microtubules were significantly shorter in both morphological forms, in comparison to WT. Beta tubulin mutants were also significantly different from each other, with tub3 mutants always having shorter microtubules. This indicates that *Ustilago* was more sensitive to beta tubulin-tub3 depletion than tub4's, even though in both cases specific phenotypes appeared. When I performed a northern blot on both types of *crg*-beta tubulin mutants, as an additional control, the results showed no detectable mRNA, in yeast-like or hyphae cells, when the *crg*-tub3 mutants were grown with added glucose, however in case of *crg*-tub4 mutants the mRNA was still detected after the promoter was switched off in yeast and hyphae. This might explain the differences between the mutants and the reason for that could be, because *crg* promoter sometimes does not get completely switched off, which probably happened in this case. The next thing to do would be to delete beta tubulins

separately and check *U. maydis* growth rate, mitosis and ability to produce long hyphae. It would also be interesting to see the effects of the deletions for the plant pathogenicity, which could be achieved by infecting plants with deletion strains and observing *Ustilago's* ability to infect them. The reason it has not been done previously is because it takes much less time to produce the *crg*-mutants than to delete beta tubulin genes. However, to achieve that especially designed plasmids, where resistance cassette could replace the ORF of the gene, would have to be introduced into *U. maydis* strain, which could be difficult, because both genes seem to be essential. Therefore getting positive transformants could be time consuming or not possible.

Furthermore, in order to check if depletion of either of *U. maydis* beta tubulins caused disturbance of molecular motors, kinesin-3 and dynein, I looked at the endosome motility in the conditional β-tubulin mutants. For this purpose, mCherry-Rab5a plasmid was transformed into those mutants to label the early endosomes (EEs). Initially, I expected the EE motility to be disturbed, because of the shorter MTs when the beta tubulin promoters were off, however I did not know if or how the motors would be affected. As a result, the EE motility recorded on the kymographs changed dramatically whilst the cells of both *crg*-tubulin mutants were cultivated in the media supplied with glucose. I discovered that both antero- and retrograde endosome velocity was significantly decreased in *crg*-tub3-mutants, but for *crg*-tub4-mutants only retrograde velocity was significantly depleted. This indicates that in *crg*-tub3 cells, kinesin-3 responsible for the plus-end movement on microtubules was affected. Perhaps *U. maydis* kinesin-3 has a preference for microtubules built with beta tubulin-Tub3. In addition, the fact that the velocity of EEs in both types of mutants was decreased could mean that dynein needs the right balance of microtubules built with different β-tubulins to move efficiently. The combined results featuring every mutant in 'on' and 'off' conditions clearly show, that *crg*-tub3 was much more sensitive to their promoter being switched off than *crg*-tub4, most probably due to tub4's promoter not shutting down completely. These experiments were only done in the yeast-like cells, because mCherry-Rab5 signal faded too quickly to enable proper EE observations and quantitative studies.

In addition, it has been demonstrated that apparently small overall differences in the structures and therefore binding energies and chemical affinities between different tubulins may translate into significant deviations in the growth and catastrophe rates for MTs (Tuszynski et al., 2006). This, together with the fact that both alpha and beta tubulins undergo a variety of posttranslational covalent modifications (PTMs) (Luduena, 1998) and several, such as polyglutamylation, polyglycylation, detyrosination, and deglutamylation, happening at the C-terminal tails (Janke, 2014) means that CTTs are crucial to our understanding of the beta tubulin gene functions. The large C-terminal extension on Tub3 probably corresponds to a higher number of potential PTM recognition sites as well as potential MAP sites, than in the shorter CTT of Tub4. This indicates that the *U. maydis* beta tubulin isoforms undergo different PTMs and their CTTs attract different MAPs. Perhaps, because the microtubules with the beta tubulin Tub3 isotype could be subjected to a higher number of modifications on their CTTs they have some very specific, yet unknown functions in the cells.

Finally, to answer the question why does *U. maydis* need two beta tubulins, much more work needs to be done. I believe that they probably interchangeable, based on the research in other fungi, however there seem to be subtle differences between them and the challenge remains to find them.

Chapter 4 – Investigating MAPs in *Ustilago maydis* using bioinformatics tools

4.1 Introduction

In most cells, microtubules are responsible for intracellular transport, organelle positioning, cell shape and motility, as well as for mitosis (Janke and Bulinski, 2011). Defects in some microtubule functions, for example microtubule-based transport, are pervasive in neurodegenerative and neurodevelopmental disorders (Hirokawa et al., 2010) (Egan et al., 2012) and therefore precise regulation of the cytoskeleton is required from the establishment of the plane of cell division to changes in cell shape, migration and polarity (Salinas, 2007).

Microtubules are also characterised by their rapid turnover and potential for reorganisation, with half-lives usually, no longer than a few minutes (Mandelkow and Mandelkow, 1995). This dynamic instability of microtubules is critical for the remodelling of the cytoskeleton that occurs during mitosis and can be modified by microtubule-associated proteins (MAPs). MAPs can be classified into three main groups: (1) motor proteins that are involved in microtubule sliding and are critical for vesicle and organelle transport along microtubules (2) enzymes such as kinases and GTPases that control the affinity of other MAPs for microtubule binding, and (3) structural proteins that form the most diverse group and act in microtubule nucleation, severing, stabilisation or plus-end binding (Figure 4.1). Together, MAPs regulate the dynamic instability of microtubules and provide an important mechanism for determining cell shape and polarity (Cooper, 2000a). Thus, regulation of microtubule dynamics is essential for proper cell function and viability, and microtubule-associated proteins (MAPs) are critical regulators of these dynamic processes. (Kiris et al., 2010).

The first MAP to be identified was dynein (Gibbons, 1965). It was found to be an ATP-dependent protein that could be selectively released and rebound to and discovered to be highly

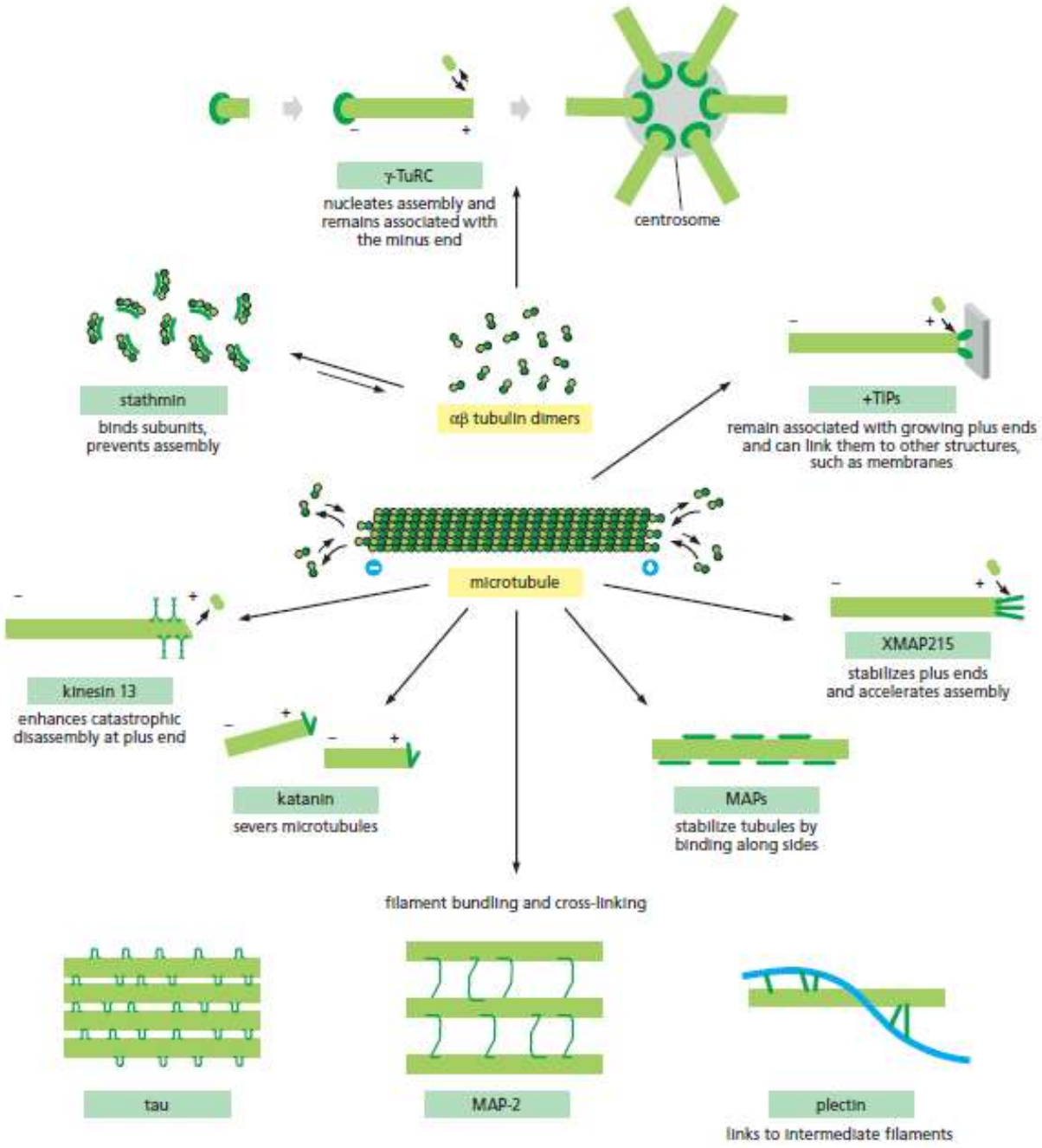

Figure 4.1 Microtubule-associated proteins and their functions

MAPs carry out numerous functions during all stages of the cell cycle. Image taken from (Alberts et al., 2008).

axonemes from *Tetrahymena* and was required for ciliary beating (Gibbons, 1963; Gibbons and Rowe, 1965). Around this time tubulin was first identified enriched in brain (Borisy and Taylor, 1967) (Weisenberg et al., 1968). This tubulin could be purified and microtubules reconstituted *in vitro* (Weisenberg et al., 1968), enabling the development of assays to characterise proteins that associated with brain microtubules (Borisy et al., 1975; Keates and Hall, 1975; Murphy and Borisy, 1975). Microtubule protein from porcine brain was separated into two fractions, containing high molecular weight component (HMW) and tubulin, which made it possible to determine the stimulating effect of HMW (an early name for a MAP) on microtubule assembly. These high molecular weight MAPs could promote tubulin assembly into microtubules and co-sedimented with microtubules with high affinity, an association that was lost when microtubules were depolymerised (Borisy et al., 1975; Keates and Hall, 1975).

A further study from the same year by Sloboda and co-workers identified two HMW proteins, named *MAP1* and *MAP2*, that co-purified with tubulin in an experiment of repeated cycles of MT assembly and disassembly, and promoted the assembly of microtubules at much lower concentrations than tubulin did alone (Olmsted, 1986; Sloboda et al., 1975). A third novel microtubule-associated protein, tau, was identified in the same way as *MAP1* and *MAP2*, when it appeared present in association with tubulin after it was purified from porcine brain by repeated cycles of polymerisation. Tau was one of the first examples of a protein proven to be essential for the assembly of microtubules in vitro (Weingarten et al., 1975). Subsequently, it was proposed that MAPs are defined as proteins that bind MTs *in vivo* (Solomon et al., 1979) (Maiato et al., 2004). Later studies showed that by adding MAPs purified from brain tissue to microtubules *in vitro*, catastrophe events could be decreased and microtubule rescue increased, suggesting the importance of MAPs for regulation of microtubule dynamic instability (Murphy et al., 1977; Pryer et al., 1992). Subsequent MAP studies were carried out on other tubulin-rich organs including liver (Collins and Vallee, 1989), and testes (Collins and Vallee, 1989), and it is now recognised that MAPs are critical for microtubule regulation in all tissues and organisms.

Discovery of the MAPs has profoundly helped in our understanding of the biology of the cell as well as some neurodegenerative disorders. As MAPs were first found in brain, they have been intensely studied there, and much is known about the role of brain MAPs in normal vertebrate development, and also in disease. For example, multiple mutations in *MAPT*, the *tau* encoding gene, can lead to a frontotemporal dementia and Parkinsonism linked to chromosome 17 (FTPP-17), also known as Pick's disease (Hutton et al., 1998), providing evidence of the role of *tau* abnormalities in the onset and progression of neurodegenerative disease (Forman et al., 2004). A second example is spastin, identified as one of the most commonly mutated genes in hereditary spastic paraplegia (Hazan et al., 1999), a human neurodegenerative disease characterised by lower extremity weakness due to axonopathy (Roll-Mecak and McNally, 2010).

MAPs have been extensively studied in many different model organisms, including budding and fission yeast, fruit fly, humans and arabidopsis, and have been found to carry out various functions (Alberts et al., 2008) (Fig.4.1). Although organism to organism variation and poor sequence conservation of some MAPs makes it difficult to identify exactly how many MAPs there are, a simple search of the online gene ontology database AmiGO (Carbon et al., 2009) for genes or their products using term 'microtubules' gives 757 records. However, it is clear that there are many more MAPs in multicellular organisms than in other organisms, with both plants and animals possessing many MAP splice variants (Gardiner, 2013). In addition, it seems that, generally, most of the known MAPs have been found to differ depending on the type of cell or tissue (Mandelkow and Mandelkow, 1995), which might indicate that there are still many unknown MAPs. For example, *MAP1* and *MAP2*, which are selectively associated with neurons and concentrated in dendrites, have relative concentrations that vary in different classes of cerebellar neurons and within different parts of the same neuron (Huber and Matus, 1984). This has huge implications for microtubules, which despite their high level of conservation, adapt to a large variety of cellular functions due to functional modification by a large panel of microtubule-associated proteins, as well as by posttranslational modifications that directly modify the microtubules (Janke, 2014).

MAPs can be divided into motor- and non-motor microtubule associated proteins (Fig. 4.1). The major families of microtubule motors are kinesins and dyneins which, besides their transport functions, can generate forces for the self-organisation of microtubule arrays, such as the mitotic spindle (Surrey et al., 2001) (Janke and Bulinski, 2011). In addition, some kinesin motors have the ability to catalyse the depolymerisation of microtubules (Howard and Hyman, 2007). The main function of the non-motor MAPs, however, is to regulate microtubule dynamics. Among them, there are proteins that stabilise microtubules (for example, the neuronal proteins tau, MAP1 and MAP2), but also severing proteins, such as spastin and katanin, which disassemble stable microtubules (Hartman and Vale, 1999). Another group of important MAPs, the plus-end tracking proteins (+TIPs), dynamically track the growing plus-ends of microtubules (Akhmanova and Steinmetz, 2010) (Schuyler and Pellman, 2001) (de Forges et al., 2012). A number of +TIPs families have been identified and these are evolutionarily conserved from yeast to humans (Blake-Hodek et al., 2010). Apart from taking part in the regulation of microtubule dynamics, they also participate in the interactions of microtubules with the chromosomes during mitosis and with the cellular cortex both in interphase and mitosis (de Forges et al., 2012) and have the ability to physically associate with a number of other +TIPs, creating a complex web of interactions (Akhmanova and Hoogenraad, 2005); (Akhmanova and Steinmetz, 2008) (Blake-Hodek et al., 2010).

Additionally, in order to carry out their functions on microtubules MAPs use a range of microtubule-binding motifs and microtubule-binding sites (Gardiner, 2013), such as SxIP microtubule-binding motif present in a number of plus-end tracking proteins (+TIPs), which acts as a general microtubule tip localisation signal (MtLS) that targets structurally and functionally diverse +TIPs to microtubule ends by binding to EBs (end-binding proteins) (Honnappa et al., 2009). Another example is the HEAT motifs (Huntington/Elongation factor 3/protein phosphatase 2A/TOR1 repeats) in proteins of XMAP215 family, which typically form protein protein interaction surfaces (Groves et al., 1999).

Although there have been many reports about MAPs in fungi, mainly in yeast, MAPs have never been systematically investigated in the filamentous fungus *Ustilago maydis*. This could be due to the fact that MAPs have been most

extensively studied the yeast model systems. Our knowledge about MAPs in *U. maydis* has been well summarised in a study by F. Banuett and co-workers (Banuett et al., 2008). They studied S*. cerevisiae* and *S. pombe* genes known to play a role in cell polarity and morphogenesis, and in the cytoskeleton as probes to survey the *U. maydis* genome and found that most of the yeast machinery is conserved in *U. maydis*, which included +TIPs and molecular motors dynein, kinesin and myosin. Given the importance of microtubule-based cellular processes in *Ustilago*, there must be many more MAPs in this organism that have not yet been identified. The availability of complete genome sequences for increasing numbers of eukaryotes of medical, economic or research importance makes it possible to identify likely orthologues of known proteins in an otherwise uncharacterised organism, without the need for time-consuming biochemical and genetic studies. The recent release of the genome sequence for *Ustilago maydis* (Kamper et al., 2006) is an invaluable resource for research on this organism, and it is interesting to see which microtubule related proteins are conserved across the fungi, as well as the unique or expanded mechanisms that are required for organism-specific biological functions. Sequence analysis using methods such as BLASTP (Altschul et al., 1990), PSI-BLAST (Altschul et al., 1997) and Hidden Markov models (Sonnhammer et al., 1998) can be used to identify putative orthologues of genes found in known cellular systems, and proteins containing known domains or active sites can be found using a variety of online search programmes such as PFAM (Finn et al., 2006) and InterProScan (Zdobnov and Apweiler, 2001). Such studies in *Ustilago* have been used to generate datasets of proteins involved in cell wall biogenesis (Ruiz-Herrera et al., 2008), cell morphogenesis and the machinery for cell polarity (Banuett et al., 2008) or meiosis (Donaldson and Saville, 2008).

Here, I set out to investigate the MAP repertoire of *Ustilago maydis* using bioinformatics methods. Given the divergent nature of some MAPs, sensitive search methods are required to identify possible orthologues. To maximise the chances of finding orthologues in *Ustilago*, this chapter uses MAP sequences from 5 well-studied eukaryotic organisms, *H. sapiens*, *D. melanogaster*, *A. nidulans*, *S. cerevisiae* and *S. pombe* as a starting point because they are well-studied in the context of microtubule biology and therefore have an extensively

characterised MAP repertoire. This analysis has revealed that there are 66 potential orthologues in *Ustilago* carrying various microtubule-related functions in different stages of the cell cycle.

4.2 Materials and Methods

4.2.1 General and specific MAP database searches

Initially, in order to find MAPs in *Ustilago maydis*, I performed searches using AmiGO database (Carbon et al., 2009) for potential microtubule-associated proteins present in *H. sapiens*, *D. melanogaster*, *A. nidulans*, *S. cerevisiae* and *S. pombe*. As well as that additional literature and searches in the databases of *H. sapiens* (Geer et al., 2010), *D. melanogaster* (St Pierre et al., 2014), *A. nidulans* (Cerqueira et al., 2014), *S. cerevisiae* (Cherry et al., 2012) and *S. pombe* (Wood et al., 2012) were used to identify MAPs. All MAP sequences found were classified according to their function and a non-redundant list of 169 proteins was made. In total 20 functional groups were differentiated with many proteins present in more than one group.

4.2.2 BLASTp, PSI-BLAST and HMM

All initially selected MAPs found in *H. sapiens*, *D. melanogaster*, *A. nidulans, S. cerevisiae* and *S. pombe* were used to query the proteome of *U. maydis* using BLASTp search (Altschul et al., 1990). Any resultant hits in *U. maydis* with an e-value below $1e^{-05}$ were then confirmed using reciprocal BLASTp. It was performed by querying the specific proteome, which generated *U. maydis* result, with the *Ustilago* sequence and considered to be a good candidate for a putative orthologue if the original sequence was returned. *U. maydis* sequences were obtained from MIPS *U. maydis* database (http://mips.helmholtz-muenchen.de/genre/proj/ustilago/).

BLASTp and reciprocal BLASTp searches (Altschul et al., 1990) were carried out using the NCBI stand-alone BLAST+ application version 2.2.28+ (Camacho et al., 2008) against BLAST-formatted proteomes.

Iterative searches were carried out using both Position-Specific Iterated (PSI)-BLAST (Altschul et al., 1997) and hidden Markov models (Finn et al., 2011). For this purpose, protein sequences annotated as homologues of specific MAPs were aligned with MAFFT (Katoh et al., 2009; Katoh and Frith, 2012; Katoh et

al., 2005; Katoh et al., 2002; Katoh and Standley, 2013; Katoh and Toh, 2007, 2008a, b, 2010) and columns containing more than 50 % gaps were removed to prevent species- or clade-specific insertions biasing the results.

PSI-BLAST searches were carried out against the full NCBI non-redundant protein database using an e-value threshold of $1e^{-05}$.

For iterative HMM searches, the alignments created with MAFFT were then used to generate a hidden Markov model using Hmmer (Sonnhammer et al., 1998). This model was used to search the NCBI non-redundant protein database. This alignment was used to generate a new model and a further round of searches was carried out. Searching was terminated when no further hits below an e-value of $1e^{-05}$ could be identified.

To find if a chosen MAP was present in other species than the initial one and *U. maydis*, BLASTp searches were conducted and the sequences with the highest e-values were considered as possible orthologues.

4.2.3 The analysis of MAPs

A number of freely available programs were used to analyse MAPs for motifs, domains or similarities to known proteins, including InterPro (Hunter et al., 2012) which searches a range of databases including PROSITE (Hulo et al., 2007) and Pfam (Finn et al., 2006), and COILS (Lupas et al., 1991) which predicts if a protein sequence contains a coiled-coil region. Due to the fact that InterPro results are produced using different databases and cannot be meaningfully compared or combined, their e-values are not given (Hunter et al., 2012). Based on domain architecture results MAPs provided by InterPro and COILS programmes, cartoons were created using DOG software **(**Domain Graph**,** version 2.0; (Ren et al., 2009b).

A MAP was regarded as a probable *Ustilago maydis* orthologue if at least one search result came back positive (with e-value below $1e^{-05}$) and domain architecture was very similar – two proteins would be considered as orthologues if most of their domains were the same. However, if no domains or motifs were

detected, alignments using an online tool T-Coffee (Goujon et al., 2010; McWilliam et al., 2013; Notredame et al., 2000) would be generated and the outcome would be judged by looking at the level of conservation of different amino-acids.

4.3 Results and Discussion

4.3.1 Compilation of a non-redundant list of known MAPs from model eukaryotes

As a first step to identify microtubule associated proteins (MAPs) in *U. maydis*, I analysed known MAPs from a range of organisms, including *H. sapiens. D. melanogaster, A. nidulans*, *S. pombe* and *S. cerevisiae,* based on published functions and AmiGO (Carbon et al., 2009) database annotations. A MAP was defined as any protein that has the ability to bind the microtubules and modify their behaviour, in accordance with the definition of (Mandelkow and Mandelkow, 1995). A non-redundant list was compiled and orthologues were removed. This gave a final list of 169 unique MAPs. These included MAPs involved in processes such as: mitotic spindle organisation, MT polymerisation and depolymerisation, MT dynamics, cell polarity, MT bundling, MT stabilisation, MT severing, formation of spindle pole bodies, tracking the plus ends of microtubules (+TIPS) or MT organisation in general. For most microtubule functions, multiple MAPs were identified.

Each MAP was analysed using pattern and profile searches to identify domain architecture (App.1). This revealed that many of the MAPs contain well-characterised PFAM domains, with CAP-Gly domains, P-loops, motor domains and calponin homology domains particularly common. Cap-Gly domains are utilised by +TIPs to target end-binding proteins at growing MT ends (Bjelic et al., 2012), P-loops are binding sites commonly present in motor proteins (Kull et al., 1998), motor domains have binding sites for both ATP and microtubules; they also generate the force for motor motility (Ruppel and Spudich, 1996). Calponin homology domains (CH) are necessary and sufficient for microtubule tip binding (Sen et al 2013). Among commonly found motifs were also coiled-coils, which often mediate protein-protein interactions (Wang et al., 2012), present in 80 % of the researched MAPs. Coiled-coils are known to interfere with simple BLAST searches (Wootton and Federhen, 1996), indicating that more sophisticated methods would likely be required to maximise identification of *Ustilago* orthologues.

4.3.2 Out of 169 MAPs 66 are conserved in *U. maydis*

Reciprocal BLASTp was used to determine conservation of the complement of the 169 known MAPs in *Ustilago*. After the first BLASTp searches were conducted, all results (hits) were subjected to reciprocal BLASTp, in order to further validate the initial search. Those that returned the starting sequence were considered as possible orthologues. 80 out of 169 proteins fulfilled the search criteria. Among the 169 MAPs examined, 8 % were present only in fungi, 3 % were found in some filamentous fungi and metazoans, 43 % were metazoan only and 4 6% of MAPs were present in all tested species. Thus, slightly less than a half of these proteins were conserved across the variety of species, while the rest were specific to certain groups of organisms, highlighting both the commonality of MAPs across eukaryotes and the organism-specific diversity of the MAP repertoire. In particular, the majority of the analysed MAPs were present only in the metazoans, represented here by *H. sapiens* and *D. melanogaster*, which presumably reflects an elaboration of the microtubule cytoskeleton in multicellular organisms.

To verify these results and minimise the risk of over/under representation of the data due to the extensive coiled-coil domains, additional, more sensitive, search methods were conducted (PSI-BLAST (Fig. 4.2) and HMM (Fig. 4.2)). These methods are more sensitive than BLASTp, because they are based on the alignments of known sequences, rather than comparison of the single amino acids. To be able to carry out PSI-BLAST and HMMs, for each MAP, known protein sequences found on NCBI website were aligned and gaps removed. The results of the extended searches validated many of the BLASTp results, but also identified an additional 21 potential orthologues (denoted as black dots in Fig. 4.2), out of which 3 were later established as correct on manual curation of the sequence data (Dam1, Spc105 and Num1). MAPs with hits above the cut-off value of e^{-5} were marked as white dots in Figure 4.2. The searches were successful as they revealed some additional potential orthologues in *Ustilago,* but also showed that in some cases the initial BLASTp search was not accurate, because PSI-BLAST and HMM denied some results.

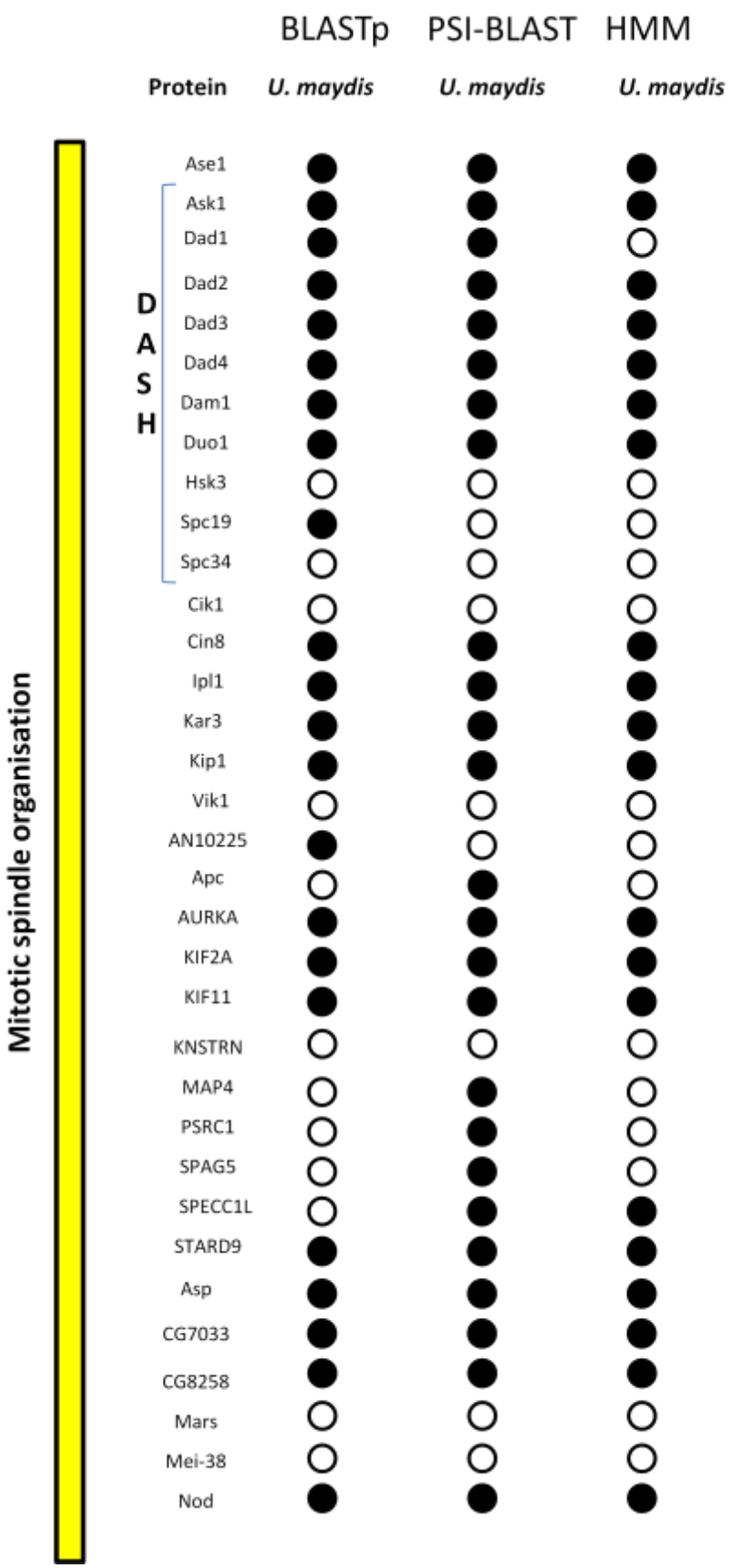
BLASTp
PSI-BLAST
HMM
Protein
U. maydis
U. maydis
U. maydis
Mitotic spindle organisation
DASH
Ase1
Ask1
Dad1
Dad2
Dad3
Dad4
Dam1
Duo1
Hsk3
Spc19
Spc34
Cik1
Cin8
Ipl1
Kar3
Kip1
Vik1
AN10225
Apc
AURKA
KIF2A
KIF11
KNSTRN
MAP4
PSRC1
SPAG5
SPECC1L
STARD9
Asp
CG7033
CG8258
Mars
Mei-38
Nod

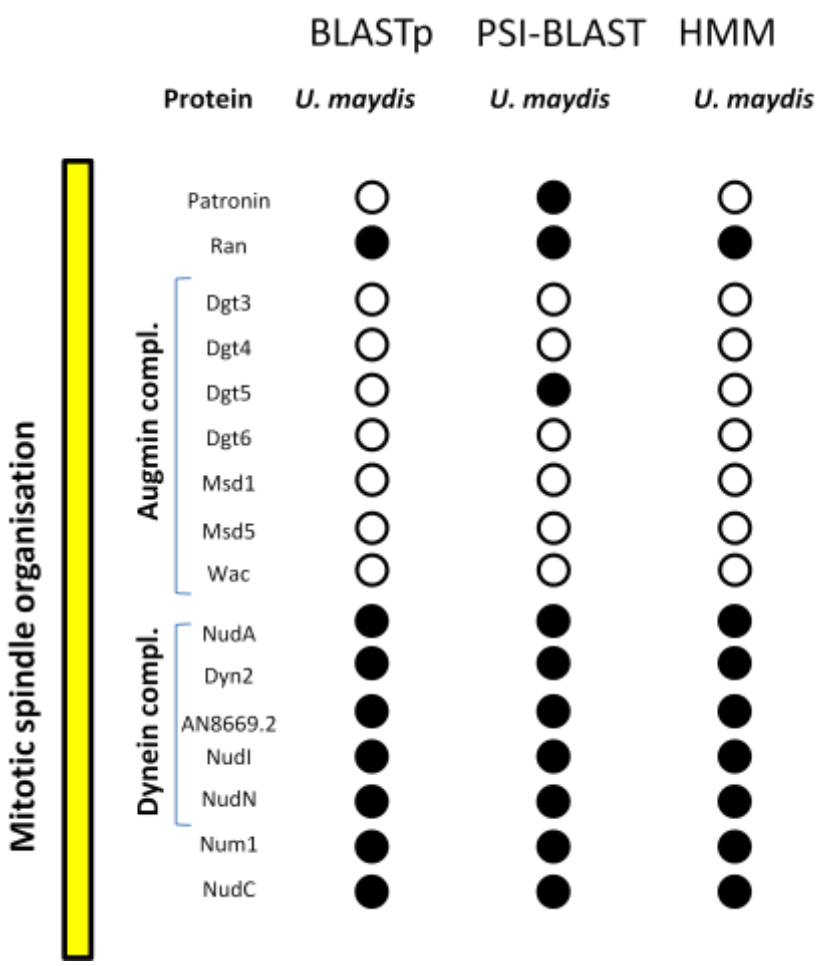
BLASTp
PSI-BLAST
HMM
Protein
U. maydis
U. maydis
U. maydis
Mitotic spindle organisation
Augmin compl.
Dynein compl.
Patronin
Ran
Dgt3
Dgt4
Dgt5
Dgt6
Msd1
Msd5
Wac
NudA
Dyn2
AN8669.2
NudI
NudN
Num1
NudC

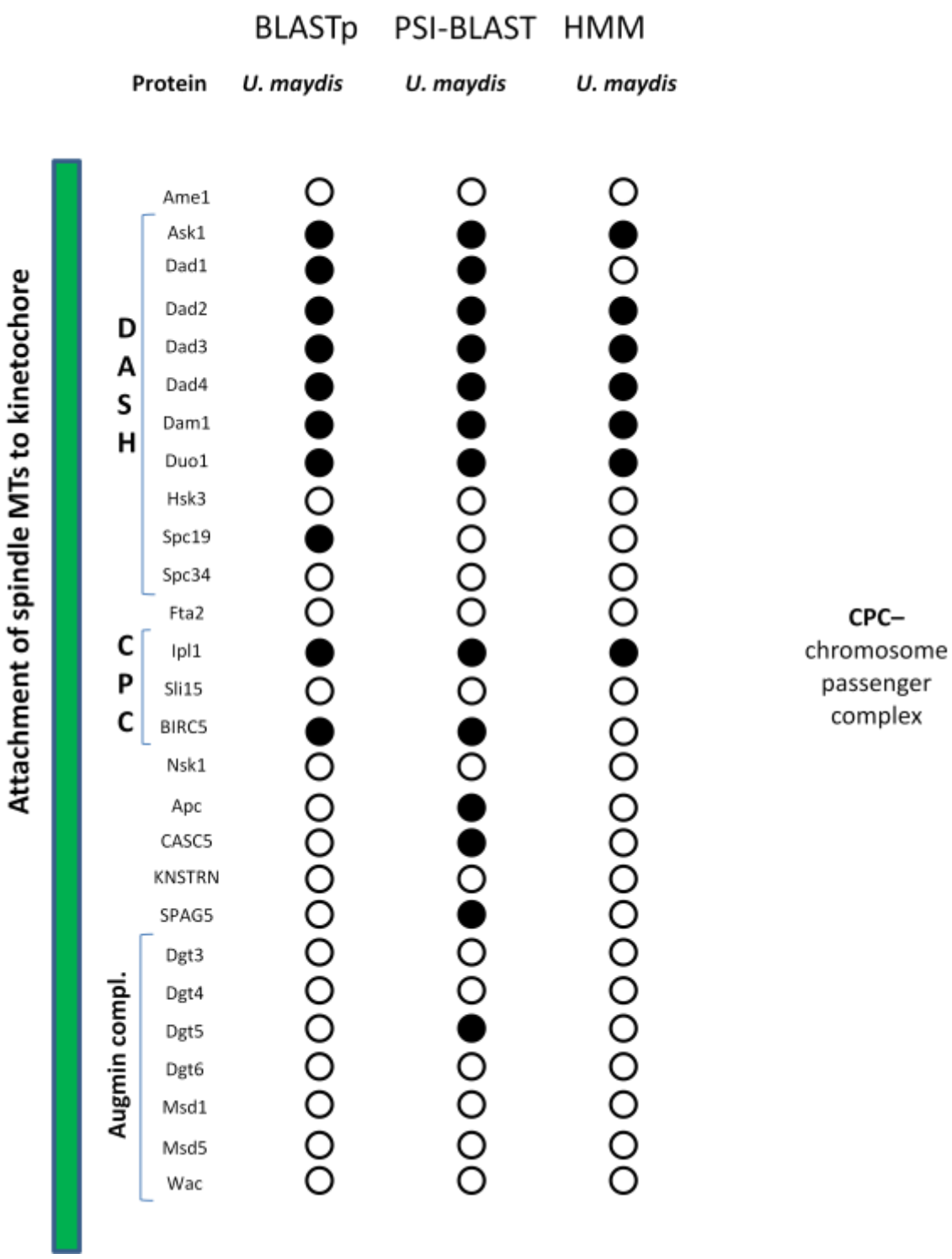
BLASTp
PSI-BLAST
HMM
Protein
U. maydis
U. maydis
U. maydis
Attachment of spindle MTs to kinetochore
DASH
CPC
Augmin compl.
Ame1
Ask1
Dad1
Dad2
Dad3
Dad4
Dam1
Duo1
Hsk3
Spc19
Spc34
Fta2
Ipl1
Sli15
BIRC5
Nsk1
Apc
CASC5
KNSTRN
SPAG5
Dgt3
Dgt4
Dgt5
Dgt6
Msd1
Msd5
Wac
CPC– chromosome passenger complex

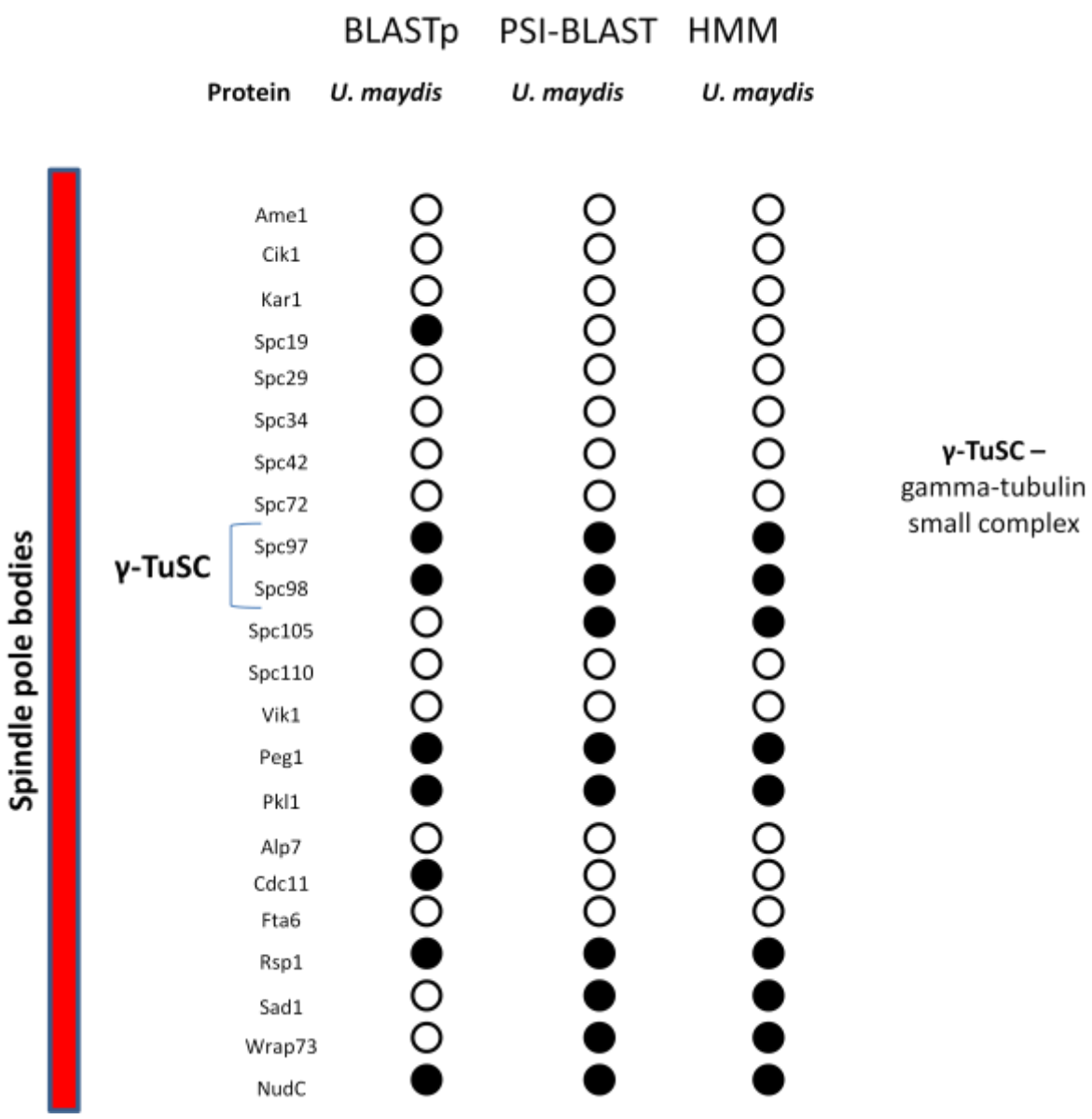
BLASTp
PSI-BLAST
HMM
Protein
U. maydis
U. maydis
U. maydis
Spindle pole bodies
γ-TuSC
Ame1
Cik1
Kar1
Spc19
Spc29
Spc34
Spc42
Spc72
Spc97
Spc98
Spc105
Spc110
Vik1
Peg1
Pkl1
Alp7
Cdc11
Fta6
Rsp1
Sad1
Wrap73
NudC
γ-TuSC –
gamma-tubulin
small complex

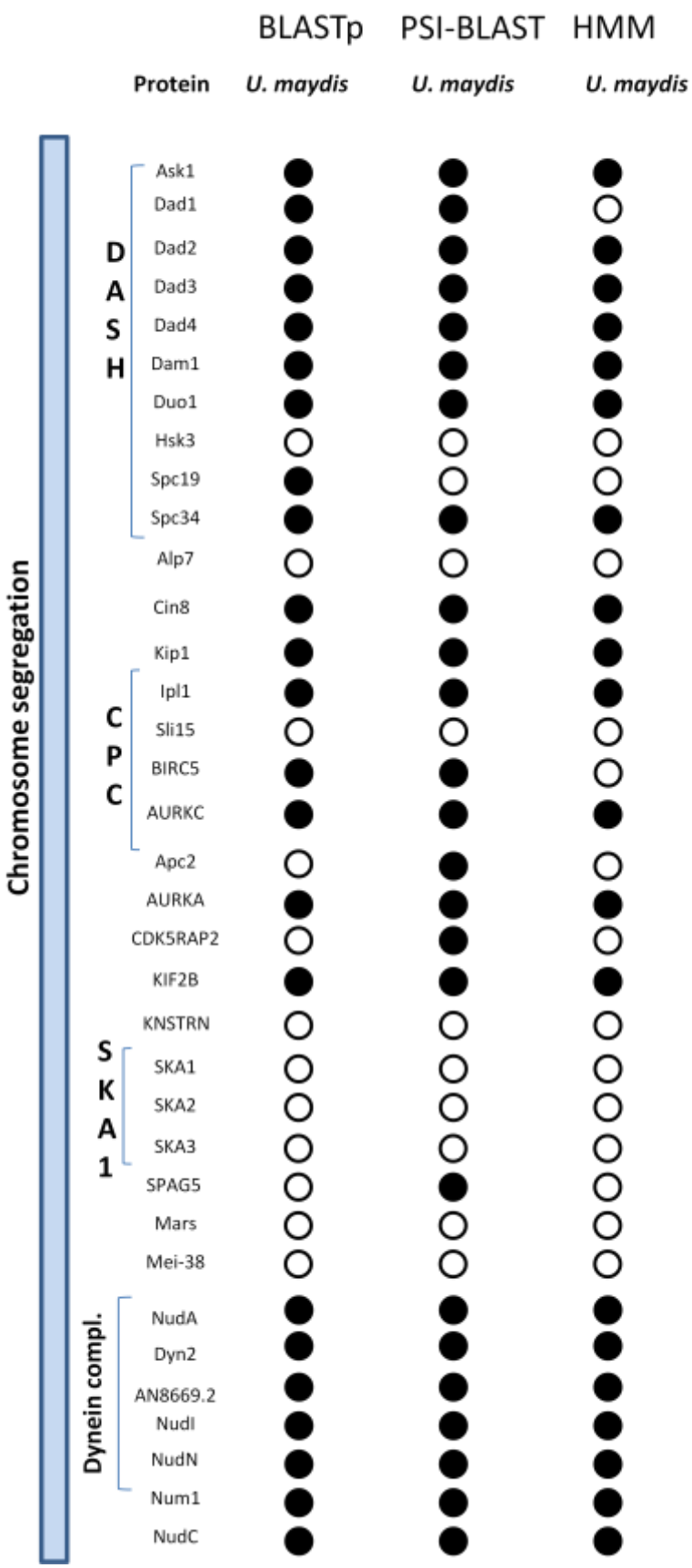
BLASTp
PSI-BLAST
HMM
Protein
U. maydis
U. maydis
U. maydis
Chromosome segregation
DASH
Ask1
Dad1
Dad2
Dad3
Dad4
Dam1
Duo1
Hsk3
Spc19
Spc34
Alp7
Cin8
Kip1
CPC
Ipl1
Sli15
BIRC5
AURKC
Apc2
AURKA
CDK5RAP2
KIF2B
KNSTRN
SKA1
SKA1
SKA2
SKA3
SPAG5
Mars
Mei-38
Dynein compl.
NudA
Dyn2
AN8669.2
NudI
NudN
Num1
NudC

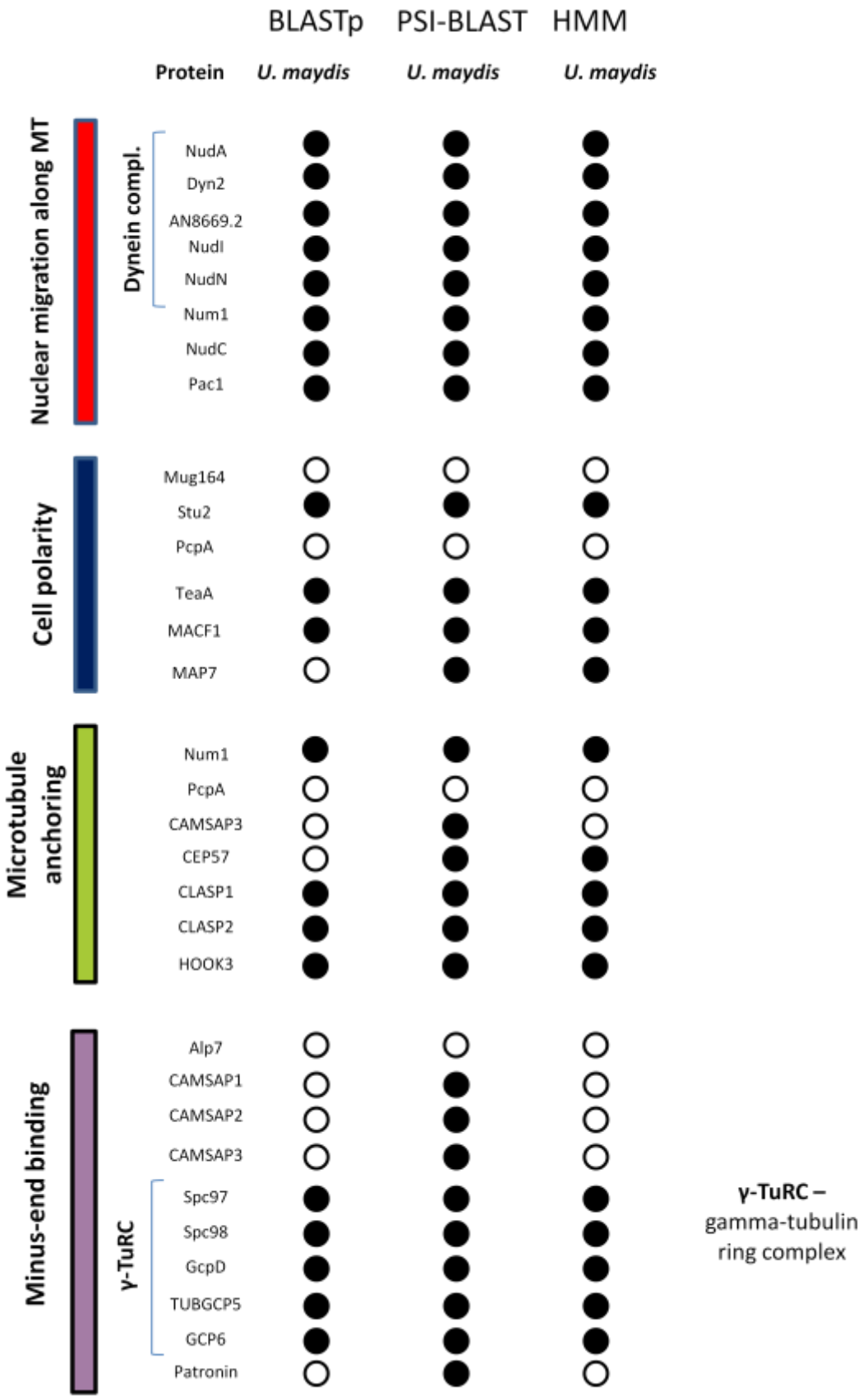
BLASTp
PSI-BLAST
HMM
Protein
U. maydis
U. maydis
U. maydis
Nuclear migration along MT
Dynein compl.
NudA
Dyn2
AN8669.2
NudI
NudN
Num1
NudC
Pac1
Cell polarity
Mug164
Stu2
PcpA
TeaA
MACF1
MAP7
Microtubule anchoring
Num1
PcpA
CAMSAP3
CEP57
CLASP1
CLASP2
HOOK3
Minus-end binding
Alp7
CAMSAP1
CAMSAP2
CAMSAP3
γ-TuRC
Spc97
Spc98
GcpD
TUBGCP5
GCP6
Patronin
γ-TuRC –
gamma-tubulin
ring complex

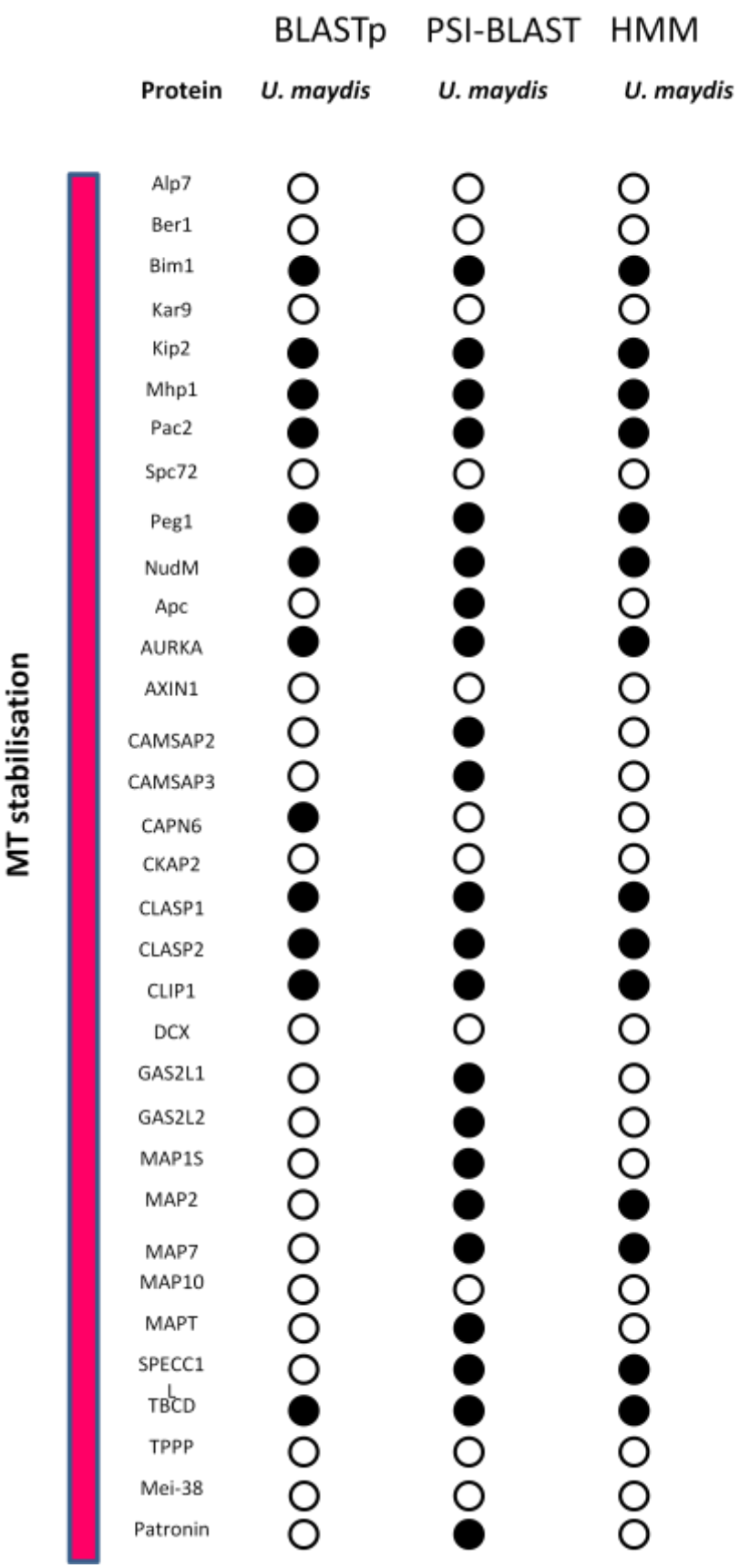
BLASTp
PSI-BLAST
HMM
Protein
U. maydis
U. maydis
U. maydis
MT stabilisation
Alp7
Ber1
Bim1
Kar9
Kip2
Mhp1
Pac2
Spc72
Peg1
NudM
Apc
AURKA
AXIN1
CAMSAP2
CAMSAP3
CAPN6
CKAP2
CLASP1
CLASP2
CLIP1
DCX
GAS2L1
GAS2L2
MAP1S
MAP2
MAP7
MAP10
MAPT
SPECC1L
TBCD
TPPP
Mei-38
Patronin

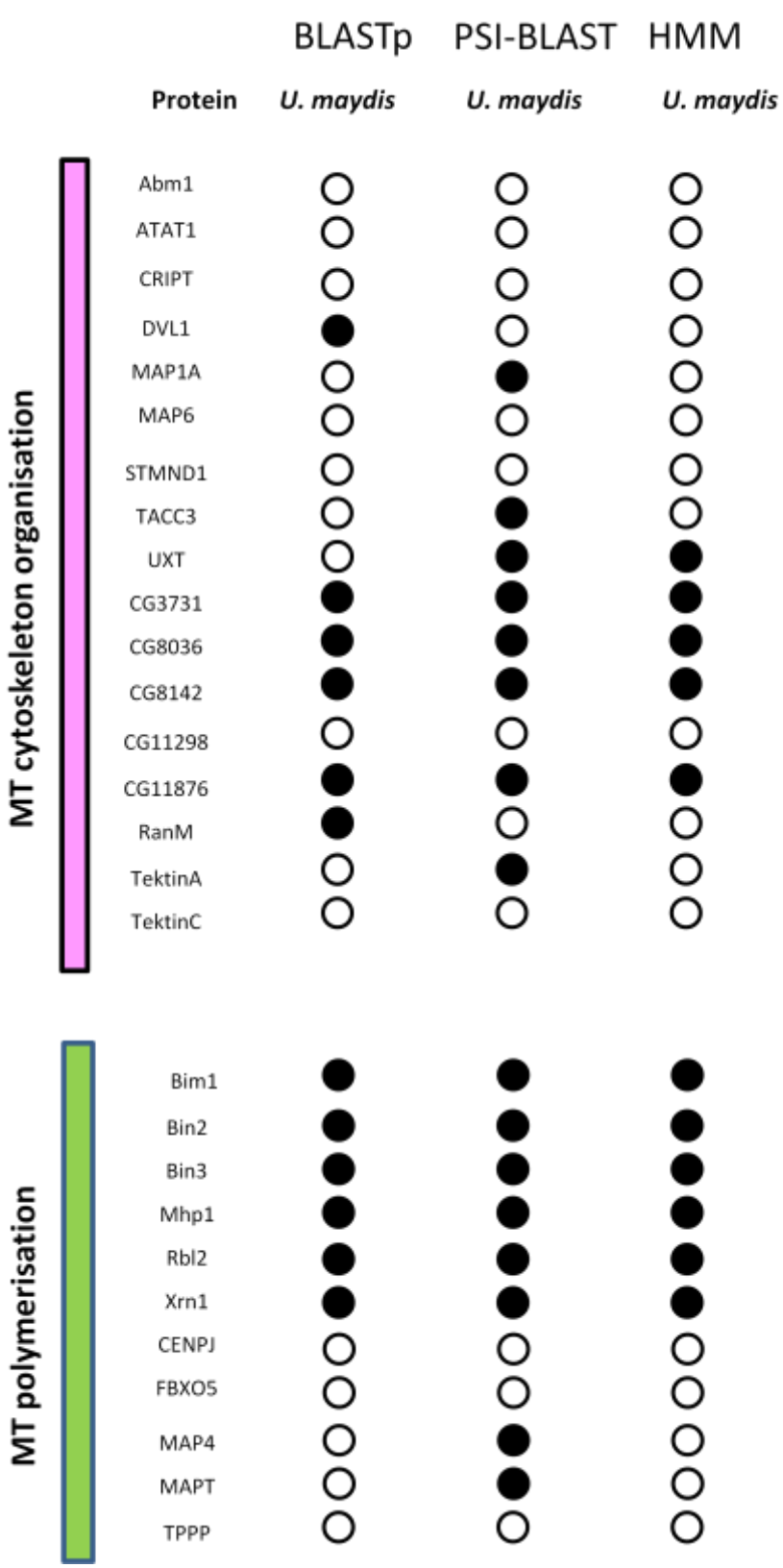
BLASTp
PSI-BLAST
HMM
Protein
U. maydis
U. maydis
U. maydis
MT cytoskeleton organisation
Abm1
ATAT1
CRIPT
DVL1
MAP1A
MAP6
STMND1
TACC3
UXT
CG3731
CG8036
CG8142
CG11298
CG11876
RanM
TektinA
TektinC
MT polymerisation
Bim1
Bin2
Bin3
Mhp1
Rbl2
Xrn1
CENPJ
FBXO5
MAP4
MAPT
TPPP

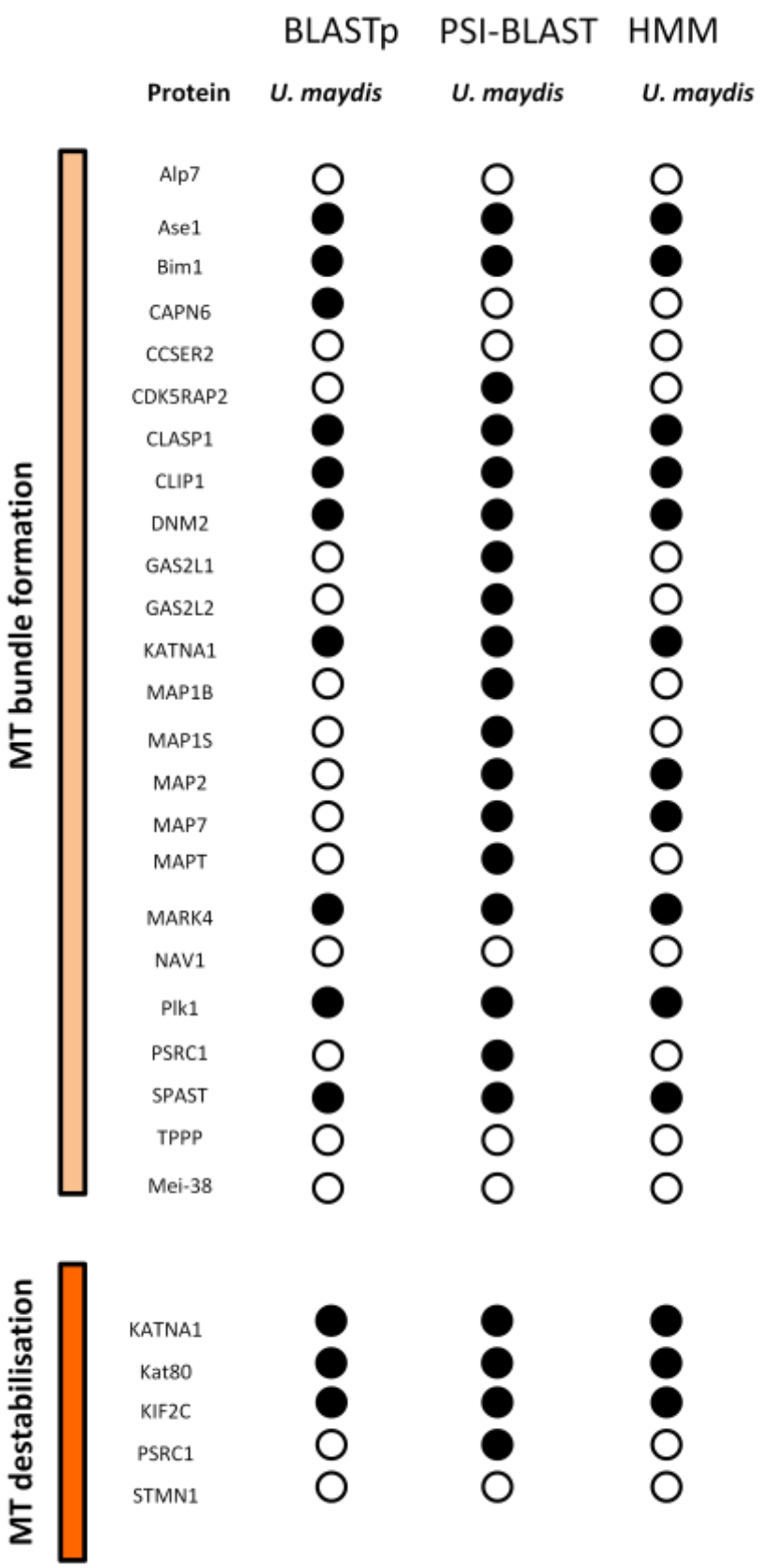
BLASTp
PSI-BLAST
HMM
Protein
U. maydis
U. maydis
U. maydis
MT bundle formation
Alp7
Ase1
Bim1
CAPN6
CCSER2
CDK5RAP2
CLASP1
CLIP1
DNM2
GAS2L1
GAS2L2
KATNA1
MAP1B
MAP1S
MAP2
MAP7
MAPT
MARK4
NAV1
Plk1
PSRC1
SPAST
TPPP
Mei-38
MT destabilisation
KATNA1
Kat80
KIF2C
PSRC1
STMN1

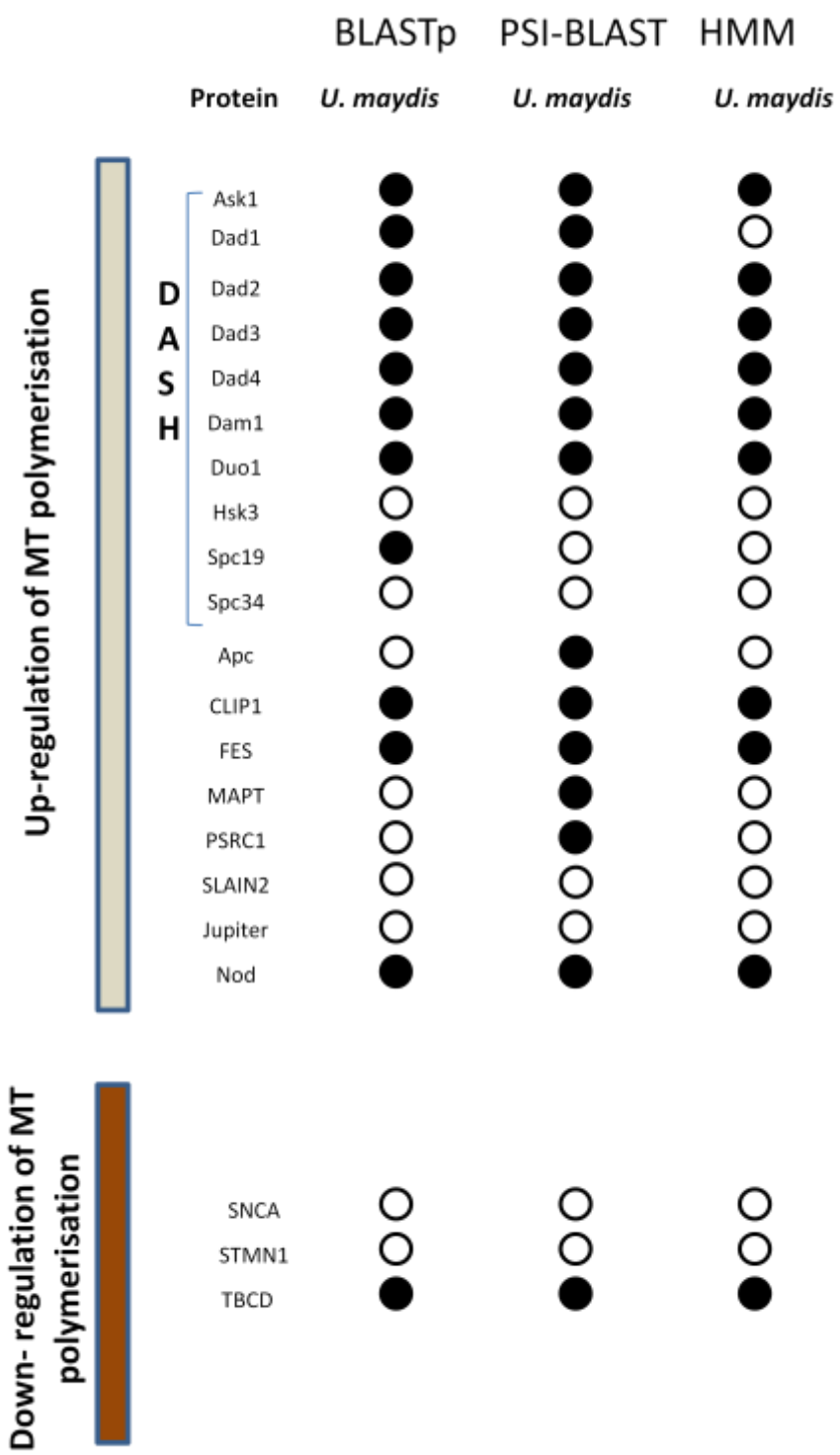
BLASTp
PSI-BLAST
HMM
Protein
U. maydis
U. maydis
U. maydis
Up-regulation of MT polymerisation
DASH
Ask1
Dad1
Dad2
Dad3
Dad4
Dam1
Duo1
Hsk3
Spc19
Spc34
Apc
CLIP1
FES
MAPT
PSRC1
SLAIN2
Jupiter
Nod
Down- regulation of MT polymerisation
SNCA
STMN1
TBCD

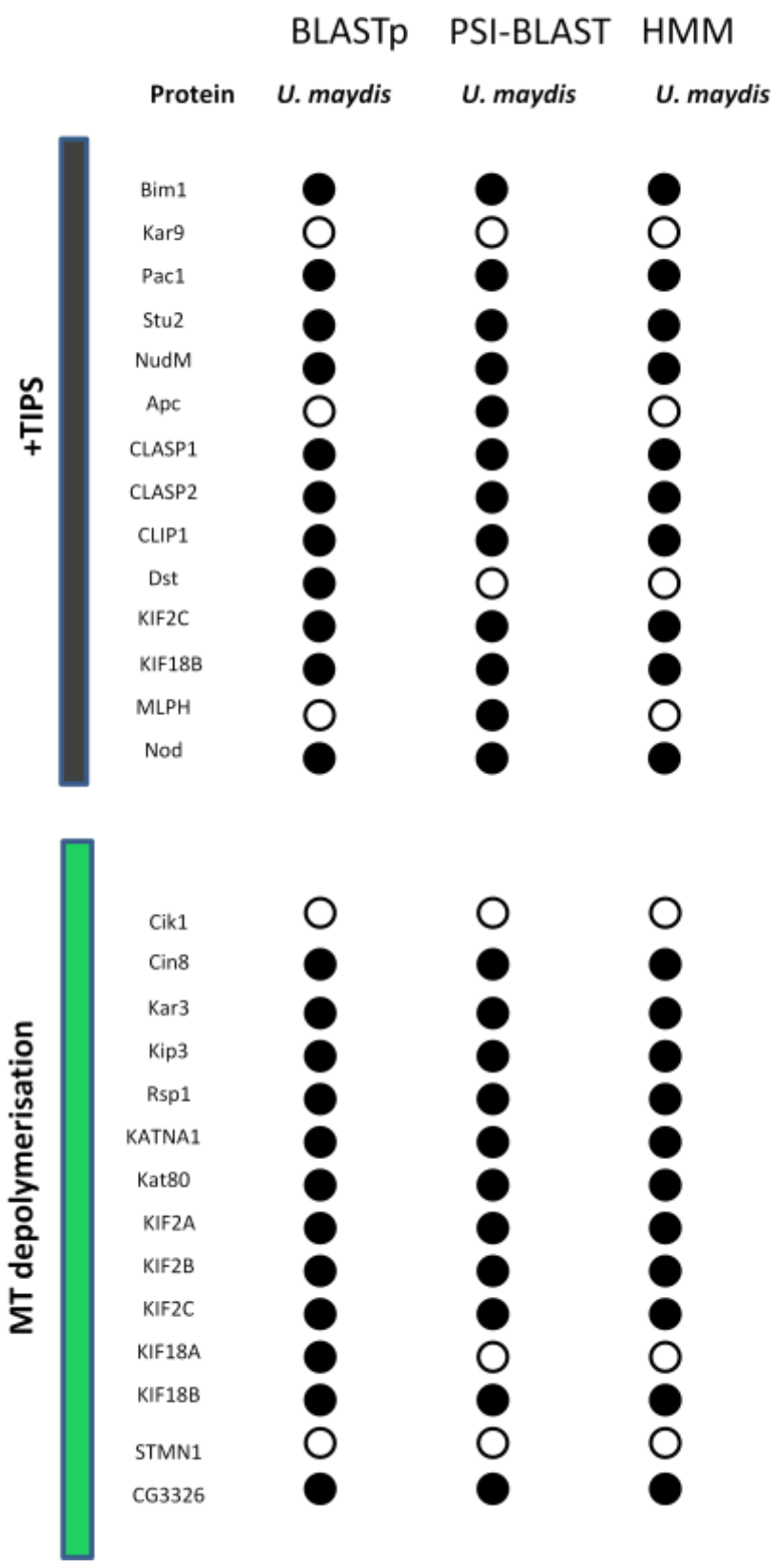
BLASTp
PSI-BLAST
HMM
Protein
U. maydis
U. maydis
U. maydis
+TIPS
Bim1
Kar9
Pac1
Stu2
NudM
Apc
CLASP1
CLASP2
CLIP1
Dst
KIF2C
KIF18B
MLPH
Nod
MT depolymerisation
Cik1
Cin8
Kar3
Kip3
Rsp1
KATNA1
Kat80
KIF2A
KIF2B
KIF2C
KIF18A
KIF18B
STMN1
CG3326

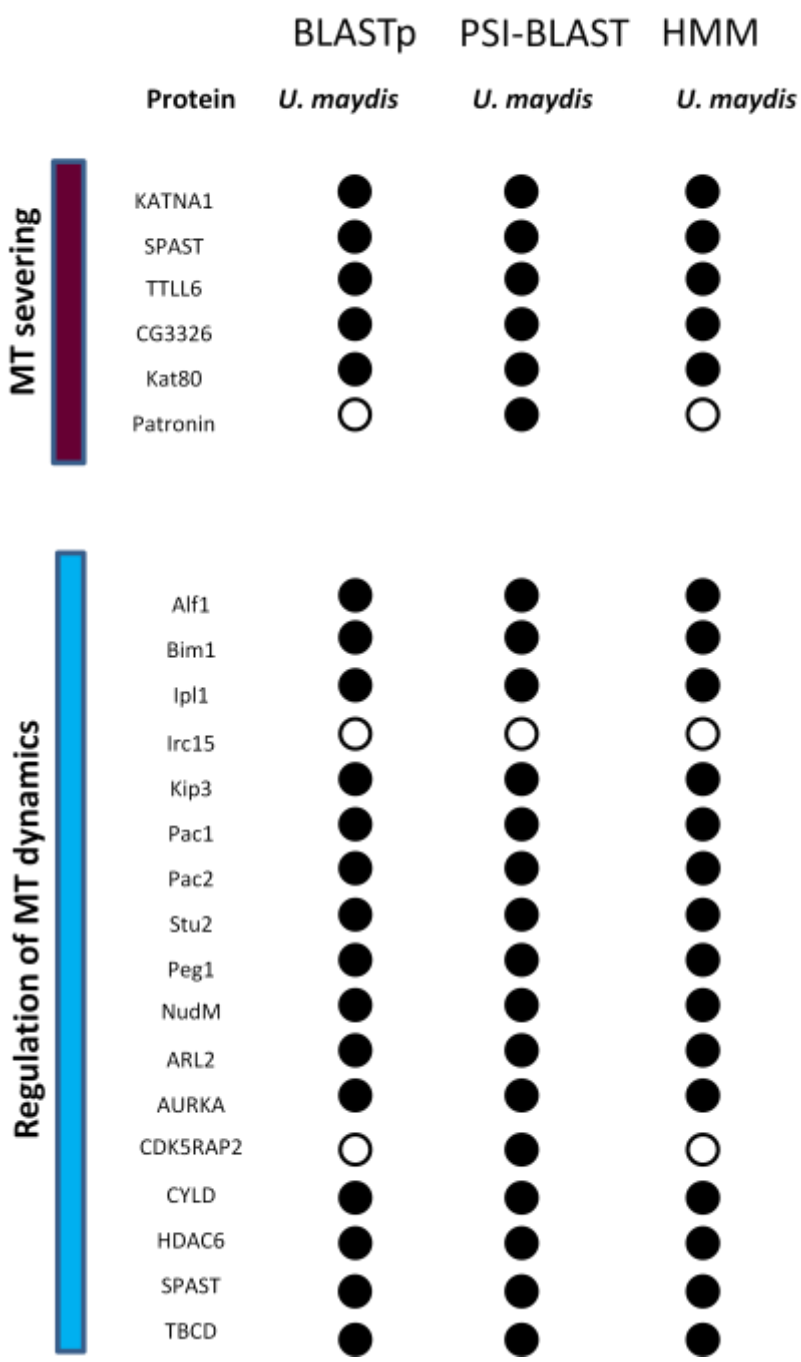
BLASTp
PSI-BLAST
HMM
Protein
U. maydis
U. maydis
U. maydis
MT severing
KATNA1
SPAST
TTLL6
CG3326
Kat80
Patronin
Regulation of MT dynamics
Alf1
Bim1
Ipl1
Irc15
Kip3
Pac1
Pac2
Stu2
Peg1
NudM
ARL2
AURKA
CDK5RAP2
CYLD
HDAC6
SPAST
TBCD

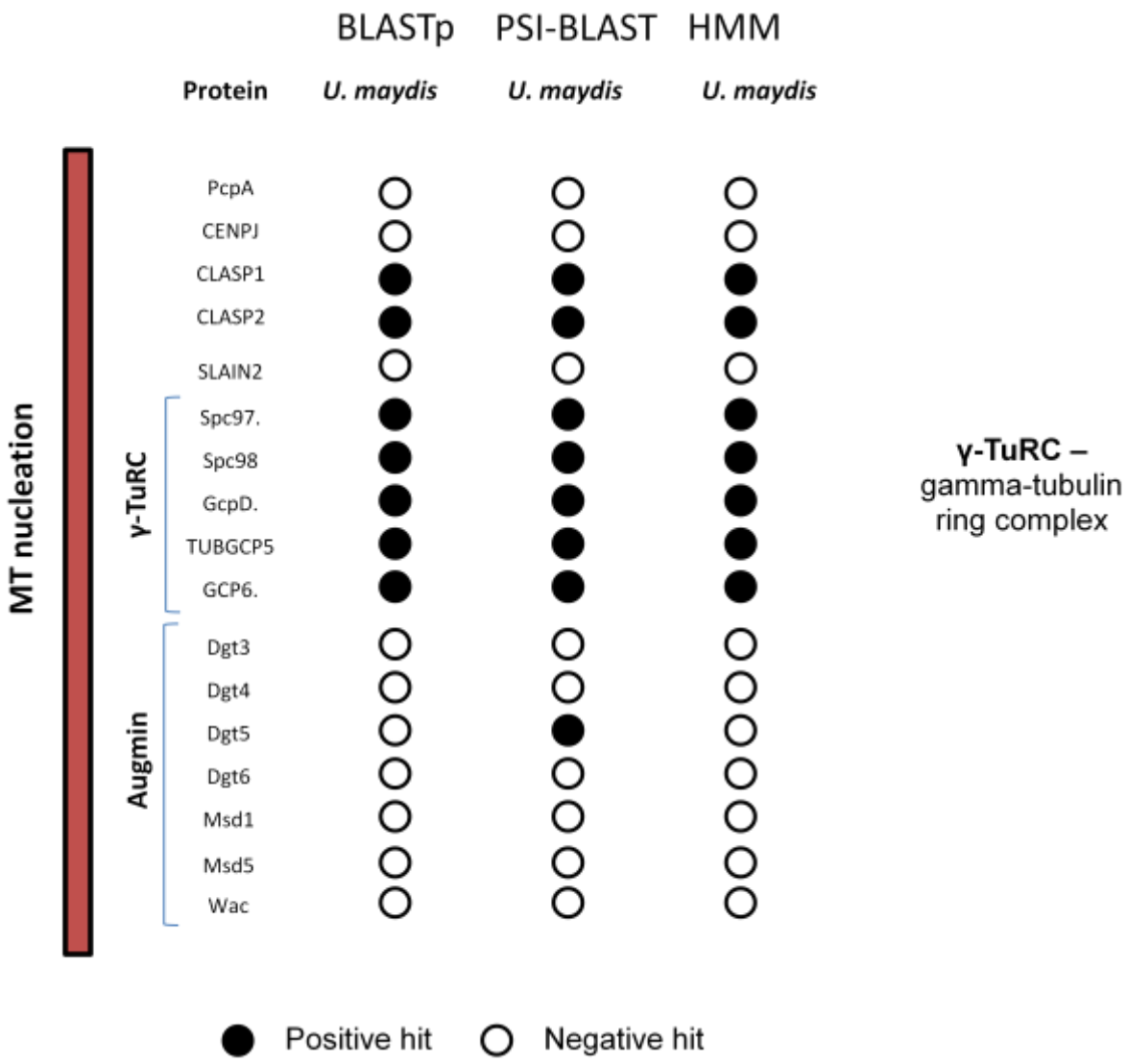

Figure 4.2 Distribution of MAPs from five eukaryotic species in *U. maydis*.

Results of 3 different search methods - BLASTp, PSI-BLAST and HMM conducted using MAP sequences from *H. sapiens*, *D. melanogaster*, *A. nidulans*, *S. cerevisiae* and *S. pombe*. Initially, out of 169 MAPs found, 80 proteins were identified as putative orthologues in *U. maydis*. Black dots denote positive hits, higher than e^{-05}; white dots indicate negative hits with scores lower than e^{-05} .

As a further step in predicting the *Ustilago* MAP repertoire, the amino acid sequences and domains of the 169 starting sequences were compared to their potential *Ustilago* orthologues as proteins with similar domain architecture are more likely to be orthologues. Domain analysis revealed that most of the *Ustilago* sequences that were identified as likely orthologues based on sequence conservation also had similar protein length and identical or similar domain architecture to their corresponding starting sequence (Figure A1). However, in a minority of cases, domain and motif analysis revealed major differences between the starting sequence and the *Ustilago* hit despite very high sequence similarity. Based on this, some proteins, for example the microtubule severing proteins katanin and spastin, were discarded. It remains possible that the sequences identified do actually represent *Ustilago* orthologues, because sequences with high similarity can be found in the *A. nidulans* and *A. fumigatus* genomes. Nonetheless, experimental data for the role of this class of MT-associated proteins are not yet available for filamentous fungi (Robson et al., 2007) and experimental validation will be required to determine the status of these sequences. However, it also had to be considered that conserved domains can lead to false positives, therefore they were manually removed in 2 yeast MAPs (Irc15 and Rsp1) and BLASTp was performed to see if the hit was correct. In addition, all dubious *Ustilago* homologues were aligned against the starting MAP sequences and compared manually.

As a final step the identity/similarity relationship between found MAPs and their potential *Ustilago* ortologues, was analysed using EMBOSS Needle (Goujon et al., 2010; McWilliam et al., 2013; Rice et al., 2000), a Pairwise Sequence Alignment tool. Average Identity/Similarity of MAPs found in *U. maydis* was 27.5 %/40.6 %, in contrast to proteins found using different search methods, but discarded due to poor e-values or incorrect domain architecture present, which had significantly lower values of 8.7 %/14.9 **%** Id/Sim. However, it is known that, in general, a firm link between protein functionality and sequence may not exist and it is not so much sequence of residue identities as that of their chemical properties and residue chain fold that really matters. This allows for greater functional diversity and flexibility, which may have important evolutionary implications (Krissinel, 2007)**.**

To make a final decision about *Ustilago* hit being a MAP orthologue, the results from 3 different search methods were analysed along with the domain architectures, alignments of *Ustilago*, MAP sequences and literature searches. A protein was considered to be a possible *U. maydis* orthologue if it was identified by at least one out of three different search methods (BLASTp, HMM or PSI-BLAST) with the e-value above e^{-05} and it had similar domain architecture to the initial MAP. Thus, the final number of MAP orthologues that could be predicted using these methods in *Ustilago* was 66 (denoted as green dots in Fig. 4.3).

4.3.3 MAPs involved in chromosome function and nuclear migration are well conserved in *Ustilago*, whereas those involved in microtubule assembly, disassembly and stability are not.

The potential orthologues found in *U. maydis*, which were previously grouped according to their functions, could be divided into 3 categories: 1. Very well conserved (more than 50 % of proteins conserved in *Ustilago*), 2. Relatively well conserved (about 50 %±2 protein conserved in *U. maydis*) and 3. Poorly conserved (less than 50 % of proteins conserved in *Ustilago*).

1. Proteins that appear to be very well conserved in *U. maydis* belong to:

- Chromosome segregation (19 out of 33 MAPs present in *Ustilago*, 19/33),
- Nuclear migration along MTs (8/8),
- Up-regulation of MT polymerisation (10/18),
- Regulation of MT dynamics (13/17).

2. Relatively well conserved proteins can be found in:

- Mitotic spindle organisation (23/48),
- Minus-end binding (5/10),
- +TIPs (6/14),
- MT polymerisation (5/11),
- Microtubule anchoring (3/7).

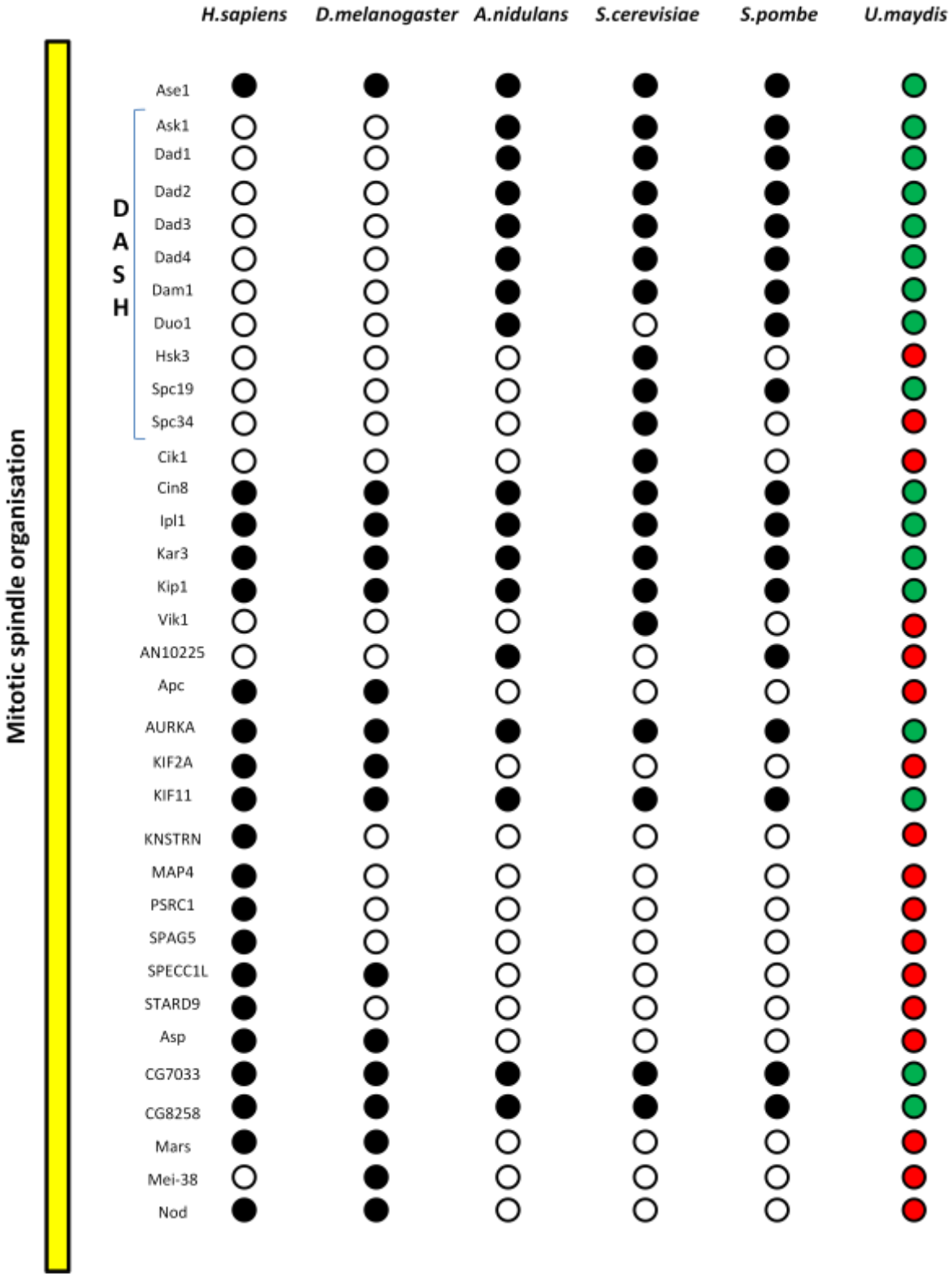
H.sapiens
D.melanogaster
A.nidulans
S.cerevisiae
S.pombe
U.maydis
Mitotic spindle organisation
DASH
Ase1
Ask1
Dad1
Dad2
Dad3
Dad4
Dam1
Duo1
Hsk3
Spc19
Spc34
Cik1
Cin8
Ipl1
Kar3
Kip1
Vik1
AN10225
Apc
AURKA
KIF2A
KIF11
KNSTRN
MAP4
PSRC1
SPAG5
SPECC1L
STARD9
Asp
CG7033
CG8258
Mars
Mei-38
Nod

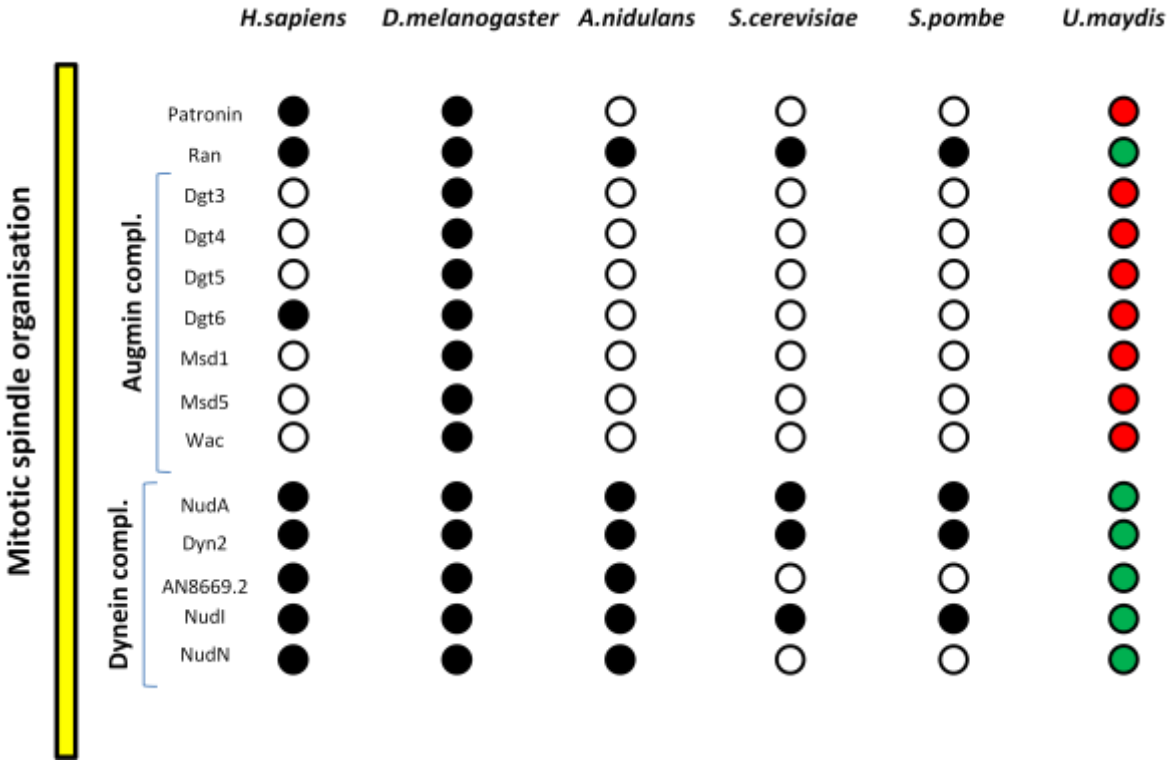
H.sapiens
D.melanogaster
A.nidulans
S.cerevisiae
S.pombe
U.maydis
Mitotic spindle organisation
Augmin compl.
Dynein compl.
Patronin
Ran
Dgt3
Dgt4
Dgt5
Dgt6
Msd1
Msd5
Wac
NudA
Dyn2
AN8669.2
NudI
NudN

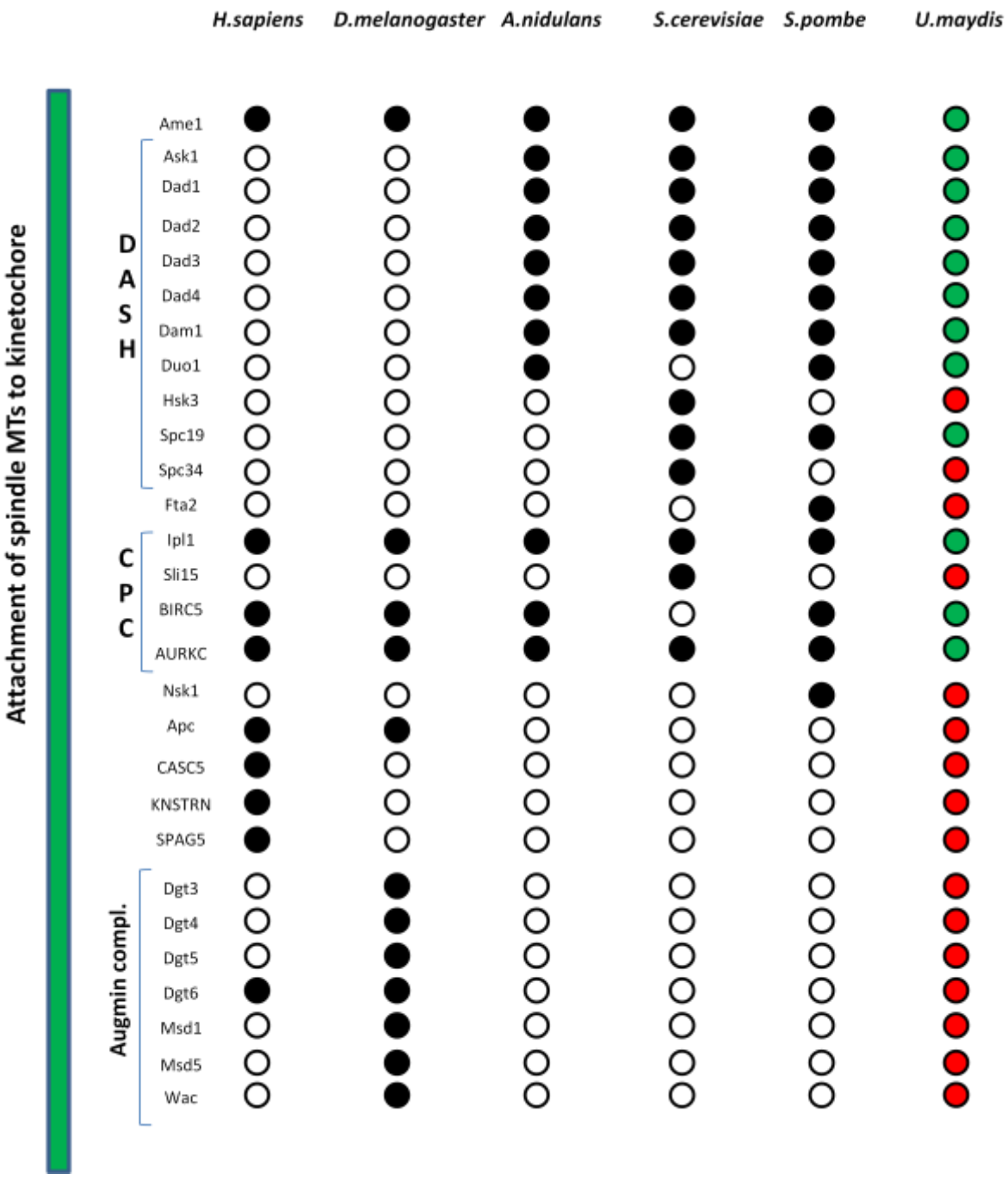
H.sapiens
D.melanogaster
A.nidulans
S.cerevisiae
S.pombe
U.maydis
Attachment of spindle MTs to kinetochore
DASH
Ame1
Ask1
Dad1
Dad2
Dad3
Dad4
Dam1
Duo1
Hsk3
Spc19
Spc34
Fta2
CPC
Ipl1
Sli15
BIRC5
AURKC
Nsk1
Apc
CASC5
KNSTRN
SPAG5
Augmin compl.
Dgt3
Dgt4
Dgt5
Dgt6
Msd1
Msd5
Wac

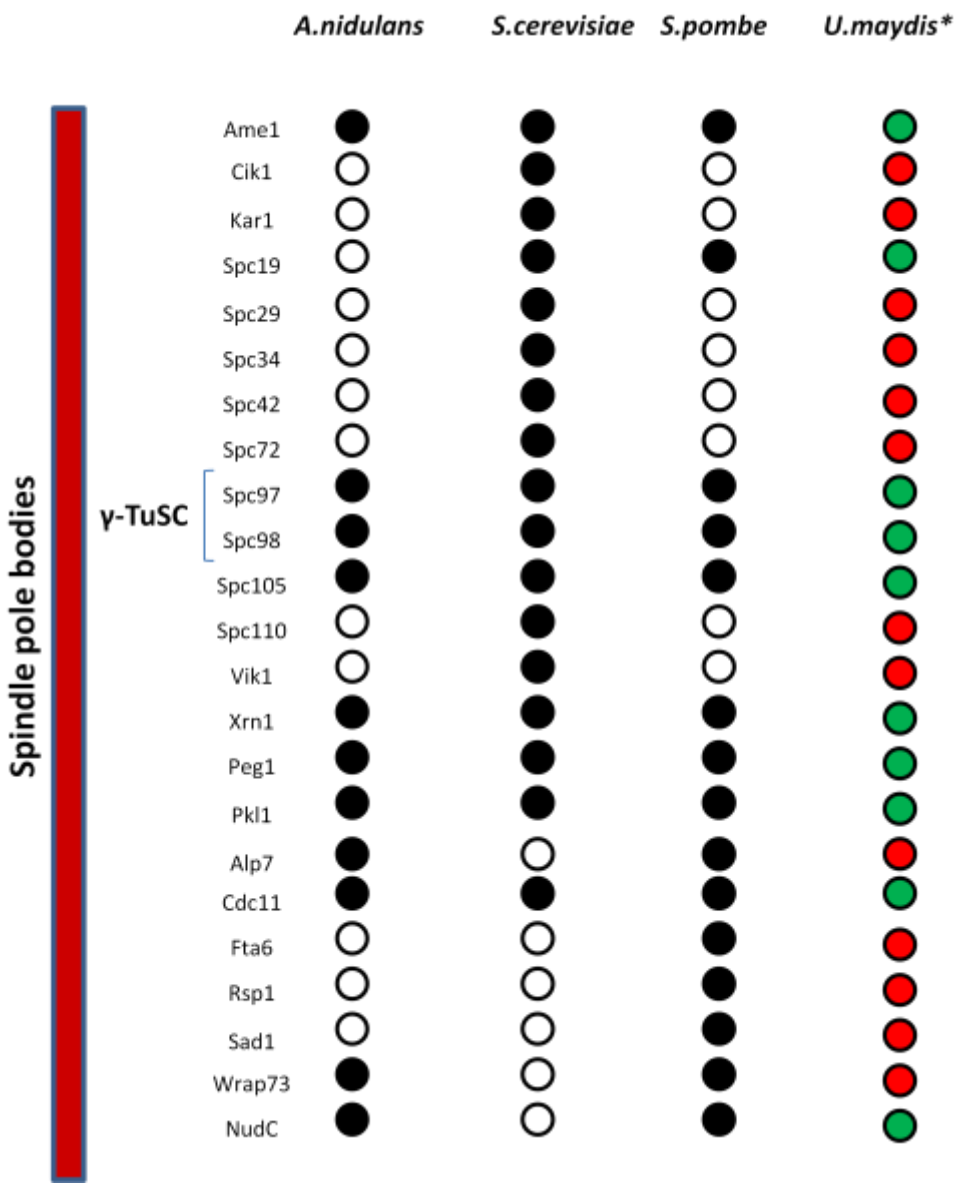

*The two species *D. melanogaster* and *H. sapiens* were not included here, because although SPBs are functionally equivalent to the centrosomes of higher eukaryotes (Rout and Kilmartin, 1990), they bear little resemblance (Pereira and Schiebel, 2001).

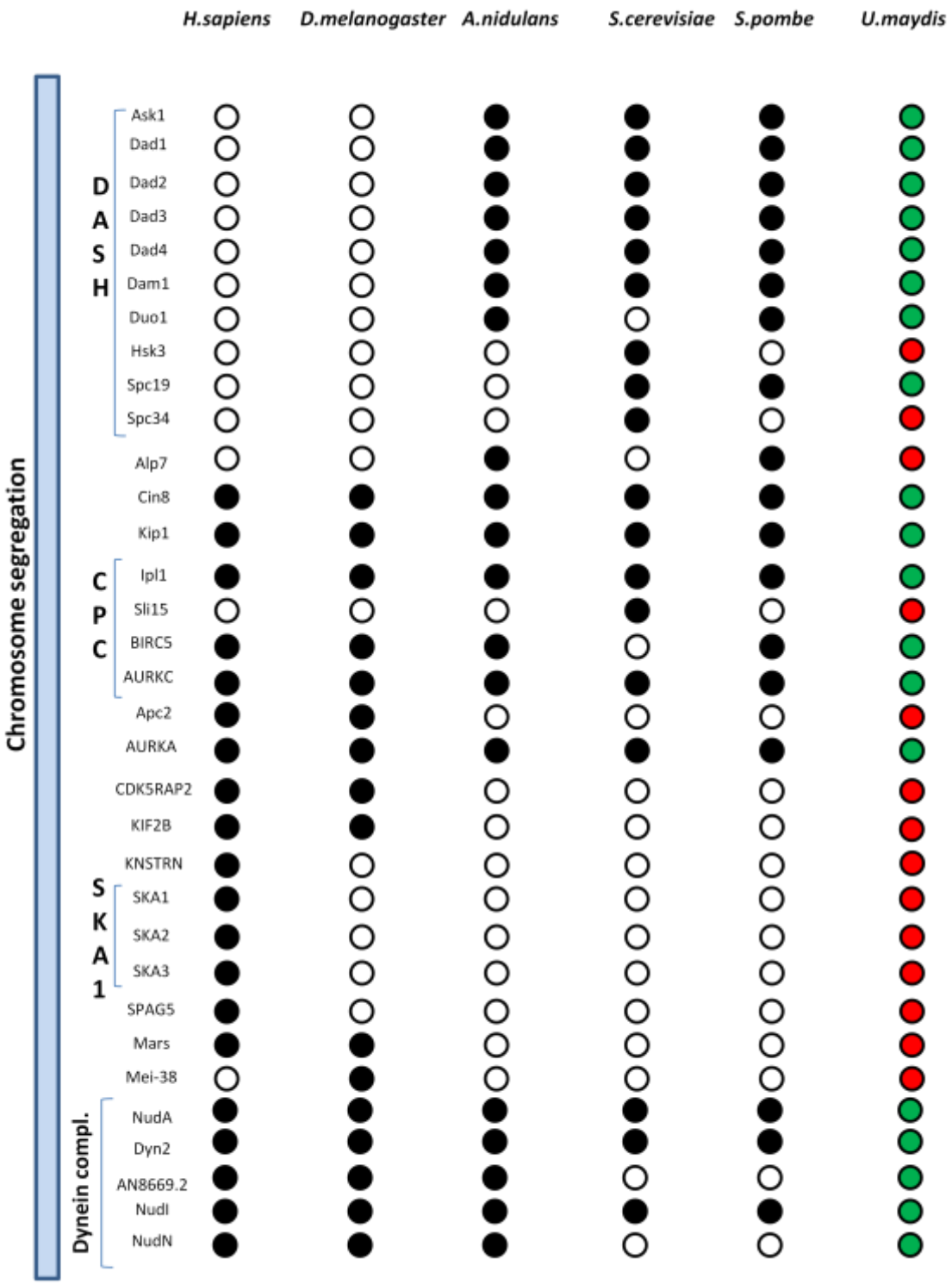
H.sapiens
D.melanogaster
A.nidulans
S.cerevisiae
S.pombe
U.maydis
Chromosome segregation
DASH
Ask1
Dad1
Dad2
Dad3
Dad4
Dam1
Duo1
Hsk3
Spc19
Spc34
Alp7
Cin8
Kip1
CPC
Ipl1
Sli15
BIRC5
AURKC
Apc2
AURKA
CDK5RAP2
KIF2B
KNSTRN
SKA1
SKA1
SKA2
SKA3
SPAG5
Mars
Mei-38
Dynein compl.
NudA
Dyn2
AN8669.2
Nudl
NudN

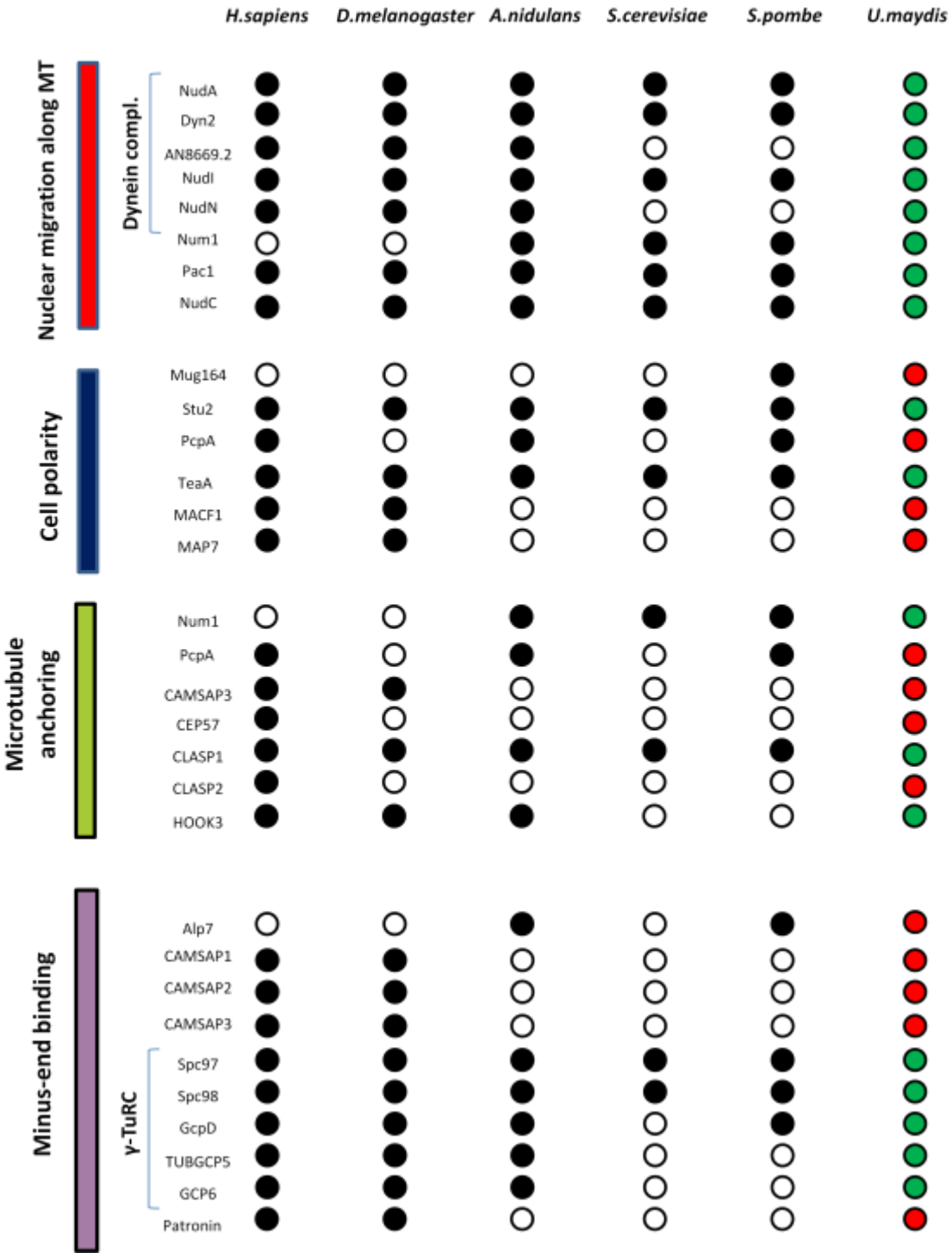
H.sapiens
D.melanogaster
A.nidulans
S.cerevisiae
S.pombe
U.maydis
Nuclear migration along MT
Dynein compl.
NudA
Dyn2
AN8669.2
NudI
NudN
Num1
Pac1
NudC
Cell polarity
Mug164
Stu2
PcpA
TeaA
MACF1
MAP7
Microtubule anchoring
Num1
PcpA
CAMSAP3
CEP57
CLASP1
CLASP2
HOOK3
Minus-end binding
γ-TuRC
Alp7
CAMSAP1
CAMSAP2
CAMSAP3
Spc97
Spc98
GcpD
TUBGCP5
GCP6
Patronin

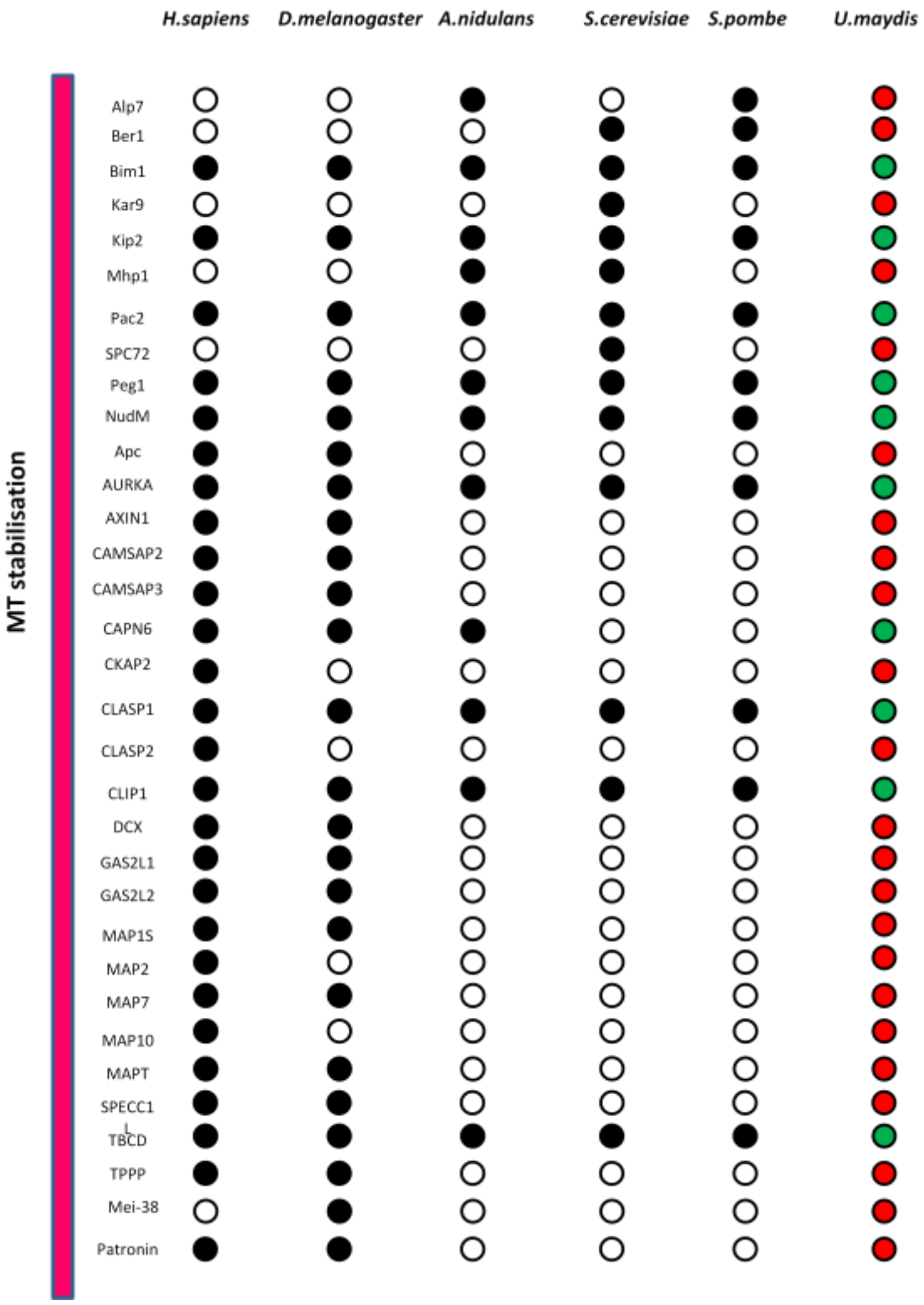
H.sapiens
D.melanogaster
A.nidulans
S.cerevisiae
S.pombe
U.maydis
MT stabilisation
Alp7
Ber1
Bim1
Kar9
Kip2
Mhp1
Pac2
SPC72
Peg1
NudM
Apc
AURKA
AXIN1
CAMSAP2
CAMSAP3
CAPN6
CKAP2
CLASP1
CLASP2
CLIP1
DCX
GAS2L1
GAS2L2
MAP1S
MAP2
MAP7
MAP10
MAPT
SPECC1L
TBCD
TPPP
Mei-38
Patronin

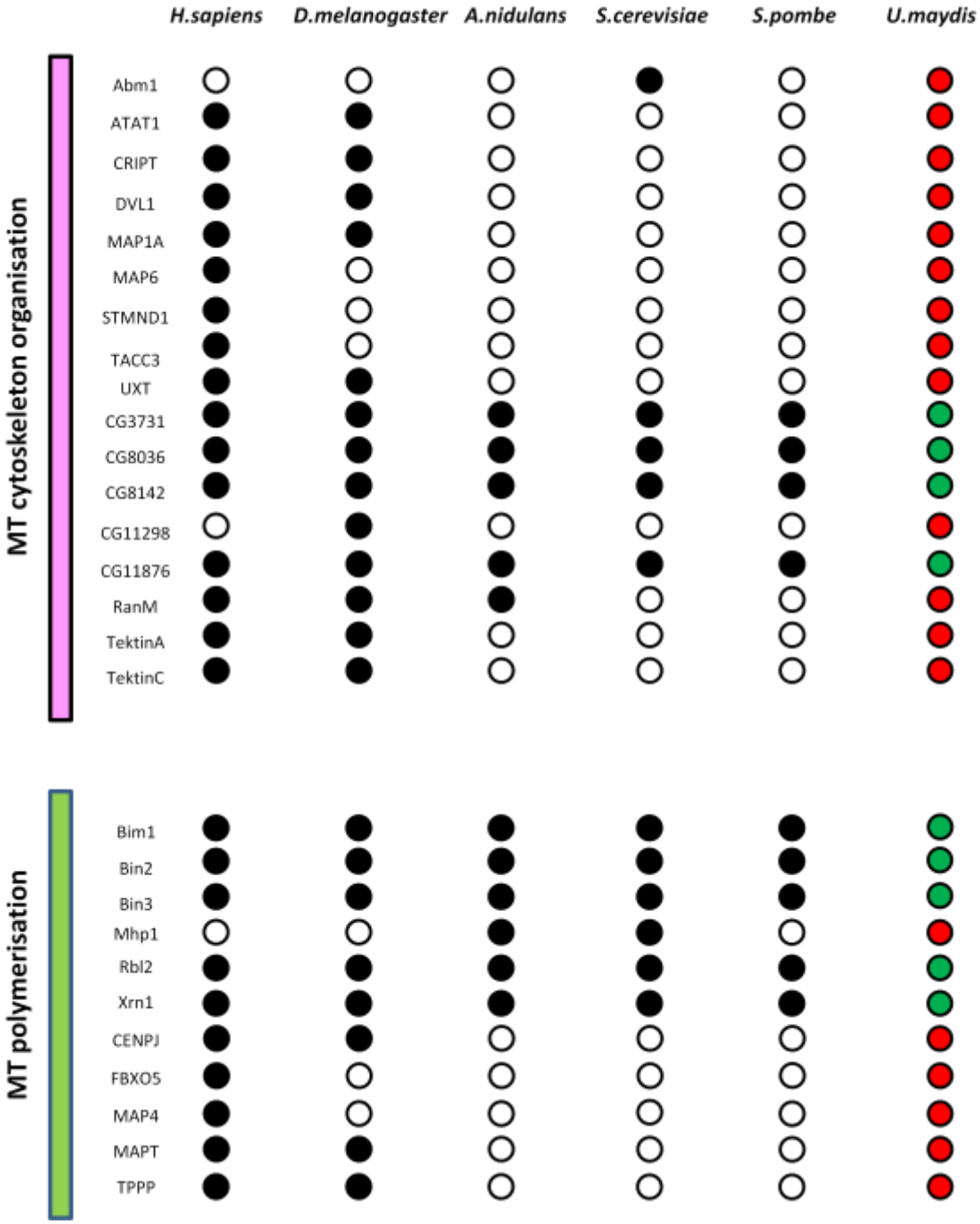
H.sapiens
D.melanogaster
A.nidulans
S.cerevisiae
S.pombe
U.maydis
MT cytoskeleton organisation
Abm1
ATAT1
CRIPT
DVL1
MAP1A
MAP6
STMND1
TACC3
UXT
CG3731
CG8036
CG8142
CG11298
CG11876
RanM
TektinA
TektinC
MT polymerisation
Bim1
Bin2
Bin3
Mhp1
Rbl2
Xrn1
CENPJ
FBXO5
MAP4
MAPT
TPPP

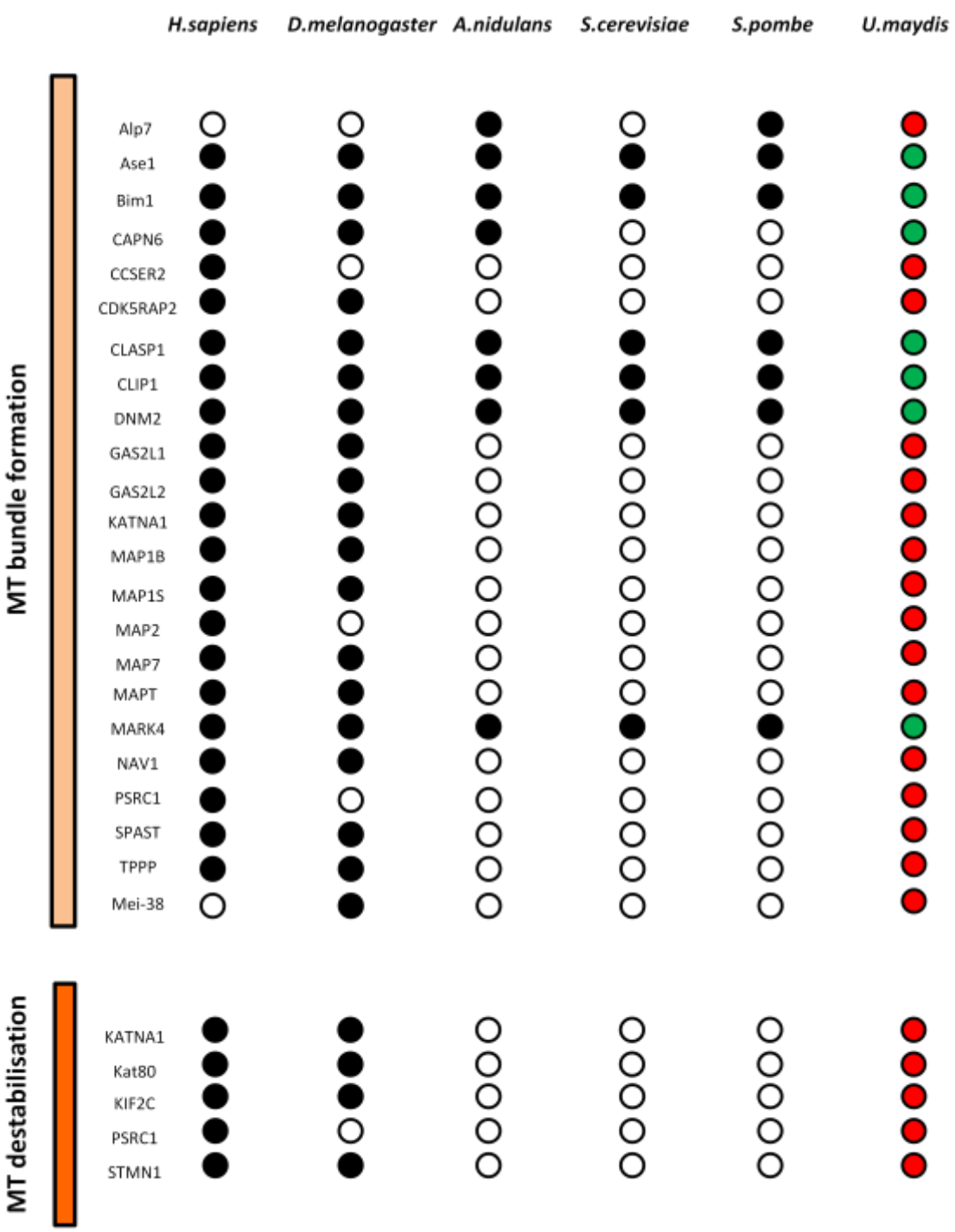
H.sapiens
D.melanogaster
A.nidulans
S.cerevisiae
S.pombe
U.maydis
MT bundle formation
Alp7
Ase1
Bim1
CAPN6
CCSER2
CDK5RAP2
CLASP1
CLIP1
DNM2
GAS2L1
GAS2L2
KATNA1
MAP1B
MAP1S
MAP2
MAP7
MAPT
MARK4
NAV1
PSRC1
SPAST
TPPP
Mei-38
MT destabilisation
KATNA1
Kat80
KIF2C
PSRC1
STMN1

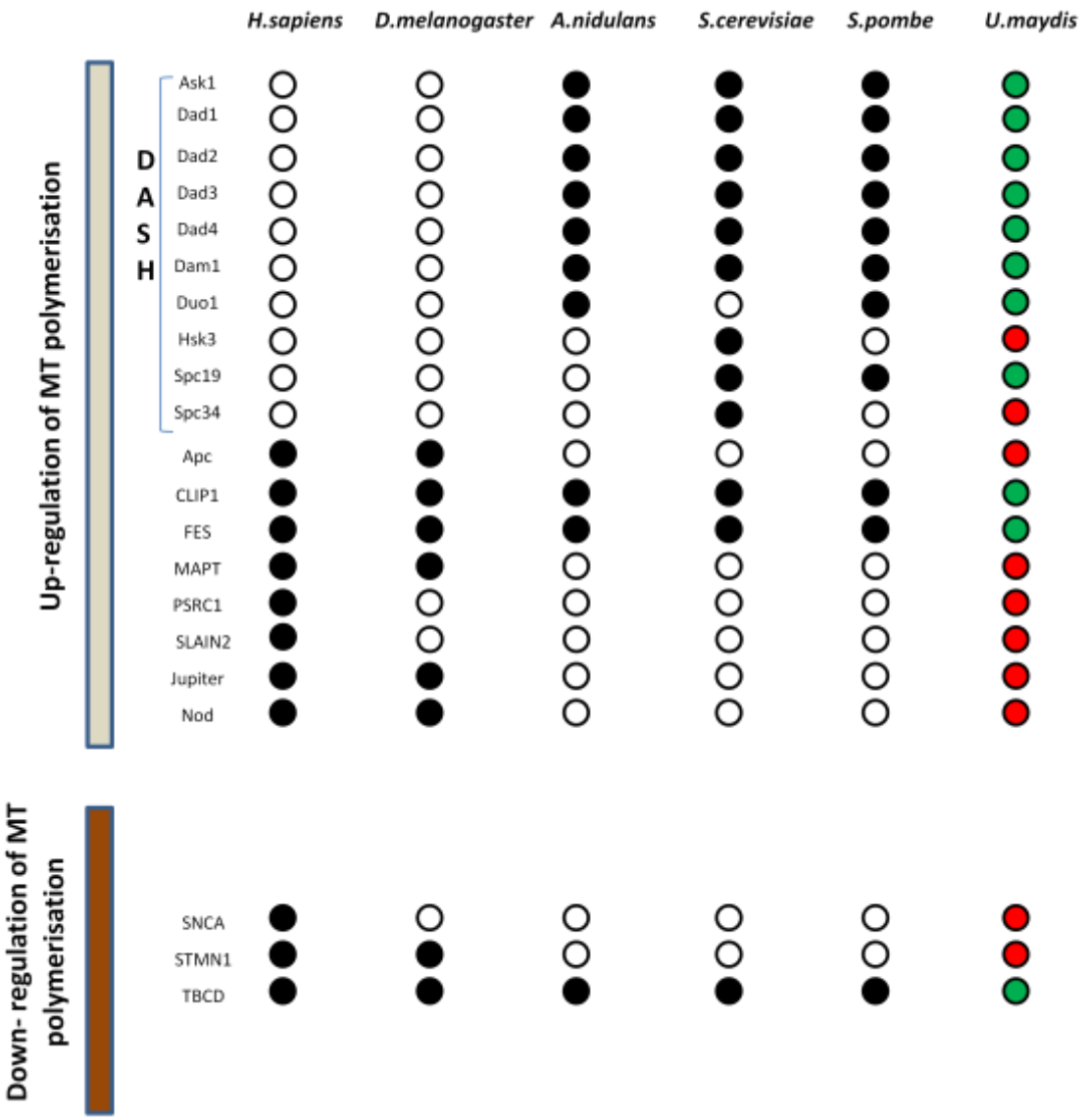
H.sapiens
D.melanogaster
A.nidulans
S.cerevisiae
S.pombe
U.maydis
Up-regulation of MT polymerisation
DASH
Ask1
Dad1
Dad2
Dad3
Dad4
Dam1
Duo1
Hsk3
Spc19
Spc34
Apc
CLIP1
FES
MAPT
PSRC1
SLAIN2
Jupiter
Nod
Down- regulation of MT polymerisation
SNCA
STMN1
TBCD

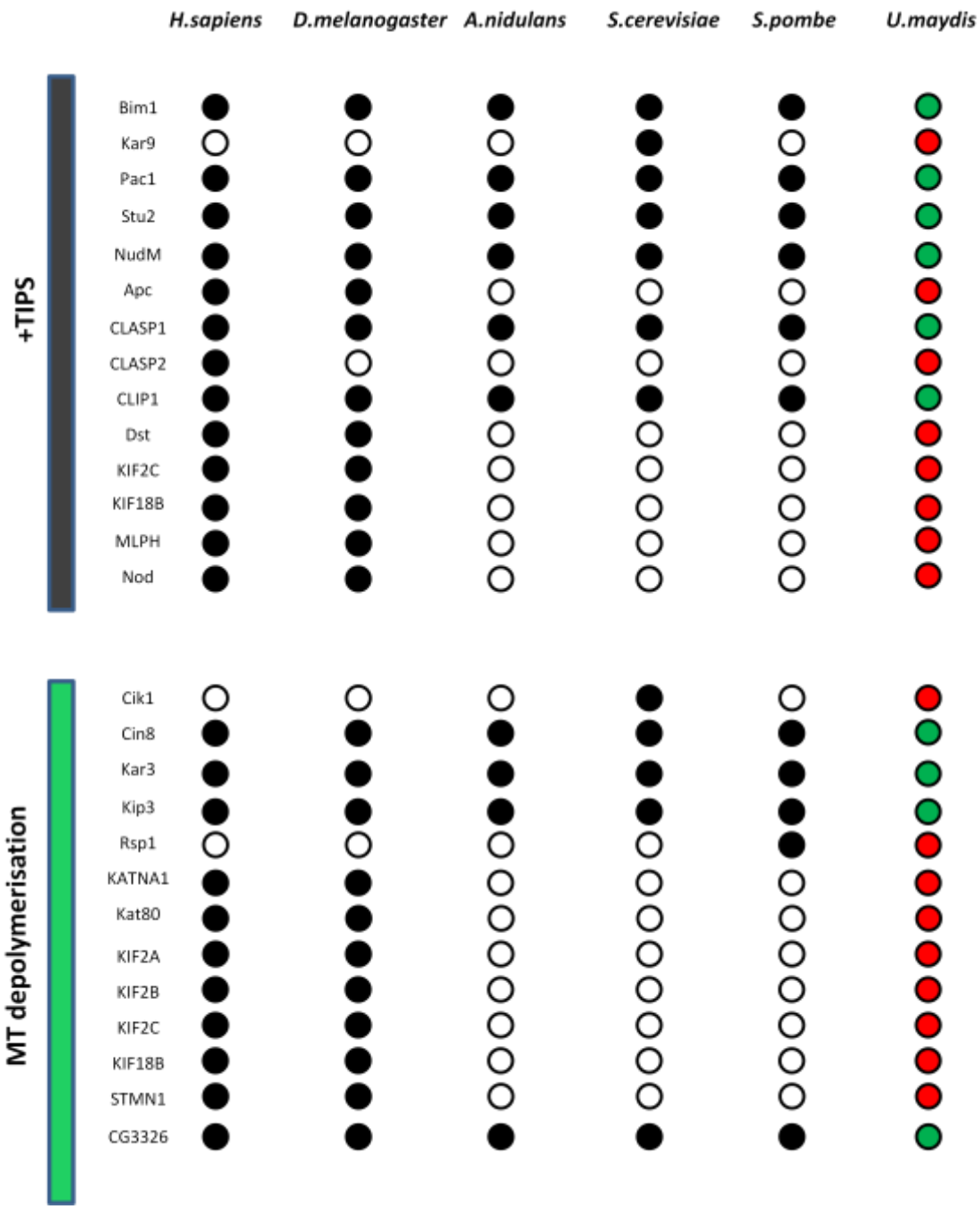
H.sapiens
D.melanogaster
A.nidulans
S.cerevisiae
S.pombe
U.maydis
+TIPS
Bim1
Kar9
Pac1
Stu2
NudM
Apc
CLASP1
CLASP2
CLIP1
Dst
KIF2C
KIF18B
MLPH
Nod
MT depolymerisation
Cik1
Cin8
Kar3
Kip3
Rsp1
KATNA1
Kat80
KIF2A
KIF2B
KIF2C
KIF18B
STMN1
CG3326

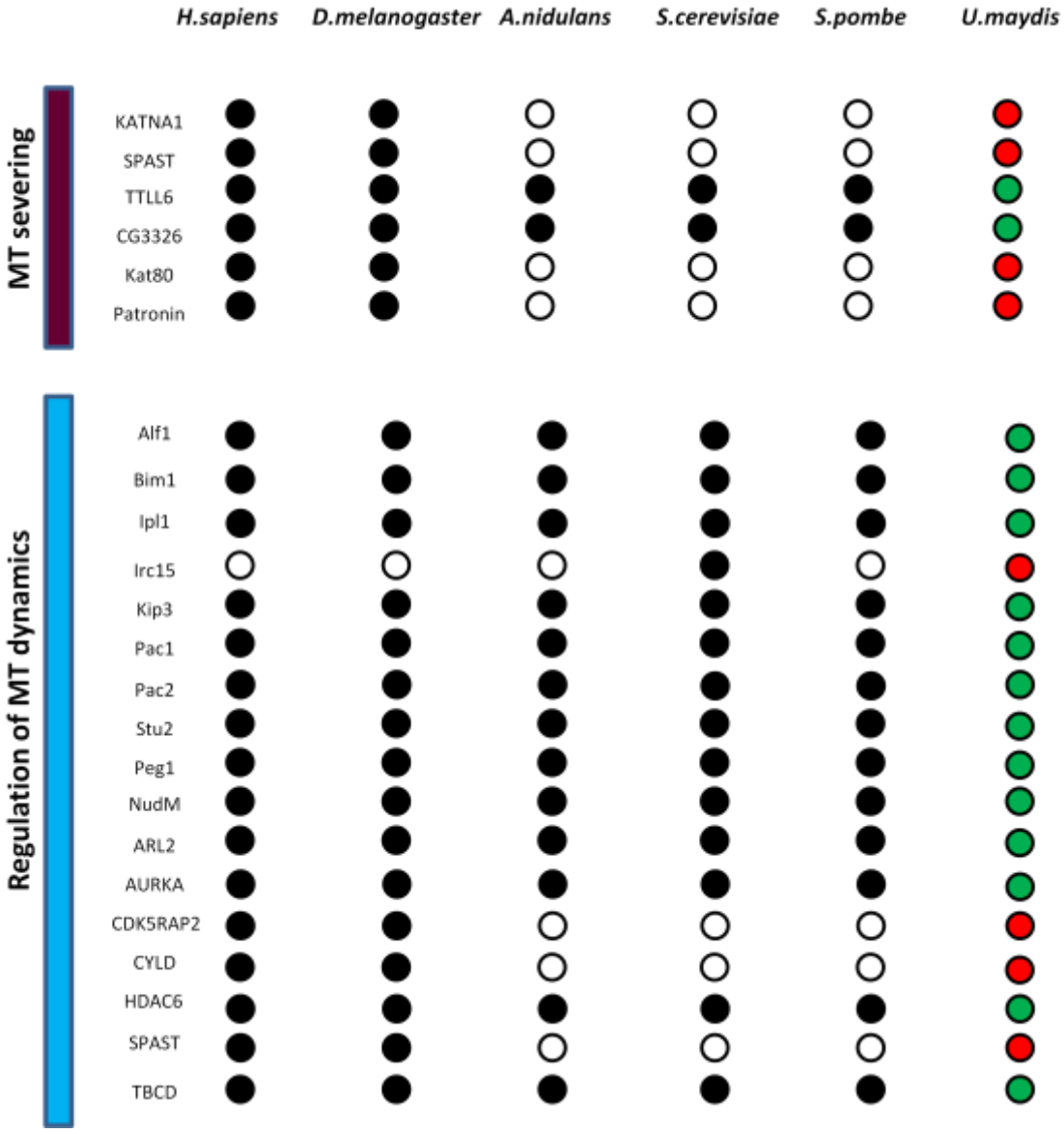
H.sapiens
D.melanogaster
A.nidulans
S.cerevisiae
S.pombe
U.maydis
MT severing
KATNA1
SPAST
TTLL6
CG3326
Kat80
Patronin
Regulation of MT dynamics
Alf1
Bim1
Ipl1
Irc15
Kip3
Pac1
Pac2
Stu2
Peg1
NudM
ARL2
AURKA
CDK5RAP2
CYLD
HDAC6
SPAST
TBCD

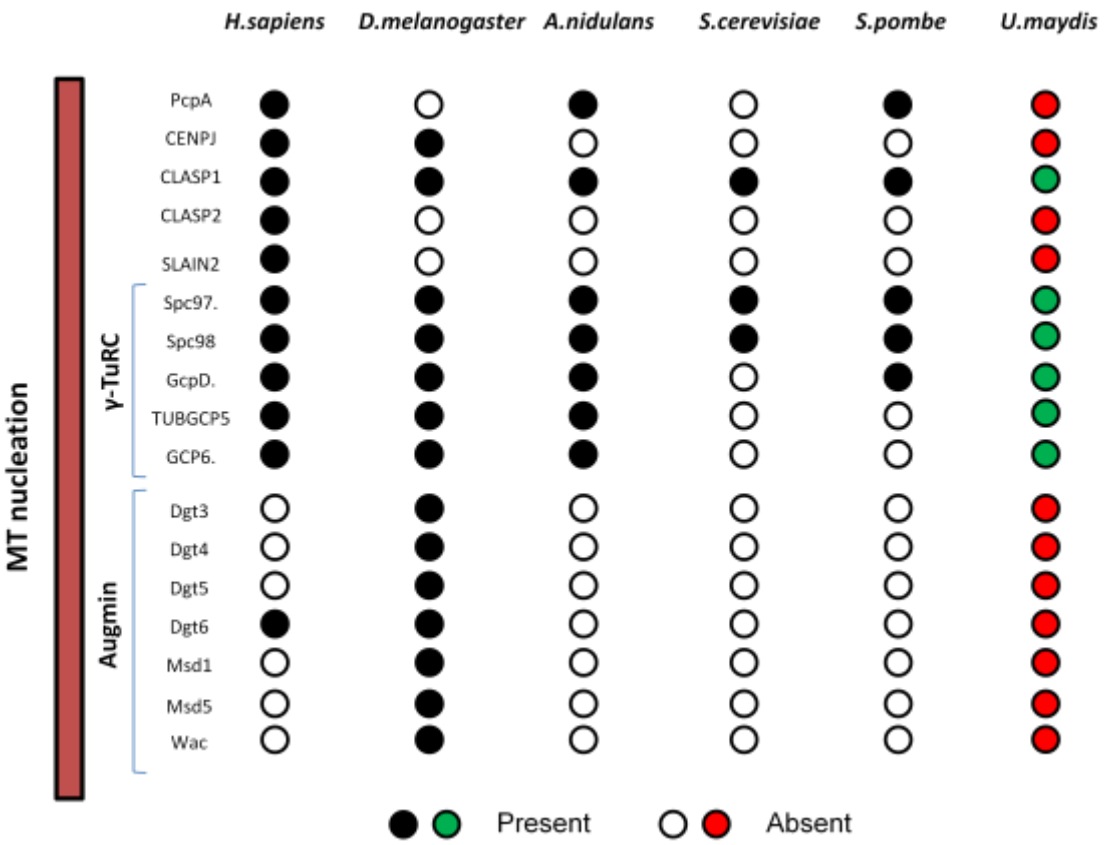

Figure 4.3 Distribution of MAPs among six different species.

Results of MAP searches in different organisms represented by dots, including final calls for *U. maydis*. In the end, 69 MAPs were marked as present in *Ustilago*. Names of the MAPs are on the left of the panel; names of the species are on the top. Black dots represent the presence of homologous sequences that are best hits to the MAPs named on the left, with the cut-off point of e^{-05} or more; white dots indicate no detectable orthologues or hits below the cut-off point of e^{-05}; green dots denote homologous sequences in *Ustilago*; red dots indicate no detectable orthologue.in *U. maydis.*

3. Proteins that are not well conserved in *U. maydis*:

- Attachment of spindle MTs to kinetochore (12/28),
- Spindle pole bodies (10/23),
- Cell polarity (2/6),
- MT stabilisation (10/33),
- MT cytoskeleton organisation (4/17),
- MTs bundle formation (7/23),
- Down-regulation of MT polymerisation (1/3),
- MT severing (2/6),
- MT depolymerisation (4/13),
- MT nucleation (6/17),
- MT destabilisation (0/5).

Analysis of the results showed that group of proteins which are not well conserved in *U. maydis* contained the highest number of functional groups, 10 out of 19, in comparison to the other two categories. It seems then, that within those functional groups, *U. maydis* must have different ways to carry out microtubule-related activities.

The first group of well-conserved proteins carries out **chromosome segregation** and also contains two complexes that belong in the attachment of spindle MTs to kinetochore's group. Those are DASH complex and CPC (chromosome passenger complex) (Appendix 1) and are essential for the chromosome segregation, however *U. maydis* does not seem to have the orthologue of yeast Sli15, which is present only in *S. cerevisiae*. It is also known that in budding yeast and other fungi there is only a single essential Aurora protein kinase, Ipl1 (Figure 4.4) (Chan and Botstein, 1993) (Francisco et al., 1994) (Buvelot et al., 2003), while in mammals, the Aurora kinases can be subdivided into three families: Aurora A, B and C (Buvelot et al., 2003). For *U. maydis*, all searches for Aurora kinases were able to find an orthologue, however the results always showed the same protein, which probably indicates that *Ustilago* has only one Aurora kinase. Another complex of proteins involved in the chromosome segregation is dynein complex. As this process requires

Chromosome segregation

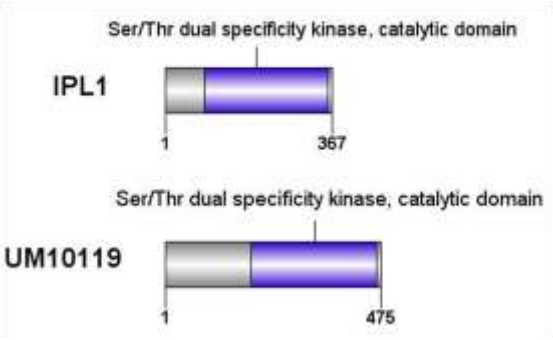

Nuclear migration along MT

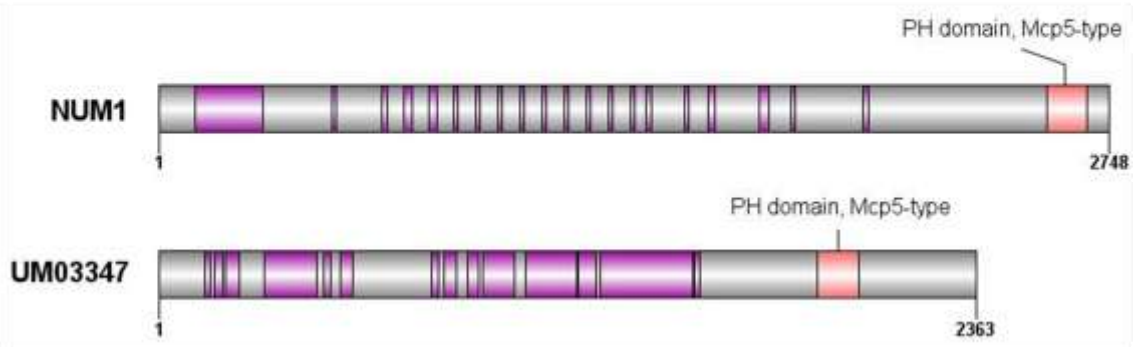

Up-regulation of MT polymerisation

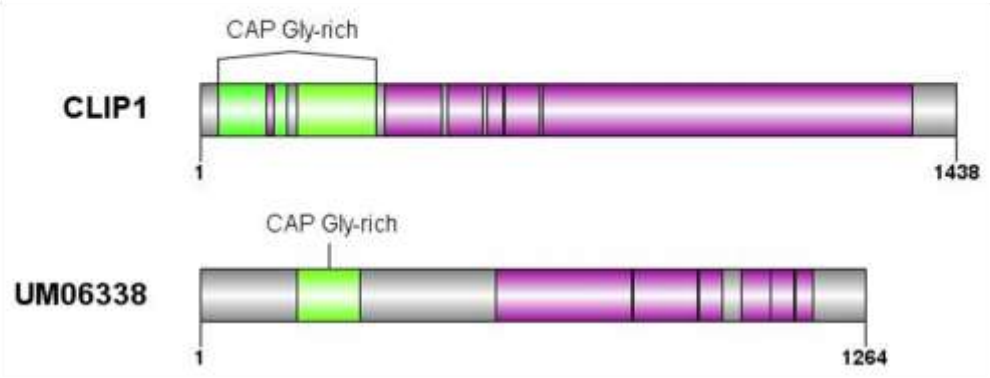

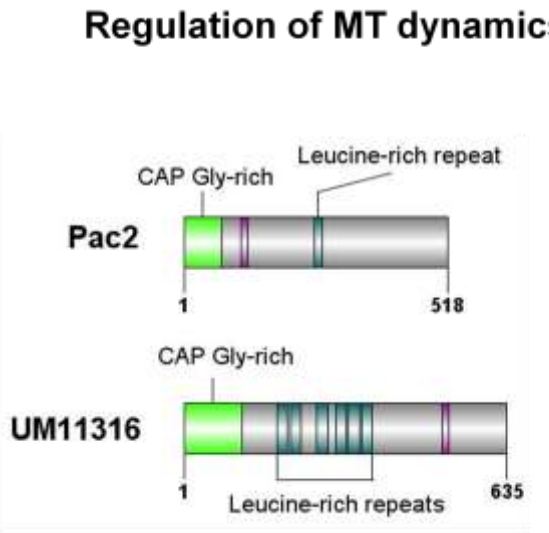

Figure 4.4 Examples of orthologues representing well conserved groups of proteins in *U. maydis.*

Each cartoon represents an example of a MAP with a potential *U. maydis* orthologue from a functional group established to be well conserved. Regions marked with different colours on each protein represent different domains.

stable bipolar attachments of spindle microtubules to kinetochores the dynein/dynactin motor complex localises transiently to kinetochores and is implicated in chromosome segregation, but its role remains poorly understood (Gassmann et al., 2008). Other proteins found to have orthologues in *U. maydis* include the *S. cerevisiae* kinesin-related gene products Cin8 and Kip1 that participate in the assembly of the bipolar mitotic spindle and have been suggested, together with Dyn1 (dynein heavy chain), to have a direct role for all three motors in generating a chromosome-separating force (Saunders et al., 1995). However, there were also proteins absent from *U. maydis*, which included *S. cerevisiae's* specific DASH components, Hsk3 and Spc34, Sli15, required for correct chromosome segregation (Kang et al., 2001), fission yeast Alp7, which forms a complex, critical for mitotic and meiotic spindle assembly and proper chromosome segregation (Tang et al., 2014), human APC2, operating at the cortex to ensure high-fidelity chromosome segregation and to prevent mitotic errors (Poulton et al., 2013), CDK5RAP2, required for spindle checkpoint function and chromosome segregation (Zhang et al., 2009b), KIF2B, a microtubule-depolymerising kinesin, that stimulates kinetochore-microtubule dynamics during distinct phases of mitosis to correct malorientation of chromosomes (Bakhoum et al., 2009), KNSTRN, an essential component of the mitotic spindle required for normal chromosome segregation and normal timing of sister chromatid segregation (Dunsch et al., 2011), SKA1 complex, an essential component of the human kinetochore, which can couple a cargo to microtubule depolymerisation and has a critical role in proper chromosome segregation (Welburn et al., 2009), SPAG5, contributes to the fidelity of chromosome alignment and mitotic progression (Dunsch et al., 2011; Thein et al., 2007), fruit fly's Mars, whose strictly controlled activity is required for accurate chromosome segregation (Li et al., 2009) and Mei-38, thought to stabilise kinetochore microtubules which in turn are important for interacting with homologous chromosomes at metaphase I of female acentrosomal meiosis (Wu et al., 2008).

Among possible orthologues found to be well conserved in *Ustilago maydis,* proteins responsible for **nuclear migration along MTs** had the highest (100 %) level of conservation. Five of those proteins belong to dynein complex NudA (dynein heavy chain), Dyn2 (dynein light chain), AN8669.2 (dynein light chain),

NudI (dynein intermediate chain) and NudN (dynein light intermediate chain), which has ability to transport of variety of cargoes and chromosome segregation (Trokter et al., 2012). The other three are yeast Num1 (Figure 4.4), a cortical protein, which controls cytoplasmic microtubule functions and nuclear migration during late anaphase by forming dynein-interacting cortical MT capture sites at both cellular poles (Farkasovsky and Kuntzel, 2001), Pac1 (homologue of human LIS1), involved in nuclear migration (Fujiwara et al., 1999), part of the dynein/dynactin pathway, which targets dynein to microtubule tips, which is necessary for sliding of microtubules along bud cortex, causing individual dynein motors to remain attached to microtubules for long periods (Lee et al., 2003), and *A. nidulans* NudC, which regulates Pac1 (NudF) protein, which in turn modulates the dynein/dynactin motor system that mediates nuclear migration (Xiang et al., 1995) (Chiu et al., 1997).

Proteins taking part in **up-regulation of MT polymerisation** also appear to be very well conserved in *U. maydis*. Among those that are likely to have orthologues in the corn smut fungus are components of the DASH protein complex, whose ring formation promotes microtubule assembly and stabilises MTs against disassembly (Westermann et al., 2005), human CLIP1 (Figure 4.4), one of the +TIPs, which was suggested by Slep and Vale, 2007 (Slep and Vale, 2007) to strongly promote MT polymerisation and act as a microtubule polymerisation chaperone and human FES, which induces dramatic tubulin polymerisation *in vitro* and may promote MT assembly (Laurent et al., 2004). Proteins without potential orthologues included Hsk3 and Spc34 from yeast DASH complex, Apc, which when added to purified tubulin *in vitro* it promotes the assembly of microtubule arrays (Munemitsu et al., 1994), MAPT (Tau), which increases the rate of polymerisation, decreases the rate of transit into the shrinking phase (catastrophe), and inhibits the rate of depolymerisation (Drechsel et al., 1992), PSRC1 (AMIGO annotation), SLAIN2, known to strongly stimulate processive MT polymerisation in interphase cells (Karpova et al., 2006; van der Vaart et al., 2011), Jupiter (Karpova et al., 2006), and Nod, that promotes polymerisation of MTs (Cui et al., 2005).

The final group of proteins well conserved in *U. maydis* is responsible for the regulation of **MT dynamics**. Within this group there are potential orthologues of yeast Stu2, a plus-end tracking protein (+TIP), which plays a central role in

regulating kinetochore-derived microtubules (Kitamura et al., 2010), Kip3, a multifunctional motor protein with microtubule depolymerase, plus-end motility, and antiparallel sliding activities (Rizk et al., 2014), and NudM, the largest subunit of the dynactin complex (Egan et al., 2012), which is thought to stabilise MTs and regulate their dynamics (Hayashi et al., 2005). There was also yeast Bim1 (human EB1) protein, which localises to growing MT ends and stabilises MTs (Slep and Vale, 2007) (Hayashi et al., 2005), Peg1, a microtubule binding protein that regulates the stability of dynamic microtubules and is required for mitotic spindle formation (Grallert et al., 2006), Alf1, responsible for the folding of alpha-tubulin (Feierbach et al., 1999) as well as MT dynamics, Pac1 (human LIS1) which targets dynein to MT tips, necessary for sliding of MTs along bud cortex (Lee et al., 2003), HDAC6, thought to function as a MAP that regulates microtubule dynamics under certain conditions (Asthana et al., 2013), and Aurora kinases, AURKA and Ipl1 (AURKB), that control MT dynamics through negative regulation of MT depolymerising KIF18B-MCAK (KIF2C) complex formation via phosphorylation of MCAK (Tanenbaum et al., 2011). The proteins which were not found in *U. maydis* included budding yeast Irc15, that regulates microtubule dynamics *in vivo* and whose loss of function leads to delayed mitotic progression (Keyes and Burke, 2009), human CDK5RAP2, a protein which exists in one of the various complexes formed by EB1 to promote MT growth and dynamics at the plus ends (Fong et al., 2009), CYLD, which modulates microtubule dynamics and cell polarisation in migrating vascular endothelial cells (Gao et al., 2010), and SPAST, suggested in a number of studies to regulate MT dynamics (Salinas et al., 2005).

The second category contains groups of proteins relatively well conserved in *U. maydis.* The first group takes part in **mitotic spindle organisation** and MAPs found to be potentially present in *Ustilago* include DASH complex proteins, which form a spindle-associated complex that has function in maintaining spindle integrity (Cheeseman et al., 2001) (Enquist-Newman et al., 2001), Ase1 (Figure 4.5), mitotic spindle midzone-localized microtubule-associated protein (MAP) family member, required for spindle elongation and stabilisation (Schuyler et al., 2003), Kip1 and Cin8, exclusively nuclear kinesin-related motor proteins (Cui et al., 2009), that are required for pole separation during spindle

Mitotic spindle organisation

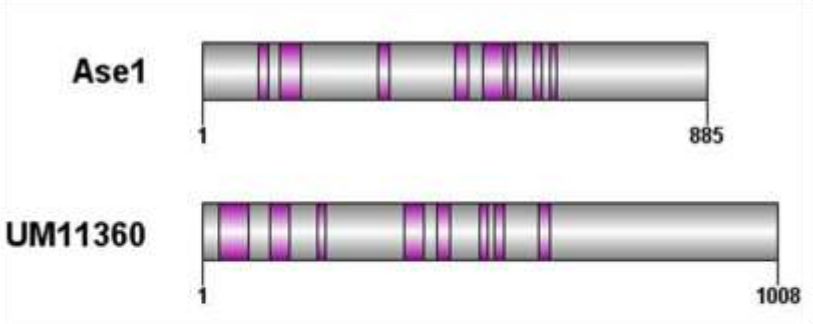

Minus-end binding

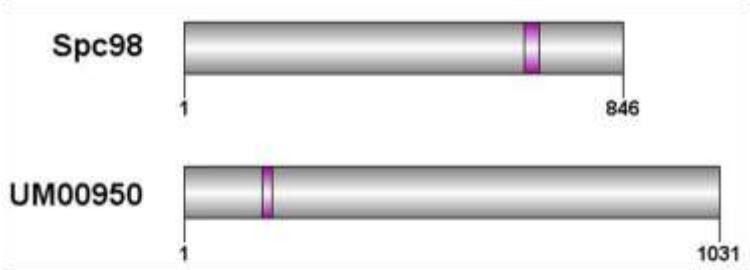

+TIPS

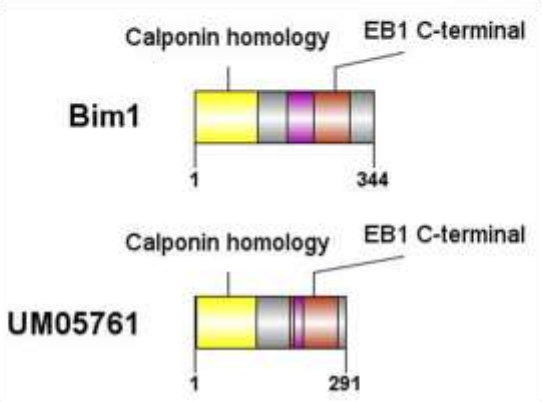

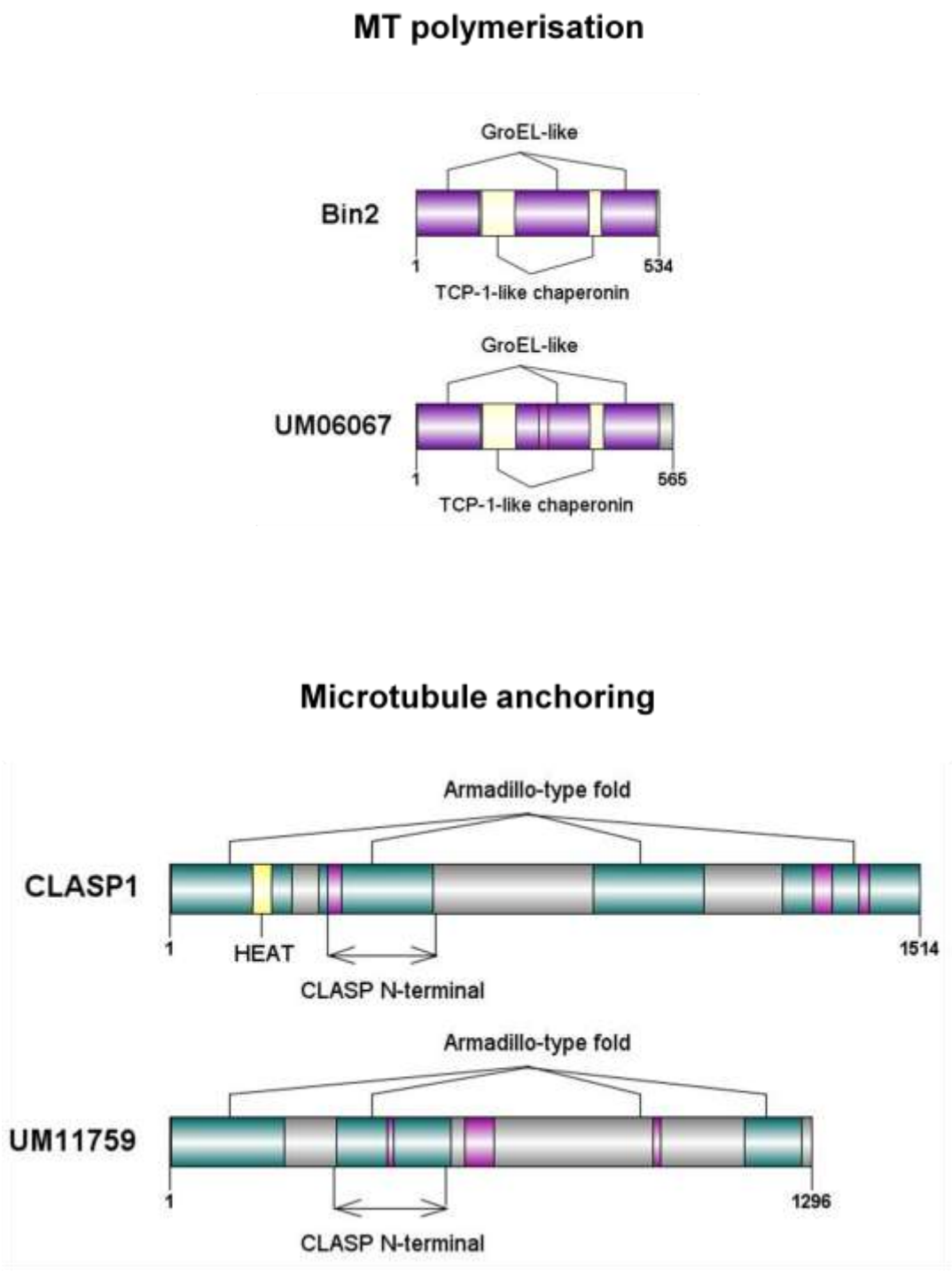

Figure 4.5 Examples of orthologues representing relatively well conserved groups of proteins in *U. maydis.*

Each cartoon represents an example of a MAP with a potential *U. maydis* orthologue from a functional group established to be relatively well conserved. Regions marked with different colours on each protein represent different domains.

assembly (Hoyt et al., 1992), Ipl1 kinase with a role in spindle disassembly that is independent from its previously identified functions (chromosome segregation and cytokinesis) (Buvelot et al., 2003), Kar3, a C-terminal kinesin with minus end-directed motility (Endow et al., 1994) (Benanti et al., 2009) which, during vegetative growth, localises to the nuclear face of the spindle pole body (SPB) and the mitotic spindle and has roles in forming, positioning, and maintaining the spindle (Manning et al., 1999) (Page et al., 1994) (Saunders et al., 1997) (Benanti et al., 2009), AURKA (Aurora kinase A), mitotic kinase that associates with the centrosome and the spindle microtubules during mitosis and plays a critical role in various mitotic events including the establishment of mitotic spindle, centrosome duplication, centrosome separation as well as maturation and chromosomal alignment (Katayama et al., 2001), KIF11, a motor protein required for establishing a bipolar spindle (Rapley et al., 2008), and Ran, a GTPase, predicted to facilitate spindle assembly by remaining in the GTP-bound state around the chromatin in mitosis (Trieselmann and Wilde, 2002). It was also concluded, using RNA interference (RNAi) screen and a bioinformatics analysis, that CG7033, CG8258, TCP1 and TCP1-zeta are involved in mitotic spindle organisation (Goshima et al., 2007) (Hughes et al., 2008) and are potentially present in *U. maydis*. The final five proteins conserved in *Ustilago* belong to dynein complex (NudA, Dyn2, AN8669.2, NudI and NudN) which is known to have functions during spindle assembly (Trokter et al., 2012). MAPs which were not found in *Ustilago* included *S. cerevisiae* specific DASH complex components Hsk3 and Spc34, yeast Cik1 that helps Kar3 in performing the spindle positioning role (Cottingham et al., 1999), Vik1, able to bind the microtubule lattice cooperatively with Kar3 and promote microtubule stabilisation (Allingham et al., 2007), *A. nidulans* AN10225 (AmiGO annotation), human Apc, thought to regulate spindle microtubule dynamics, probably through its interaction with the microtubule plus-end binding protein, EB1 (Caldwell and Kaplan, 2009), KIF2A, localised to spindle poles in vivo to control bipolar spindle assembly (Ganem and Compton, 2004) (Jang et al., 2008), KNSTRN (kinastrin), a component of the mitotic spindle required for maintenance of spindle pole architecture and progression into anaphase (Dunsch et al., 2011). Also MAP4, a Tau-related protein essential for maintaining spindle position and the correct cell-division axis in human cells (Samora et al., 2011), PSRC1, a MT-destabilising protein which regulates mitotic spindle dynamics (Jang et al.,

2008), SPAG5 (Astrin), a mitotic spindle–associated protein required for the correct alignment of all chromosomes at the metaphase plate and normal spindle architecture (Dunsch et al., 2011), SPECC1L, which is a cytoskeletal cross-linking protein involved in spindle orientation and cell polarity (Saadi et al., 2011), STARD9, a mitotic kinesin involved in mitotic spindle assembly (Torres et al., 2011) could not be found. In addition, *Drosophila's* Asp helping to organise both the spindle poles and the central spindle (Wakefield et al., 2001), Mars, required for the interaction of the centrosomal microtubules with the nuclear envelope and the spindle microtubules (Zhang et al., 2009a), Mei-38, identified due to its role in mitotic spindle assembly in (Wu et al., 2008), Nod, identified in a genetic screen for proteins that contribute to spindle assembly (Goshima et al., 2007), Patronin, regulating mitotic spindle elongation (Goshima et al., 2007), and Augmin complex, which plays critical role in the central spindle formation during anaphase (Uehara et al., 2009) do not have orthologues in *U. maydis*.

Minus-end binding proteins which fulfil the MAPs criteria seem to be relatively well conserved in *U. maydis*, particularly the gamma-tubulin complex (gamma-TuC) proteins. Two members of this complex, yeast Spc97 (hGCP2) and Spc98 (hGCP3) (Figure 4.5), are part of a gamma-tubulin small complex (gamma-TuSC), which is the immediate template for growing microtubule ends (Wiese and Zheng, 2006) and component of the gamma-TuC (Raynaud-Messina and Merdes, 2007). Gamma-TuC also consists of at least three more GCPs (gamma-tubulin complex proteins) (Xiong and Oakley, 2009) - A*. nidulans* GcpD (hGCP4), human GCP5 and GCP6 - and is part of gamma-tubulin ring complex (gamma-TuRC). Members of gamma-TuRC help in the assembly and stability of large gamma-TuCs (Xiong and Oakley, 2009). Proteins that were not found to be conserved in *U. maydis* were *S. pombe's* Alp7, required for organisation of bipolar spindles (Sato et al., 2004), human CAMSAPs (1-3) which regulate microtubule minus-end growth and are specifically deposited on the lattice formed by microtubule minus-end polymerisation (Jiang et al., 2014), and finally Patronin, that binds with high selectivity to microtubule minus ends and acts as a "cap", stabilising these ends and protecting them against the actions of microtubule depolymerases (Goodwin and Vale, 2010).

Furthermore, microtubule plus-end binding proteins (**+TIPS**), which localise to the dynamic plus ends of microtubules where they stimulate microtubule growth and recruit signalling molecules (Slep and Vale, 2007), were found to be relatively well conserved in *U. maydis*. The potential orthologues include (1) Bim1 (human EB1) (Figure 4.5) and (2) CLIP1, well-studied plus-end tracking proteins that target growing microtubule plus ends in the form of comet tails and regulate microtubule dynamics (Lopus et al., 2012), (3) Pac1, which targets dynein to microtubule plus ends, necessary for sliding of microtubules along the bud cortex (Lee et al., 2003), (4) Stu2 (XMAP215), which has an intrinsic ability to promote microtubule polymerisation (Gard and Kirschner, 1987) (Charrasse et al., 1998) (Ohkura et al., 2001), (5) NudM, important for cytoplasmic dynein function *in vivo* (Schroer, 2004; Yao et al., 2012), and (6) CLASP1, involved in the ability to bind and influence the dynamic properties of spindle microtubules (Maiato et al., 2003). Among the proteins not present in the corn smut fungus were Kar9, thought to track microtubule plus-ends by a surfing mechanism (movement of a +TIP on the potential energy "wave" created by the existence of an end-specific conformation or protein (Folker et al., 2005) (Liakopoulos et al., 2003), CLASP2, which marks the distal ends of MTs at the leading edge of the cell and is involved in organising stabilised MTs (Akhmanova et al., 2001), Dst (AmiGO annotation), KIF2C and KIF18B, which physically interact and enhance each other's affinity for MT plus ends, strongly suggesting that they act together to promote MT plus-end depolymerisation (Tanenbaum et al., 2011), MLPH (AmiGO annotation), and Nod, preferentially localised to the plus ends of MTs and stimulating MT polymerisation (Cui et al., 2005).

Finally **microtubule anchoring** MAPs are relatively well conserved in *Ustilago*. Two proteins from this group were found to have orthologues in *Ustilago*: CLASP1 (Figure 4.5), bound to the growing MT in human cells is able to anchor very short MT fragments at the cell cortex formed in the proximity of the Golgi membranes and by coating them prevent their disassembly to allow them to serve as seeds for polymerisation (Efimov et al., 2007), and human HOOK3 responsible for microtubule anchoring at centrosome (Carbon et al., 2009). The rest of the proteins, which included *S. cerevisiae* Num1, suggested to have the ability to attach the dynein motor domain and the plus-end of cytoplasmic MTs to the cellular cortex (Farkasovsky and Kuntzel, 2001), *A. nidulans* PcpA

(pericentrin-related), suggested to play a role in anchoring interphase microtubules to cortical membranes for stabilising the position of the nucleus (Chen et al., 2012), human CAMSAP3, specifically required for the biogenesis and the maintenance of zonula adherens by anchoring the minus-end of microtubules to zonula adherens and by recruiting the kinesin KIFC3 to those junctional sites (Meng et al., 2008), CEP57 and CLASP2, bound to the growing MT tip and associated with the cell cortex at the same time, bringing the MT end in very close proximity to the cell edge (Mimori-Kiyosue et al., 2005), were not found to be present in *Ustilago*.

The third category of MAPs consists of proteins that are not well conserved in *Ustilago* and it contains the highest number of groups in comparison to the other two categories. The first group of proteins includes MAPs taking part in the **attachment of spindle MTs** to kinetochore (12/28), where less than half of proteins were present in *U. maydis*. In this group there were proteins that belong to the well-conserved DASH complex (Ask1, Dad1, Dad2, Dad3, Dad4, Dam1, Duo1, Hsk3, Spc19 and Spc34), a microtubule-binding complex, containing around 8-10 subunits in yeasts, that is transferred to the kinetochore prior to mitosis, thereby defining a new step in kinetochore maturation (Li et al., 2002b). It forms part of the kinetochore, associates with microtubules when the kinetochore attaches to the spindle and plays a role in spindle attachment, chromosome segregation and spindle stability (Li et al., 2005). The results show that *U. maydis* lacks two of them, Hsk3 and Spc34. Other possible orthologues in *U. maydis* include yeast Ame1, essential kinetochore protein associated with microtubules and SPBs, involved in spindle checkpoint maintenance (Pot et al., 2005), and human AURKC (Aurora-C kinase), a component of the chromosomal passenger complex (CPC) which acts as a key regulator of mitosis in humans (Sasai et al., 2004). There are also Ipl1 (human Aurora B) Figure 4.6), Sli15 (human INCENP), and Bir1 (human BIRC5) that belong to the chromosomal passenger complex, CPC, which is an essential regulator of chromosome segregation, spindle checkpoint, and cytokinesis (Ruchaud et al., 2007). Proteins without possible orthologues in *Ustilago* also included fission yeast Fta2, essential kinetochore protein, required for bipolar chromosome attachment (Kerres et al., 2006), and Nsk1, promoting proper kinetochore-MT interactions (Chen et al., 2011), as well as human APC, which modulates

Attachment of spindle MTs to kinetochore

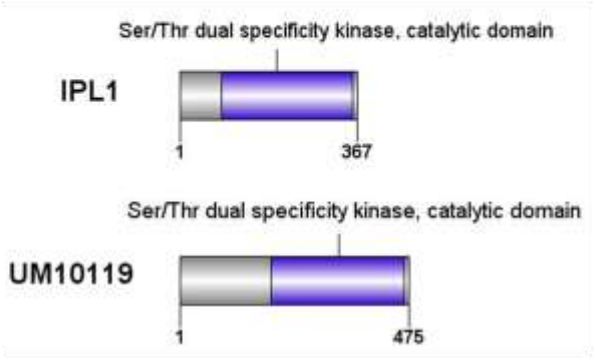

Spindle pole bodies

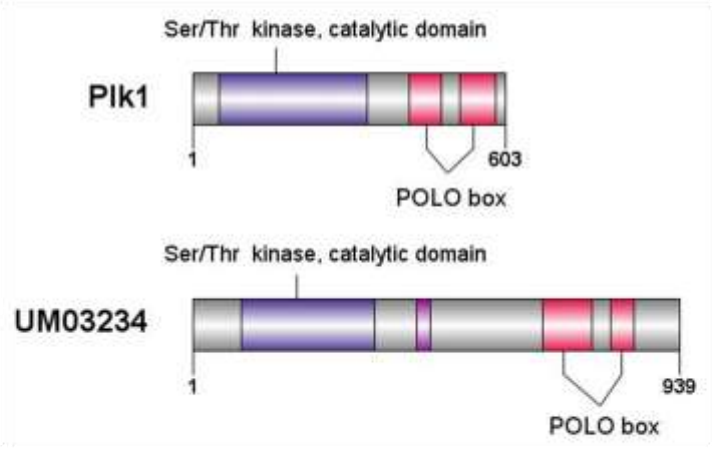

Cell polarity

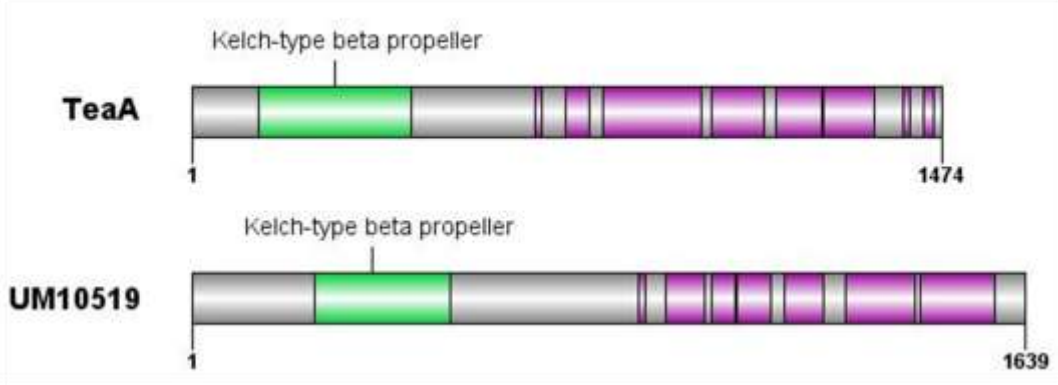

MT stabilisation

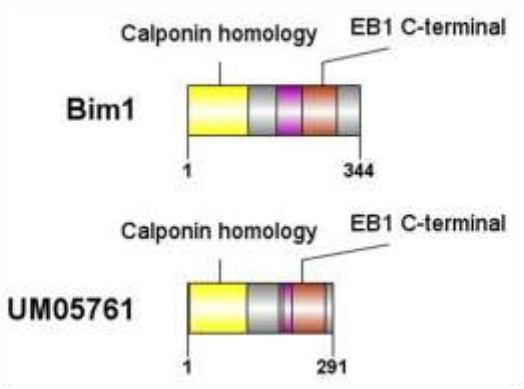

MT cytoskeleton organisation

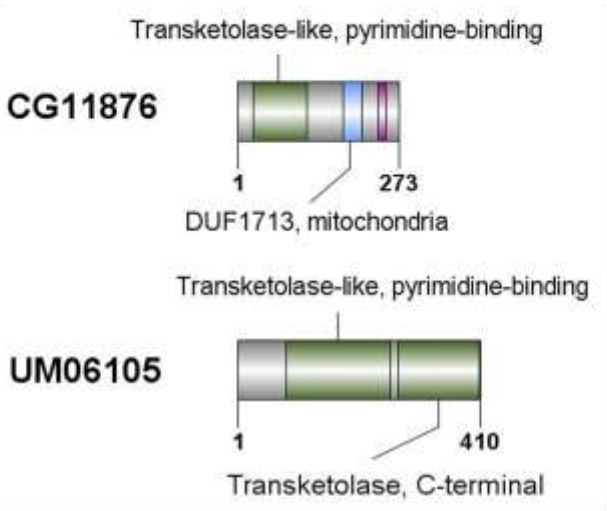

MT bundle formation

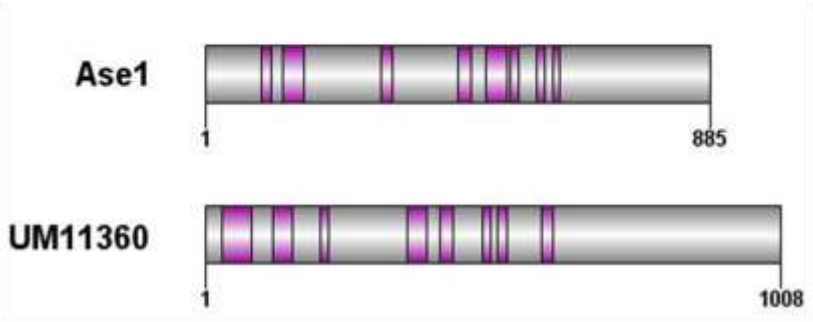

Down- regulation of MT polymerisation

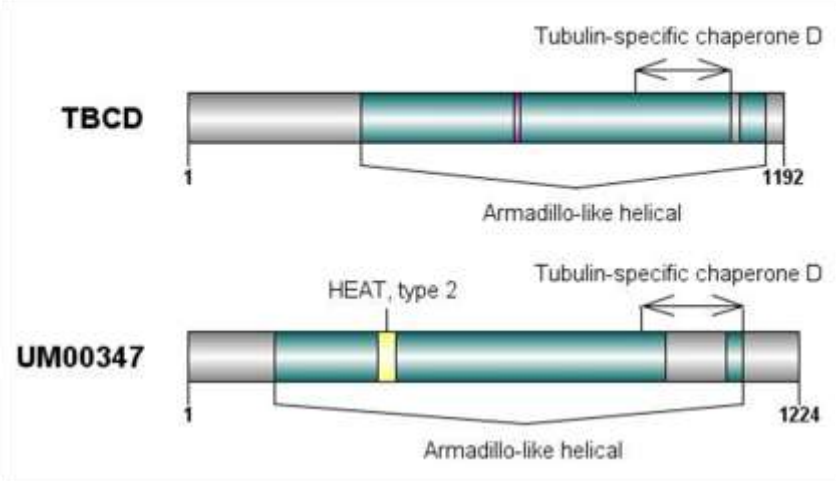

MT severing

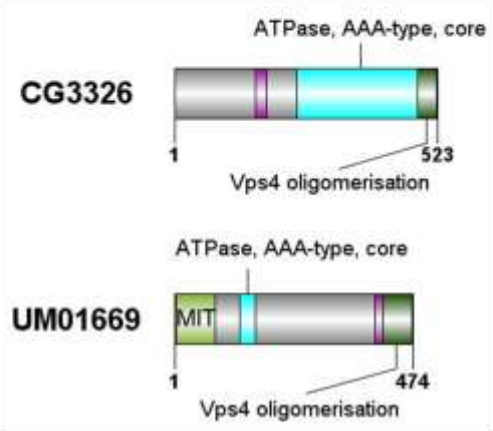

MT depolymerisation

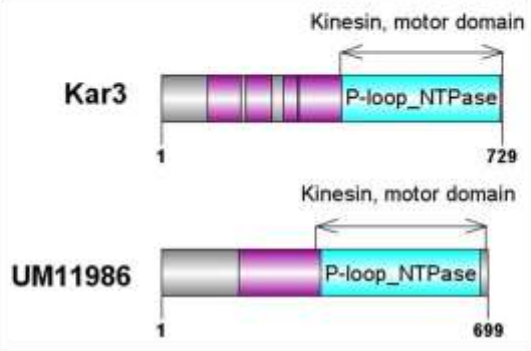

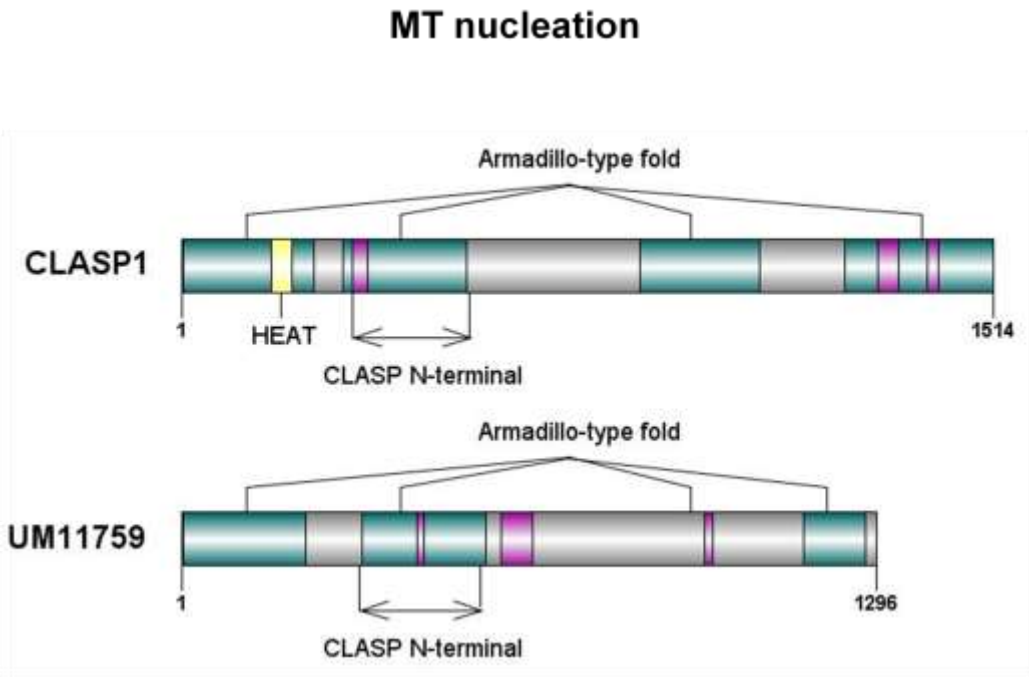

Figure 4.6 Examples of orthologues representing not well conserved groups of proteins in *U. maydis*.

Each cartoon represents an example of a MAP with a potential *U. maydis* orthologue from a functional group established not to be well conserved. Regions marked with different colours on each protein represent different domains.

kinetochore-microtubule attachments (Caldwell and Kaplan, 2009), CASC5, kinetochore protein with a role in the association with checkpoint proteins Bub1 and BubR1, but also in the attachment to the spindle microtubules (Kiyomitsu et al., 2007), KNSTRN, which helps in regulation of attachment of spindle microtubules to kinetochore (Dunsch et al., 2011; Huang et al., 2012), SPAG5, promoting stable microtubule-kinetochore attachments (Dunsch et al., 2011), and Augmin complex, which, in human cells, plays critical and non-redundant roles in the kinetochore–MT attachment and also central spindle formation during anaphase (Uehara et al., 2009).

Proteins in the **spindle pole bodies** group contain MAPs supporting mitosis at that particular spot in the cell. The spindle pole body (SPB) is the microtubule organising centre in yeast cells and has a crucial role in bipolar spindle assembly (Lim et al., 2009). It is also functionally equivalent to the centrosome of higher eukaryotes (Rout and Kilmartin, 1990). However, unlike the centrosome the SPB does not contain centrioles, and generally centrosomes and SPBs bear little resemblance (Pereira and Schiebel, 2001). Proteins found to be conserved in *U. maydis* include Ame1: an essential kinetochore protein associated with microtubules and SPBs, involved in spindle checkpoint maintenance (Pot et al., 2005); Spc97 (hGCP2) and Spc98 (hGCP3), the components of the spindle pole body (SPB) and part of the gamma-tubulin small complex (gamma-TuSC), the essential core of the microtubule nucleating machinery which interacts with Spc110 at the SPB inner plaque (Nguyen et al., 1998) (Knop et al., 1997) (Kollman et al., 2010); Spc110, an essential structural component of the SPB that spans between the central and inner plaques of this multilamellar organelle (Nguyen et al., 1998), in addition, it stabilises gamma-TuSC rings into extended filaments and is required for oligomer formation under physiological buffer conditions (Kollman et al., 2010); Spc19, essential subunit of DASH complex, localised to the nuclear side of the spindle pole body (Li et al., 2002b); Cdc11, which acts as a bridge between SIN (septation initiation network) proteins mediating their association with the spindle pole body (SPB), which is required for cytokinesis (Morrell et al., 2004) (Krapp and Simanis, 2014); Peg1, CLIP170- associated protein, required for spindle and astral microtubules formation (Grallert et al., 2006); yeast Pkl1, in particular its Tail domain, is required for the establishment of bipolarity *in vivo* in *S. pombe*

(Simeonov et al., 2009); and finally, *A. nidulans* NudC protein, which plays a broad role during mitosis, and interacts directly with NudF at spindle-pole bodies at different stages of the cell cycle (Helmstaedt et al., 2008). Proteins without identified orthologues included yeast Cik1, SPB-associated component that is important for proper organisation of microtubule arrays and the establishment of a spindle during vegetative growth (Page and Snyder, 1992), Kar1, involved in spindle pole body duplication during mitosis (Spang et al., 1995), Spc29, linking the central plaque component Spc42 to the inner plaque component Spc110, also required for SPB duplication (Elliott et al., 1999), Spc34, essential component of the DASH complex, also localised to nuclear side of spindle pole body (Li et al., 2002b), Spc42, involved in SPB duplication and which may facilitate attachment of the SPB to the nuclear membrane (Bullitt et al., 1997), Spc72, required for astral microtubule formation at the SPB half-bridge (Hoepfner et al., 2002), Spc110, involved in connecting nuclear microtubules to SPB (Mirzayan et al., 1992), Vik1 protein which localises Kar3 at the spindle pole bodies and it was suggested that their role is to focus and crosslink microtubules for bipolar spindle assembly and stabilisation (Allingham et al., 2007), Alp7, which forms a complex which is critical for mitotic and meiotic spindle assembly with Alp14 (Tang et al., 2014), Fta6 (AmiGO annotation), Rsp1 (AmiGO annotation), Sad1, which a maintains a functional interface between the nuclear membrane and the microtubule motor proteins (Chikashige et al., 2006), and Wrap73 (AmiGO annotation).

MAPs responsible for the **establishment or maintenance of cell polarity regulating cell shape** are not well conserved in *U. maydis*. The only ones I found to have potential orthologues in *U. maydis* were Stu2 (AlpA in *A. nidulans*), an orthologue of the MT polymerase CKAP5 in mammals (Brouhard et al., 2008), and cell-end marker protein TeaA, important for localising the growth machinery at hyphal tips (Takeshita et al., 2008). It has been suggested that there is a functional connection between TeaA and AlpA, both present at MT plus-ends, for proper regulation of MT growth at hyphal tips (Takeshita and Fischer, 2011). The convergence of MT plus-ends at polarised growth sites is thought to be important for the fine-tuning of polarity in highly polarised filamentous fungi tip (Takeshita et al., 2013). The proteins that were not found to be present in *U. maydis* were fission yeast Mug164, involved in the cell

polarity process and in regulation of microtubule growth (Martin-Castellanos et al., 2005), *A. nidulans* PcpA, which has important roles in nuclear positioning and in polar growth (Chen et al., 2012) and human MAPs MACF1, required for correct polarity of the oocyte (Gupta et al., 2010), and MAP7, a microtubule-stabilising protein that may play an important role during reorganisation of microtubules during polarisation and differentiation of epithelial cells (Masson and Kreis, 1993).

Another group of proteins that are not well conserved in *Ustilago* is responsible for **MT polymerisation**. Five of them were found to be present and they included budding yeast Bim1 (EB1), which has an intrinsic activity of promoting MT assembly, which can be stimulated upon binding APC or p150^{glued} to the EB1 tail (Nakamura et al., 2001) (Ligon et al., 2003) (Fong et al., 2009), Bin2 (Figure 4.6) and Bin3, the components of yeast cytoplasmic chaperonin complex required for assembly of microtubules and actin *in vivo* (Chen et al., 1994), Rbl2 which may participate as a scaffolding protein for beta tubulin in the assembly of the tubulin heterodimer (Archer et al., 1998) and Xrn1, which has a direct structural role in microtubule formation in yeast (Interthal et al., 1995) . In addition, fourteen were not found to be present in *U. maydis*. Those were budding yeast protein Mhp1, promoting microtubule assembly *in vivo* (Irminger-Finger and Mathis, 1998), human CENPJ, binding to tubulin heterodimers and inhibiting microtubule assembly (Hung et al., 2004), FBXO5 (AmiGO annotation), MAP2, originally discovered for and characterised by its ability to bind and stabilise microtubules (Dehmelt and Halpain, 2005), MAP4, which promotes MT polymerisation (Kitazawa et al., 2000), MAPT, involved in promoting microtubule assembly (Yoshida and Goedert, 2012) and TPPP, which induces tubulin self-assembly into intact frequently bundled microtubules (Hlavanda et al., 2007).

MAPs regulating **MT stabilisation** are also poorly conserved. Among potentially conserved proteins were budding yeast proteins: Kip2, which stabilises microtubules by targeting Bik1 to the plus ends of MTs (Carvalho et al., 2004), Bim1 (humanEB1), which together with dynactin complex (represented here by NudM) is thought to stabilise microtubules by forming a plus-end complex at microtubule growing ends with ill-defined mechanisms (Hayashi et al., 2005),

Pac2 (human TBCE) shown to be required for normal microtubule stability in vivo together with TBCD (Sce Cik1) (Hoyt et al., 1997), fission yeast Peg1 promoting microtubule stability in mitosis (Grallert et al., 2006), human AURKA, a cell cycle-regulated kinase that appears to be involved in stabilising spindle microtubules during chromosome segregation in a kinase-independent manner (Toya et al., 2011), CAPN6, a microtubule-stabilising protein expressed in embryonic tissues that may be involved in the regulation of microtubule dynamics and cytoskeletal organisation (Tonami et al., 2007), CLASP1 (Figure 4.6), CLIP-associated protein, that can induce MT stabilisation when present only at the distal ends of MTs (Akhmanova et al., 2001), and CLIP1, suggested to act cooperatively with EB1 to regulate microtubule dynamics by the stabilisation of microtubule plus ends, which may involve modification of an aspect of the stabilising cap (Lopus et al., 2012). Proteins that were not found to be conserved in *Ustilago* include fission yeast Alp7, required for stability of microtubule bundles (Zheng et al., 2006), budding yeast Ber1, thought to be involved in microtubule stability in yeast (Fiechter et al., 2008), Kar9, suggested by Huisman, 2004 (Huisman et al., 2004) and Cuschieri, 2006 (Cuschieri et al., 2006) to promote microtubule stabilisation within the bud, Mhp1, stabilising interphase microtubules in yeast (Irminger-Finger and Mathis, 1998), Spc72, required for stabilisation of astral microtubules at the SPB outer plaque (Hoepfner et al., 2002), human APC which associates with MT ends and correlates directly with their increased growth stability (Kita et al., 2006). Moreover, AXIN1, which associates with microtubules and unexpectedly stabilises MTs through DVL (Ciani et al., 2004), CAMSAP2 and CAMSAP3 which are specifically deposited on the growing MT minus-ends and form stable MT stretches that can serve as ‘‘seeds’’ for repeated MT outgrowth (Jiang et al., 2014), CKAP2, whose regulation of microtubule dynamics may be vital for tumour suppression (Tsuchihara et al., 2005), CLASP2, which carries the same function in MT stabilisation as CLASP1, DCX (doublecortin), a MAP which directly interacts with microtubules and, which results in MT stabilisation (Horesh et al., 1999), DVL1, associated with axonal MTs and regulating MT stability through the inhibition of GSK-3beta (ser/thr kinase) (Ciani et al., 2004). In addition, GAS2L1 and GAS2L2 which have properties that allow them to stabilise MTs and protect them from depolymerisation by nocodazole (Goriounov et al., 2003), MAP10, known to directly stabilise MTs participate in

cytokinesis (Fong et al., 2013), MAP1S, which via its light chain stabilises the MTs (Orban-Nemeth et al., 2005), MAP7, with a role in stabilising and reorganising the microtubule cytoskeleton during epithelial cell polarisation and differentiation (Fabre-Jonca et al., 1999; Masson and Kreis, 1995), MAPT, which promotes microtubule stability and might be involved in the establishment and maintenance of neuronal polarity (Yoshida and Goedert, 2012). Finally there are *D. melanogaster* Mei-38, required for the stability of parallel microtubules, including the kinetochore microtubules (Wu et al., 2008), Patronin which caps and stabilises microtubule minus ends, a critical activity in the organization of the microtubule cytoskeleton (Goodwin and Vale, 2010), SPECC1L, whose role in microtubule stability was suggested after experiments in which this protein was overexpressed (Saadi et al., 2011), and TPPP which is able to stabilise the microtubules, which is fulfilled via its bundling activity (Olah et al., 2006).

Proteins found to take part in the **organisation of the microtubule cytoskeleton** were also not found to be well conserved in *U. maydis*. For most of them, not much is known, apart from helping to organise MTs. From out of 18 potential candidates, only 5 had possible orthologues. Those are CG3731, CG8036, CG8142 and CG11876, all of which were found in a study that aimed to identify novel MAPs from early *Drosophila* embryos by Hughes, 2008 (Hughes et al., 2008). There is also TBCB (Tubulin folding cofactor B), whose actual role as MT organiser is still unknown (Kortazar et al., 2007). The proteins that were not found conserved in *U. maydis* are yeast Abm1, human ATAT1, CRIPT, DVL1, MAP1A, MAP6, STMND1, TACC3, UXT and fruit fly's CG11298, RanM, TektinA, and TektinC.

Next group of proteins that are not well conserved in *U. maydis* is responsible for **MT bundle formation.** Only 7 out of 23 MAPs were found have potential orthologues in *Ustilago*. These are Ase1, which is a dosage-dependent microtubule-bundling factor (Yamashita et al., 2005), Bim1 (EB1), known to, together with CDK5RAP2, induce MT bundling (Fong et al., 2009), CAPN6, causing the formation of microtubule bundles (Tonami et al., 2007), CLASP1, whose microtubule binding region bundles microtubules, rendering them non-dynamic (Maiato et al., 2003), CLIP1, responsible for promoting microtubule

growth and microtubule bundling (Slep and Vale, 2007), DNM2, known to be involved in producing microtubule bundles and to bind and hydrolyse GTP (Thompson et al., 2002), and MARK4, a serine/threonine kinase which can perform microtubule bundle formation (Naz et al., 2013). The rest of the proteins which have not been found to be conserved in *U. maydis* are fission yeast Alp7, proposed to allow the existence of stable microtubule bundles (Zheng et al., 2006), human CCSER2 (AmiGO annotation), CDK5RAP2, a part of complex with EB1 which promotes MT growth and induces MT bundling in vitro (Fong et al., 2009), GAS2L1 and GAS2L2, both possessing MT bundling activity (Goriounov et al., 2003), KATNA1 (AmiGO annotation), MAP1B (AmiGO annotation), MAP1S, its light chain binds and bundles the microtubules (Orban-Nemeth et al., 2005), MAP2 and MAPT (tau) which have the ability to induce microtubule bundles in heterologous cell systems (Lewis et al., 1989) (Weisshaar et al., 1992) (Dehmelt and Halpain, 2005), MAP7 (GO annotation), NAV1 (AmiGO annotation), PSRC1 (AmiGO annotation), SPAST which has an intrinsic bundling activity (Salinas et al., 2005), TPPP, shown to have MT bundling activity in many experiments (Hlavanda et al., 2002), and *Drosophila's* Mei-38 that has the microtubule-binding and bundling activities (Goshima, 2011).

Another group of proteins that was not found to be well conserved in *U. maydis* is responsible for **down-regulation of MT polymerisation**. It seems that only one protein (out of three) has a potential orthologue, human TBCD (Figure 4.6), which is capable of inducing tubulin and microtubule destruction *in vivo*, but that this reaction is inhibited by interaction of TBCD with Arl2 and potentially other interacting effectors (Tian et al., 2010). SNCA (α-synuclein), which causes MT instability in neurons, Tau that protects microtubules from α-synuclein (Qureshi and Paudel, 2011), and STMN1, which destabilises microtubules, however it is not known how (Cassimeris, 2002), were among the proteins without potential *Ustilago* representatives.

MT severing proteins are not well-represented in *Ustilago's* proteome. Only human TTLL6 (tubulin polyglutamylase) that participates in tubulin polyglutamylation, thought to potentially regulate MT severing (Lacroix et al., 2010) and *Drosophila's* fidgetin (CG3326), which may sever MTs, though this has not been demonstrated experimentally (Zhang et al., 2007), have potential

orthologues. The rest of the proteins include katanin, a heterodimer consisting of a 60-kD catalytic subunit (KATNA1), which has the microtubule-severing activity (Hartman et al., 1998; McNally and Thomas, 1998) and an 80-kD targeting and regulatory subunit (Kat80), which severs microtubules from the centrosome during mitosis (Keating et al., 1997), SPAST, an ATP-dependent microtubule severing protein that can act directly on microtubules (Evans et al., 2005) and Patronin, which regulates MT severing (Goshima et al., 2007).

MT depolymerisation proteins are not well conserved in *U. maydis*. These proteins appear to have orthologues: Cin8, during yeast mitosis promotes microtubule catastrophe in a length-dependent manner to mediate chromosome congression (Gardner et al., 2011); Kar3 (Figure 4.6) functions in the cytoplasm during mating, where it catalyses the depolymerisation of microtubules, bringing the two nuclei together (Maddox et al., 2000) (Sproul et al., 2005) (Benanti et al., 2009); Kip3 was previously shown to destabilise MTs *in vitro* and *in vivo (Gupta et al., 2006)* (Gardner et al., 2011), and *Drosophila's* CG3326 (Fidgetin) (Figure 4.6), stimulates MT minus-end depolymerisation and flux (Zhang et al., 2007). MAPs that are not conserved are Cik1, which in complex with Kar3 promotes the depolymerisation of microtubules (Benanti et al., 2009), Rsp1, part of a chaperone-based mechanism that disassembles the eMTOC (equatorial MTOC) into satellites, contributing to the dynamic redistribution of MTOC components for organisation of interphase microtubules (Zimmerman et al., 2004), katanin (KATNA1 and Kat80 subunits) which contributes to MT minus-end depolymerisation and flux (McNally et al., 1996; McNally and Vale, 1993), KIF2A, which disassembles microtubules at their minus ends at spindle poles in association with poleward microtubule flux (Ganem et al., 2005) (Manning et al., 2007), KIF2B and KIF2C which are microtubule-depolymerising kinesins which stimulate kinetochore-microtubule dynamics during distinct phases of mitosis to correct maloriented attachment of chromosomes to spindle microtubules (Bakhoum et al., 2009), KIF18B which acts together with MCAK (KIF2C) to promote MT depolymerisation in mitosis (Tanenbaum et al., 2011), and STMN1 which destabilises microtubules, although the mechanism of destabilisation is currently controversial (Howell et al., 1999).

Potential orthologues involved in **MT nucleation** are relatively well conserved in *U. maydis*. They include CLASP1, required for nucleation of non-centrosomal microtubules at the trans-Golgi network (Efimov et al., 2007) and gamma-TuC proteins. The gamma-tubulin complex is a large multiprotein complex that is required for microtubule nucleation at the centrosome in animal cells (Murphy et al., 2001) or at the SPBs in filamentous fungi (Xiong and Oakley, 2009). Proteins without *Ustilago* orthologues are *A. nidulans* PcpA, which plays an important role in nucleus positioning by affecting microtubule organisation and nucleation (Chen et al., 2012), CENPJ, a part of the γ-tubulin complex and which may participate in microtubule nucleation (Hung et al., 2000), CLASP2, with a similar function to CLASP1 (Efimov et al., 2007), SLAIN2 which promotes cytoplasmic microtubule nucleation and elongation (van der Vaart et al., 2011), and Augmin which is a protein complex critically required for spindle microtubule-based MT nucleation, as observed in *Drosophila* and human cells (Johmura et al., 2011).

Finally, none of the **destabilising** MAPs were present in *Ustilago*. They included the two best characterised destabilising proteins katanin and stathmin (STMN1). Katanin destabilises the mitotic spindle by severing MTs and STMN1 sequesters the α/β-tubulin dimers and stimulates catastrophes (Kline-Smith and Walczak, 2004; Yang et al., 2008). There were also KIF2C (MCAK), a soluble catastrophe factor (Kline-Smith et al., 2004) and PSRC1, which controls spindle dynamics and mitotic progression by regulating MT depolymerases (Jang et al., 2008).

4.3.4 Comparison of orthologues found in the selected species

In addition, to gain better understanding of the above results, searches for orthologues against the initial protein sequences in all previously selected model organisms (*H. sapiens. D. melanogaster, A. nidulans*, *S. pombe* and *S. cerevisiae*) were conducted. After comparison of orthologues found in different organisms, several patterns emerged (Figure 4.3).

In the first category, of the proteins that appear to be very well conserved in *U. maydis,* proteins involved in chromosome segregation can be found. Most of the potentially conserved proteins were grouped in three complexes: fungal DASH, CPC and dynein, whose components were present in most species. As well as

that, 8 MAPs were found in all six researched species, 7 were fungal specific (DASH complex), 3 were metazoan specific and 1 (AN8669.2) was present only in the filamentous fungi, and metazoans. These results indicate that chromosome segregation is a very well conserved process among the species.

In the group of proteins responsible for nuclear migration along MTs all proteins appear to be present in *U. maydis* (Fig. 4.3). The level of conservation among different species is extremely high as well, because 5 out of 8 proteins were present everywhere, 2 proteins (AN8669.2 and NudN), which belong to dynein complex, were specific to the filamentous fungi and metazoans, and only 1 protein is fungal specific (Num1). It is probably due to the dynein complex components being a majority in this group.

Another process with well-conserved MAPs in *U. maydis* is up-regulation of MT polymerisation. In this group only 2 proteins were present in all researched organisms, another 8 were fungal specific (DASH complex components) and 4 were metazoan specific. In comparison to nuclear migration proteins, the level of conservation within this group is much lower. It looks like metazoan species share only 2 proteins with fungi, therefore the up-regulation of MT polymerisation is more conserved within closely related groups of species. The final group of MAPs well conserved in *U. maydis* control regulation of MT dynamics. All 13 proteins potentially present in the corn smut fungus were found in all of the selected organisms (Fig. 4.3). In addition, 3 MAPs were metazoan specific and 1 was specific to the budding yeast. The results indicate that MT dynamics, generally, could be regulated in a similar way by many different species.

The second category of MAPs consists of 5 groups of relatively well conserved proteins in *Ustilago*. The first one is responsible for mitotic spindle organisation, where 15 proteins are present in all tested species, 8 proteins are fungal specific, 9 proteins are metazoan only, 4 proteins are *S. cerevisiae* specific, 5 are present only in humans and 7 are *D. melanogaster* specific. It also contains 3 well known complexes: fungal DASH complex, Augmin and dynein complex. In the Figure 4.3, only Dgt6 is shown to be present in humans, however other

augmin complex components have been identified in humans (Uehara et al., 2009), but could not be found by sequence homology searches performed here.

The second group takes part in the minus-end binding and all 5 proteins present in *Ustilago* belong to the gamma-TuRC complex. Within this complex, 2 proteins were present in all tested species (Spc97 and Spc98) and they build the gamma-TuSC, while the other 3 were not found only in the yeast species. Additionally, 4 MAPs were metazoan specific and 1 (Alp7) was present only in *A. nidulans* and *S. pombe*. Therefore, overall in this group of MAPs, the level of conservation is much higher between metazoan species and filamentous fungi than yeast species, which might indicate that species with more specialised cell types, carrying out long-distance transport, need more sophisticated MT nucleating machinery.

The next group consists of +TIPs, where 6 proteins seem to be present in *U .maydis* as well as all tested species, 5 proteins are metazoan specific, 1 (CLASP2) is *H. sapiens* specific and 1 (Kar9) *S. cerevisiae* specific (Fig.4.3). In this group conservation level between different species is relatively high and metazoan species have few more +TIPS than fungi, most probably due their high complexity.

Moreover, MT polymerisation appears to be a relatively conserved process in *U. maydis* as well as the other tested species. All 5 proteins detected in *U. maydis* are present in all of the species (Fig. 4.3). The rest of MAPs consist of 3 proteins present only in animal cells, 2 proteins human specific and 1 protein (Mhp1) that was found in *S. cerevisiae* and *A. nidulans*. It looks like different species are able to polymerise MTs using similar proteins however the animal cells need more of them than fungi, perhaps due to a much higher variety of types of cells.

Finally, microtubule anchoring process, similarly to the cell polarity regulation, has 7 MAPs, out of which 3 are conserved in *U. maydis* (Num1, CLASP1 and HOOK3) (Figure 4.3). However, only CLASP1 was present in all checked species, while Num1 was found only in fungal species and HOOK3 appeared to be absent from the yeasts, which indicates that it is present only in organisms

conducting long-distance transport. Indeed, it has been reported that *U. maydis* orthologue, Hok1, regulates bidirectional EE trafficking along microtubules and the Hok1 adapter complex increases the motor number on organelles, thereby enabling extended runs of up to 90μm (Bielska et al., 2014b; Schuster et al., 2011). There were also 2 human specific MAPs (CLASP2 and CEP57), 1 present in animal cells only (CAMSAP3) and PcpA, described in the cell polarity group. Again, a very low level of evolutionary conservation can be seen here.

The third category of MAPs contains proteins that are not well conserved in *U. maydis* and it has more MAP groups than the other 2 categories taken together. In the first group there are proteins taking part in the attachment of spindle MTs to kinetochore. Three of the proteins (Ame1, Ipl1 and AURKC) were found to have homologues in all of the organisms and seven were species specific. It is also clear that there is a very high level of conservation between all the fungal species (10 proteins), especially the filamentous fungi (*A. nidulans* and *U. maydis*), which share eleven proteins. Proteins that have orthologues in *U. maydis* belong to two complexes, DASH and CPC. DASH is a fungi specific complex, essential only in *S. cerevisiae*, and absent from metazoans (Thakur and Sanyal, 2011). Most in components are present in yeasts and filamentous fungi, except for Hsk3 and Spc34 present only in *S. cerevisiae*. CPC (chromosome passenger complex) usually consists of Ipl1, Sli15 and BIRC5, while in animals there are additionally AURKC and borealin, and is conserved from yeast to humans (Nakajima et al., 2009). Even though, the sequence search for orthologues in the selected organisms using Sli15 (INCENP) indicated no orthologues, it is known that this protein is conserved from yeast to human. The reason why it was not found using methods used here is probably, because the sequence homology between Sli15 and metazoan INCENP is largely restricted to the COOH-terminal IN box domain (binds to Ipl1) (Kang et al., 2001), therefore the search methods did not prove to be sensitive enough here.

In the second group, spindle pole bodies, only fungal proteins were considered, because, although SPBs have functional equivalents in animal cells in the form of centrosomes, structurally, centrosomes and SPBs have little resemblance (Lim et al., 2009). Out of 10 proteins conserved in *U. maydis*, 8 were present in

all tested fungi, 1 (NudC) was not found only in *S. cerevisiae* and 1 (Spc19) was absent from *A. nidulans*. Among the proteins which were not detected in *Ustilago* there were 8 *S. cerevisiae* specific proteins, 3 *S. pombe* specific and 1 (Wrap73) found in *A. nidulans* and *S. pombe* (Figure 4.3). It also seems that the level of conservation is much higher among the filamentous fungi than between the yeast species and *U. maydis*.

The next group of proteins helps to maintain or establish cell polarity and there are only 6 MAPs here, 2 of which (Stu2 and TeaA) are probably present in *Ustilago*, as well as all researched species. The rest of the proteins were either human specific (MACF1 and MAP7), fission yeast specific (Mug164) or detected only in *H. sapiens, A. nidulans* and *S. pombe*, (PcpA). The last protein, a putative pericentrin-related protein homologue in *A. nidulans* that has many functions, one of which is in polar growth, is known to have orthologues in *S. cerevisiae* and *D. melanogaster* (Chen et al., 2012), even though my searches did not find them. This might mean that, potentially, there is an orthologue in *Ustilago*, but more sensitive methods would have to be applied to test that. Overall, apart from two well-conserved proteins, MAPs in this group are poorly conserved, which could mean that cell polarity functions are very much specific to different groups of species.

Proteins responsible for MT stabilisation have 10 potential orthologues in *U. maydis*, of which 9 are present in all tested species and 1 (CAPN6) is absent from the yeast species, suggesting possible function in stabilising MTs in long, elongated cells, such as hypha. Also, 13 proteins were found in metazoans only, 4 were *H. sapiens* specific, 2 were *S. cerevisiae* specific (Kar9 and Spc72), 1 was *Drosophila* specific, 1 (Mhp1) was present only in *A. nidulans* and *S. pombe* and 1 (Ber1) only in the yeasts. These results show that MAPs present in *Ustilago* were generally well-conserved among other species, however, in general, most MT stabilising proteins were found only in metazoans and the most primitive, in terms of evolution, yeast species had the least number of these MAPs. It is not surprising, as more sophisticated fungi and multicellular organisms have more specialised cells, which need more MAPs carrying different functions.

MT cytoskeleton organisation group contains proteins that could not be categorised anywhere else, because there was no other evidence. Most in this group were found in humans and fruit flies, therefore 11 out of 18 proteins are present in both of these species or in either. One protein (Abm1) seems to be budding yeast specific, another one (RanM) was conserved in humans, fruit flies and *A. nidulans* and five MAPs found to be potentially conserved in the corn smut fungus were also present in all of the species. It is hard to judge this result, as the proteins might have different, unknown functions, which would make them difficult to compare.

MAPs involved in the MTs bundle formation were not found to be well conserved in *U. maydis* or other fungi, because only 6 out of 23 proteins appeared to be present in all chosen species (Fig. 4.3) and one (human CAPN6) was found also in fruit fly and both filamentous fungi, but not the yeasts. There was also *S. pombe's* Alp7, present in *A. nidulans* as well, but after that 11 proteins were metazoan specific and 4 more MAPs were either *H. sapiens* (CCSER2, MAP2 and PSRC1) or *D. melanogaster* specific (Mei-38). This means that fungi probably use very different mechanisms to bundle their MTs, in comparison to the animals.

Down-regulation of MT polymerisation is generally known to stop or reduce the frequency of microtubule polymerisation and I found 3 MAPs in this group, out of which only one (TBCD) is present in *Ustilago* as well as the rest of the species. Two others were only present in humans (SNCA) or humans and fruit flies (STMN1), therefore there is not a huge variety of MAPs here and there might be others that are not known yet.

The subsequent group of MT severing MAPs contains 6 proteins out of which only 2 (TTLL6 and CG3326) were found to be conserved in all tested organisms, including *Ustilago*. The rest of them were present only in metazoan species, however proteins such as katanin and spastin, could be conserved, because sequences with high similarity can be found in *A. nidulans* (Robson et al., 2007) and *U. maydis* (this thesis). It is also interesting that there were no other MT severing proteins found in fungi, which may mean that they have not been discovered yet.

Furthermore, MAPs that belong to the MT depolymerisation group were found not to be well conserved in *U. maydis*, as only 4 out of 13 were present (Fig. 4.3). The proteins potentially conserved there were also found in the rest of the species. There was also 1 (Cik1) *S. cerevisiae* specific protein and 1 (Rsp1) *S. pombe* specific. However, the rest of the proteins (7) were metazoan specific. In this case, the most MT depolymerising MAPs can be found in the animal cells, while fungi can function without them or perhaps using different mechanisms.

The penultimate group, MT nucleation, contains 2 large complexes, gamma-TuRC, with all its components conserved in *U. maydis* and augmin complex, not detected in *U. maydis*, in addition to 5 other proteins (Fig. 4.3). Firstly, only 6 out of 17 proteins were detected in *Ustilago* and of those 3 were found in all tested species, 2 only in metazoans and filamentous fungi, and 1 (GcpD) was absent only from *S. cerevisiae*. None of the augmin proteins was detected in any of the fungal species and only one component, Dgt6, was found in humans, although it was mentioned earlier that augmin complex was found in humans. Apart from that there were 2 human specific MAPs, 1 (CENPJ) metazoan and 1 (PcpA), detected in *H. sapiens*, *A. nidulans* and *S. pombe*. Generally, the level of conservation is best between the filamentous fungi, and also between metazoan species, however it is not high in general, which probably shows that species, which are closely related might nucleate MTs in a similar fashion.

The final group of MAPs, which causes MT destabilisation, did not seem to be conserved at all in *U. maydis* or any other fungi. There were 5 proteins, with 4 present in humans and fruit flies, and PSRC1 human only. This probably means that there must be a different mechanism used by fungi to destabilise their MTs.

4.3.5 The pattern of evolutionary conservation allows prediction of MAPs important for yeast or hyphal stage *U. maydis*

Ustilago can exist in either a yeast or hyphal form. These two cell stages are morphologically very different, and it might be expected that different MAPs would be required for each stage. Analysing the pattern of MAP conservation across eukaryotes with differing biology allows predictions to be made. For

example, hyphal cells have a requirement for long-range microtubule transport similar to that found in human and fly brain and in other filamentous fungi, but not observed in fission yeast or budding yeast. Thus, MAPs conserved between *Ustilago*, human and/or fly and *A. nidulans,* but absent in *S. cerevisiae* and *S. pombe* might be predicted to have an important role in this process and be critical for the hyphal cell stage. 6 MAPs fulfilled these criteria: 2 dynein complex components, NudN (dynein light intermediate chain) and AN8669.2 (dynein light chain), 2 gamma-TuRC proteins, GCP5 and GCP6, as well as human CAPN6 and HOOK3.

Furthermore, several proteins were conserved only between fungi, implying important roles for this group of organisms. These included all DASH complex components, Alp7, Mhp1 and Num1. Most of them, apart from Mhp1, have functions in mitosis (Franco et al., 2007; Li et al., 2002b; Sato et al., 2004; Siller and Doe, 2009).

4.3.6 *Ustilago* MAPs are enriched in P-loop NTPase, CH and CAP Gly domains, Armadillo folds and WD40 repeats

The occurrence of protein domains and folds was analysed to examine if certain structural features were dominant in the MAP dataset (Table 4.1). P-loop NTPase (P-loop containing nucleoside triphosphate hydrolase) and kinesin motor domains were present in most proteins, although out of 23 P-loop containing proteins, 18 were motor-proteins, which was not surprising, since it is known that most molecular-motor proteins are members of the P-Loop NTPase superfamily (Berg et al., 2002). A phosphate-binding loop (P-loop) typically consists of a glycine-rich sequence followed by a conserved lysine and a serine or threonine (Saraste et al., 1990), and typically, P-loop NTPases show substantial substrate preference for either ATP or GTP (Leipe et al., 2004). In addition, P-loop NTPase fold is the most prevalent domain in proteins encoded in the genomes of most cellular life-forms (Milner-White et al., 1991; Saraste et al., 1990; Vetter and Wittinghofer, 1999) (Leipe et al., 2004; Vetter and Wittinghofer, 1999).

Table 4.1 List of domains found in MAPs

Domains	Number of MAPs
P-loop containing nucleoside triphosphate hydrolase, including ATPase, AAA-type, core (6 MAPs)	23
Kinesin, motor domain	17
Calponin homology domain	12
Armadillo-type fold, incl. Armadillo-like helical	7
CAP Gly-rich domain	6
TCP-1-like	4
WD40 domain or repeats	4
GroEL-like	4
CKK domain	4
Growth-arrest-specific protein 2 domain	4
h-arrest-specific protein 2 domain	4
Protein kinase-like domain	3
CLASP N-terminal domain	3
HEAT	3
Spectrin/alpha-actinin	3
Zinc finger, incl 1 of CCCH-type, 1 of RING/FYVE/PHD-type, 1 of FYVE	3
Beta-lactamase-like	3
Serine/threonine- /dual specificity protein kinase, catalytic domain	3
Small GTP-binding protein domain	3
Armadillo domain	2
SAMP	2
DIX domain	2
Calmodulin-regulated spectrin-associated protein	2
Spindle associated	2
Cep57 centrosome microtubule-binding domain	2

Pleckstrin homology domain	2
Plectin repeat	2
EF-hand domain	2
PDZ domain	2
Vps4 oligomerisation	2
Spindle and kinetochore-associated protein	2
Kelch repeat; Kelch-type beta propeller	2
Microtubule associated protein, tubulin-binding repeat	2
Sad1/UNC-like	2
Ubiquitin-like domain	2
Leucine-rich repeat	2
Transketolase	2
EB-1 binding	1
Protein kinase C-like, phorbol ester/diacylglycerol binding	1
Protein of unknown function DUF1395	1
MIT	1
Acyl-CoA N-acyltransferase	1
Regulator of G protein signalling domain	1
Axin beta-catenin binding	1
Baculoviral inhibition of apoptosis protein repeat	1
Peptidase C2, calpain,	1
Casc1 domain	1
Cyclin	1
T-complex protein 10	1
Cep57 centrosome localisation domain	1
Ubiquitin carboxyl-terminal hydrolases family 2	1
Doublecortin domain	1
Dynamin, GTPase domain; Dynamin central domain;	1
Dishevelled protein domain	1
DEP domain	1
F-box domain	1

FCH domain	1
SH2 domain	1
Tyrosine-protein kinase	1
Histone deacetylase domain	1
Kinesin-associated microtubule-binding domain	1
Sterile alpha motif	1
BTB/POZ	1
RII binding domain	1
Ubiquitin-associated/translation elongation factor EF1B, N-terminal,	1
Kinase associated domain 1	1
Rab effector MyRIP/Melanophilin	1
POLO box duplicated domain	1
Tubulin-specific chaperone D, C-terminal	1
Prefoldin alpha-like	1
Kinetochore protein Nuf2	1
Kinetochore-Ndc80 subunit Spc24	1
Dynein associated protein	1
PPC89 centrosome localisation domain	1
Major facilitator superfamily domain	1
Dynein heavy chain, domain-1	1
ATPase, dynein-related, AAA domain	1
Dynein heavy chain, coiled coil stalk	1
HSP20-like chaperone, CS domain	1
Dynein 1 light intermediate chain	1
Spindle associated	1
Pericentrin/AKAP-450 centrosomal targeting domain	1
EB1 C-terminal domain	1
Dynein light chain, type ½	1
Pyridine nucleotide-disulphide oxidoreductase, FAD/NAD(P)-binding domain	1
Karyogamy protein	1
ARK-binding domain	1

Mto2p-binding domain	1
Putative 5-3 exonuclease	1
Tacc	1
Central kinetochore-associated	1
Dynein family light intermediate chain	1
Kinetochore Sim4 complex subunit Fta2	1
DnaJ domain	1
Translation initiation factor	1
Myosin-like IQ motif-containing domain	1
Vps4 oligomerisation	1
Peptidase M16 domain	1
Replication factor C	1
Katanin p80 subunit, C-terminal	1
Guanylate-kinase-associated protein	1
RuvA domain 2-like	1
Helix-hairpin-helix DNA-binding motif	1
B30.2/SPRY domain	1
Concanavalin A-like lectin/glucanases superfamily	1
SPla/RYanodine receptor subgroup	1
LisH dimerisation motif	1
CRA domain	1

All protein domains were segregated according to the number of MAPs they were found in. All domains were identified with InterPro online software (Hunter et al., 2012).

Potentially more interesting is the abundance of calponin homology domains (present in 12 MAPs), CAP Gly-rich domains (found in 6 proteins), Armadillo-type fold (present in 7 MAPs) and WD40 repeats (in 4 proteins). The calponin homology domain (or CH domain) consists of approximately 100 amino acid residues that functions mainly as an actin filament-binding domain, in both cytoskeletal proteins and signal transduction proteins (Castresana and Saraste, 1995), but can also bind MTs (Dougherty et al., 2005; Gimona et al., 2002). Among the proteins which have a CH domain, only yeast Bim1 (EB1) is known to use it to bind MTs (Bu and Su, 2003; Dougherty et al., 2005; Hayashi and Ikura, 2003). Others, like human CAMSAP1, Dst or MACF1 are thought to use CH domain to bind actin, which is regulated by the two CH domains working in tandem (Gimona et al., 2002) and some, such as human SPECC1L or *Drosophila's* Asp, have a single CH-domain, but its function is not yet clear (Banuelos et al., 1998). CAP Gly-rich is a conserved glycine-rich cytoskeleton associated protein domain, first discovered in restin (or CLIP-170), it is the prototype +TIP and its amino acid sequence is conserved from the simple single cell *S. cerevisiae* to humans (Li et al., 2002a). It is thought to be responsible for MT binding (Feierbach et al., 1999; Pierre et al., 1994; Saito et al., 2004; Scheel et al., 1999). MAPs containing this domain included yeast Alf1, Bik1 and Pac2, *A. nidulans* NudM (p150 dynactin subunit), human CLIP1 and CYLD. However, in the case of CYLD it is not known whether it colocalises with MT and whether the CAP-Gly domains are capable of MT binding (Saito et al., 2004).

Armadillo-type fold repeats are approximately 40 amino acid long sequence motifs, which have function in various processes, including intracellular signalling and cytoskeletal regulation, amongst others (Hatzfeld, 1999). Proteins with armadillo repeats are present in all eukaryotic kingdoms and the structure of the Arm containing domain allows for proteins to have many interaction partners and functions in the cell (Coates, 2003). MAPs found to have Armadillo-type fold repeats include such proteins as Stu2, APC, APC2 and CLASPs, all of which have multiple binding partners and different roles in regulating MT dynamics.

The WD40 repeat (also known as the WD or beta-transducin repeat) is a short structural motif of approximately 40 amino acids, often terminating in a tryptophan-aspartic acid (W-D) dipeptide (Neer et al., 1994). WD-repeat proteins are a large family found in all eukaryotes, but not prokaryotes, implicated in a variety of functions ranging from cell division, signal transduction and transcription regulation to vesicle fusion and apoptosis (Neer et al., 1994) (Li and Roberts, 2001). WD40 domain-containing proteins have 4 to 16 repeating units (van der Voorn and Ploegh, 1992), that act as a site for protein-protein interaction and proteins containing WD40 repeats are known to serve as platforms for the assembly of protein complexes or mediators of transient interplay among other proteins (van Nocker and Ludwig, 2003). The specificity of the proteins is determined by the sequences outside the repeats themselves (Smith et al., 1999). MAPs with WD40 repeats included Pac1 and NudI, involved in the nuclear migration along MTs, fission yeast Wrap73 implied to have a role at SPBs and Kat80, a subunit of katanin, a MT severing protein.

4.3.6 *Ustilago* is a model organism for the study of human genetic disease

While it is well-recognised that budding yeast makes excellent model system for studying fundamental biological processes in higher eukaryotes, *Ustilago* actually shares more genes in common with humans than *S. cerevisiae* (Munsterkotter and Steinberg, 2007). This makes *Ustilago* an excellent model system for the study of human biology, particularly in respect to processes such as long-range microtubule transport, where the hyphal cells mimic many of the transport processes that occur in neurons (Steinberg and Perez-Martin, 2008). There are many inherited diseases of humans that are associated with MAP dysfunction. Therefore, to test if *Ustilago* could represent a good model system to study the function of these MAPs to better understand human health and disease, the OMIM (Online Mendelian Inheritance in Man) database was used to compile a list of MAPs analysed in this study that are associated with genetic conditions in humans. Mutation or dysfunction in 31 of the MAPs studied in this chapter causes genetic diseases in humans (Table 4.2), and 12 of these (39%) have predicted *U. maydis* orthologues. Among those, there are 22 human proteins that cause serious diseases particularly associated with the central nervous system, for example lissencephaly, a rare brain formation disorder

Table 4.2 MAPs responsible for diseases and conditions in humans

Human proteins

Gene	Human disease	Affected organ	*Ustilago* hit
Apc	Adenoma, periampullary, somatic; Adenomatous polyposis coli; Brain tumor-polyposis syndrome 2; Colorectal cancer, somatic; Desmoid disease, hereditary; Gardner syndrome; Gastric cancer, somatic; Hepatoblastoma, somatic;	brain, colon, stomach, liver	no hits
APC2	Familial adenomatous polyposis, basal cell carcinoma,	colon, uterus	no hits
AURKA	Colon cancer	colon	no hits
AXIN1	Caudal duplication anomaly; Hepatocellular carcinoma, somatic	liver	no hits
CASC5	Microcephaly 4, primary, autosomal recessive	brain	no hits
CDK5RAP2	Microcephaly 3, primary, autosomal recessive	brain	no hits
CENPJ	Microcephaly 6, primary, autosomal recessive; Seckel syndrome 4	brain;	no hits
CEP57	Mosaic variegated aneuploidy syndrome 2	heart; facial dysmorphism;	no hits
CYLD	Brooke-Spiegler syndrome; Cylindromatosis, familial; Trichoepithelioma, multiple familial, 1;	skin;	no hits
DCX	Lissencephaly, X-linked; Subcortical laminal heteropia, X-	brain;	no hits

	linked		
DNM2	Charcot-Marie-Tooth disease, axonal, type 2M; Charcot-Marie-Tooth disease, dominant intermediate; Lethal congenital contracture syndrome; Myopathy, centronuclear	muscles; nervous system;	um05378
Dst	Epidermolysis bullosa simplex, sutosomal recessive; Neuropathy, hereditary sensory and autonomic, type VI	skin; heart; muscles	no hits
HDAC6	Chondrodysplasia with platyspondyly, distinctive brachydactyly, hydrocephaly, and microphthalmia	brain;	um02102
GCP6	Microcephaly and chorioretinopathy with or without mental retardation	brain;	um02520
KIF2A	Cortical dysplasia, complex, with other brain malformations 3	brain;	um06251
KIF11	Microcephaly with or without chorioretinopathy, lymphedema, or mental retardation;	brain; eyes; central nervous system; face;	um10678
MAPT; Tau	Dementia, frontotemporal, with or without parkinsonism; Pick disease; Supranuclear palsy, progressive atypical; Tauopathy and respiratory failure;	brain	no hits
MLPH	Griscelli syndrome, type 3	skin	no hits
SNCA	Dementia, Lewy body	brain;	no hits

	Parkinson disease 1 Parkinson disease 4		
SPAST	Spastic paraplegia 4, autosomal dominant	brai	no hits
SPECC1L	Facial clefting, oblique, 1	face (facial bones)	no hits
TACC3	Bladder cancer susceptibility.	bladder	no hits

Human diseases and conditions caused by mutations or defects in MAPs, found in *H. sapiens, D. melanogaster, A. nidulans, S. cerevisiae* and *S. pombe.* The names in brackets next to some of the proteins, in the first column, are the names of the orthologues, used by OMIM's search engine. The last column, called *Ustilago* hit, shows potential *Ustilago maydis* orthologues and their numbers in the *U. maydis* database. This data was found using NCBI OMIM database.

caused by defective neuronal migration during gestation resulting in a lack of development of brain folds and grooves (Dobyns, 1987) and Parkinson's disease, a degenerative disorder of the central nervous system. Five have potential orthologues in *U. maydis*, DNM2, HDAC6, GCP6, KIF2A and KIF11. Thus, the overwhelming pattern observed is that the disease-causing MAPs with potential *Ustilago* orthologues affect the brain, muscles or nervous system.

Interestingly, in this group there was 1 protein, GCP6, a subunit of gamma-TuRC complex, which not only causes brain problems, but also is only present in metazoans and filamentous fungi. GCP6 could not be detected in fission or budding yeast, although it has been suggested that *S. pombe* might have an additional component, closely related to GCP6 called Alp16, because the deletion revealed that it is required for the formation of normal interphase microtubules (Fujita et al., 2002). All of the conserved MAPs function in microtubule organisation, stabilisation and regulation rather than microtubule disassembly, highlighting the need to analyse them in the context of a well-developed and stable microtubule network. Therefore *Ustilago* represents an excellent model system for studying the function of these proteins, particularly in the hyphal cell stage, where the cell morphology and subcellular processes mimic those observed in neurons.

Finally, as *U. maydis* and humans share proteins and cellular processes that are not found in the fungal model *S. cerevisiae*, such as long-distance transport along the microtubule cytoskeleton (essential in neurons), or the removal of the nuclear envelope in mitosis (Pruyne et al., 2004) (Munsterkotter and Steinberg, 2007), EST databases were used to examine the expression pattern of human MAPs conserved in *Ustilago* to see if any were particularly enriched in the central nervous system. Only 5 human MAPs and 1 found in fruit fly were enriched almost exclusively in brain or nerves, but none of them had possible orthologues in *U. maydis* (Table 4.3). Each is a brain-specific MAP and highlights the limitations of using a unicellular organism to study multicellular biology. Indeed, in comparison to fungal species, metazoans or plants have a variety of known unique MAP families (Gardiner, 2013), with many of them organ specific, for example MAP1, tau or MAP2 in brain. Thus, while *Ustilago* represents a good model system to study fundamental cellular processes that

Table 4.3 List of MAPs mostly expressed in brain or nerves

Human proteins

Gene	Human EST profile	Mouse EST profile	*Ustilago* hit
APC2	nerves and brain	brain	no hits
DCX	brain	brain and nerves	no hits
MAP1A	brain	brain and other organs	no hits
MAP6	brain and nerves	brain and nerves	no hits
MAPT (Tau)	mostly in brain and nerves	mostly in brain and nerves	no hits

***D. melanogaster* proteins**

Gene	Human EST profile	Mouse EST profile	*Ustilago* hit
Mars (DLGAP3)	brain	different organs	No hits

EST (expressed sequence tag) profiles of MAPs found in the NCBI database. None of the MAPs found to have a high expression in brain were present in *U. maydis*. Names of the proteins in brackets indicate their names in the database.

are sometimes associated with disease in humans, it is necessary to take tissue-specific functions into account and choose the most appropriate model system on a case by case basis.

4.3.8 The MAP repertoire of the corn smut fungus, *Ustilago maydis*

The range of MAPs in *U. maydis* has never been systematically investigated. Previously, studies in *Ustilago* on proteins with cytoskeleton-related functions focused on particular groups of proteins, rather than on the comprehensive analysis. For example, in a study of the machinery for cell polarity, cell

the genes used to query *U. maydis* genome in that study, such as +TIPs Pac1, Kar9 or Bim1, were also in my collection of tested proteins and we obtained the similar results, evidence for the reliability of this current dataset. A second study (Schuchardt et al., 2005) analysed the role of microtubule motors in hyphal growth of *U. maydis*, and showed that kinesin-1 and kinesin-3 have essential roles in long-range hyphal growth and supplied detailed information of the kinesin superfamily in *U. maydis.* Finally, one study provided a genome-wide comparison of the predicted proteome of *U. maydis*, humans and the budding yeast *S. cerevisiae,* and demonstrated that *U. maydis* shares more proteins with humans than with the budding yeast (Munsterkotter and Steinberg, 2007).

The analysis presented in this chapter represents the first comprehensive study of the MAP repertoire in the corn smut fungus and should be a valuable resource for understanding the regulation of the microtubule cytoskeleton in this organism. Out of 169 proteins 66 are most probably conserved in *Ustilago maydis*. They included 10 MAPs found only in the fungal species, 6 found in filamentous fungi and metazoans and the rest (50 proteins) conserved across most species (Figure 4.7). Most *U. maydis* MAPs are conserved between fungi and metazoans, and only some proteins are fungal specific. MAPs are a highly diverse group of proteins and the analysis here relies on a list of known MAPs as starting material. Therefore it is highly likely that *Ustilago* has additional MAPs, which could not be detected using the search methods used in this chapter, because they are either unique to this fungus or have such a highly diverged sequence that orthologues could not be identified using the methods in this chapter. Biochemical methods will be critical for the identification of further

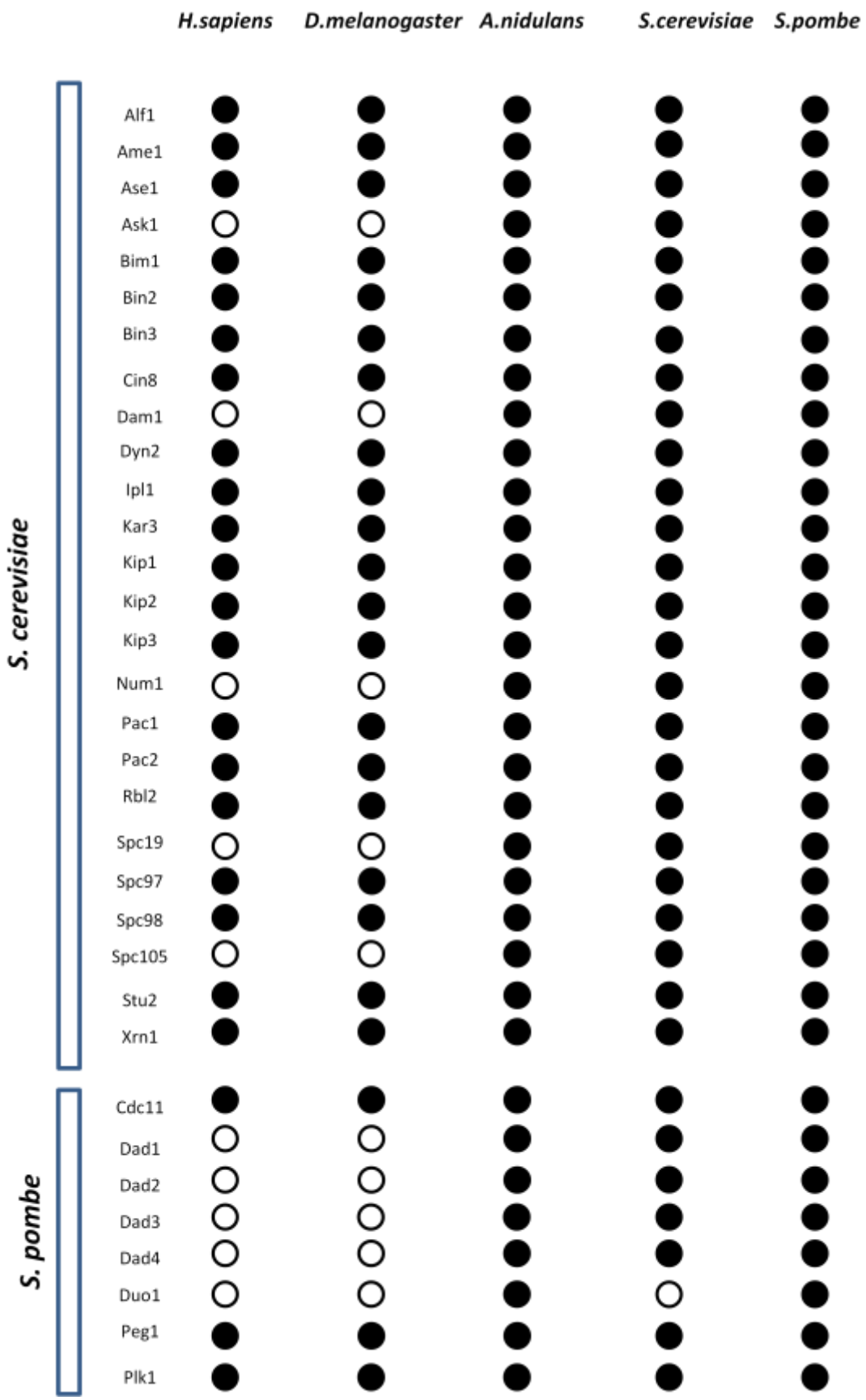
H.sapiens
D.melanogaster
A.nidulans
S.cerevisiae
S.pombe
S. cerevisiae
S. pombe
Alf1
Ame1
Ase1
Ask1
Bim1
Bin2
Bin3
Cin8
Dam1
Dyn2
Ipl1
Kar3
Kip1
Kip2
Kip3
Num1
Pac1
Pac2
Rbl2
Spc19
Spc97
Spc98
Spc105
Stu2
Xrn1
Cdc11
Dad1
Dad2
Dad3
Dad4
Duo1
Peg1
Plk1

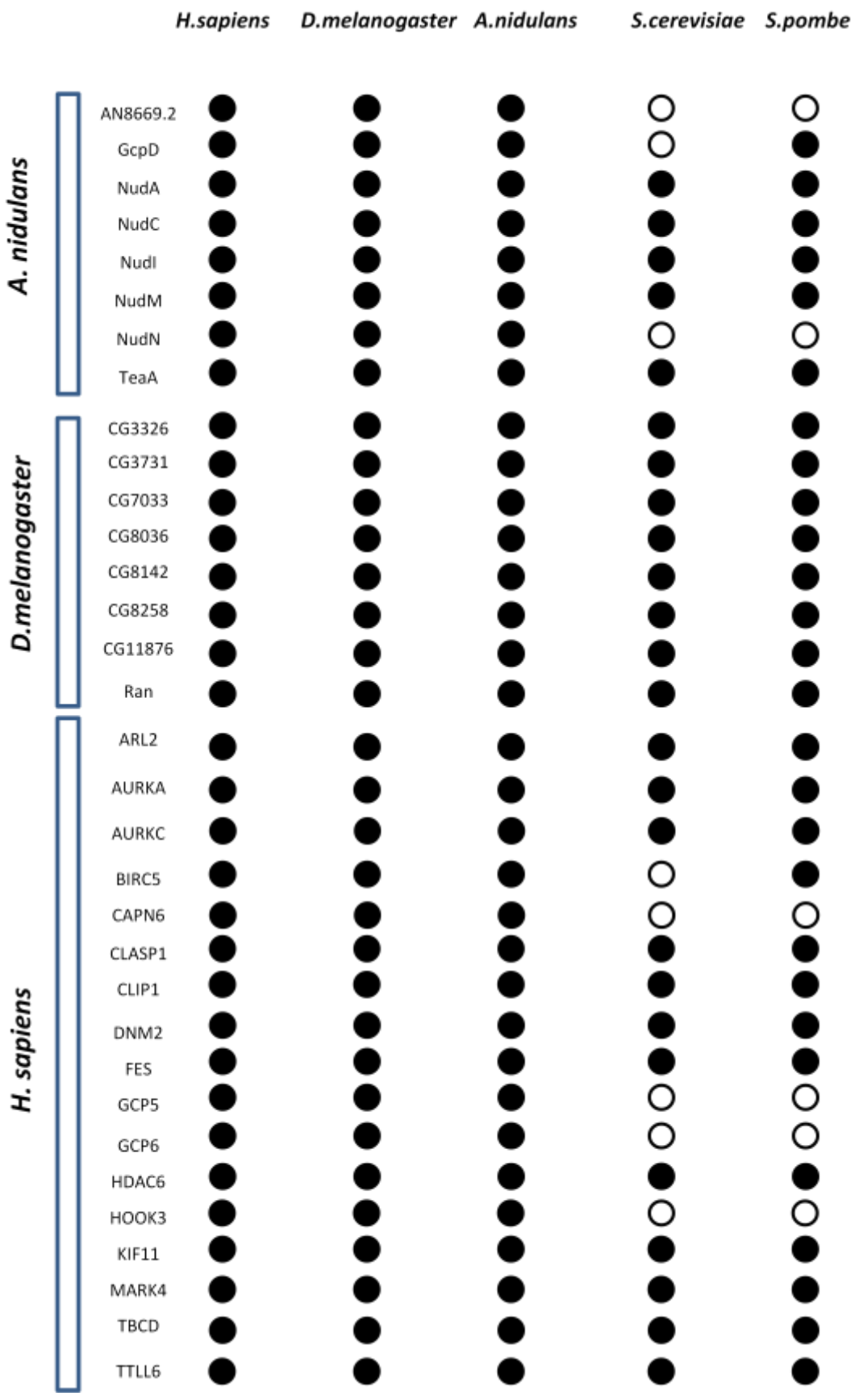

Figure 4.7 Distribution of *U. maydis* MAPs across five different species.

Results of MAP searches in different organisms are represented by dots. The proteins were grouped into five groups, depending on the species whose database generated the initial protein sequence. Each group of proteins From 66 MAPs conserved in *Ustilago maydis*, 10 included MAPs found only in the fungal species, 6 found in filamentous fungi and metazoans and the rest (50 proteins) conserved across most species. Names of the MAPs are on the left of the panel; names of the species are on the top. Black dots represent the presence of homologous sequences that are best hits to the MAPs named on the left, with the cut-off point of e^{-05} or more; white dots indicate no detectable orthologues or hits below the cut-off point of e^{-05}.

Ustilago MAPs, especially as MAPs that regulate fundamental aspects of microtubule dynamics such as microtubule disassembly, microtubule bundling and cell polarity were very poorly conserved in this organism.

Multiple search methods were used to find the MAP homologues. The initial searches were done using BLASTp, a method that aims to find the highest scoring locally optimal alignments between a query sequence and a database (Altschul et al., 1990). Although BLASTp search is a fast method and sequences do not require much preparation, it is not the optimal method, because it cannot detect weak signals as they could be be masked (marked to be ignored), because these segments might initiate too many spurious alignments of a query with unrelated targets (Moreno-Hagelsieb and Latimer, 2008). Therefore, to be able to detect weak relationships between query and members of the database iterative searches were carried out using both Position-Specific Iterated (PSI)-BLAST (Altschul et al., 1997) and Hidden Markov Models (Finn et al., 2011). The reason for performing two of those searches was that, because they use different algorithms, they can be more helpful in identifying distant orthologues than BLASTp. These search methods can be time-consuming, which is their only downside, as they use alignments to query database. For this purpose, for each MAP all known and validated homologues had to be found first, aligned and finally columns containing more than 50% gaps had to be removed to prevent species- or clade-specific insertions biasing the results. However, to be sure that the obtained results are correct, I had to check the domain architecture, of all potential homologues and corresponding MAPs by using the online software, such as InterPro (Hunter et al., 2012) for domains and COILS for coiled-coil motifs (Lupas et al., 1991). It appeared that in most cases the potential orthologues had similar length, as well as very similar domains and coiled-coils configuration in the sequence, which would indicate that they could carry out similar functions.

Furthermore, as *U. maydis* is a dimorphic fungus, which can exist in a yeast-like form or as elongated hyphae, to validate the bioinformatics searches and check the importance of a particular MAP in different cell stages, expression analysis via RT-PCR experiment could be performed. This method would show if a MAP

is expressed, indicate if it is functional and would be helpful in prioritisation of localisation work and functional studies, for example.

To validate the results obtained in this chapter and to facilitate the identification of *Ustilago*-specific MAPs, a combined approach of bioinformatics and experimental methods of cell biology will be critical. With the advancement of technology in the fields of mass spectrometry, bioinformatics, RNA interference, combined with the complete genome sequences for an increasing number of eukaryotic organisms, large-scale screens become a possibility. The importance of MAPs in regulating MT dynamics is clear, and as mitosis is a process which heavily involves MT dynamic regulation, several recent screens for novel MAPs have focussed on this process. Several hundred previously unidentified MAPs were identified in two screens for mitotic MAPs in *Drosophila* (Goshima et al., 2007; Hughes et al., 2008). One study carried out in *Drosophila* S2 cells by Goshima and co-workers (Goshima et al., 2007) sought to identify genes contributing to spindle assembly using a combination of bioinformatics methods with a genome-wide RNA interference screen as well as protein localisation studies. It resulted in identification of 200 genes involved in spindle assembly. A second multidisciplinary study identified over 250 MAPs in the early *Drosophila* embryo. The data were gained using bioinformatics, and also biochemical and cytological methods, which taken together serve as functional sieves, focussing the study on putative MAP complexes with roles in cell cycle regulation and cell division (Hughes et al., 2008).

The sheer number of novel MAPs isolated in these studies is a reminder of how much remains opaque about the regulation of microtubule dynamics in individual subcellular processes. Together, these data indicate that there are many MAPs that are poorly characterised, and much work remains to be carried out before we have a full picture of the complement and function of MAPs in whole cells.

Chapter 5 – A genetic screen to find novel factors organising microtubules in *Ustilago maydis*

5.1 Introduction

The purpose of the work described in this chapter was to enhance our understanding of the mechanisms by which microtubule cytoskeleton is organised. The main task was to identify novel factors involved in organising the microtubules using a genetic screen.

Ustilago maydis is a dimorphic fungus that grows as yeast, but under experimental conditions can be easily converted into hyphal form. If yeast-like cells have a faulty interphase MT array, it will result in lateral budding, but will not affect the survival of the cell (Straube et al., 2003), whereas in hyphae MTs are crucial for extended hyphal growth (Fuchs et al., 2005). Based on the knowledge of difference between yeast-like and hyphal cells, a genetic screen was designed prior to my involvement in the project. In the screen, a strain, which can be switched to filamentous growth after plating on a nitrate-containing medium and can express GFP-alpha-tubulin (AB33_GT), was UV-mutagenised at survival rate of 3-5% (34mJ/cm^2). The idea was that cells with defective interphase microtubules would grow as yeast-like cells on standard plates, but when shifted onto the plates stimulating hyphal growth, would only be able to form smooth and 'greyish' colonies indicating impaired hyphal growth. Such colonies would look completely different from fuzzy, white colonies of unaffected cells and would be very easy to distinguish. The first round of UV-mutagenesis resulted in 145 mutants with impaired filamentous growth, from which four mutants were chosen for further work and the second one created ca. 100 more mutants and only one was chosen to work with. All 5 mutants contained short, fragmented microtubules <10 μm length and were not able to produce long hyphae. Such MT array would result in problems with intracellular transport, including membrane trafficking, previously shown by GFP-Rab5a, an early endosome marker.

Genetic screens proved to be a very successful tool in finding new genes involved in the organising MTs. In a study of *Schizosaccharomyces pombe*, cells were mutagenised using a chemical N-methyl-N'-nitro-N-nitrosoguanidine

and then visually screened for temperature-sensitive mutants defective in cell morphology, which enabled identification of completely new genes by Snell and Nurse (1994) (Snell and Nurse, 1994) and Verde et al., (1995) (Verde et al., 1995). Among newly found genes were *tea1*, *tea2 and tip1*. The *Tea1* gene encodes a protein Tea1 that is always present at the plus-ends of the microtubules, therefore it acts as an end marker and it is also known to have the ability to influence MT organisation, in order to maintain correct cell polarity (Mata and Nurse, 1997). The next gene, *tea2*, which was shown to encode a kinesin-like protein (KLP) that is necessary for establishment of proper cellular morphology, localises to the cell poles and plus-ends of most MTs (Browning et al., 2000). It is also known that Tea2 can act as a plus-end directed kinesin motor transporting Tip1 protein along the MTs toward their growing ends, where both of these proteins accumulate via Mal3 mediated mechanism, so it has been suggested that by transporting the factors like Tip1 to the MTs growing ends the kinesin Tea2 can regulate microtubule growth (Busch et al., 2004). The last out of the three genes mentioned, *tip1*, was found to encode Tip1, a member of CLIP-170 protein family. Tip1 was shown to be able to regulate MT organisation in the cell by playing a crucial role in a guidance mechanism for MTs, where it was located, at the growing ends of microtubules (Brunner and Nurse, 2000). Basically, Tip1 can delay the catastrophe of MTs until they have reached the cell ends and can also distinguish different cortical regions of the cell to modify MT dynamics accordingly (Brunner and Nurse, 2000; Busch et al., 2004).

Another example of successful genetic screen which helped in finding novel factors involved in organising the microtubule cytoskeleton is an overexpression screen done in fission yeast which identified a rim protein Amo1. This newly found factor localises in dots at the nuclear periphery in a pattern similar to nuclear pore complex (NPC) proteins, but most certainly does not affect NPC proteins, motility; its overexpression leads to MT bundling on one side of the cells and cells without Amo1 showed abnormal MTs confirming involvement of Amo1 in MT organisation (Pardo and Nurse, 2005). Lastly, an insertional mutagenesis screen, designed to identify genes regulating cell polarity in fission yeast (Samejima et al., 2005; Snaith and Sawin, 2003), led to discovery of novel proteins Mto1 and Mto2. It was shown that Mto2 plays a very important role in

the regulation of *S. pombe* microtubule nucleation mediated by Mto1 and the γ-tubulin complex (γ-TuC) (Samejima et al., 2005), by being able to influence the ability of the γ-TuC to nucleate specific sets of cytoplasmic microtubules (Venkatram et al., 2005). Mto1 however, is a γ-TuC-associated protein that mediates γ-TuC recruitment specifically to cytoplasmic MTOCs (Sawin et al., 2004; Venkatram et al., 2005; Zimmerman and Chang, 2005). It is also documented that Mto1 can physically associate with Mto2, mirror each other in localisation pattern and depend upon each other for proper localisation (Venkatram et al., 2005).

In this chapter I set out to describe the identification of novel factors organising microtubules in *Ustilago maydis*, which come from the genetic screen.

This work was built on previous work and was undertaken with the help of co-workers. Mr. Christoph Hemetsberger performed a first round of UV-mutagenesis, which resulted in 4 mod (**M**icrotubule **O**rganisation **D**efect) mutants, mod1, mod2, mod3 and mod4. He complemented mod1 and mod3, for which he confirmed rescue plasmids, and transformed genomic library into mod4. Dr. Darren Soanes assembled raw data from Illumina sequencing and analysed them, which resulted in a list of proteins with mutations. University of Exeter Sequencing Service performed genomic library construction and the Illumina sequencing. The software, which identified SNPs within genes and which produced non-silent mutations was written by Dr. David Studholme and adapted by Dr. Darren Soanes, while script used to identify SNPs that are present in introns or promoters was written by Dr. Darren Soanes.

In order to find gene or genes responsible for defective MT cytoskeleton in hyphae of UV-mutants, I performed the second round of UV-mutagenesis, from which I selected mod9 for further work. I conducted benomyl sensitivity studies on plates and at the microscope, tested ‘complementing’ plasmids for mod1 and mod3, and attempted complementation of mod2, mod4, and mod9. Also, I quantified the length of MT tracks in mod mutants in comparison to wild-type. In addition, I analysed all proteins with mutations to see if they could be causing the phenotype in mod mutants. I performed domain architecture analysis of all

proteins found to have mutations. As a result, proteins with potential links to the cytoskeleton were identified.

5.2 Materials and methods

5.2.1 UV-Mutagenesis of *U. maydis*

To generate *U. maydis* mutants, AB33_GT strain was grown overnight in a liquid culture, as described in General Materials and Methods. From that, ca. 6000 cells were taken and transferred into a 300 µl volume of complete medium, supplemented with 1 % glucose (CM-Glu), and plated on 120x120 mm CM-Glu plates. Next, they were treated with UV at 254 nm to 3 % survival rate in the UV crosslinker (CL 508S, UVITEC, Cambridge, UK) where intensity of 32 mJ/cm^2 was applied. Afterwards, plates were wrapped in aluminium foil and incubated at 28 °C for 3-5 days in the dark to avoid DNA photo-repair, followed by replica-plating using sterile silk cloths onto nitrate minimal medium plates, supplemented with 1 % glucose (NM-Glu) to induce filamentous growth. After another 3-5 days at 28 °C colonies were screened visually and only 'non-fuzzy' (no long hyphae) ones were collected to be checked further in a liquid culture and under a microscope. Only strains without the ability to produce long hyphae and with short, fragmented microtubules were considered for complementation (Wedlich-Soldner et al., 2000) and (Hemetsberger, 2008)).

5.2.2 Genetic screen

For complementation studies, each mutant was transformed with a genomic library. This contained *U. maydis* DNA, partially digested with *Sau*3AI into fragments of 7-9 kb that were cloned in a self-replicating plasmid pNEBUH (Figure 5.1), containing hygromycin resistance cassette (Hemetsberger, 2008).
5 µg of DNA was transformed following the protocol described in General Materials and Methods. The transformation mixture was plated on 120x120 mm plates. Colonies appeared after 4-5 days and were replica-plated onto nitrate minimal medium supplied with glucose (NM-Glu-hyg) using sterile silk cloths, then left for 3-5 days at 28 °C. After that, colonies with a rescued phenotype (white and fuzzy) were identified on the NM-Glu plates. They were picked from the corresponding transformation plate and grown on separate plates. Single colonies were used to inoculate CM-Glu buffer, which was shifted after 9 h to NM-Glu, to induce filamentous growth. The phenotype was analysed microscopically by observing GFP-alpha-tubulin and hyphae. A transformant

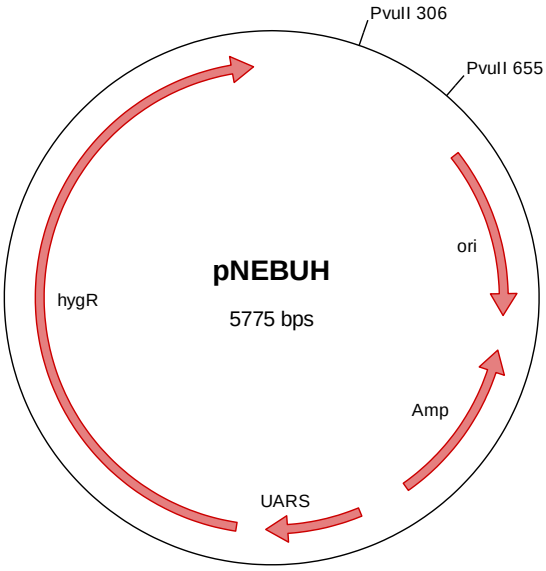

Figure 5.1 *E. coli* vector pNEBUH

This plasmid contains two selectable markers for: *E. coli* (*Amp*R) and *U. maydis* (*hyg*R) and UARS motif which makes it a self-replicating plasmid. Two restriction sites for *Pvu*II provide the 3.55 kb backbone. Graphic map was generated in Clone Manager 9 Professional Edition (Scientific & Educational Software).

was confirmed as ‘rescued’ if it was able to produce typical long filaments that contained unbroken microtubules. Only transformants with the rescued phenotypes were selected for further study. Colonies without GFP-α-tubulin signal were not analysed further. All plates and liquid cultures were supplied with 0.4 % hygromycin (200 µg/ml; Roche, West Sussex, UK).

Next, DNA isolation was performed on the selected transformants, according to the protocol in General Materials and Methods. The isolated DNA was transformed into *E. coli* electro-competent cells (General Materials and Methods section), for each selected transformant. After *E. coli* transformation, many colonies were picked for the plasmid DNA isolation. An individual *E. coli* colony was inoculated in approximately 3 ml dYT + Ampicillin in a glass tube. After overnight incubation at 37 °C, 200 rpm, 1.5 ml of culture was transfered into Eppendorf reaction tube and centrifuged for 1 min at 13,000 rpm. Supernatant was discarded, which was followed by the addition of 350 µl STET-Buffer and the tube was vortexed to resuspend the pellet. Next, 25 µl Lysozyme (10 mg/ml) (Merck) was added, the tube was inverted to mix and left for 10 min at room temperature. Tube was then incubated for 1 min at 99 °C in a thermomixer and centrifuged for 10 min at 13,000 rpm. The pellet was removed with a toothpick and discarded. 50 µl of 3M sodium acetate, pH 4.8 and 400 µl isopropanol were added, and the tube was inverted to mix before incubation for 10 min at room temperature. The eppendorf tube was then centrifuged for 15 min at 13,000 rpm, supernatant discarded and pellet was washed for 5 min at 13,000 rpm with 70 % ethanol. Again, the supernatant was removed and pellet dried at 37 $^{\circ}$C in thermomixer. Afterwards, 20 µl H_2O/RNase at 10 mg/ml was added to the pellet which was resuspended. Newly isolated plasmid was stored at -20 $^{\circ}$C.

STET-Buffer: for 1 L, 5.845 g NaCl, 10 ml 1M Tris-HCl pH 8.0, 2 ml 0.5 EDTA and 50 ml Triton X were mixed with ddH_2O. pH-value was adjusted to 8.0 with 5M NaOH and then autoclaved.

After isolating plasmid DNA from the selected transformants, the plasmids were analysed using digestions with restriction enzymes. The main enzyme was *Pvu*II, which provided a 3.55 kb fragment of the backbone (Fig. 5.1). Other enzymes, included *Eco*RV and *Hind*III, were used to digest the plasmids further.

This helped in identifying similarities or differences in plasmids according to obtained bands on the gel electrophoresis. One plasmid from each digestion pattern group was further analysed.

Plasmids were transformed then into the corresponding mod mutant strains according to the procedures described in General Materials and Methods. For example, if the plasmids were isolated from the selected transformants from mod1, they were transformed into the mod1 mutant, to check if they could restore the mutants' phenotype from before UV-mutagenesis. Obtained transformants were checked under the microscope, after growing in the liquid culture of NM-Glu, for the ability to grow long hyphae and long, unbroken microtubules. If most of them showed the ability to grow long hyphae and had long, complete MTs, then the plasmid was regarded as a potential 'rescue plasmid' and its DNA sequence was analysed by Eurofins MWG Operon.

On the occasion that more than one gene were present on a rescue plasmid, the genes would be either selectively removed from the plasmid, using digestions with restriction enzymes and then re-introduced into the corresponding mutants or they would be sub-cloned into the pNEBUH vector.

5.2.3 Growth conditions

All cultures of *U. maydis* with exception of complemented mutant strains were grown as described earlier. All complemented mutant strains in liquid cultures and on plates were always supplemented with hygromycin, thus they would not lose complementing plasmid that had that antibiotic resistance in its backbone.

5.2.4 Benomyl sensitivity studies

Prior to the experiments shown in this chapter, the amount of MT depolymerising drug benomyl used for the sensitivity studies was determined in a series of tests on plates (not shown). The aim was to find an optimal benomyl concentration, which would be able to show clear differences between the mod mutants. Serial dilutions with tested benomyl concentrations spanned between

0.5 µM and 3 µM. From those, I concluded that 1.2 µM benomyl would be optimal for showing differences. Therefore I used this in my experiments on plates and under the microscope.

Serial dilutions

Serial dilutions of *U. maydis* AB33_GT and microtubule organisation defect (mod) mutants were applied onto CM-glucose agar plates containing 1.2 µM of methyl [1-[(butylamino)carbonyl]-1H-benzimidazol-2-yl]carbamate, commonly known as benomyl. Each strain was grown to the OD_{600} of 0.7. The control plates contained the corresponding amount of the solvent DMSO. The plates were incubated at 28 $^{\circ}$C for 48 hours prior to observation of cell growth.

5.2.5 Preparation of genomic DNA for Illumina sequencing

DNA was isolated from AB33_GT and 5 mod mutants as described previously. Sequencing was performed by the University of Exeter Sequencing Service. DNA samples were prepared for sequencing by producing a paired-end library using the SpriWork library preparation protocol.

Ustilago maydis DNA was diluted in TE buffer to a final volume of 200 µl and sonicated in a Biorupter for 15 minutes (30 s pulse : 30 s rest) on ice with medium power. All samples contained a good proportion of fragments in the size range of 200-600 bp. Libraries were prepared, with 300-600 bp size selection using TruSeq Indexed adapters and were amplified by 15 cycles of PCR resulting in samples shown below in Table 5.1. Libraries were denatured and diluted to 6.5 pM for clustering on the cBot and 100 paired end reads were sequenced on the Illumina HiSeq2000.

Table 5.1 Concentrations and fragment sizes of newly prepared libraries.

Sample	Concentration [nM]	Fragment length
526	80	416 bp
mod1	67	441 bp
mod 2	38	452 bp
mod 3	96	407 bp
mod 4	86	414 bp
mod 9	76	435 bp

5.2.6 *De novo* assembly of *Ustilago maydis* AB33_GT and the mod mutants

De novo assembly of the genomes was performed by the University of Exeter Sequencing Service. In brief, samples were filtered using the FASTX toolkit (v 0.13) (Blankenburg et al., 2010). All reads containing adaptor sequence were removed. Reads were assembled using Velvet algorithms (1.1.04) (Zerbino and Birney, 2008). At the same time, the raw reads were aligned against reference genome of *Ustilago* (5.21) using BWA (Li and Durbin, 2009) resulting in alignment files, which were manipulated with SAMtools (Li et al., 2009), creating pileup file. In addition, BEDTools software (Quinlan and Hall, 2010) was utilised to estimate gene coverage. The genes that were looked for had less than 90% coverage in MOD mutant strains, but 100% coverage in wild-type strain. Each sequenced strain was checked for a presence of 6522 gene sequences from *U. maydis* wild type genome using BLASTn, as well as BLASTp search in NCBI database. An e-value cut off of $1e^{-5}$ was used to identify all genes and therefore the hit sequences below that value were not regarded as significant. Mutations in the genes were identified using software, written at the University of Exeter, which identified SNPs (Single Nucleotide Polymorphisms) that fell within genes, promoters or introns and which would produce non-silent mutations.

5.3 Results

5.3.1 Genetic screen

In order to identify the novel factors organising the microtubules, I utilised a genetic screen, which was previously done in our lab by UV-mutagenesis of AB33_GT strain, which can be switched to filamentous growth after change of medium to nitrate-containing and which can express GFP-alpha-tubulin. The main principle of the screen was to select for transformants with defective microtubule array in the hyphae of *U. maydis*. Such transformants would happily grow as yeast, therefore would not have faulty mitotic MTs, but after media change they would fail to produce long hyphae and MTs would not be properly organised.

Initial UV mutagenesis was performed and mutants were obtained. It was previously shown (Hemetsberger, 2008), that to achieve 1 mutation per cell it is necessary to obtain a 3 % survival rate. To test which UV intensity should be used, 3 independent experiments were carried out. The results were plotted onto the graph, which shows that to achieve a 3 % survival rate an intensity of 33 mJ/cm^2 should be used (Figure 5.2).

The first UV-mutagenesis provided 145 mutants with impaired filamentous growth and the second one, 160 mutants. For further work, five mod (Microtubule Organisation Defect) mutants were selected: mod1, mod2, mod3, mod4 and mod9. These had similar phenotype under the microscope which is short, fragmented microtubules and inability to produce long, elongated hyphae (Figure 5.3, panel C), in comparison to the wild-type, where long, unbroken MTs can be seen spanning throughout the whole length of hyphae (Figure 5.3, panel A and B). On NM-plates (Figure 5.4), they formed smooth, ‘greyish’ colonies, which were clearly distinguished from white and ‘fluffy’ wild-type colonies.

In order to quantify the differences in MT length between the WT and the MOD mutants, they were grown during the day in a CM-Glu medium and then filamentous growth was induced overnight by changing media to NM-Glu. Three

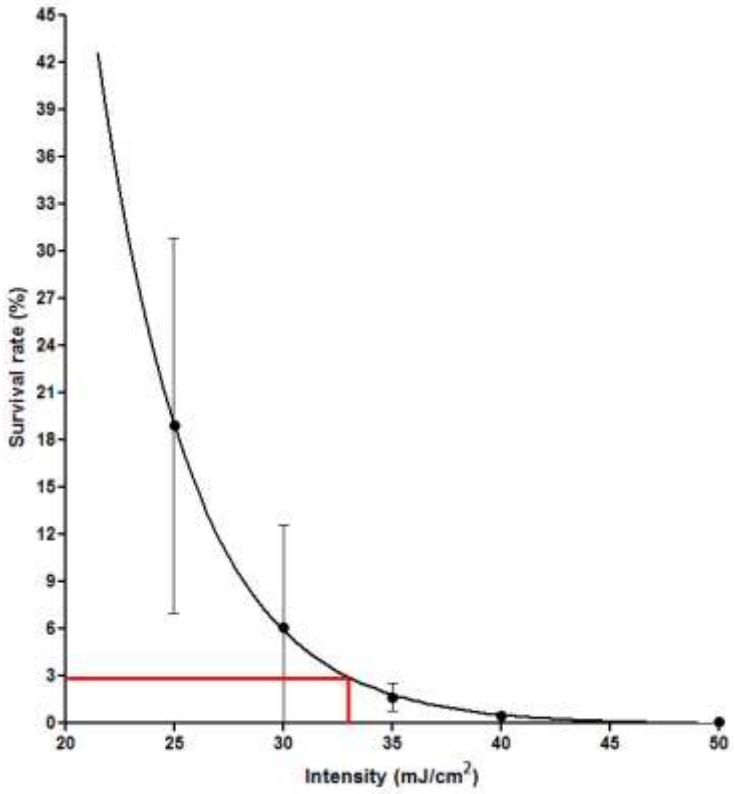

Figure 5.2 Survival curve of UV-mutagenised AB33_GT strain.

For induction of ca. 1 mutation per cell it was necessary to achieve a ~ 3% survival rate, previously shown (Hemetsberger, 2008). For AB33_GT strain an intensity of 33 mJ/cm² of UV_{254} had to be applied in the second round of UV-mutagenesis. Results were obtained after performing 3 independent experiments and plotted onto the graph.

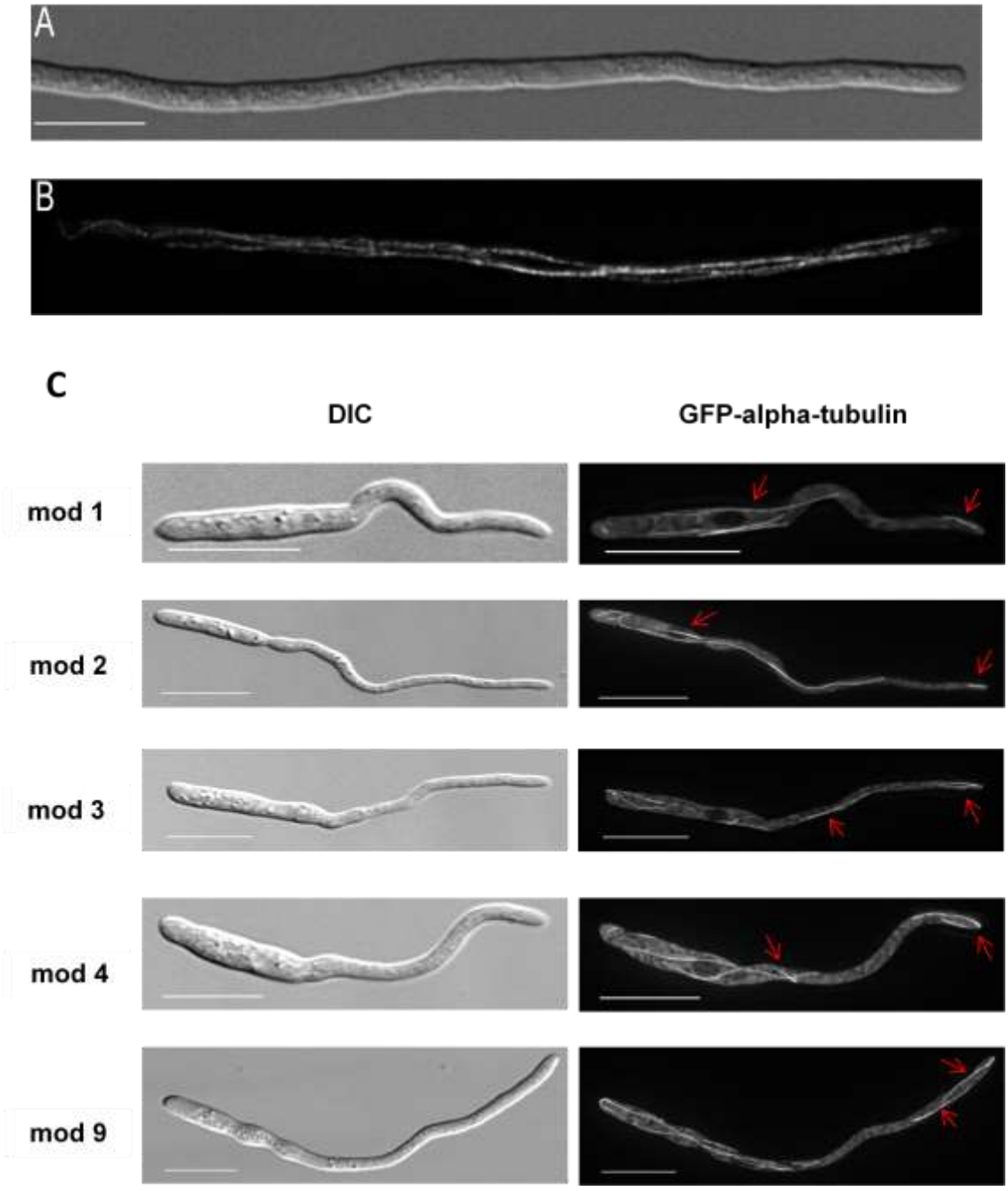

Figure 5.3 Phenotype of WT strain and the mod mutants under the microscope.

The upper panel (**A**) shows a DIC image of WT hyphae. The lower panel (**B**) shows typical, unbroken microtubules visualised with GFP-alpha-tubulin in WT. Image (B) presents maximum projection obtained from *z*-axis stack.

Panel (**C**) shows mod (**M**icrotubule **O**rganisation **D**efect) mutants from the genetic screen used for identification of novel factors organising MTs. Column on the left contains DIC images and the right one microtubules visualised with

GFP-alpha-tubulin. Images on the right present maximum projection obtained from *z*-axis stacks. Short microtubules are highlighted by the red arrowheads. Scale bars=10µm.

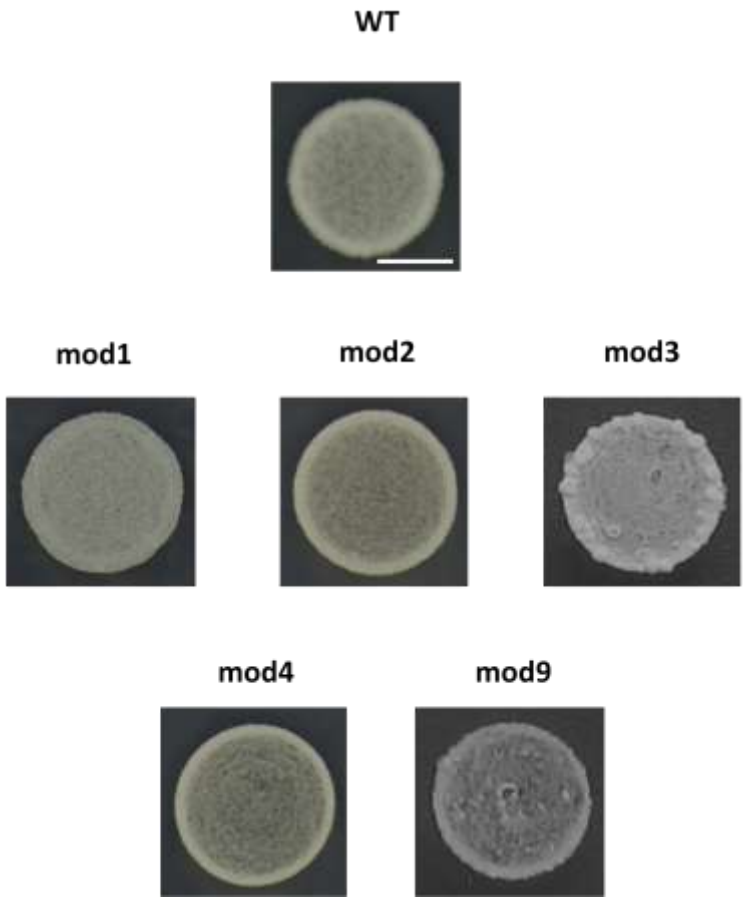

Figure 5.4 Phenotype of mod mutants on NM-Glu plates

WT strain (AB33_GT) produces white, fluffy colonies, while mutant shows greyish, smooth colonies.Scale bar=10µm.

independent experiments were carried out and z-axis stacks from at least 10 cells were made for each strain at the microscope. Then, length of MT tracks in each cell was measured using MetaMorph (Molecular Devices) and values were entered into GraphPad Prism 5.03 software to check whether there were significant differences in MT tracks length. This analysis showed that for all mod mutants the length of MT tracks was significantly smaller than the WT (Figure 5.5). It seems that mod2 strain can produce the longest microtubules of all mods, but they were never longer than 20 μm, while the WT produced MTs longer than 70 μm.

5.3.2 The mod mutants and benomyl sensitivity

The mod mutants, from the genetic screen, had very similar phenotypes on plates and when observed under the microscope, therefore, in order to better characterise the mutants, serial dilutions were made on plates containing benomyl, a fungicide that inhibits microtubule polymerisation and depolymerises existing microtubules by binding to beta-tubulin and changing conformation of α/β heterodimer (Kilmartin, 1981; Sweet et al., 2007). The aim was to find and test a benomyl concentration that would potentially show different levels of sensitivity by the mod mutants in their yeast-like stage. Firstly, I tested which concentration was optimal to show differences between MODs (not shown) and found that it was 1.2 μM of benomyl.

Plates with serial dilutions were made to compare mod mutants visually (Figure 5.6). For the purpose of this study, the mutant strains were compared with WT and classified as hyposensitive (growing faster and forming bigger colonies than WT on benomyl supplemented plate), hypersensitive (with visibly reduced growth and smaller colonies) or neutral (with phenotype similar to WT). On the plates containing 1.2 μM benomyl all strains, except for mod2, showed reduced growth, in comparison to the DMSO supplied plate. Moreover, the serial dilution from the benomyl plates indicated that mod1, mod3 and mod4 mutants could be classified as hypersensitive, mod2 was hyposensitive, and mod9 looked neutral. These results showed that the MOD mutants, despite their similar phenotypes after switching to filamentous growth, can be distinguished using a MT depolymerising drug, benomyl. It could mean that the UV-mutagenesis potentially affected genes responsible for microtubule stability in the mod

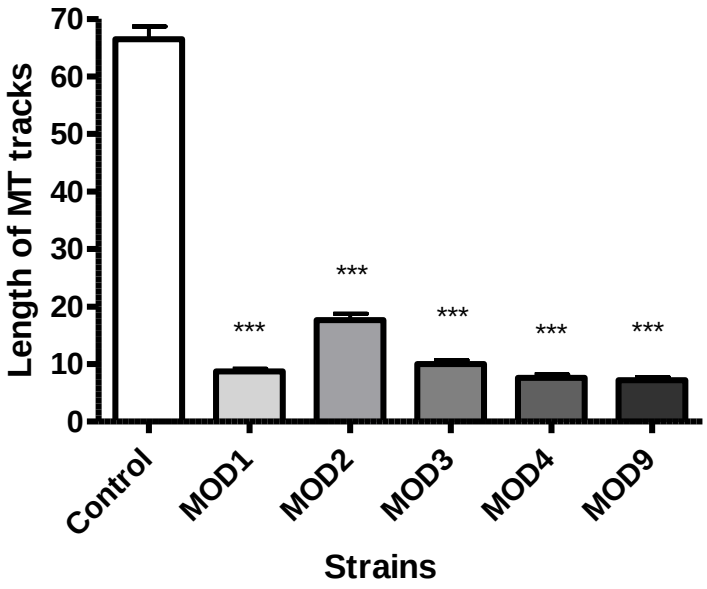

Figure 5.5 Microtubule tracks in the hyphae of mod mutants are significantly shorter than in the wild-type.

WT strain (AB33_GT) produces long hyphae with MT tracks reaching 70 μm, while mutants can only produce short hyphae with MTs no longer than 20μm. Data was collected from 3 independent experiments. All bars are given as mean±SEM.

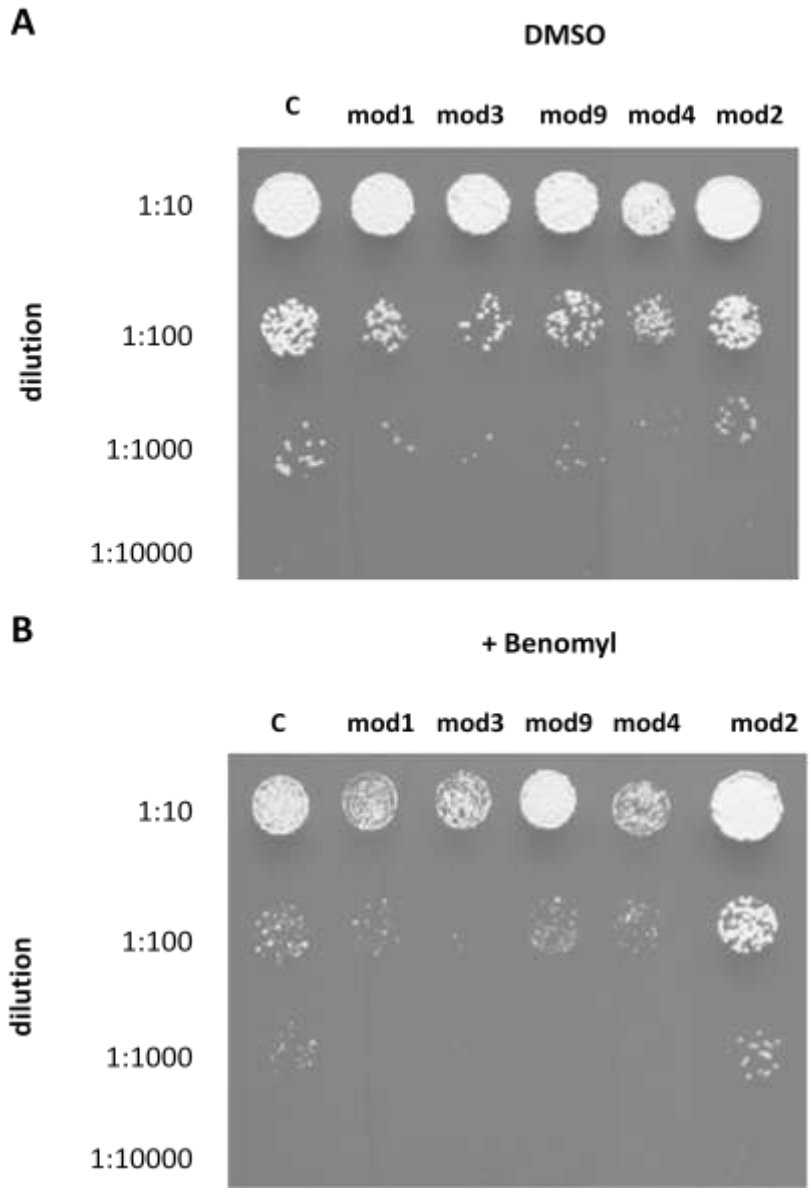

Figure 5.6 The influence of benomyl on mod mutants.

(**A**) On DMSO containing plate all strains were grown in a similar way to the control strain AB33_GT (C). Cell dilutions are given. Starting OD_{600} was 0.6.

(**B**) On benomyl containing medium mod2 seems to grow even better than the control strain, AB33_GT (shown as C). It was the only hyposensitive mutant found. mod1, mod3 and mod4 were hypersensitive and mod9 was neutral. Concentration of benomyl was 1.2 µM. Cell dilutions are given. Starting OD_{600} was 0.6.

mutants. It caused less stable MT array in some mutants (hypersensitive), but also more stable MTs in the hyposensitive mod2 mutant.

To check the appearance of MTs in benomyl treated mod mutants, all strains were grown in a liquid medium with addition of 1.2 μM benomyl and observed at the microscope (Figure 5.7). All mod mutants showed a disrupted MT array, lateral growth and had a cell separation defect. Despite being classified as hyposensitive, mod2 mutant did not appear to be less sensitive to benomyl than other strains. These discrepancies between plate assays and microscope observations may have occurred, because perhaps benomyl lost its properties during 2-3 days at 28 $^{\circ}$C and is not as effective as at the beginning of the experiment.

5.3.3 Complementation of MOD mutants with a genomic library

mod1

For mod1, I utilised an available transformant, selected previously from the complementation plate, to find potential 'rescue' plasmids. In total, I obtained 14 plasmids, but only 5 of them contained the 3.55 kb backbone from the genomic library. Those were chosen for further work, which included transforming each of them into mod1 mutant, to check if they could restore WT-like phenotype. From each transformation, many colonies were obtained, however, after checking them with the microscope none of them complemented the mutant, which meant that the plasmids did not carry genes necessary to restore desired phenotype. The plasmids, which did not contain the 3.55 kb backbone were not studied further and were treated as incorrect, because they did not contain hygromycin resistance cassette.

I also checked, whether DNA sequence of the 4 genes present on the previously identified 'rescue' plasmid had mutations, using sequencing analysis performed by Eurofins MWG Operon and found no mutations in any of the genes. To identify which of the four genes (Figure 5.8) is responsible for restoring WT phenotype, I removed 4.06 kb fragment containing Gene 2 and

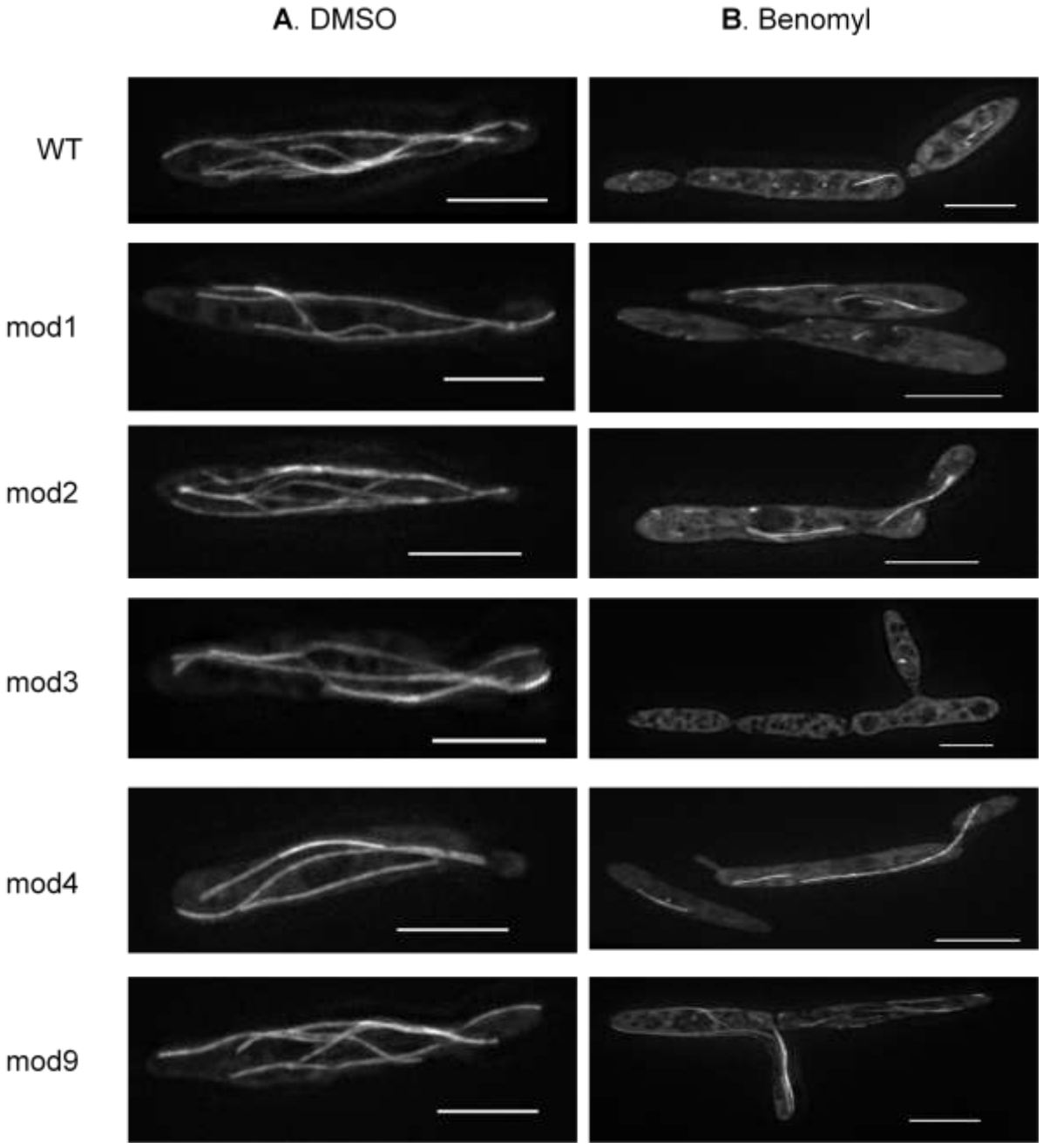

Figure 5.7 The effect of benomyl on the MT cytoskeleton in yeast-like cells of control strain AB33_GT and mod mutant strains.

(**A**) DMSO treated cells have a proper MT array and display normal growth. The amount of added DMSO was equal to the volume of added benomyl. All cultures were grown to the OD_{600} of 0.6-0.7. Scale bar=5 µm. All cells expressed GFP-alpha-Tub.

(**B**) Control cells grown in a liquid medium with 1.2 µM benomyl show a disrupted MT array, lateral growth and have a cell separation defect.

All images present maximum projection obtained from *z*-axis stacks.

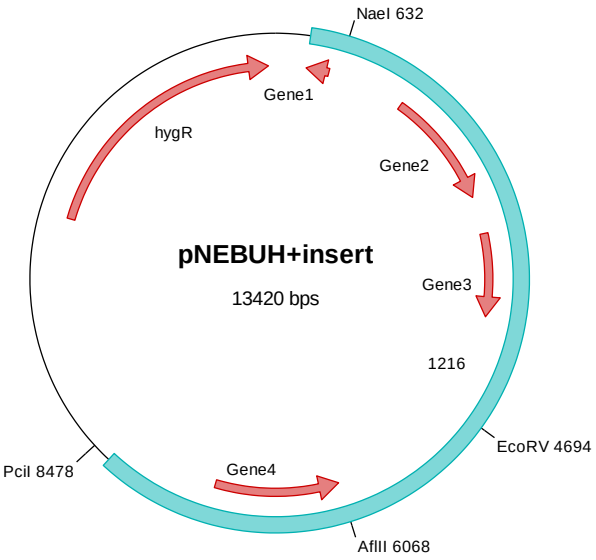

Figure 5.8 *E. coli* vector pNEBUH with insert, which acts as a 'rescue' plasmid for MOD1 mutant.

This plasmid contains 3.55 kb backbone of pNEBUH plasmid and an insert found to restore MOD1 mutant's phenotype into WT-like. The 9.8 kb insert contains four genes, one of which, Gene 1, appears to be truncated. The restriction sites for *Nae*I and *Eco*RV were used to remove 4.06 kb fragment containing Gene 2 and Gene 3, while *Pci*I and *Afl*II sites were used to remove 2.4 kb fragment containing Gene 4. Graphic map was generated in Clone Manager 9 Professional Edition (Scientific & Educational Software).

Gene 3 using restriction endonucleases *Nae*I and *Eco*RV and then transformed plasmid with the remaining 2 genes into mod1 strain. It did not restore the WT phenotype. Similarly, I removed 2.4 kb fragment containing Gene 4 using *Pci*I and *Afl*II restriction enzymes from the rescue plasmid, but plasmid with Gene1, 2 and 3 was not able to complement the mutant. In conclusion, it seems that all of the genes are needed 'rescue' 3.55 kb 1 mutant's phenotype.

mod2

The complementation of mod2 mutant with the genomic library resulted in 5 'rescued' strains. Their DNA was isolated and plasmids transformed into *E. coli*, resulting in many colonies, which provided potential rescue plasmids. As before, each plasmid was checked for the presence of 3.55 kb backbone. In order to investigate which plasmid restores the wild-type phenotype of mod2, *Ustilago* transformations were carried out using 9 different plasmids. Each plasmid was transformed separately into mod2 mutant. All transformations produced hundreds of colonies that were then checked under the microscope for intact MTs and long hyphae, after shifting to NM-Glu. Unfortunately, none of those plasmids was able to complement the mutant.

mod3

For mod3 mutant, already available 'rescue' plasmid, able to restore correct MT array and long hyphae, contained only 1 gene belonging to the family of serine/threonine kinases. Its DNA sequence was checked by Eurofins MWG Operon. The results showed that there was not a single mutation in the kinase.

I also prepared a vector with aim to overexpress ser/thr kinase in mod3 mutant, to see if it rescues it. However, after performing many transformations, done in duplicates, there were no transformants obtained, suggesting that too many copies of the ser/thr kinase are lethal for *U. maydis.* This result could also be tested by overexpressing the ser/thr kinasein wild-type.

mod*4*

For mod4 I used 2 available transformants, to find potential 'rescue' plasmids. Although none of them contained the 3.55 kb backbone from the genomic

library, I decided to transform them back into mod4, but as expected they did not restore the correct phenotype.

mod 9

The mod9 mutant was identified by me in the second round of UV-mutagenesis, as described in 5.2.1 section. It was then confirmed on NM-Glu plate (Fig. 5.4) and in a liquid culture (Fig. 5.3). Complementation of mod9 was done according to the protocol described in section 5.2.2. As a result, I obtained 40 potential rescued transformants, from which I chose one for further experiments.

After DNA isolation and transformation into *E. coli,* I found 2 different plasmids, distinguished by different digestion patterns and both had the expected 3.55 kb backbone from the genomic library. I transformed them into mod9, but, neither of them seemed to rescue mod9. Perhaps both plasmids should be transformed together into the mutant, which would mean that more than one gene is responsible for the mutants' phenotype.

5.3.4 Genomic sequencing of *U. maydis* AB33_GT strain and mod mutants.

In order to succeed in identifying the potential factors responsible for the phenotype of the modmutants, I sent them along with the wild-type strain for Illumina sequencing. DNA gel electrophoresis containing DNA samples submitted to the University of Exeter Sequencing Service are shown in Figure 5.9.

As a result of the Illumina sequencing, six strains were successfully sequenced and results were analysed by Dr. Darren Soanes. In brief, 6519 gene sequences from wild-type were checked for presence in each mutant strain using protein BLAST with $1e^{-5}$ e-value cut-off. By comparing the genomes of WT and mod strains, the software indicated possible gene deletions in mod1 and mod9 mutants, as the genes were not present in the mutants' genomes (Table 5.2). Genes deleted from mod1 mutant were annotated as a reverse transcriptase and gene with unknown function, while mod9 does not have a telomere-associated DNA helicase and a gene with unknown function.

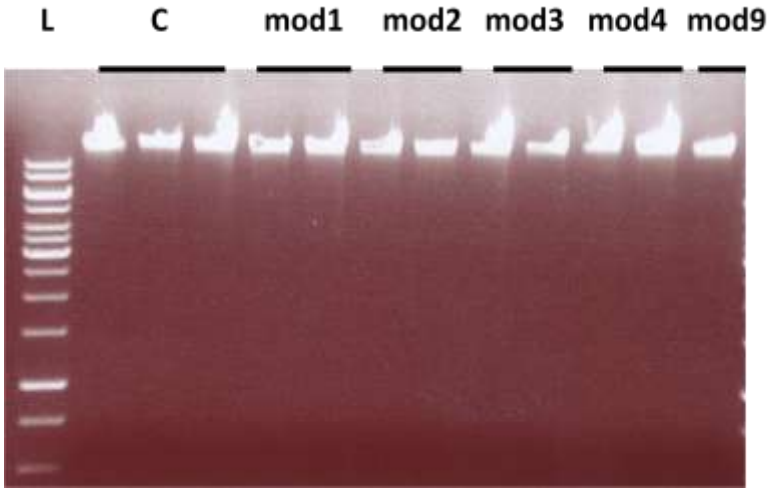

Figure 5.9 Agarose gel electrophoresis of *U. maydis* AB33_GT (C) and MOD mutants genomic DNA submitted for Illumina sequencing.

DNA was extracted using standard procedures and treated with Rnase. 1µl of DNA was loaded in a 1% agarose. (L) is 1kb Fermentas ladder, (C) marks AB33_GT.

Table 5.2 Number of genes present in the wild-type strain and mod mutants established by the Illumina sequencing

Strain	Number of genes
Wild-type	6519
mod1	6517
mod 2	6519
mod 3	6519
mod 4	6519
mod 9	6517

Therefore, it would be interesting to investigate the gene with unknown function by tagging it with GFP in a wild-type to find out where it localises in the cell, as well as by deleting it in a wild-type strain, to see what phenotype it causes. The software was also used to search for SNPs (single-nucleotide polymorphisms) in the mutant strains by comparing DNA sequences from mutants to the wild-type strain sequence, in order to find mutated genes. All details regarding SNPs are in the Excel spreadsheets (Figure A2 in the Appendix). Among the SNPs there were 36 silent and 37 non-silent mutations. Only genes with silent mutations were not analysed further, because non-silent mutations in the promoters could, for example, stop RNA-polymerase or transcription factors from binding, therefore stopping the gene expression. Also mutations in the introns could potentially be of importance, because of the alternative splicing. It is known that alternative splicing occurs in app. 2.3 % of *Ustilago's* genes (Grutzmann et al., 2013) and there is evidence of all varieties of alternative splicing, however, the majority are intron retention events (Ho et al., 2007). This means that part of the intron stays in the mRNA and mutations could potentially cause a shift in the reading frame, which would lead to change in the expression of a gene.

Moreover, detailed analysis of the non-silent mutations (Table 5.3.) in the mod mutants showed that mod1 contains the highest number of mutations in the coding sequences (ORFs), promoters and introns. It was also apparent that most predicted genes contained only 1 mutation per sequence, apart from a gene present in mod3 that had 2 mutations. Mod1 and mod4 each have a gene with 3 mutations, although some of them are silent.

Table 5.3 Non-silent mutations present in the MOD mutants found using Illumina sequencing.

Non-silent mutations			
Mutant	**ORF[1]**	**Promoter[2]**	**Intron[3]**
mod1	19	12	4
mod 2	3	8	1
mod 3	5	0	3
mod 4	7	0	1
mod 9	3	5	0

The ORF[1] column represents mutations found in the open reading frame of the affected genes, Promoter[2] shows mutations found in the promoter region defined as 1-1.5kb before the start codon and Intron[3] column represents mutations found in the introns.

5.3.5 Analysis of mutations identified in the mod mutants

mod1

The Illumina sequencing showed that in mod1, 19 genes were found to have mutations in their coding sequences, 4 genes had mutations in their introns and 12 genes had mutations in their promoters (Table 5.3). Firstly, a BLAST search was done across databases of 53 different organisms to check for presence of homologues of the mutated genes, to test if there are any genes known as potential microtubule interactors. Then, for each gene, a corresponding protein sequence was analysed using the Interpro website to check for domain architecture (Figures 5.10-5.12). The purpose of this was to see if there are any MT-binding motifs, indicating involvement in MT array organisation. Among all mutated genes, 17 were found to encode proteins with known functions. 18 genes were found to encode proteins annotated as 'uncharacterised' or 'putative' in the *Ustilago maydis's* database MIPS, which means that there might be novel factors organising MTs among them.

In the group of genes with known functions, there were 2 involved in a ubiquitin pathway, UM02440 (Figure 5.11) and UM05402 (Figure 5.12), which plays role in the regulation of many basic cellular processes, for example, cell cycle and division, differentiation and development, DNA repair or response to stress (Ciechanover, 1998). However, UM05402 together with UM03762 (Figure 5.12) have a WD40-repeat containing domain, a protein-protein interaction domain. Proteins with WD40 domain are involved in a wide range of cellular functions, such as signal transduction, vesicular trafficking, cytoskeleton assembly, cell-cycle control, apoptosis, chromatin dynamics and transcription regulation (Xu and Min, 2011). UM03762 is also required for nuclear pore complex structure and function, according to annotation in MIPS. Based on these findings, it was not very likely for UM02440 to cause mod1's phenotype. However, in case of the genes encoding proteins with WD40 domain (UM5402 and UM03762) it is possible that one of them may be important for this mutants' phenotype.

Another group of genes identified from the Illumina sequencing has functions in DNA repair and processivity. These include a mismatch base pair and cruciform DNA

mod1

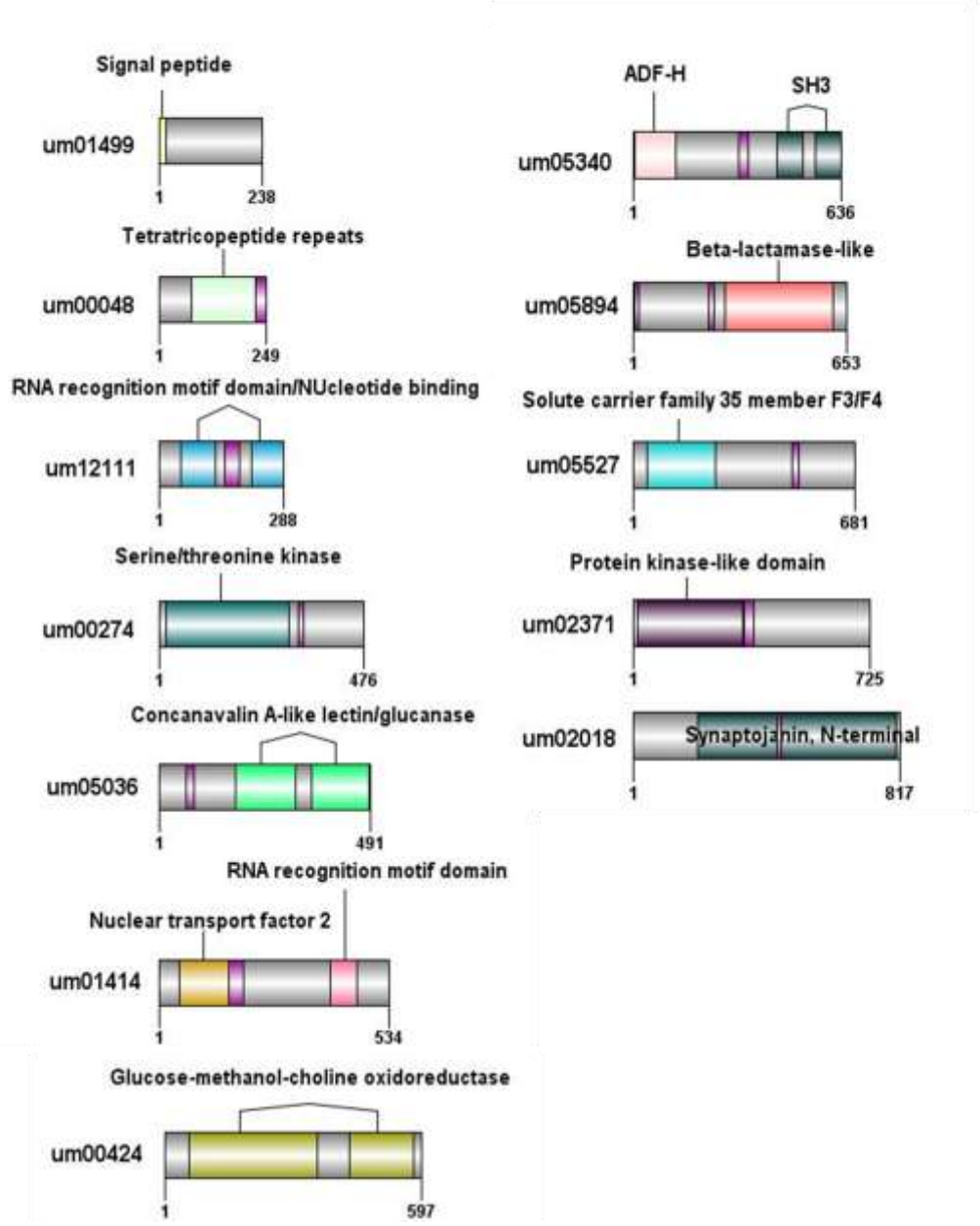
Signal peptide
um01499
1
238
Tetratricopeptide repeats
um00048
1
249
RNA recognition motif domain/NUcleotide binding
um12111
1
288
Serine/threonine kinase
um00274
1
476
Concanavalin A-like lectin/glucanase
um05036
1
491
RNA recognition motif domain
Nuclear transport factor 2
um01414
1
534
Glucose-methanol-choline oxidoreductase
um00424
1
597
ADF-H
SH3
um05340
1
636
Beta-lactamase-like
um05894
1
653
Solute carrier family 35 member F3/F4
um05527
1
681
Protein kinase-like domain
um02371
1
725
um02018
Synaptojanin, N-terminal
1
817

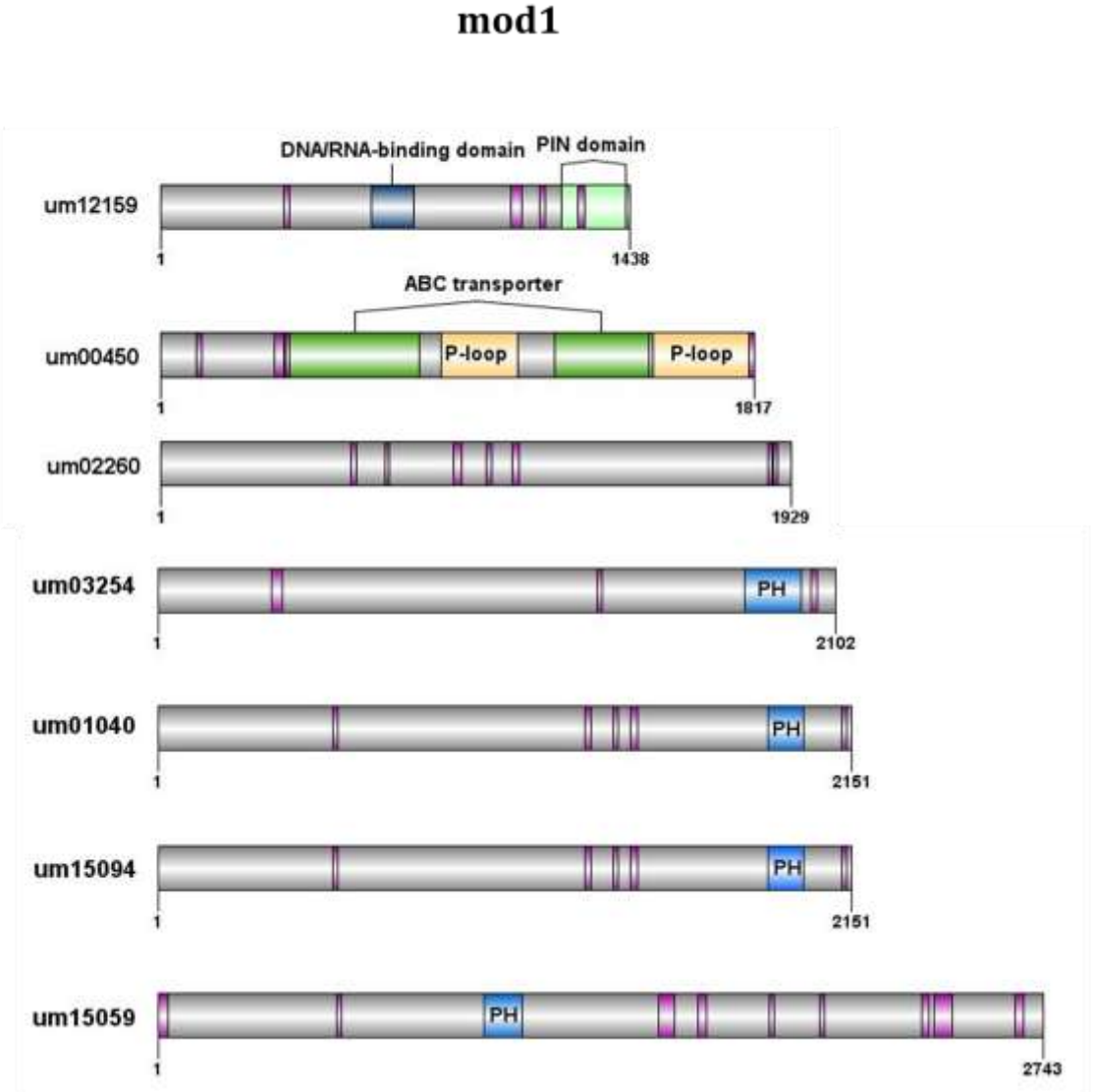

Figure 5.10 Domain architecture of the genes with mutations in the ORFs found by the Illumina sequencing in the MOD1 mutant

mod1

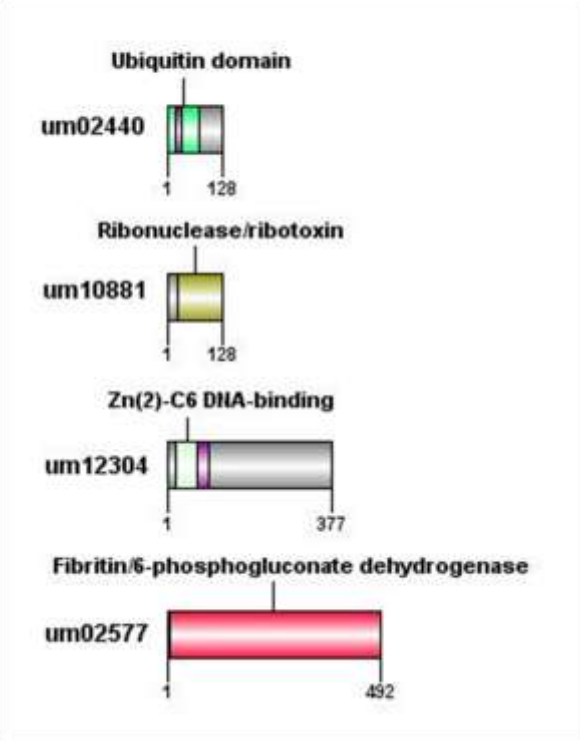

Figure 5.11 Domain architecture of the genes with mutations in the introns found by the Illumina sequencing in the MOD1 mutant.

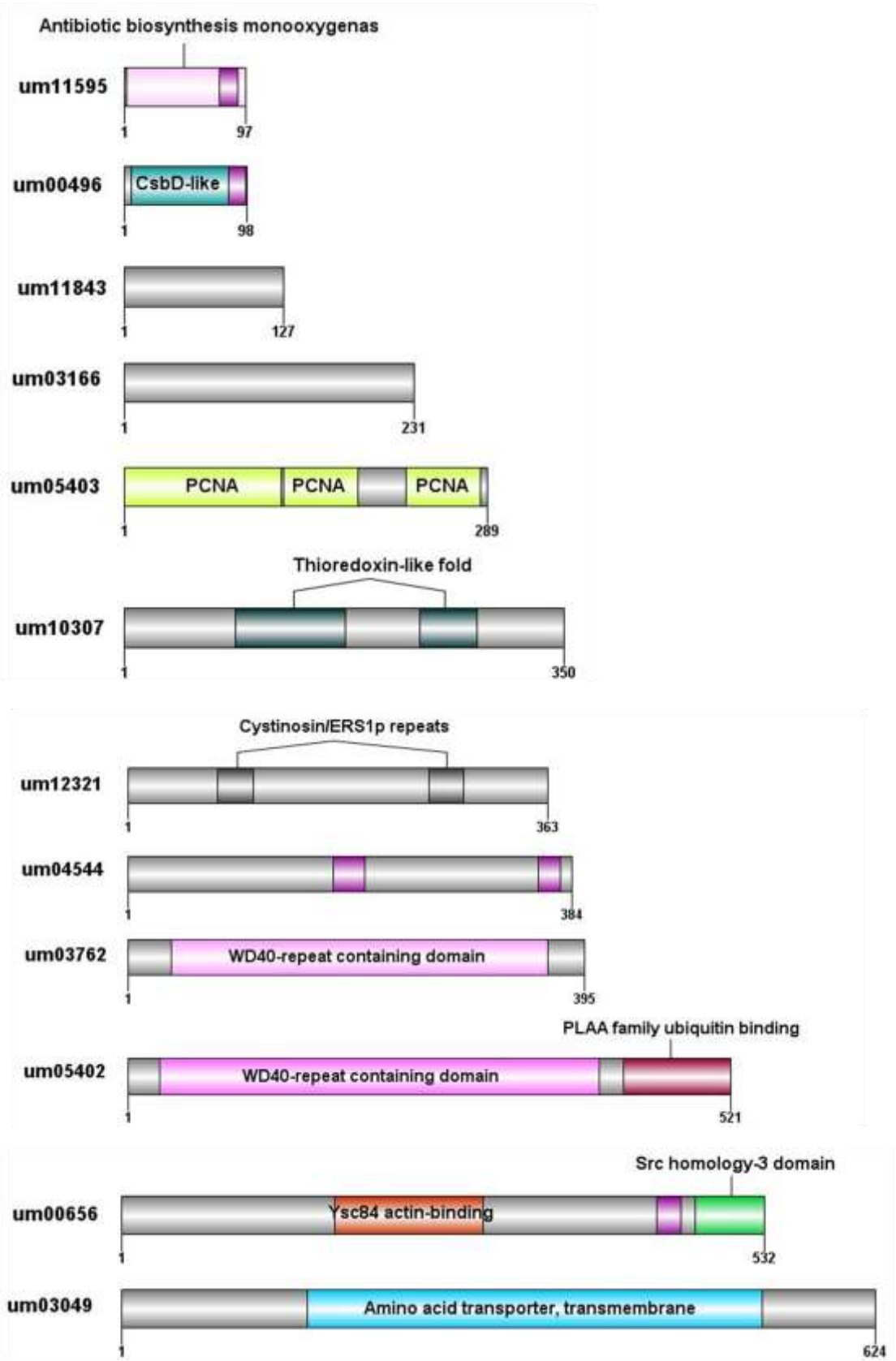

Figure 5.12 Domain architecture of the genes with mutations in the promoters found by the Illumina sequencing in the MOD1 mutant.

For each protein, I show their domain architecture, determined using the InterPro online software (Hunter et al., 2012). All cartoons were drawn using DOG 2.0 software. The purple-coloured motif, present in most proteins, is a coiled-coil region. The rest of domains are denoted with different colours and names.

recognition protein UM00496 (Figure 5.12), a casein kinase I UM00274 (Figure 5.10), acting as a regulator of signal transduction pathways in most eukaryotic cell types involved, for example, in nucleo-cytoplasmic shuttling of transcription factors, DNA repair, and DNA transcription (Eide and Virshup, 2001) and DNA polymerase processivity factor UM05403 (Figure 5.12). In addition, there were 2 genes encoding proteins interacting with RNA. One of them, UM12111 (Figure 5.10), is a snRNP, which is a part of spliceosome (Liang and Lutz, 2006) and the second one, UM10881 (Figure 5.11), is a ribonuclease responsible for RNA degradation. Most probably none of them would be responsible for the disrupted MT cytoskeleton in the mod mutant.

Furthermore, among the identified genes were ones responsible for cellular transport, such as UM01414 (Figure 5.10), related to Ras family of small GTPases that can regulate all-receptor mediated transport between the nucleus and the cytoplasm (Steggerds and Paschat, 2002), UM03049 (Figure 5.12), a neutral aminoacid permease which catalyses the transport of neutral amino acids into the cell (Grenson et al., 1970) and UM00450 (4.10), a multidrug resistance protein that belongs to ATP-binding cassette (ABC) transporter superfamily. Most ABC transporters are responsible for the active transport of different compounds through the biological membranes (Klein et al., 1999; Leslie et al., 2005). Judging by the functions, the genes do not seem as good candidates for novel regulators of MT cytoskeleton.

Moreover, there were 2 proteins found to have direct links to the cytoskeleton. They were annotated as drebrin-f-like, UM05340 (Figure 5.10) and TPR repeat protein, UM00656 Figure (5.12). Drebrin is an actin filament (F-actin)–binding protein involved in organising the dendritic pool of actin (Grintsevich et al., 2010), with crucial roles in neuritogenesis and synaptic plasticity (Worth et al., 2013). The TPR-repeat protein is annotated in MIPS as a protein involved in the organisation of the actin cytoskeleton. BLAST search against numerous databases showed that this protein is a potential orthologue of yeast protein Ysc84, which represents a class of actin-binding proteins conserved from yeast to humans. It contains a novel N-terminal actin-binding domain Ysc84 actin binding (YAB), which can bind and bundle actin filaments (Robertson et al., 2009) In addition, it also has SH3 domain previously identified in several

cytoskeleton-associated proteins such as myosin 1B and spectrin (Parker et al., 1996).

The rest of the genes with known function appeared to encode enzymes involved in different biochemical reactions inside the cell, such as phosphorylation by ser/thr kinase UM02371 (Fig. 5.10), breaking down glucans, UM05036 (Fig. 5.10), phosphogluconate dehydratase activity, UM02577 (Fig. 5.11) and choline dehydrogenase activity, UM00424 (Figure 5.10).

Finally, among the group of 'uncharacterised proteins' 4 genes encoded proteins with similar domain architecture: UM03254, UM01040, UM15094 and UM15059 (Figure 5.10). Basically, they all contained a PH (pleckstrin homology) domain found in many proteins important for signal transduction and cytoskeletal function (Wang et al., 1994). This means that all of these genes could potentially be good candidates for factors that disrupted MT cytoskeleton in mod1.

Other genes encoded proteins involved in RNA processing, for example UM00048 and UM12159 (Figure 5.10), RNA polymerase associated protein and telomerase binding protein with nuclease activity, respectively.

There was also a group of proteins with no homologues in other organisms identified, but only with known domains found using Interpro search. Those were UM01499 (Figure 5.10), which had a short signal peptide, indicating potential destination into a secretory pathway (Blobel and Dobberstein, 1975), UM11595 (Figure 5.12) with antibiotic biosynthesis monooxygenase domain found in proteins potentially able to synthesise antibiotics (Sciara et al., 2003) and UM10307 (Figure 5.12) that had thioredoxin-like folds that ubiquitously regulate cellular redox status (Qi and Grishin, 2004). None of the above proteins seemed like good candidates for novel MT cytoskeleton organisers.

There were also genes that could not be grouped with others, because they had separate functions, for example, UM02018 (Figure 5.10) has homologues which regulate Golgi membrane morphology and mitotic spindle organisation in mammals (Liu et al., 2008), in addition to regulation of lipid storage and

maintenance of vacuole morphology in fission yeast (Foti et al., 2001). UM12304 (Figure 5.11) has homologues that localise to the nucleus, UM05894 (Figure 5.10) potentially localises in the inner membrane protein and UM05527 (Figure 5.10) takes part in glycosaminoglycan degradation. Only UM02018 seems promising, because it is able to influence cytoskeleton behaviour.

The rest of the uncharacterised genes, UM02260 (Figure 5.10), UM03166, UM11843, UM04544 and UM12321 (Figure 5.12), did not seem to have any homologues in other organisms or domains recognised by the available software with the exception of UM12321, whose domain is called cystinosin, but its function is unknown. It is therefore difficult to predict if they played an important role in mod 1's phenotype. Those genes could potentially be interesting and perhaps could be tagged in wild-type.

mod 2

Illumina sequencing results for MOD2 showed 3 genes with mutations in their coding sequences (Panel A, Figure 5.13), 8 genes in the introns and I gene had mutation in the promoter (Table 5.2). As before, BLAST search was done across databases of 53 different organisms in order to find potential MT interactors and no proteins with links to the MT cytoskeleton were found. It revealed though, that the mutations in the coding sequences included a gene, UM00415 (Panel A, Figure 5.13) with homologues containing an HD domain identified using SMART website (Schultz et al 1998; Letunic et al 2012). According to SMART HD domain is found in a superfamily of enzymes with a predicted or known phosphohydrolase activity. There was also a gene, UM04371 (Figure 5.13), related to a translation initiation factor eIF2A, which has function in the early steps of protein synthesis of a small number of specific mRNAs (Zoll et al., 2002). Interestingly, it has a WD40 domain, which can be responsible for the cytoskeleton assembly, among other functions (Xu and Min, 2011), which means that it may be a good candidate for the factor that caused MOD2's phenotype and it should be further investigated. Another gene, UM10099 (Figure 5.13), had a DnaJ domain. Proteins with DnaJ domain are members of the Hsp40 family of molecular chaperons that can regulate the activity of 70-kDa heat-shock proteins (Walsh et al. 2004). The remaining genes

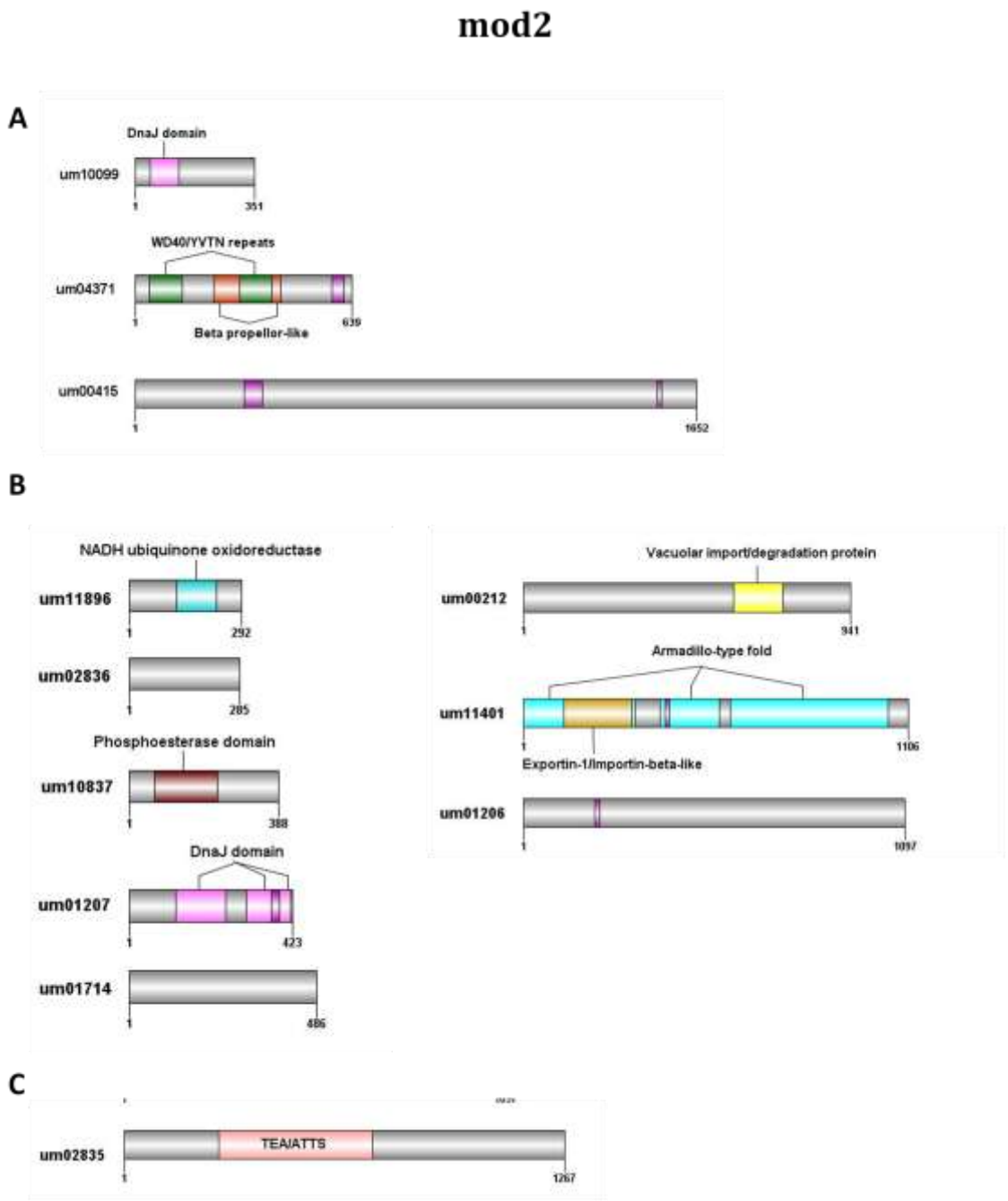

Figure 5.13 Domain architecture of the genes with mutations in the ORFs, promoters and introns found by the Illumina sequencing in the mod2 mutant.

(A) Proteins with mutations in the ORFs

(B) Protein with mutations in the intron

(C) Protein with mutations in the promoter

For each protein, I show their domain architecture, determined using the InterPro online software (Hunter et al., 2012). All cartoons were drawn using DOG 2.0 software. The purple-coloured motif, present in most proteins, is a coiled-coil region. The rest of domains are denoted with different colours and names.

encoded mainly proteins with enzymatic or transport activity, indicated by their domains and therefore do not seem likely to be heavily involved in MT cytoskeleton (Figure 5.13).

mod3

As a result of the sequencing there were 5 genes with mutations in the ORFs found and 3 genes with a mutation in the introns. Among the genes with a mutation in the ORF there was a gene identified by BLAST search as similar to MDN1, a dynein-related AAA-type ATPase, UM04878. The AAA+ ATPases are enzymes containing a P-loop NTPase domain, and function as molecular chaperones (Iyer et al., 2004). Another gene with ORF mutation was coding for a protein with a RING-type zinc finger domain, identified using Interpro website, whose homologue in *S. cerevisiae* may play a role in activation of the filamentous growth pathway (Foster et al., 2013). This gene might be the potential causing agent of mod3's specific phenotype. Other genes included a DNA mismatch repair protein, UM11009, aminotransferase class IV, UM06258 and related to potassium/hydrogen antiporter, UM04319, (Panel A, Figure 5.14).

mod4

In this mutant Illumina sequencing showed 7 genes with mutations in the ORFs (Panel A, Figure 5.15) and 1 with mutation in the intron (Panel B, Figure 5.15). Two of the genes, UM06043 encoding amidase and UM02177 encoding related to DRAP deaminase RIB2 (Figure 5.15) have function in the cell metabolism. The first one, which is a hydrolytic enzyme containing a conserved stretch of approximately 130 amino acids, known as the AS sequence, can catalyse the hydrolysis of amide bonds (Valina et al., 2004), while the second one is involved in the metabolism of vitamins, cofactors and prosthetic groups (Oltmanns and Bacher, 1972). These proteins are not very likely to have role in the MT cytoskeleton regulation.

Next set of genes was found to encode proteins taking part in the intracellular transport and membrane trafficking. Those were UM01535, which contains no known motifs and it takes part in the post-translational delivery of tail-anchored membrane proteins to the endoplasmic reticulum (ER) membrane (Mariappan

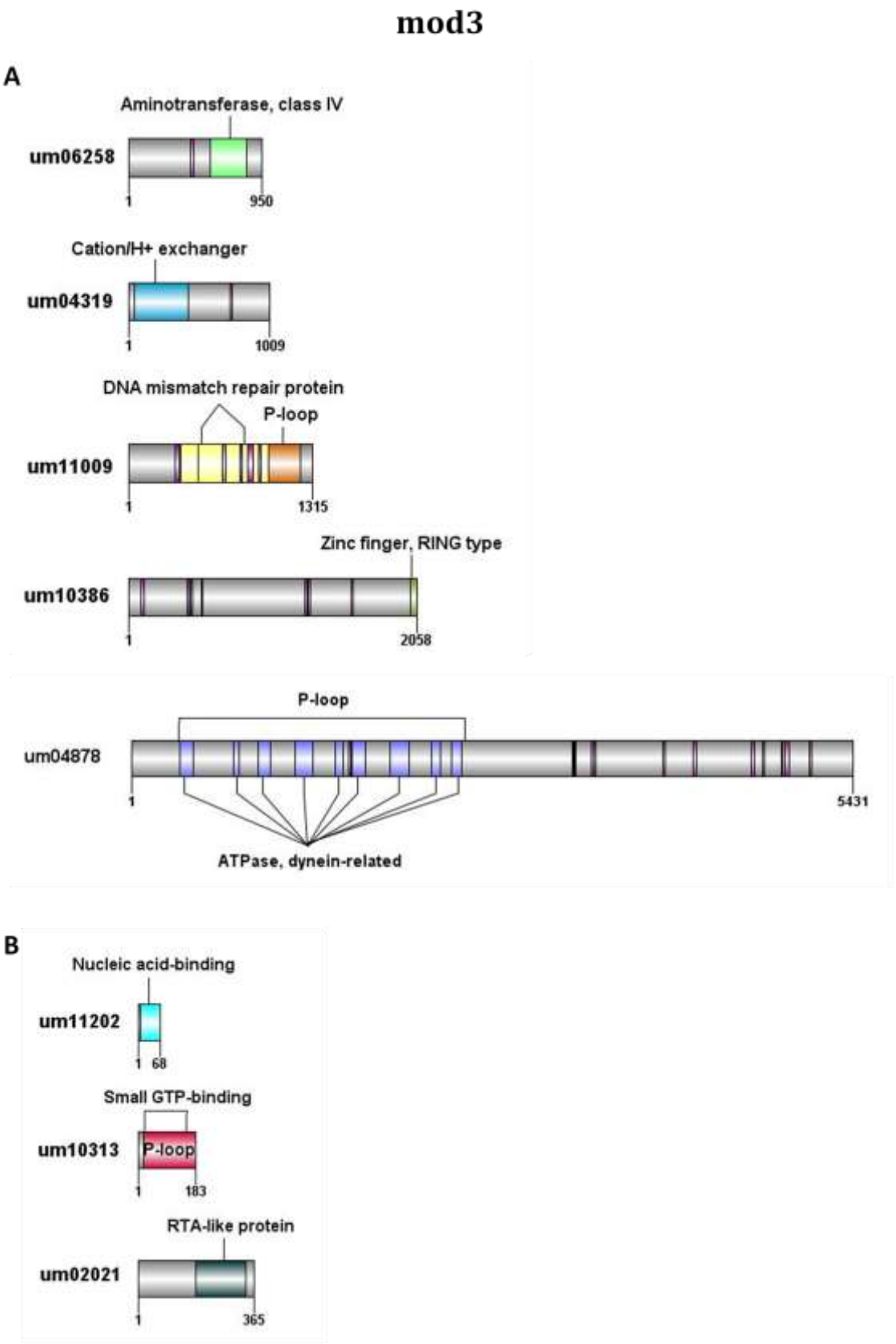

Figure 5.14 Domain architecture of the genes with mutations in the ORFs and introns found by the Illumina sequencing in the mod3 mutant

(A) Proteins with mutations in the ORFs

(B) Proteins with mutations in the intron

For each protein, I show their domain architecture, determined using the InterPro online software (Hunter et al., 2012). All cartoons were drawn using DOG 2.0 software. The purple-coloured motif, present in most proteins, is a coiled-coil region. The rest of domains are denoted with different colours and names.

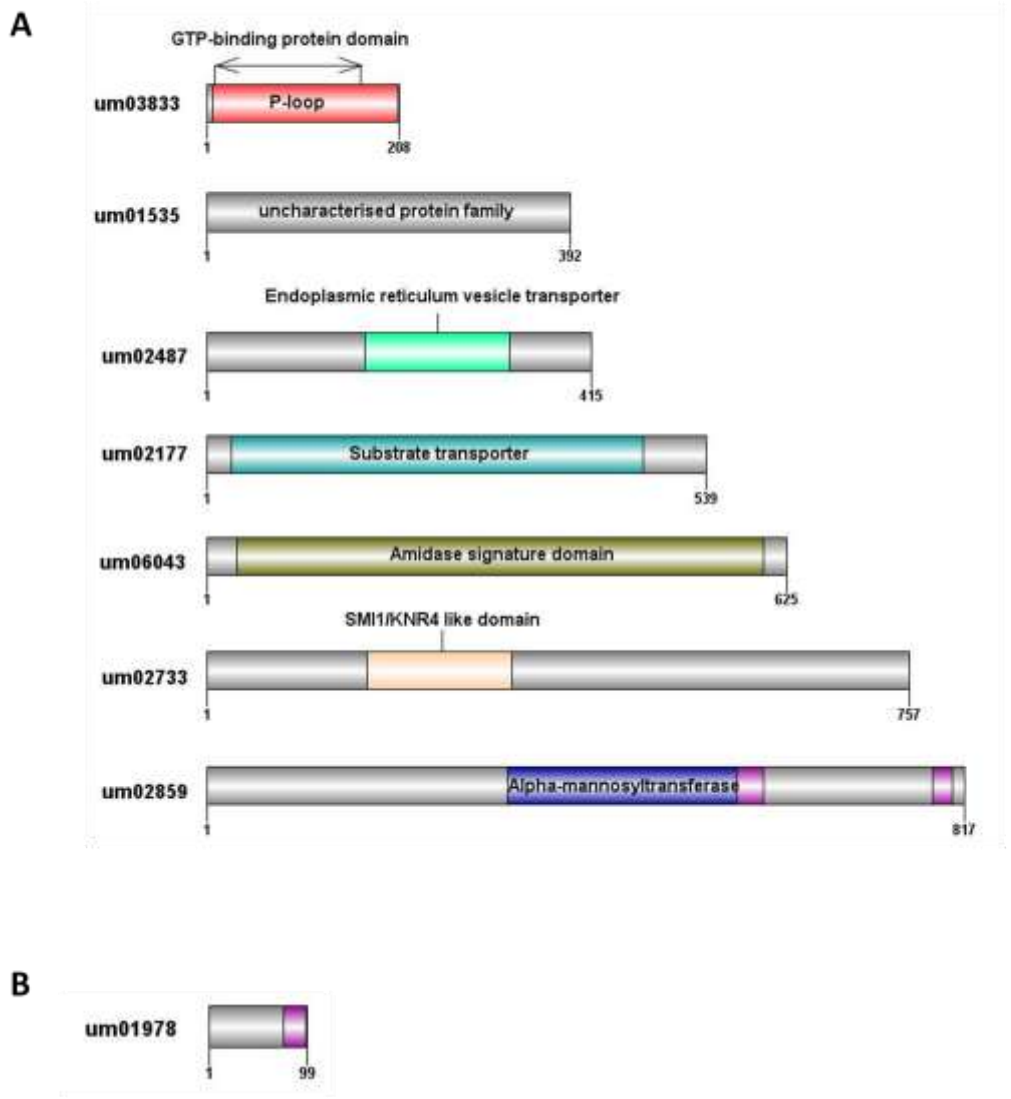

Figure 5.15 Domain architecture of the genes with mutations in the ORFs and introns found by the Illumina sequencing in the mod4 mutant.

(A) Proteins with mutations in the ORFs

(B) Protein with mutations in the intron

For each protein, I show their domain architecture, determined using the InterPro online software (Hunter et al., 2012). All cartoons were drawn using DOG 2.0 software. The purple-coloured motif, present in most proteins, is a coiled-coil region. The rest of domains are denoted with different colours and names.

et al., 2010), UM02859, that facilitates the transport of large macromolecules including RNA and proteins across nuclear membrane to the cytoplasm (Nguyen et al., 2012), UM03833, a GTP-binding protein YPT1, involved in trafficking of secretory vesicles from the ER to the Golgi (Yoo et al., 1999) and UM02733 (Figure 5.15), an integral transmembrane protein that resides in the Golgi and ER and enables transport of vesicles (Otte et al., 2001). None of these proteins are good candidates for factors organising the microtubules.

Another gene with mutation in the ORF was UM02733 (Figure 5.15) found to encode a protein involved in the regulation of the cell wall synthesis (Martin-Yken, et al., 2003). Again, it does not seem likely for this gene to be able to disrupt MT cytoskeleton.

Although, according to the *U. maydis* database, the gene with a mutation in the intron, UM01978 (Figure 5.15) was an 'uncharacterised protein', the BLAST search in different organisms showed that all homologues were HYPK proteins. HYPK is an intrinsically unstructured huntingtin (HTT)-interacting protein with chaperone-like activity, apoptosis, protein synthesis and cell cycle regulation functions (Choudhury et al., 2012). Also, the *U. maydis* gene, UM01978, does not have any known domains, apart from a single coiled-coil structure. Mutated genes identified by BLAST search are mainly involved in intracellular transport or metabolism. Also, domain architecture of the found genes did not indicate genes with obvious function in cytoskeleton organisation (Figure 5.15).

mod9

Sequencing of mod9 revealed 3 genes with mutations in ORFs (Panel A, Figure 5.16) and 5 with the mutations in the promoter (Panel B, Figure 5.16). Among those genes there was one encoding glycerophosphoinositol transporter, UM01868, alpha-1,3-mannosyltransferase, UM05152 which localises to ER membrane and is involved in protein glycosylation (Gao et al., 2004), and a protein which may be involved in vesicular transport and has a Golgi complex domain, UM03238 (Figure 5.16). None of them seems to be likely candidates for the disruption of MT cytoskeleton. There was also one gene, for which

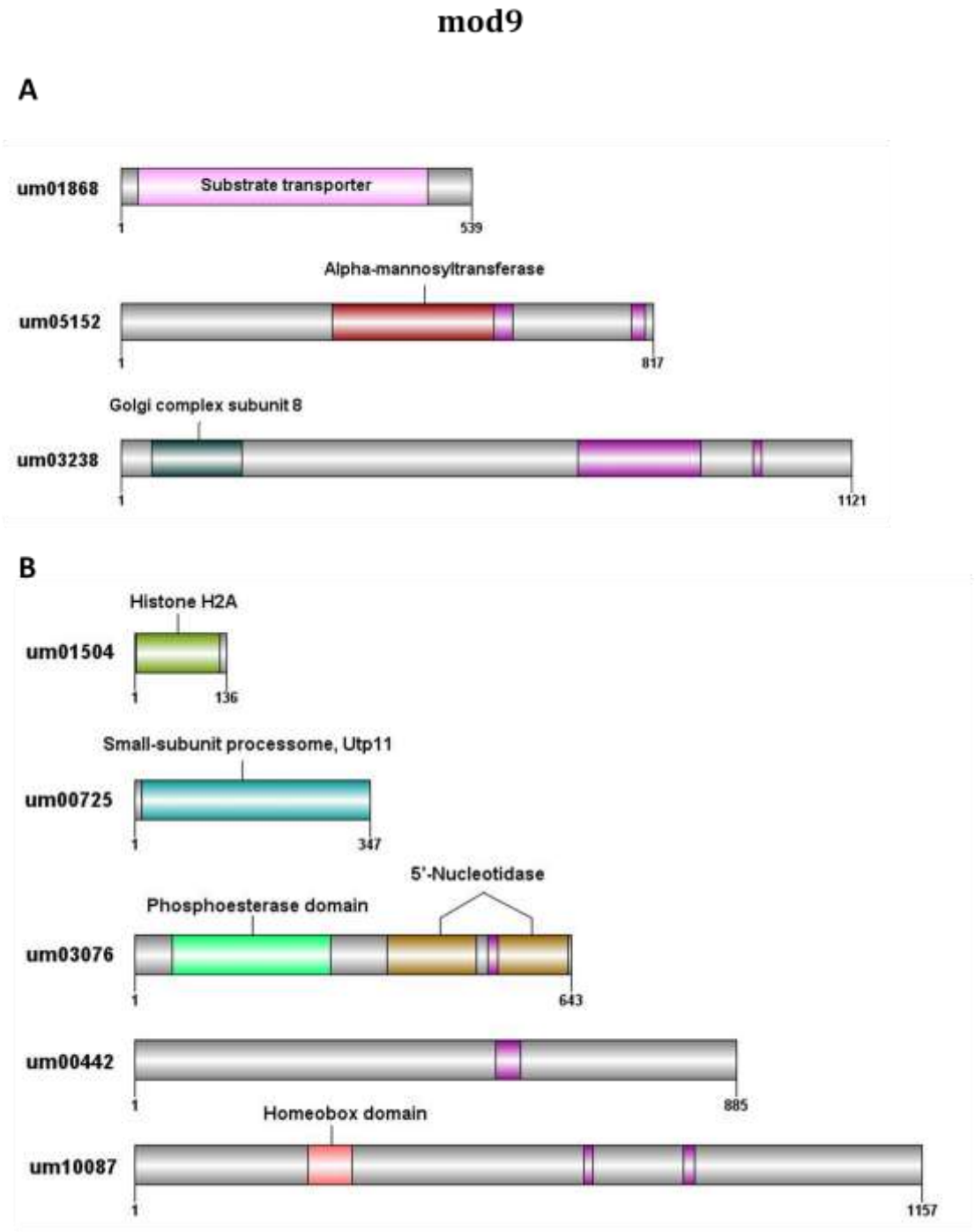

Figure 5.16 Domain architecture of the genes with mutations in the ORFs and introns found by the Illumina sequencing in the mod9 mutant.

(A) Proteins with mutations in the ORFs

(B) Proteins with mutations in the promoter

For each protein, I show their domain architecture, determined using the InterPro online software (Hunter et al., 2012). All cartoons were drawn using DOG 2.0 software. The purple-coloured motif, present in most proteins, is a coiled-coil region. The rest of domains are denoted with different colours and names.

BLAST search did not find any possible homologues and Interpro website did not find any domains.

5.4 Discussion

The aim of the work summarised in this chapter was to find novel factors organising interphase microtubule cytoskeleton in *U. maydis.* I made use of a strain AB33_GT which was UV-mutagenised and generated mutant strains. In order to identify the gene and mutation responsible for this, two different strategies were employed, complementation with a genomic library and Illumina sequencing.

Firstly, from over a hundred mutants obtained as a result of UV-mutagenesis, five (mod1, mod 2, mod3, mod4 and mod9) were chosen for the initial studies. They were selected based on the microscopy observations of MT cytoskeleton. All of them have short, fragmented MTs and are defective in extended hyphal growth.

Although the mutants look very similar on a plate and in the liquid culture, I managed to show that they exhibit different sensitivity to low doses of benomyl, microtubule-depolymerising drug. Surprisingly, in a plate assay one of the mutants (Figure 5.6), mod2, appeared to be hyposensitive to benomyl, in fact, it grew slightly better than control strain. At the same time, the rest of the mutants showed higher (mod1, mod3 and mod4) or lower (mod9) level of hypersensitivity. These results may suggest, that a mutation in one of mod2 genes caused a change in protein or proteins that resulted in microtubules that are more stable and resistant to benomyl. In the past, studies with benomyl revealed that in benomyl sensitive fungus *Coprinus cinereus,* some strains with mutations in the structural gene beta-tubulin became more resistant to the effects of benomyl (Matsuo et al., 1999), however in my genetic screen none of the mutants had mutations in beta-tubulin. Perhaps it is possible that mutation in one of the genes (found in mod2), UM04371 (Figure 5.13), which has a WD40 domain and might be help the cytoskeleton assembly, among other functions (Xu and Min, 2011), could be responsible for mod2 mutant's hyposensitivity to benomyl. Furthermore, it was not possible to distinguish different levels of benomyl sensitivity in the liquid cultures, which might be due to the fact that benomyl was used only for a short period of time, 1-2 hours, therefore it did not degrade and microtubules could not recover. On plates

though, experiments were carried out for 3 days and benomyl probably degraded due to its chemical properties, therefore making possible observations of the differences between mod mutant strains.

Secondly, complementation with genomic library on prospective mod mutants did not bring any conclusive results. Although, rescue plasmids for mod1 and mod3 were available and were confirmed to rescue those mutants phenotype, no mutations were found in the genes present on them. Identified 'rescue' plasmid for mod1 mutant contained three full genes which were not able to rescue the phenotype, unless all of them were present. According to the MIPS database they are positioned next to each other on a chromosome, however BLAST or SMART search did not indicate that their products are interacting partners or act the same pathway. If that was the case it would seem obvious that disruption of one element would affect the others. Additionally, mod3 rescue plasmid contained only one gene, a serine/threonine kinase, which might be a key factor in a pathway involved in proper MT assembly and filamentous growth. After the kinase gene was put under a constitutive, overexpressing promoter and transformed back into the mutant, despite many attempts, no transformants were ever obtained. This result could indicate that overexpression of the kinase is lethal. Also, the kinase gene did not have any mutations. It could, perhaps, indicate that the kinase gene acted as a multicopy suppressor. It is known that increased abundance of some cellular component could either help functioning of the mutated gene product or compensate for the retardation caused by the mutated gene product (if they act in sequence) (Ueguchi and Ito, 1992). These results were confirmed later by the Illumina sequencing, which did not show any mutations in the genes found through complementation. Moreover, to check instantly what happens to a WT strain when newly found kinase is turned off, the plan was to use site-directed mutagenesis of the ATP-binding pocket within the kinase, which could be inhibited by a known kinase inhibitor NA-PPI (Calbobiochem), previously done by Böhmer et al., 2008. This experiment would give a definite proof that the kinase is or is not a novel MT organising factor, however could not be done due to time constrictions.

Furthermore, the Illumina sequencing used to support a search for novel factors necessary for organisation of the interphase microtubules, revealed mutations mostly in genes associated with metabolism, cell cycle and DNA processing. Although a lot of the mutations were found in conserved proteins, unexpectedly, no mutations were found present in any known microtubule cytoskeleton organising proteins. However, more detailed analysis of Illumina sequencing results showed three genes with some links to the cytoskeleton. Two of them, involved in the organisation of the actin cytoskeleton, were found in mod1 mutant, which has the highest number of mutations. The first one was identified by BLAST search as related to Drebrin F, a mammalian neuronal protein. Drebrin is an actin filament (F-actin)–binding protein involved in organising the dendritic pool of actin (Grintsevich et al., 2010), with crucial roles in neuritogenesis and synaptic plasticity (Worth et al., 2013). Drebrin couples dynamic microtubules to F-actin in growth cone filopodia via binding to the microtubule-binding +TIP protein EB3 and organises F-actin in dendritic spines (Worth et al., 2013), the receptive regions of most excitatory synapses that play a crucial role in higher brain functions (Mikati et al., 2013). However, it is unknown how drebrin interacts with F-actin and how this is regulated. In fungi, drebrin's homologue is Abp1, a member of the Abp family (Actin-Binding-Proteins) (Lappalainen et al., 1998). Abp1/Drebrins are relatively large proteins composed of an N-terminal ADF-H domain followed by a variable region and a C-terminal SH3 domain, which interacts only with actin filaments and do not promote filament depolymerisation or fragmentation (Interpro website; Lappalainen et al., 1998). *U. maydis* domain architecture appears to be typical for the proteins from Abp1 family (Figure 5.10 in the Results section), therefore it is not likely to cause mod1 aberrant phenotype. The second protein (from mod1), has a mutation in the promoter region and is annotated in MIPS as a protein involved in the organisation of the actin cytoskeleton. BLAST search against numerous databases showed that this protein is a potential orthologue of yeast protein Ysc84, which represents a class of actin-binding proteins that are conserved from yeast to humans. It contains a novel N-terminal actin-binding domain termed Ysc84 actin binding (YAB), which can bind and bundle actin filaments (Robertson et al., 2009).

However, it is also possible that a large number of mutations might have a pleiotropic effect on mod1, causing its phenotype. Another interesting mutation was found among mutated genes in mod3 mutant. It was identified by BLAST search as related to MDN1, a huge dynein related AAA-type ATPase. This gene belongs to dynein/midasin family and contains a P-loop ATPase domain, typical for molecular motors, but also found in nucleotide-binding proteins, synthases and kinases (Saraste et al., 1990). Previously, it was shown that both dynein and midasin contain 6 tandem AAA+ domains in the same polypeptide (Iyer et al., 2003; Mocz and Gibbons, 2001; Neuwald et al., 1999). Dynein is a microtubule-associated motor, which uses energy from ATP hydrolysis to power a wide variety of cellular functions, including intracellular transport, mitosis, cell polarisation and directed cell movement (Hook and Vallee, 2006). At least a single copy of dynein is encoded in all sequenced eukaryotic genomes, suggesting that it was present in the last common ancestor of eukaryotes (Iyer et al., 2003). Midasin also appears to be present in all eukaryotes (Garbarino and Gibbons, 2002) and is associated with the nuclear pore complex involved in cytoplasmic export of the 60S ribosomal particle (Bassler et al., 2001; Garbarino and Gibbons, 2002). By analogy to dynein, midasin might act as a motor in the translocation of the ribosomal particles across the nuclear pore (Iyer et al., 2003).

Finally, it is possible that the best candidates for novel factors organising the microtubules are the unknown genes for which BLAST searches did not find any potential homologues. Those were present in mod1 (7 genes), mod2 (1 gene) and mod9 (1 gene). It would be interesting to delete each of those genes in the wild-type strain or make conditional mutants, where their promoter could be easily switched off.

The analysis of the mutants also revealed that in mod1 and mod9 gene deletions occurred. In both cases 2 genes were found to be deleted and they included a telomere-associated DNA helicase and reverse transcriptase. It might be possible that gene deletions are responsible for the specific phenotype of mod1 and mod9, so in the future, it would be useful to delete the genes in the wild-type strain. In addition, the types of mutations the most commonly present

in the mutants were missense mutations and mutations in promoters, and these were found in most unknown proteins.

Chapter 6 - General Discussion

The studies undertaken in this thesis provide new understanding of different aspects of the microtubule cytoskeleton organisation in *U. maydis*.

Firstly, I have provided evidence that there are two functional beta tubulin genes in *U. maydis*. Using bioinformatics tools, I have shown that *U. maydis* beta tubulins differ mostly in their C-terminal domains (C-terminal tails, or CTTs). CTTs are known to be sites of post-translational modifications, which result in unique interactions with microtubule-associated proteins for specific cellular functions (Sirajuddin et al., 2014). Moreover, RT-PCR revealed that both beta tubulins are expressed in yeast and hyphal forms of *U. maydis*. This means that, most probably, both isotypes take part in building the MT cytoskeleton during the *U. maydis* life cycle. Subsequently, *in vivo* studies revealed that at least one of the beta tubulins, Tub3, seems to be present on all visible interphase and mitotic (not shown) MTs. However, the most significant finding was that depletion of Tub3 led to disruption of the molecular motors kinesin 3 and dynein, which are responsible for early endosome motility, while down-regulation of Tub4 caused significant disruption of dynein function only. This means that when Tub 3 was not expressed, Tub 4 was unable to maintain fully functional microtubules, which led to disrupted intracellular transport. Tub 3, however, was able to sustain more efficient MT tracks, when Tub 4 was down-regulated, because only the velocity of dynein was significantly decreased. Perhaps, kinesin 3 has a preference towards Tub3-containing microtubules, whereas dynein needs both kinds of MTs. Therefore, both beta tubulin isotypes are essential to the fully functional MT cytoskeleton in *U. maydis*. In the future, it would be interesting to observe both beta tubulins during mitosis to see whether they have distinct functions during this process. For example, each beta tubulin could be tagged with a different fluorescent protein and then tracked in yeast-like cells during mitosis. Also, *crg*-mutants could be used in order to see how down-regulation of beta tubulins affects mitotic microtubules and mitotic progression. When considered together, I can conclude that both beta tubulins are essential to the fully functional *U. maydis* MT cytoskeleton, but there are many more questions that remain to be answered regarding the specific functions of Tub3 and Tub4. For example, it would be useful to know if all

microtubules in a cell are built by one isotype of beta tubulin or if one beta tubulin is more important than the other one at a particular developmental stage, and if so, in which cell stage or morphological form of *U. maydis* this occurs. Another aspect that is worth investigating in future, is *U. maydis* beta tubulin localisation during plant infection. Perhaps, one isotype of beta tubulin is more important for this stage of *U. maydis* development than the other. It would be very useful to know this, in the context of antifungal drug development targeted at *U. maydis*-infecting corn plants.

A significant component of this thesis is the investigation of the MAP repertoire in *U. maydis*, which has previously not been systematically carried out. For the first time, I showed the full repertoire of MAPs in *U. maydis*. In order to achieve this, I first performed searches of MAPs found in five organisms: *H. sapiens, D. melanogaster, A. nidulans*, *S. pombe* and *S. cerevisiae,* using the AmiGO protein database (Carbon et al., 2009), but also databases of each specific species as well as the available literature. The aim of using a variety of model organisms was to ensure that there would be a good collection of MAPs important in different cell-cycle stages and cell forms (yeast and filamentous). Initially, I had a list of about 500 proteins, which had to be verified using different databases as well as the literature. I then had to prepare a non-redundant list, which led to the collection of 169 MAPs, involved in various microtubule-oriented cellular functions, for example, mitotic spindle organisation, microtubule bundling, microtubule severing, microtubule stabilisation and other functions. For the purpose of this study I divided all of the MAPs into 20 functional groups with many of the proteins present in more than one group, highlighting the multiple, or redundant functions of MAPs. The largest group consisted of 48 MAPs that are involved in mitotic spindle organisation. Among all MAPs studied, 8 % were present only in fungi, 3 % were found in both filamentous fungi and metazoans, 43 % were metazoan only and 46 % of MAPs were present in all tested species. This shows that slightly less than a half of these proteins were conserved across the variety of species observed, while the rest were specific to certain groups of organisms. Therefore, the majority of specific MAPs were present only in multicellular organisms, represented here by *H. sapiens* and *D. melanogaster*. The reason for this, most probably, because they are multicellular organisms displaying

complex morphogenesis and cellular differentiation In comparison to fungal species, metazoans or plants have a variety of known unique MAP families (Gardiner, 2013), with some of them organ-specific, for example MAP1, tau or MAP2 in the brain. The final results showed that 66 out of 169 proteins are conserved in *Ustilago maydis*. Those included 10 MAPs found only in the fungal species, 6 found in filamentous fungi and metazoans and the rest (50 proteins) conserved across all most species. This result shows that most of *U. maydis* MAPs are conserved between fungi and metazoans, and only some proteins are fungal specific, which is not surprising. It is also possible that *U. maydis* has additional MAPs, which could not be detected using the chosen search methods, because they are unique to this fungus. When I checked the functions of the *U. maydis* MAPs it appeared that the majority (64 % of MAPs) were involved in multiple functions at all stages of the cell cycle, 24 % were found to take part in mitosis and 12 % of MAPs could carry out their functions only at interphase. The analysis of MAPs presented in this thesis provided valuable information with regard to factors organising microtubules in fungi. In this study, 66 MAPs were identified to be present in the corn smut fungus, but as our knowledge of these proteins expands there can be many more identified. The MAP collection included proteins previously characterised to have roles in MT cytoskeleton organisation in *U. maydis* as well as the proteins, whose function has not been studied. The next step in this project would be to perform RT-PCR, in order to see which uncharacterised MAPs are expressed in different morphological forms of *U. maydis.* After this, localisation studies should be carried out to see how each MAP functions in living cells. In this way it should prove possible to extend the functional classification based on spatio-temporal dynamics of gene expression and cellular localisation patterns. This would be followed by systematic targeted mutagenesis to test their roles functionally. It is, of course, possible that a sub-set of the MAPs will prove to be essential functions and therefore will not prove possible to delete using targeted gene replacement. In these instances, it will be necessary to carry out conditional mutant generation by means of temperature-sensitive mutant identification, especially where orthologous genes in other organisms have been identified in this way. Otherwise, it may prove necessary to use new technologies such as CRISPR-Cas9-mediated gene editing to generate point mutants, or gene

silencing procedures to produce conditionally silenced mutants to study gene function.

Finally, a genetic screen was carried out to search for novel factors organising interphase MT array using UV-mutants. Those mutants were characterised by having a defective interphase MT cytoskeleton in hyphal form, which manifested itself as development of short, fragmented microtubules. Therefore, in order to find out which gene, or genes, were disrupted and caused the specific phenotype, complementation with a genomic library and Illumina whole genome sequencing were both performed. This study focused on five mutants, which exhibited the same phenotype. Interestingly, the mutants appeared to have differential sensitivity to a microtubule-depolymerising drug, benomyl. One mutant, mod2, was shown to be hypo-sensitive, as it was more resistant to benomyl than a control strain, while the rest of the mutants were hypersensitive to benomyl (mod1, mod3, mod4 and mod9). Unfortunately, complementation with the genomic library was inconclusive, because none of the genes found on the 'rescue' plasmids contained mutations. However, as a consequence of Illumina sequencing, I was able to demonstrate that when the interphase MT cytoskeleton is disrupted, it was probably due to mutation of a whole set of genes, rather than one particular gene. This result is not surprising and it proves that proper MT organisation in hyphae requires a complex network of proteins to be involved. For example, MTs undergo rapid cycles of rapid growth and disassembly, also known as dynamic instability and has been observed both *in vitro* and *in vivo* (Desai and Mitchison, 1997; Nogales, 2001), which is orchestrated by numerous MAPs. Among the genes carrying mutations, no common microtubule organising proteins were found, which is surprising, because one might expect those genes to be affected, in the first instance. The majority of genes detected to have mutations were responsible for DNA processing, metabolism and cell cycle control. The only three proteins found to have some links to cytoskeleton organisation were either actin-binding proteins (drebrin and Ysc84) or related to midasin, which might act as a motor in the translocation of the ribosomal particles across the nuclear pore (Iyer et al., 2003). In addition, the analysis of the genes with mutations in the UV-mutants indicated that there is a group of uncharacterised proteins, which may have important functions for the microtubule function in *U. maydis*, but have not been

studied. It would be very interesting to check the expression of those genes in *U. maydis*, as well as localise those proteins in yeast and hyphae to see if they have roles in organising the microtubules. The critical next step in this study would be systematic complementation analysis using the specific genes identified by whole genome sequence analysis, in order to define clearly which genes are likely to be responsible, singly or in combination, for the observed phenotypes. This should, however, be accompanied by genetic analysis to observe the segregation patterns of the mutants so that greater focus could be brought to bear on the single gene mutations exerting the greatest effect on MT organisation. In this way, it should prove possible to identify the key process and underlying genes associated with MT organisation. This would also allow the synthesis of each part of this PhD thesis to provide new and fundamental insight into the organisation and genetic regulation of MT function in the corn smut fungus *U. maydis.*

Appendix

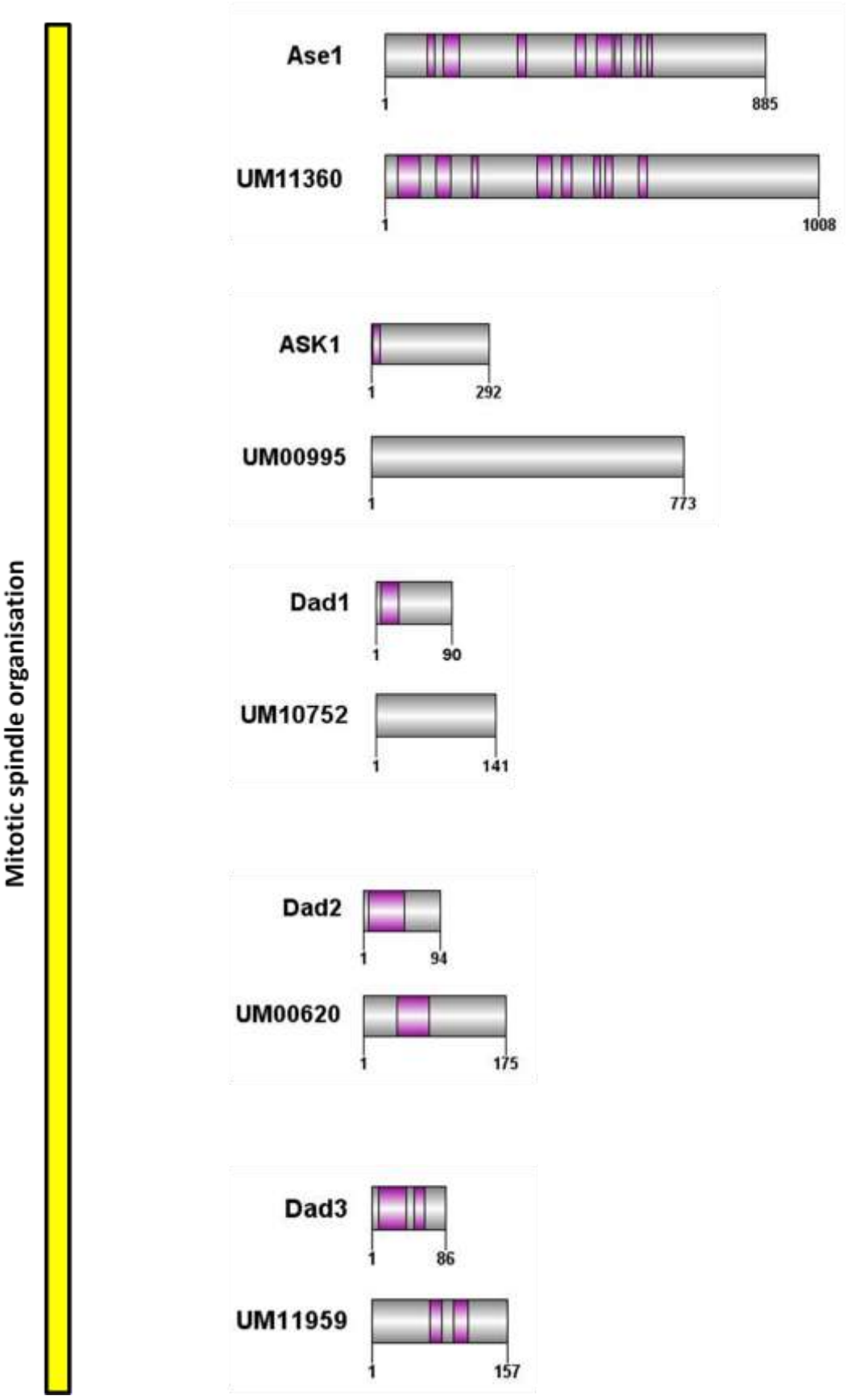
Mitotic spindle organisation
Ase1
1
885
UM11360
1
1008
ASK1
1
292
UM00995
1
773
Dad1
1
90
UM10752
1
141
Dad2
1
94
UM00620
1
175
Dad3
1
86
UM11959
1
157

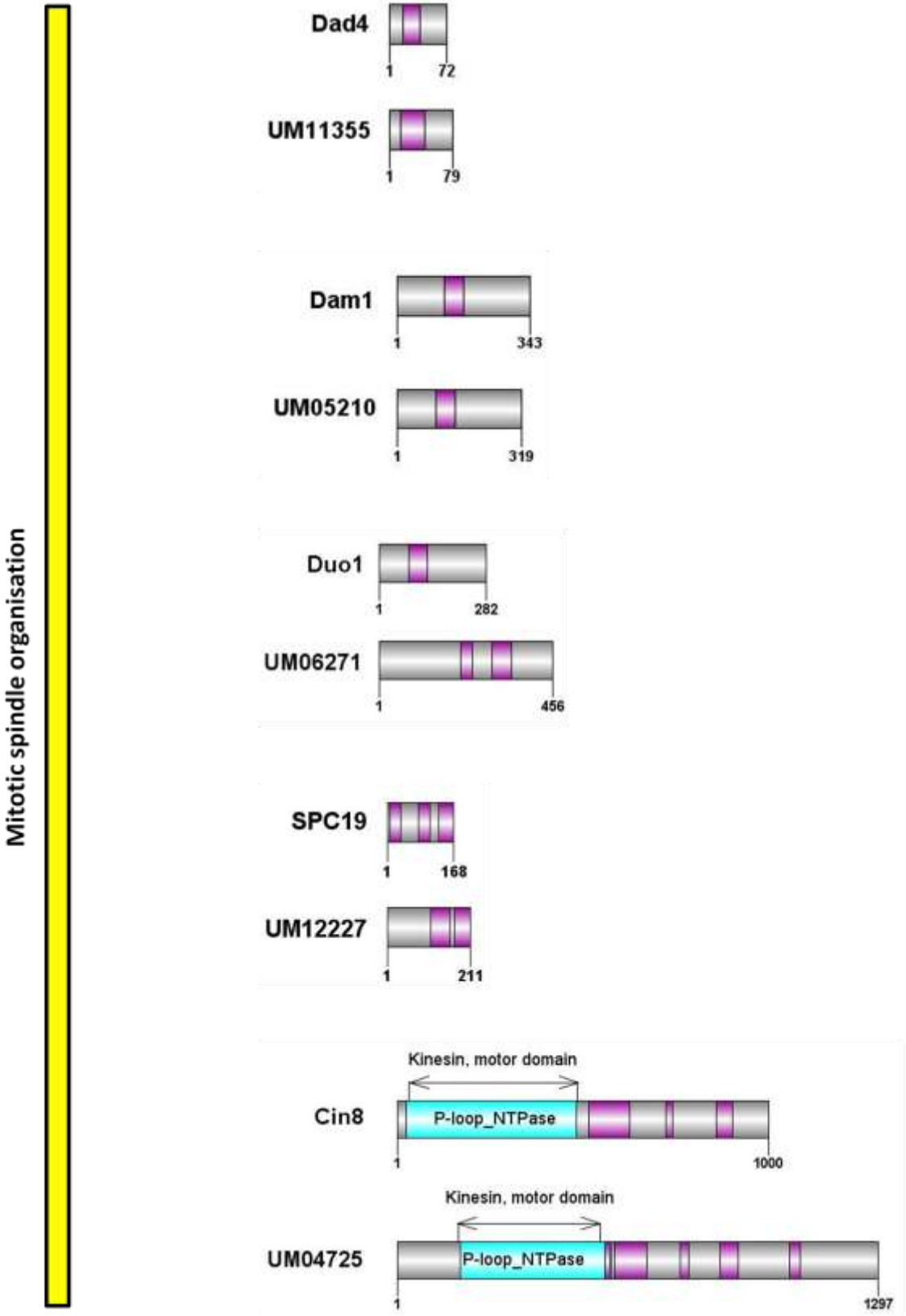
Mitotic spindle organisation
Dad4
1
72
UM11355
1
79
Dam1
1
343
UM05210
1
319
Duo1
1
282
UM06271
1
456
SPC19
1
168
UM12227
1
211
Kinesin, motor domain
Cin8
P-loop_NTPase
1
1000
Kinesin, motor domain
UM04725
P-loop_NTPase
1
1297

Mitotic spindle organisation

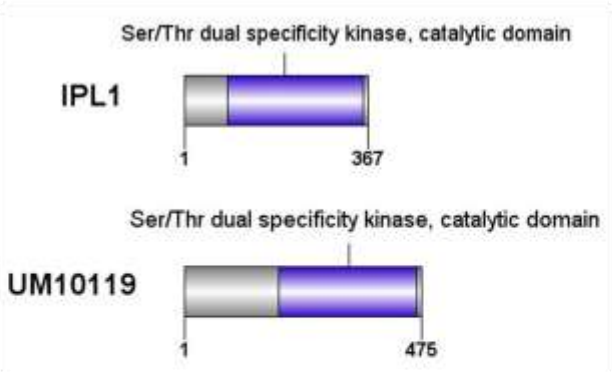

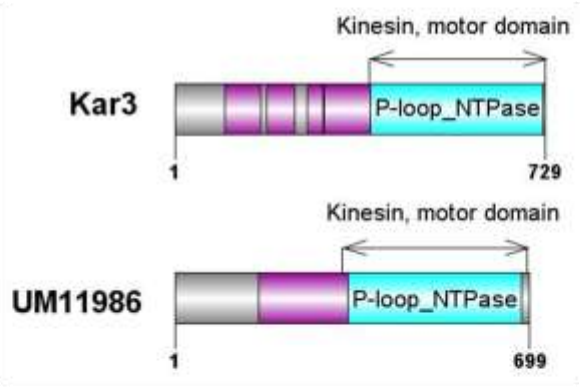

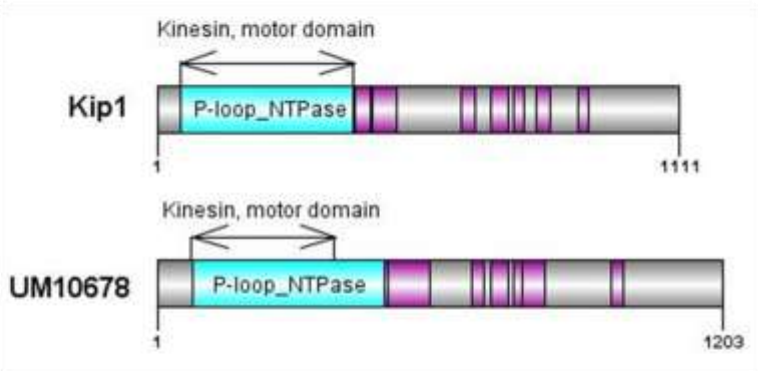

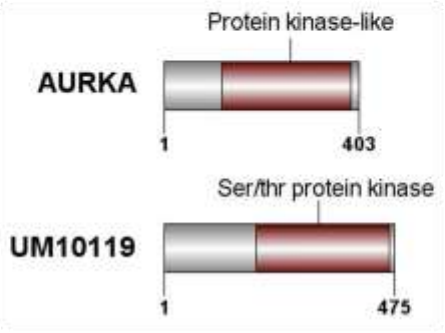

Mitotic spindle organisation

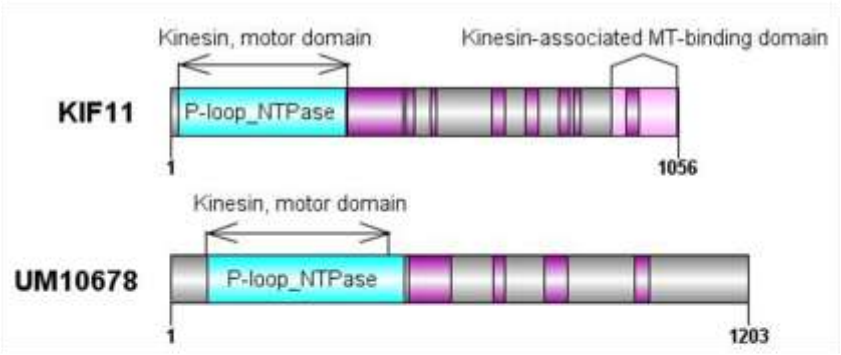

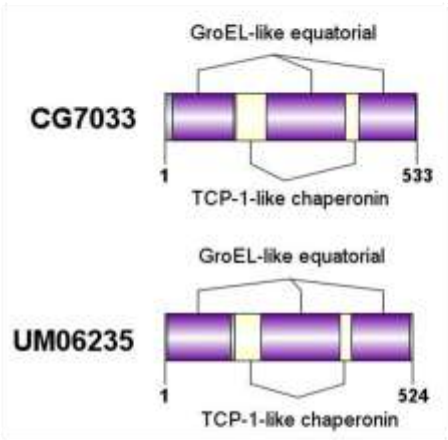

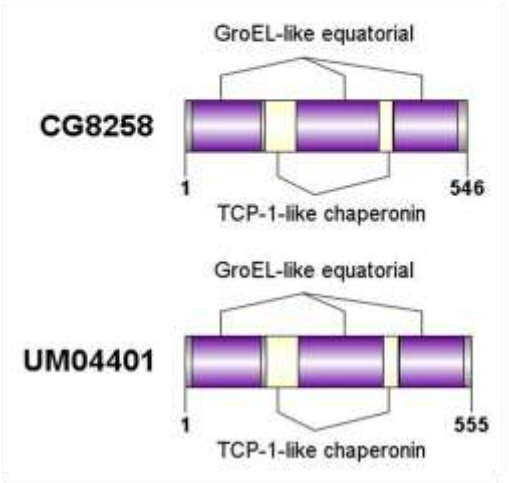

Mitotic spindle organisation

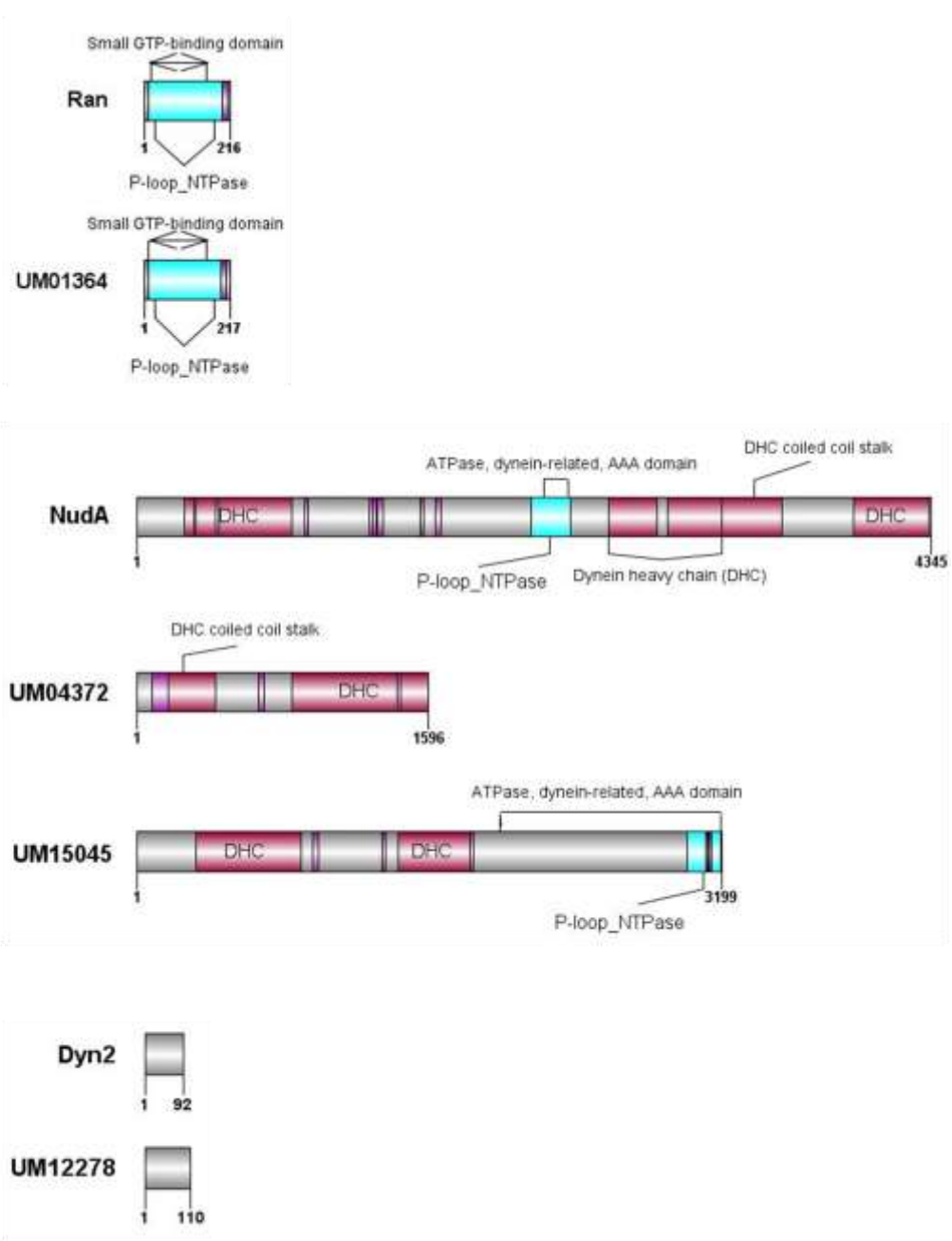

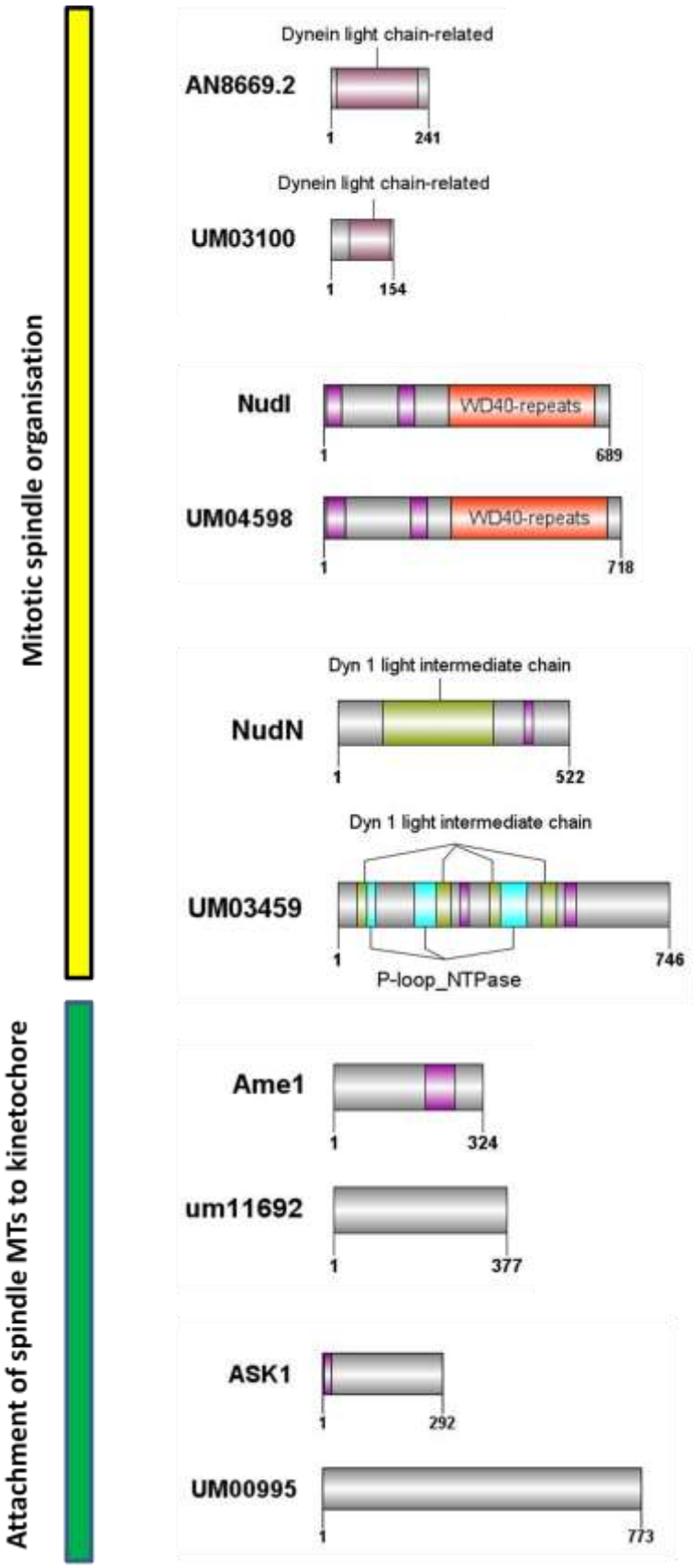
Mitotic spindle organisation
Attachment of spindle MTs to kinetochore
Dynein light chain-related
AN8669.2
1
241
Dynein light chain-related
UM03100
1
154
NudI
WD40-repeats
1
689
UM04598
WD40-repeats
1
718
Dyn 1 light intermediate chain
NudN
1
522
Dyn 1 light intermediate chain
UM03459
1
746
P-loop_NTPase
Ame1
1
324
um11692
1
377
ASK1
1
292
UM00995
1
773

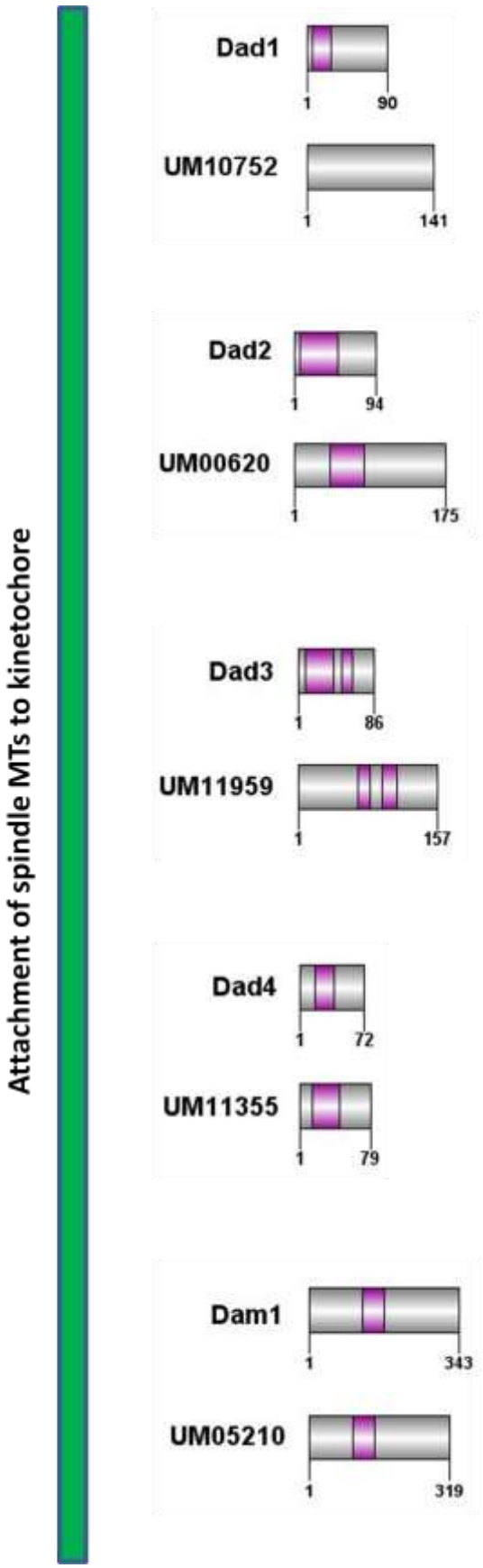
Attachment of spindle MTs to kinetochore
Dad1
1
90
UM10752
1
141
Dad2
1
94
UM00620
1
175
Dad3
1
86
UM11959
1
157
Dad4
1
72
UM11355
1
79
Dam1
1
343
UM05210
1
319

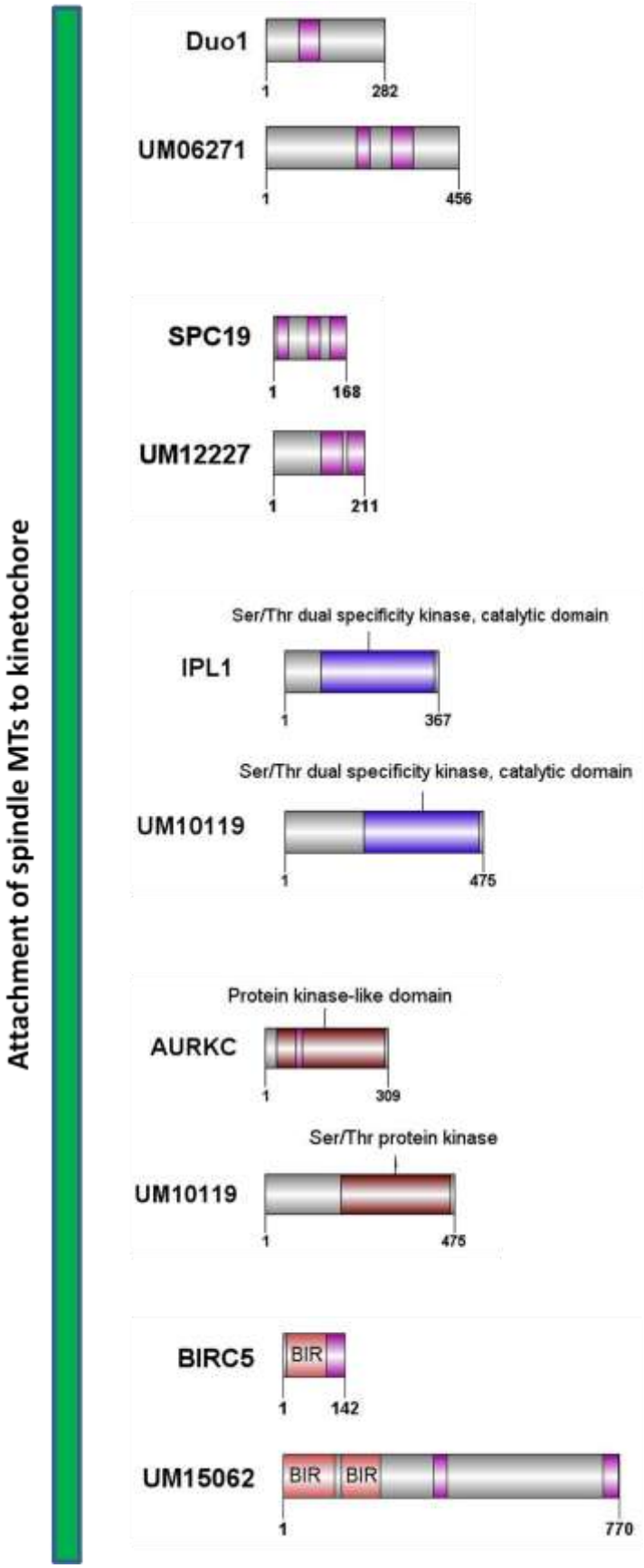
Attachment of spindle MTs to kinetochore
Duo1
1
282
UM06271
1
456
SPC19
1
168
UM12227
1
211
Ser/Thr dual specificity kinase, catalytic domain
IPL1
1
367
Ser/Thr dual specificity kinase, catalytic domain
UM10119
1
475
Protein kinase-like domain
AURKC
1
309
Ser/Thr protein kinase
UM10119
1
475
BIRC5
BIR
1
142
UM15062
BIR
BIR
1
770

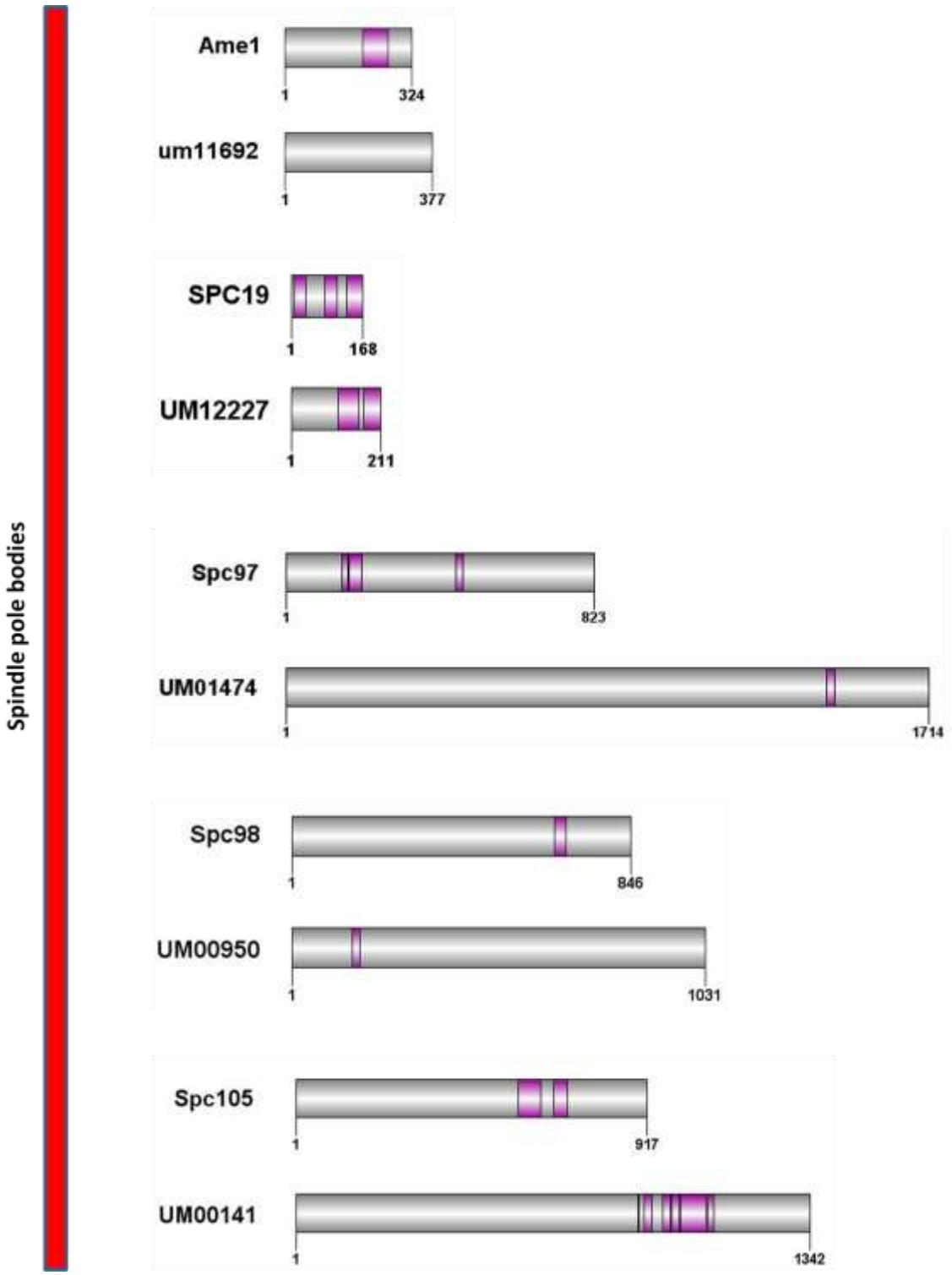
Spindle pole bodies
Ame1
1
324
um11692
1
377
SPC19
1
168
UM12227
1
211
Spc97
1
823
UM01474
1
1714
Spc98
1
846
UM00950
1
1031
Spc105
1
917
UM00141
1
1342

Spindle pole bodies

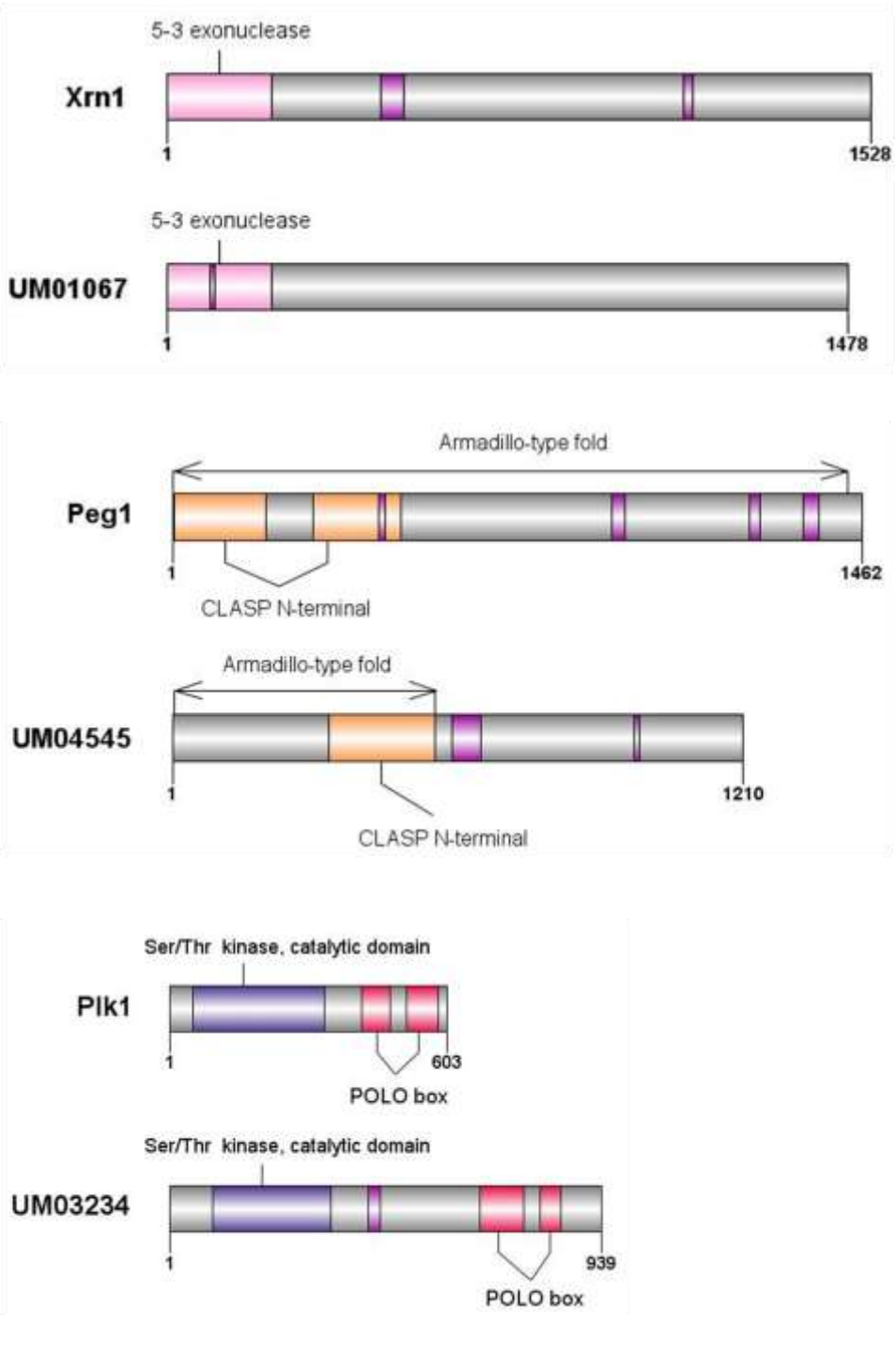

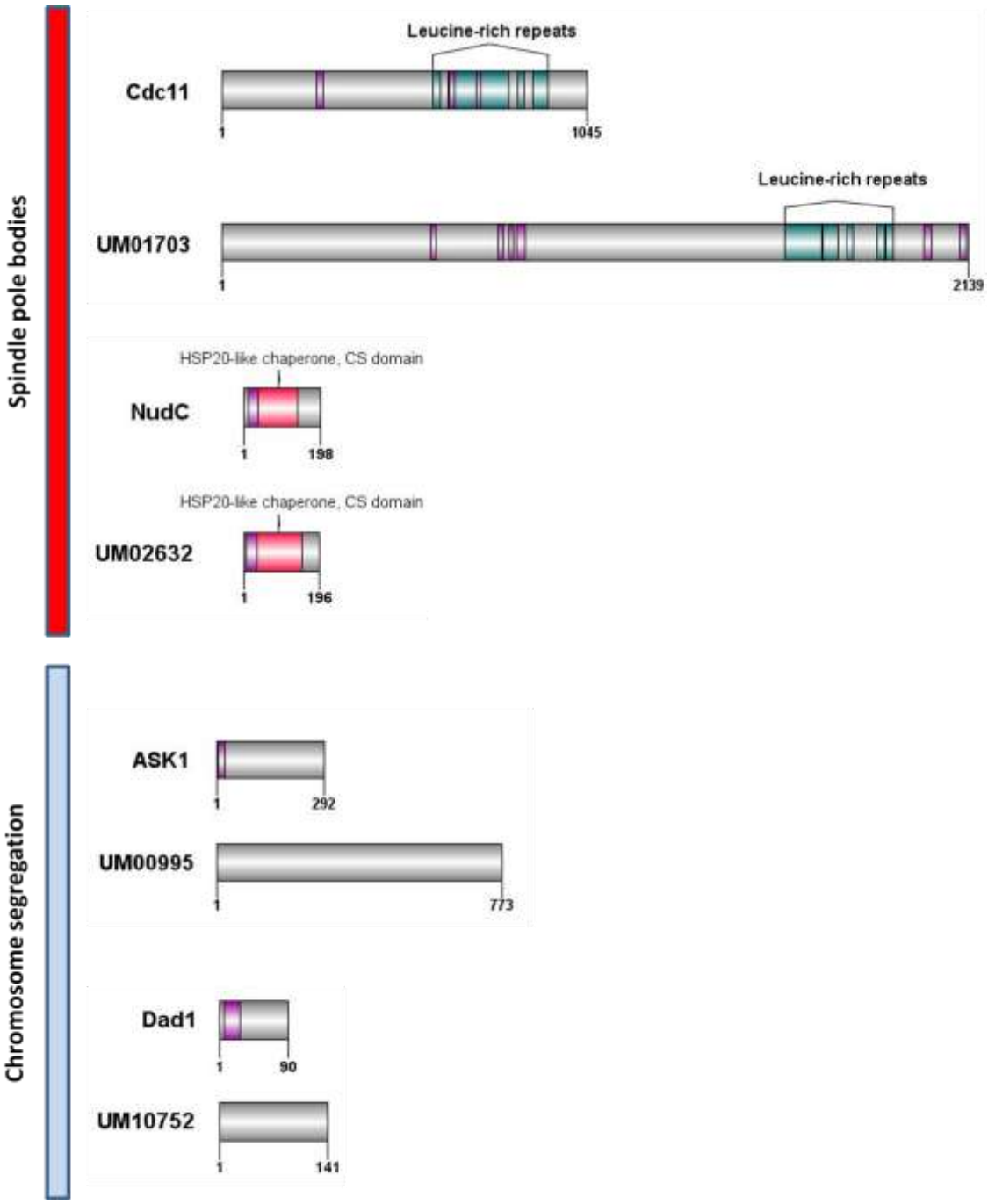
Spindle pole bodies
Leucine-rich repeats
Cdc11
1
1045
Leucine-rich repeats
UM01703
1
2139
HSP20-like chaperone, CS domain
NudC
1
198
HSP20-like chaperone, CS domain
UM02632
1
196
Chromosome segregation
ASK1
1
292
UM00995
1
773
Dad1
1
90
UM10752
1
141

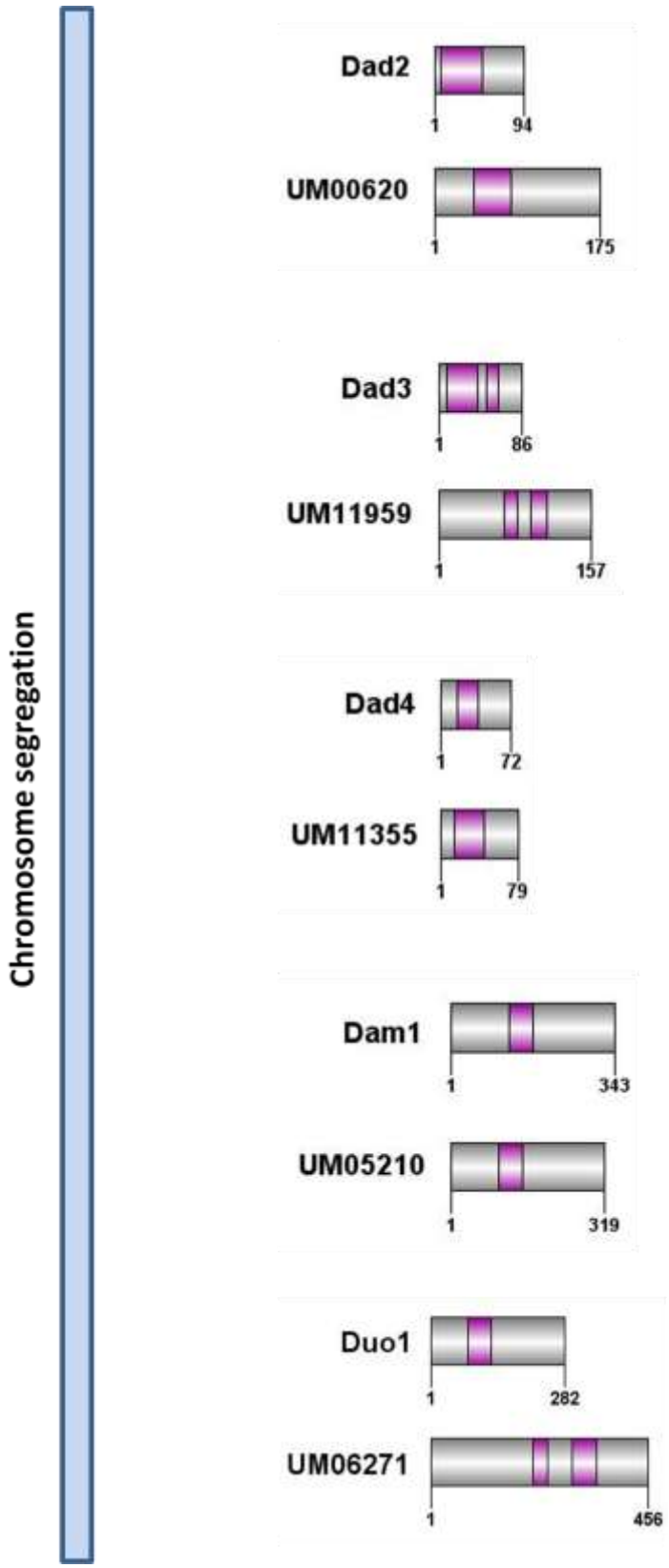
Chromosome segregation
Dad2
1
94
UM00620
1
175
Dad3
1
86
UM11959
1
157
Dad4
1
72
UM11355
1
79
Dam1
1
343
UM05210
1
319
Duo1
1
282
UM06271
1
456

Chromosome segregation

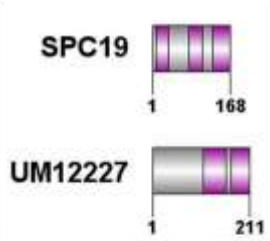

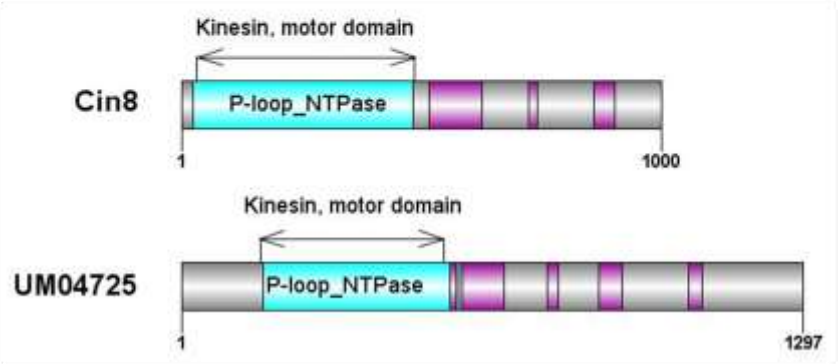

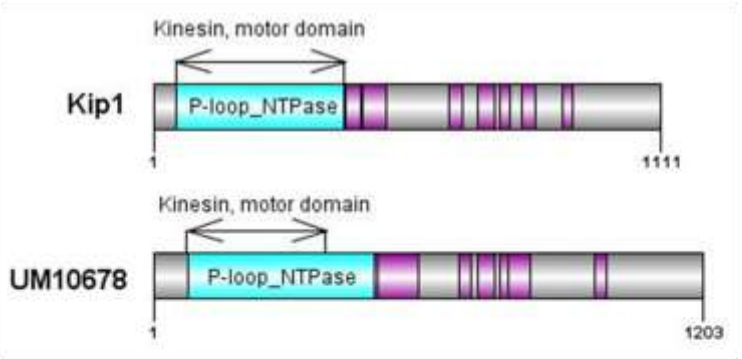

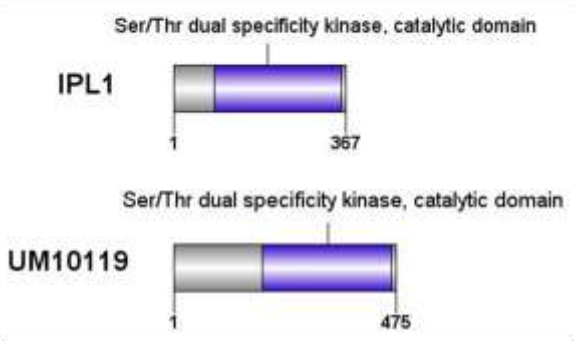

Chromosome segregation

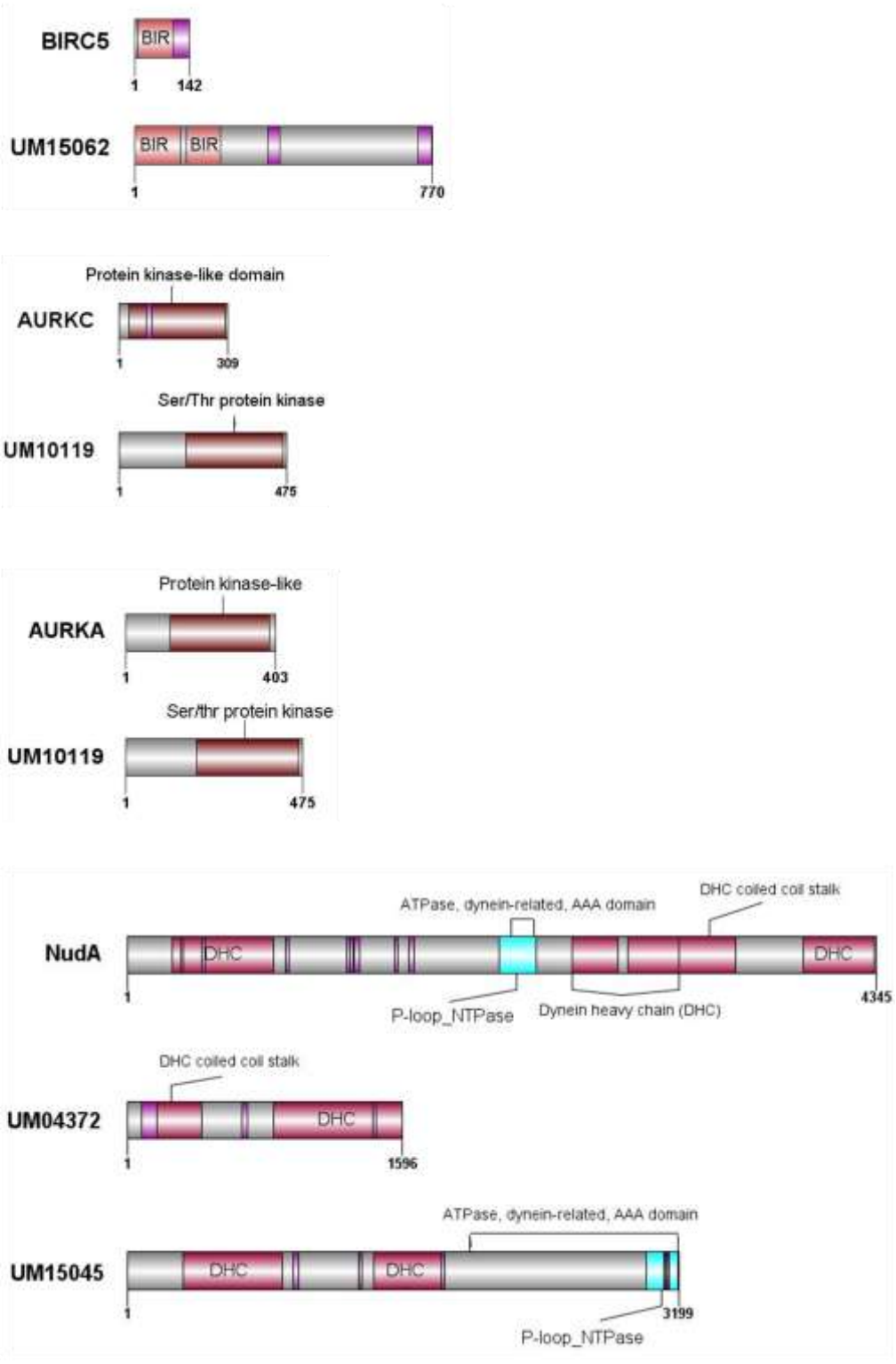

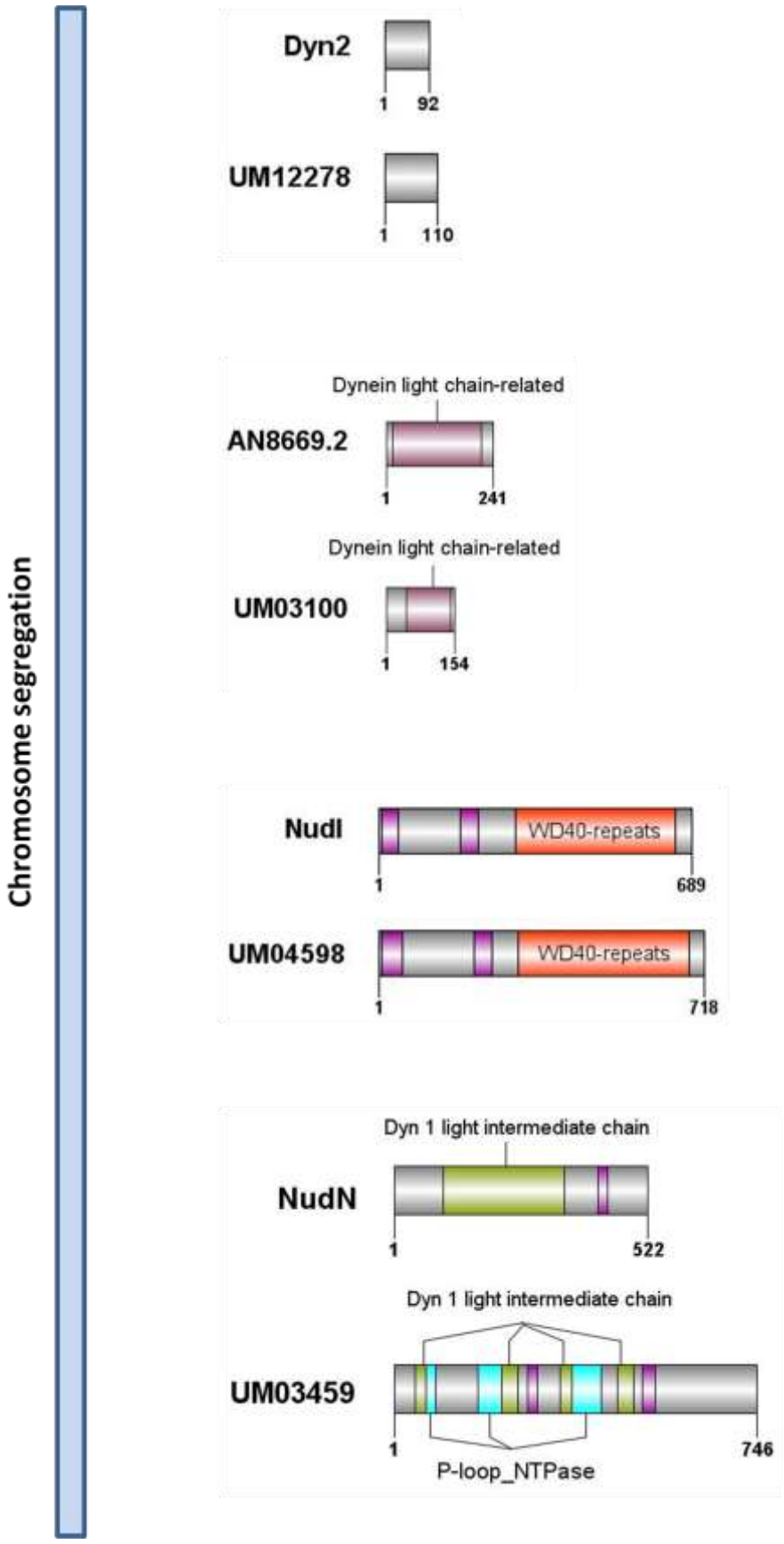
Chromosome segregation
Dyn2
1
92
UM12278
1
110
Dynein light chain-related
AN8669.2
1
241
Dynein light chain-related
UM03100
1
154
NudI
WD40-repeats
1
689
UM04598
WD40-repeats
1
718
Dyn 1 light intermediate chain
NudN
1
522
Dyn 1 light intermediate chain
UM03459
1
746
P-loop_NTPase

Nuclear migration along MT

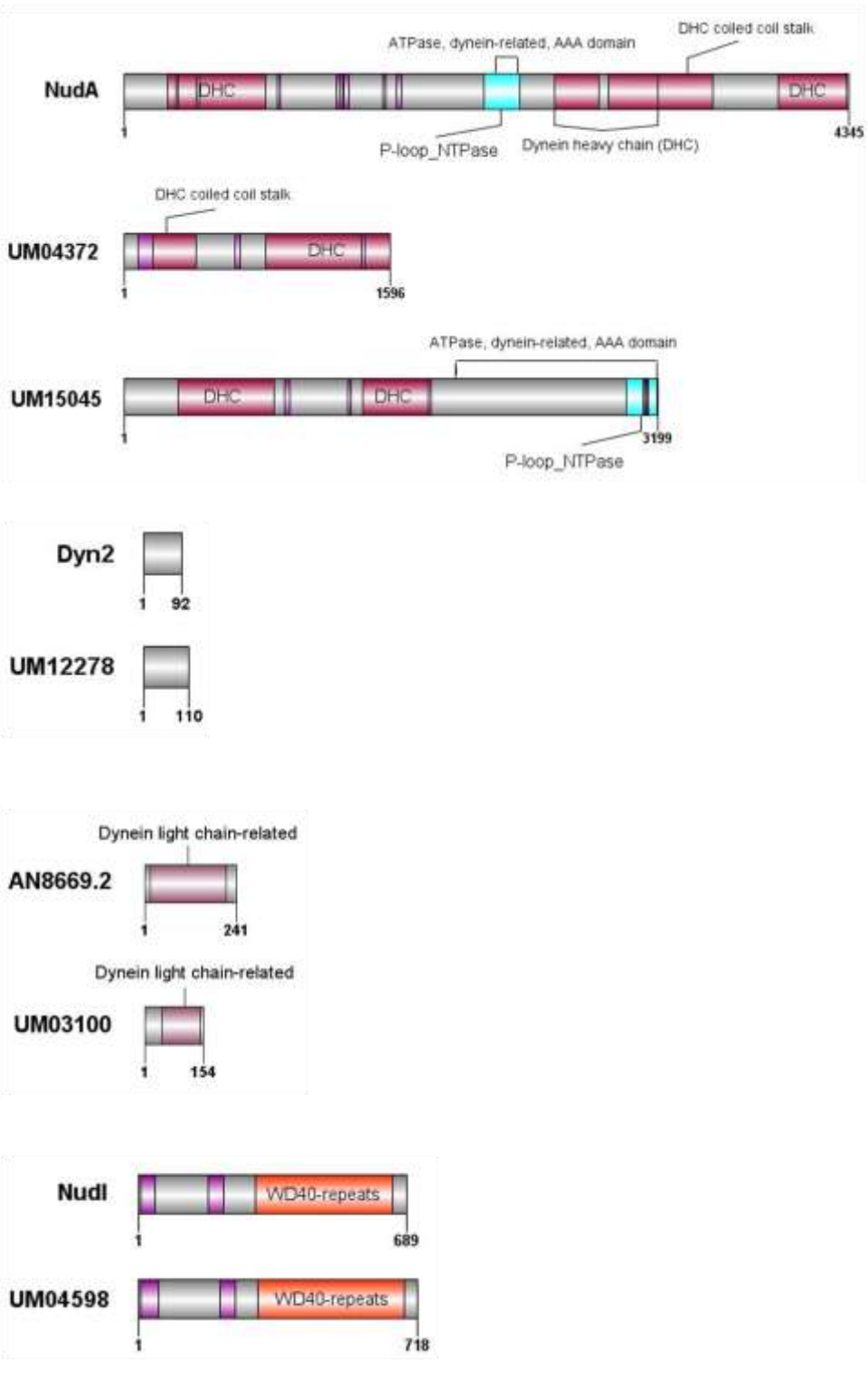

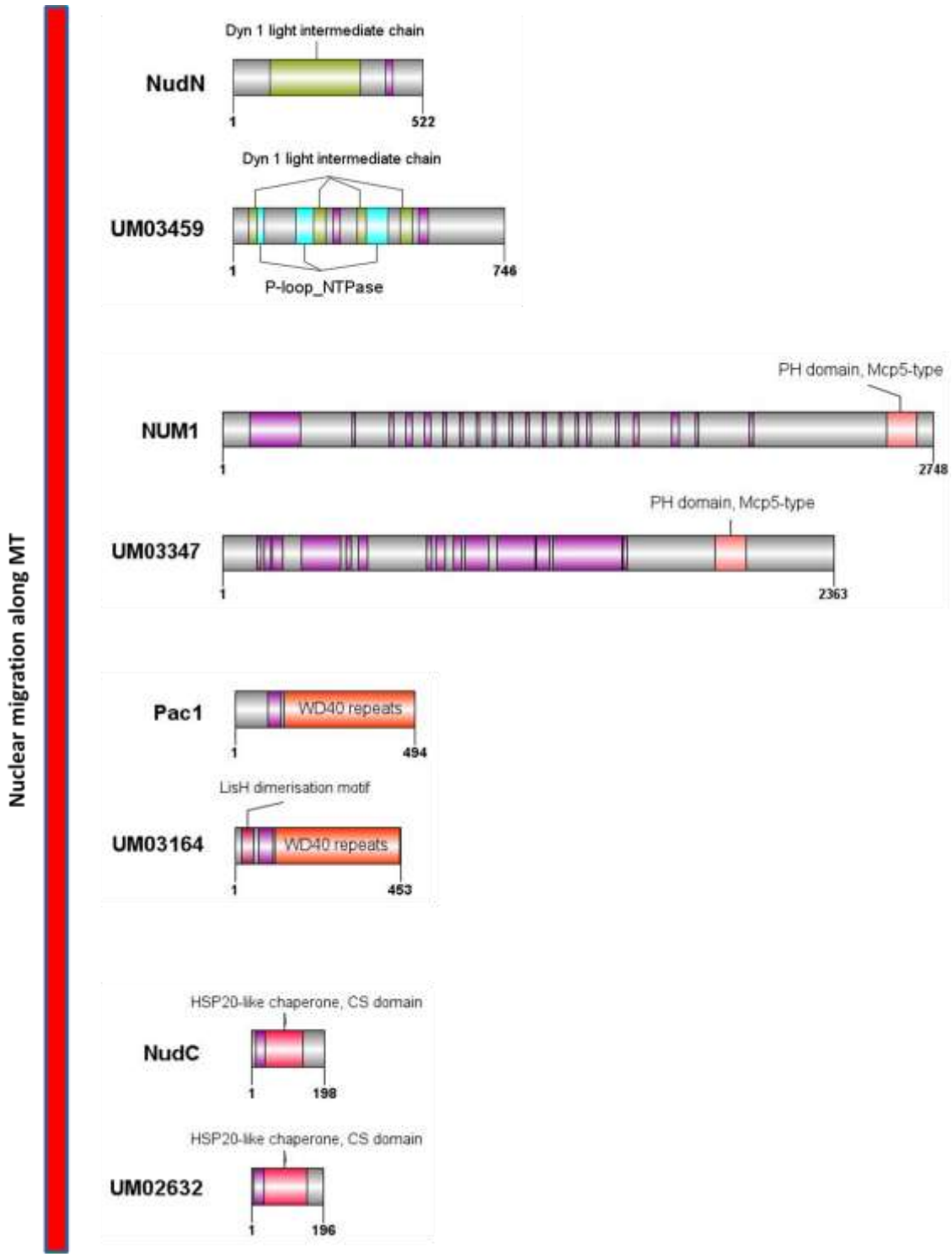
Nuclear migration along MT
Dyn 1 light intermediate chain
NudN
1
522
Dyn 1 light intermediate chain
UM03459
1
746
P-loop_NTPase
PH domain, Mcp5-type
NUM1
1
2748
PH domain, Mcp5-type
UM03347
1
2363
Pac1
WD40 repeats
1
494
LisH dimerisation motif
UM03164
WD40 repeats
1
453
HSP20-like chaperone, CS domain
NudC
1
198
HSP20-like chaperone, CS domain
UM02632
1
196

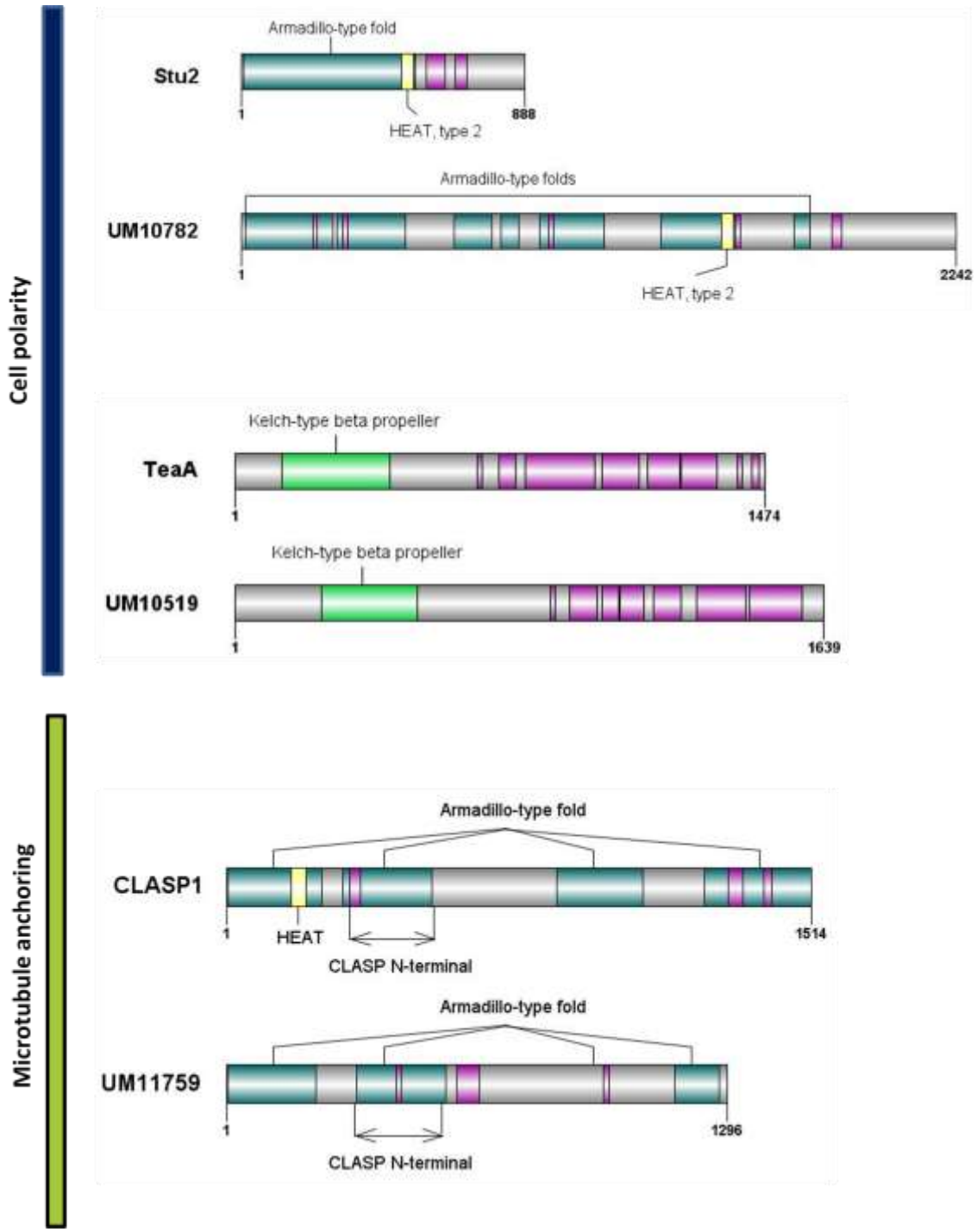
Cell polarity
Stu2
Armadillo-type fold
1
888
HEAT, type 2
UM10782
Armadillo-type folds
1
2242
HEAT, type 2
TeaA
Kelch-type beta propeller
1
1474
UM10519
Kelch-type beta propeller
1
1639
Microtubule anchoring
CLASP1
Armadillo-type fold
1
1514
HEAT
CLASP N-terminal
UM11759
Armadillo-type fold
1
1296
CLASP N-terminal

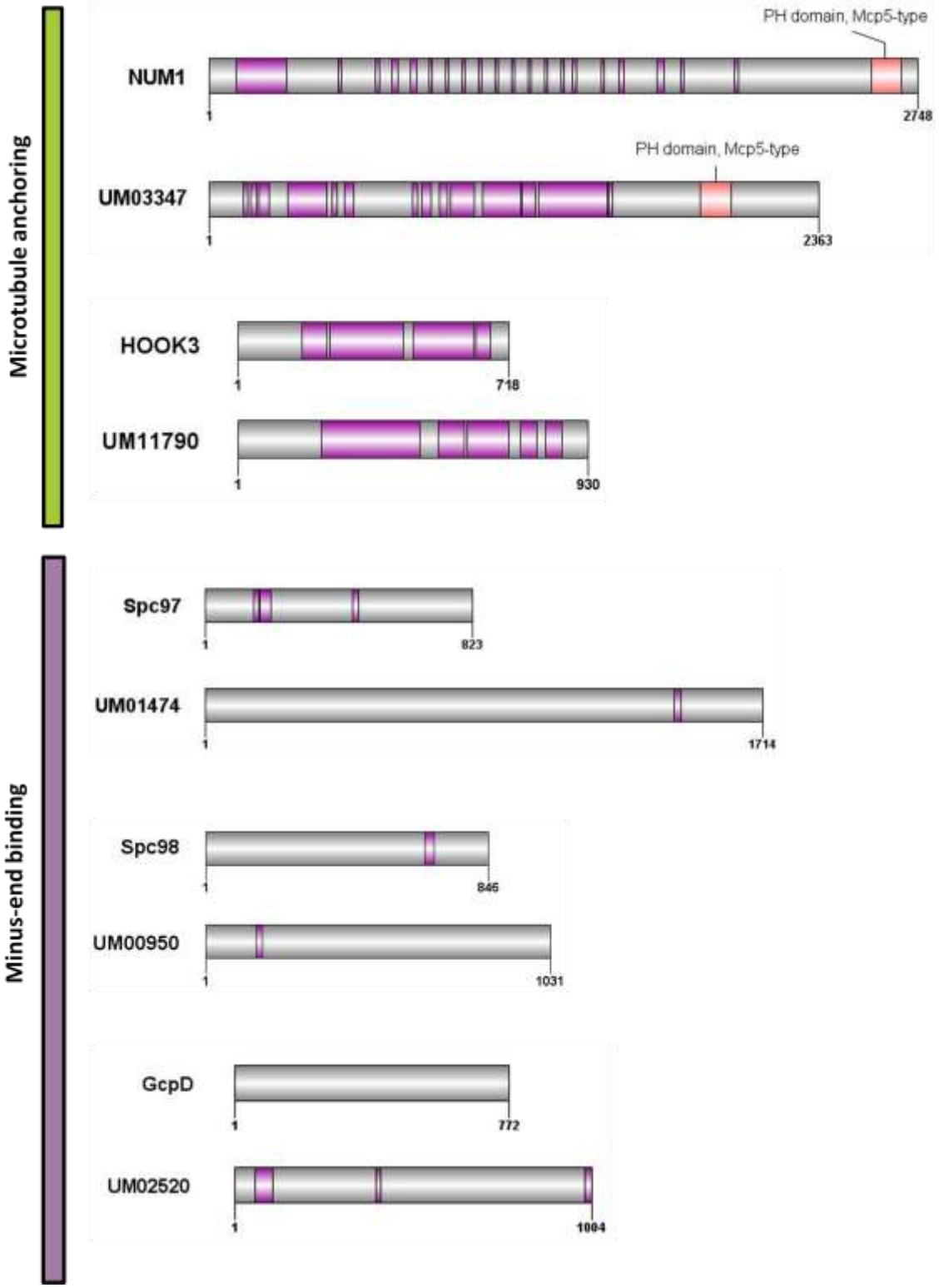
Microtubule anchoring
Minus-end binding
PH domain, Mcp5-type
NUM1
1
2748
PH domain, Mcp5-type
UM03347
1
2363
HOOK3
1
718
UM11790
1
930
Spc97
1
823
UM01474
1
1714
Spc98
1
846
UM00950
1
1031
GcpD
1
772
UM02520
1
1004

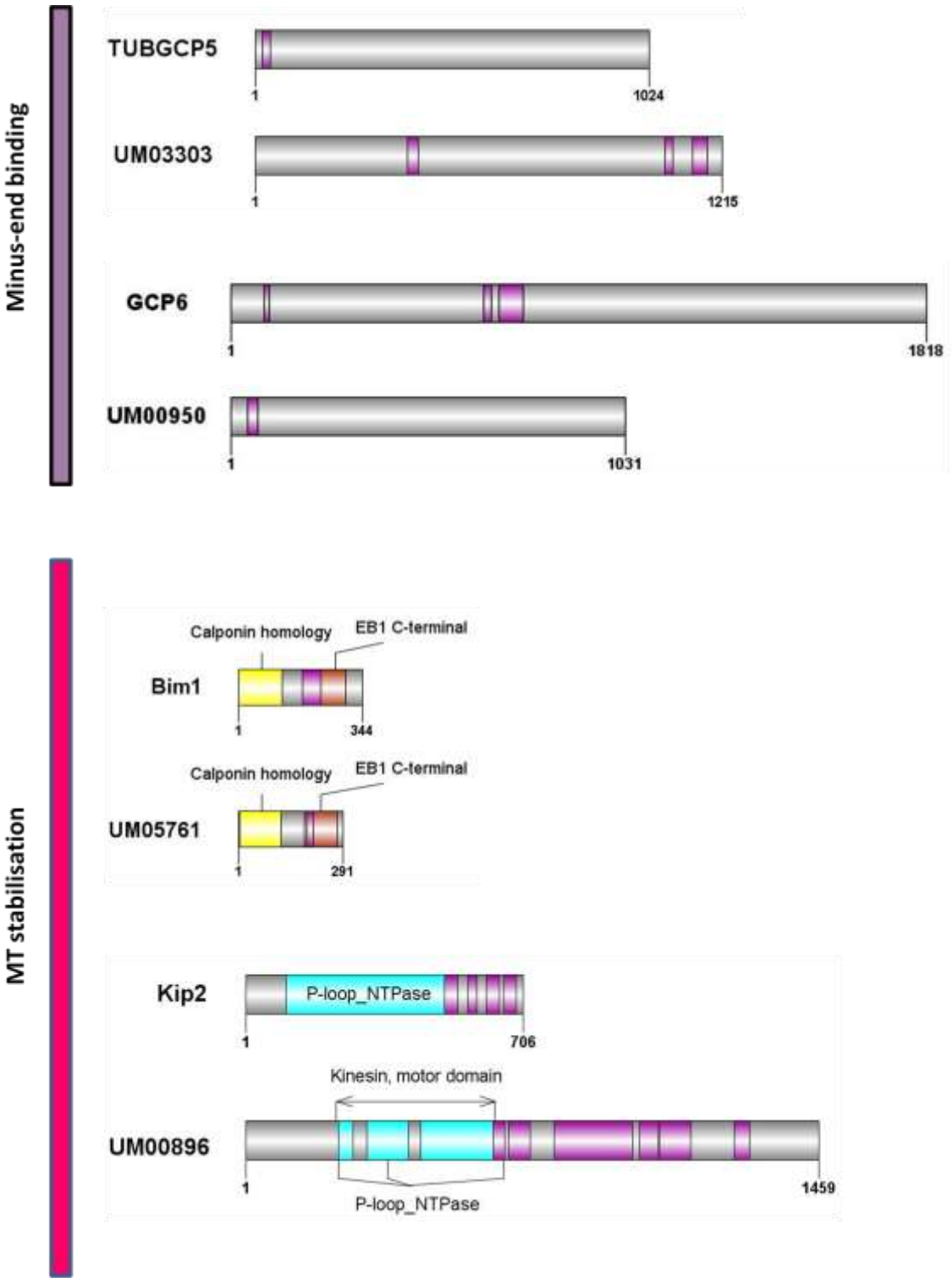
Minus-end binding
TUBGCP5
1
1024
UM03303
1
1215
GCP6
1
1818
UM00950
1
1031
MT stabilisation
Calponin homology
EB1 C-terminal
Bim1
1
344
Calponin homology
EB1 C-terminal
UM05761
1
291
Kip2
P-loop_NTPase
1
706
Kinesin, motor domain
UM00896
1
1459
P-loop_NTPase

MT stabilisation

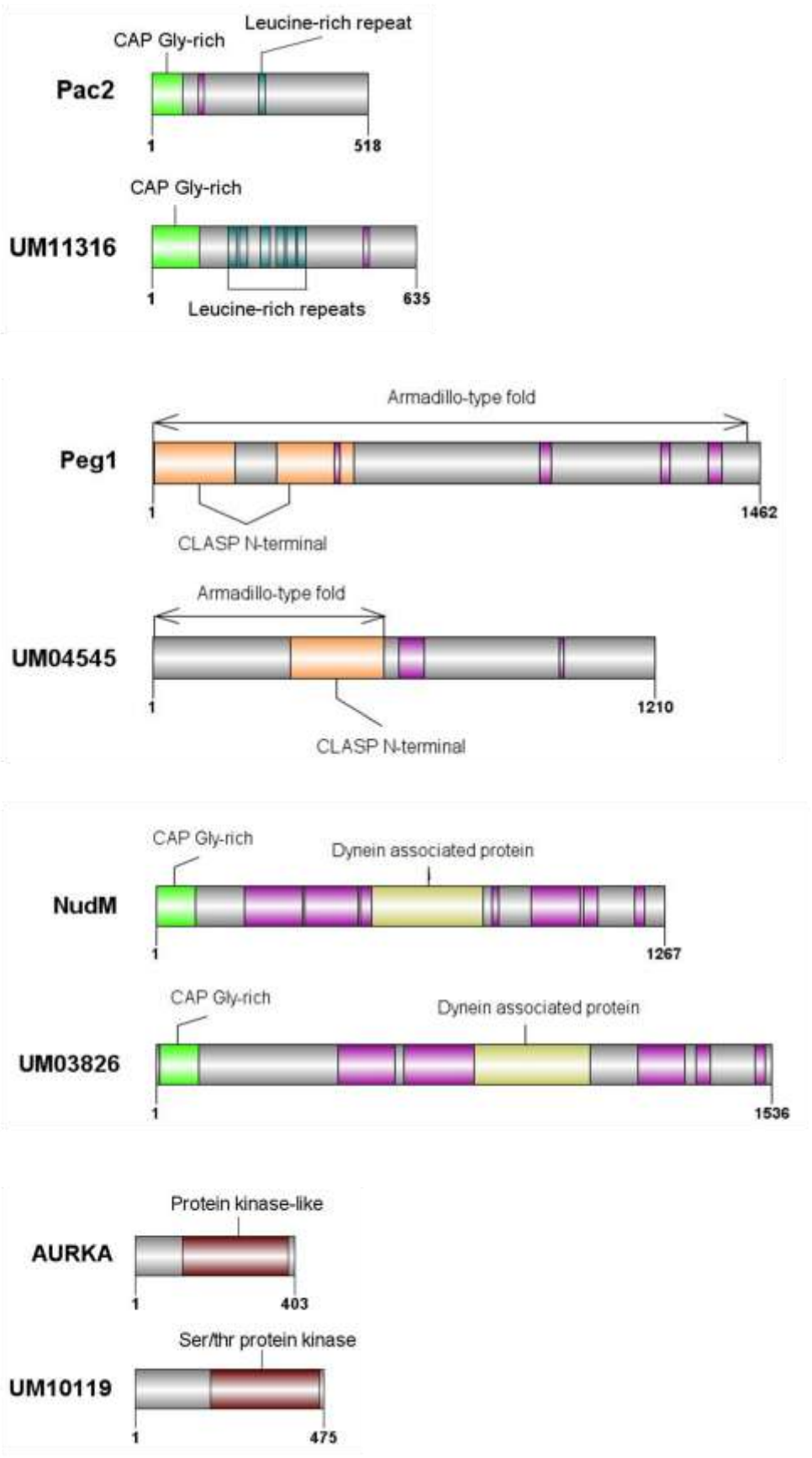

MT stabilisation

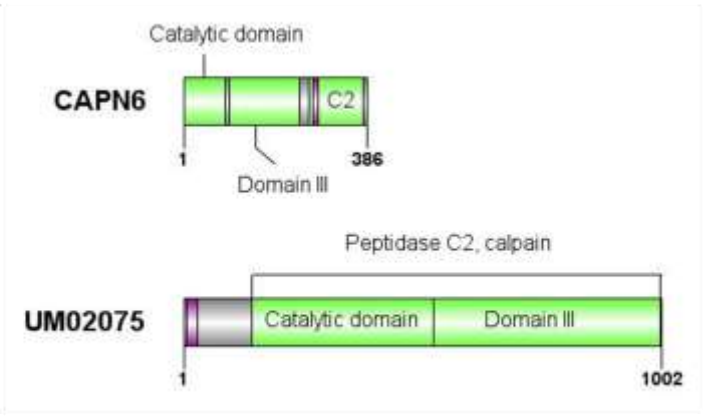

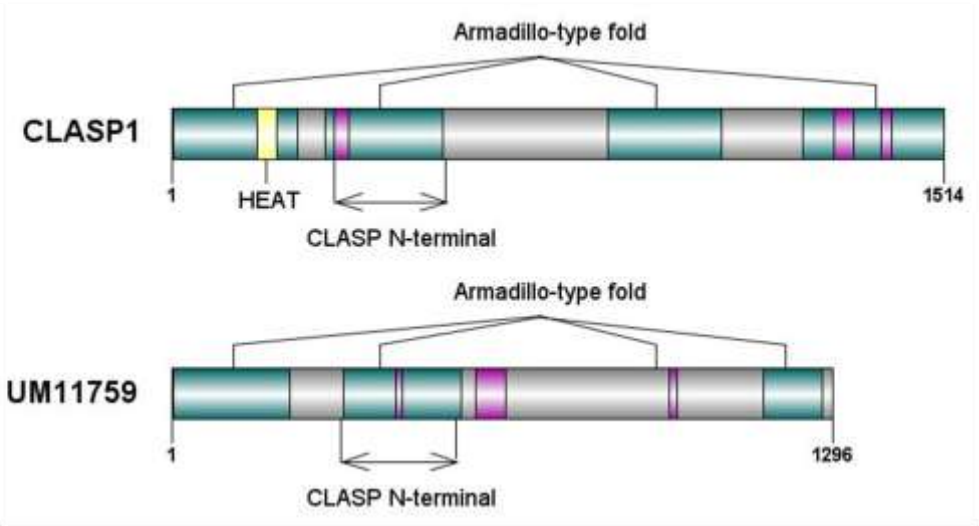

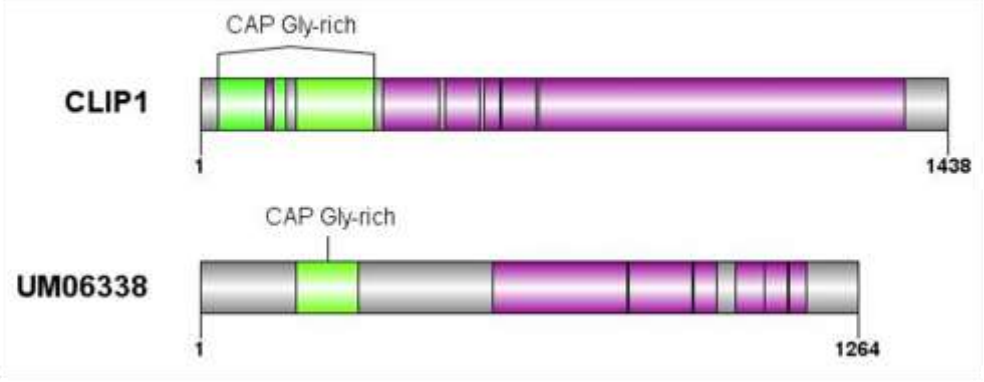

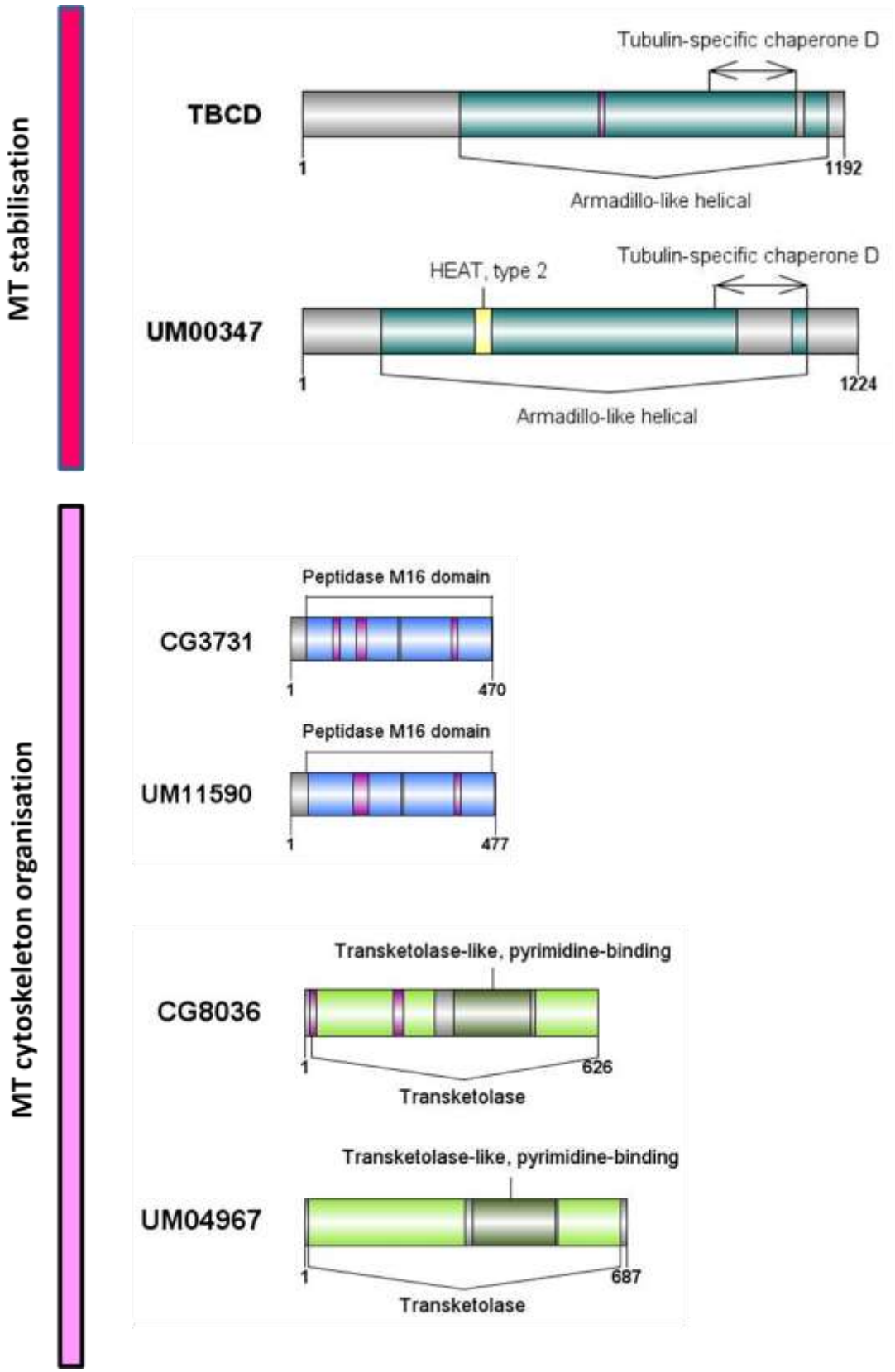
MT stabilisation
TBCD
Tubulin-specific chaperone D
1
1192
Armadillo-like helical
UM00347
HEAT, type 2
Tubulin-specific chaperone D
1
1224
Armadillo-like helical
MT cytoskeleton organisation
CG3731
Peptidase M16 domain
1
470
UM11590
Peptidase M16 domain
1
477
CG8036
Transketolase-like, pyrimidine-binding
1
626
Transketolase
UM04967
Transketolase-like, pyrimidine-binding
1
687
Transketolase

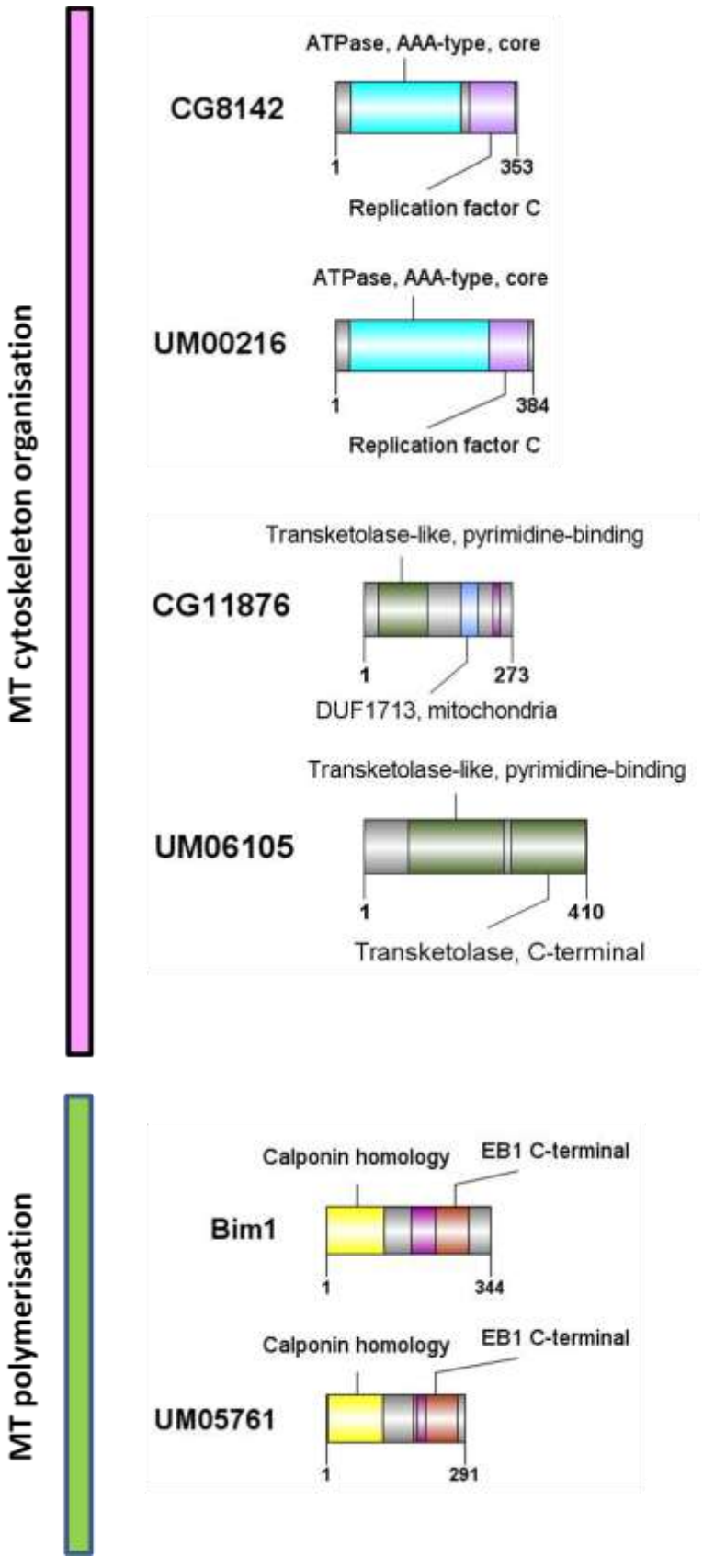
MT cytoskeleton organisation
CG8142
ATPase, AAA-type, core
1
353
Replication factor C
UM00216
ATPase, AAA-type, core
1
384
Replication factor C
CG11876
Transketolase-like, pyrimidine-binding
1
273
DUF1713, mitochondria
UM06105
Transketolase-like, pyrimidine-binding
1
410
Transketolase, C-terminal
MT polymerisation
Bim1
Calponin homology
EB1 C-terminal
1
344
UM05761
Calponin homology
EB1 C-terminal
1
291

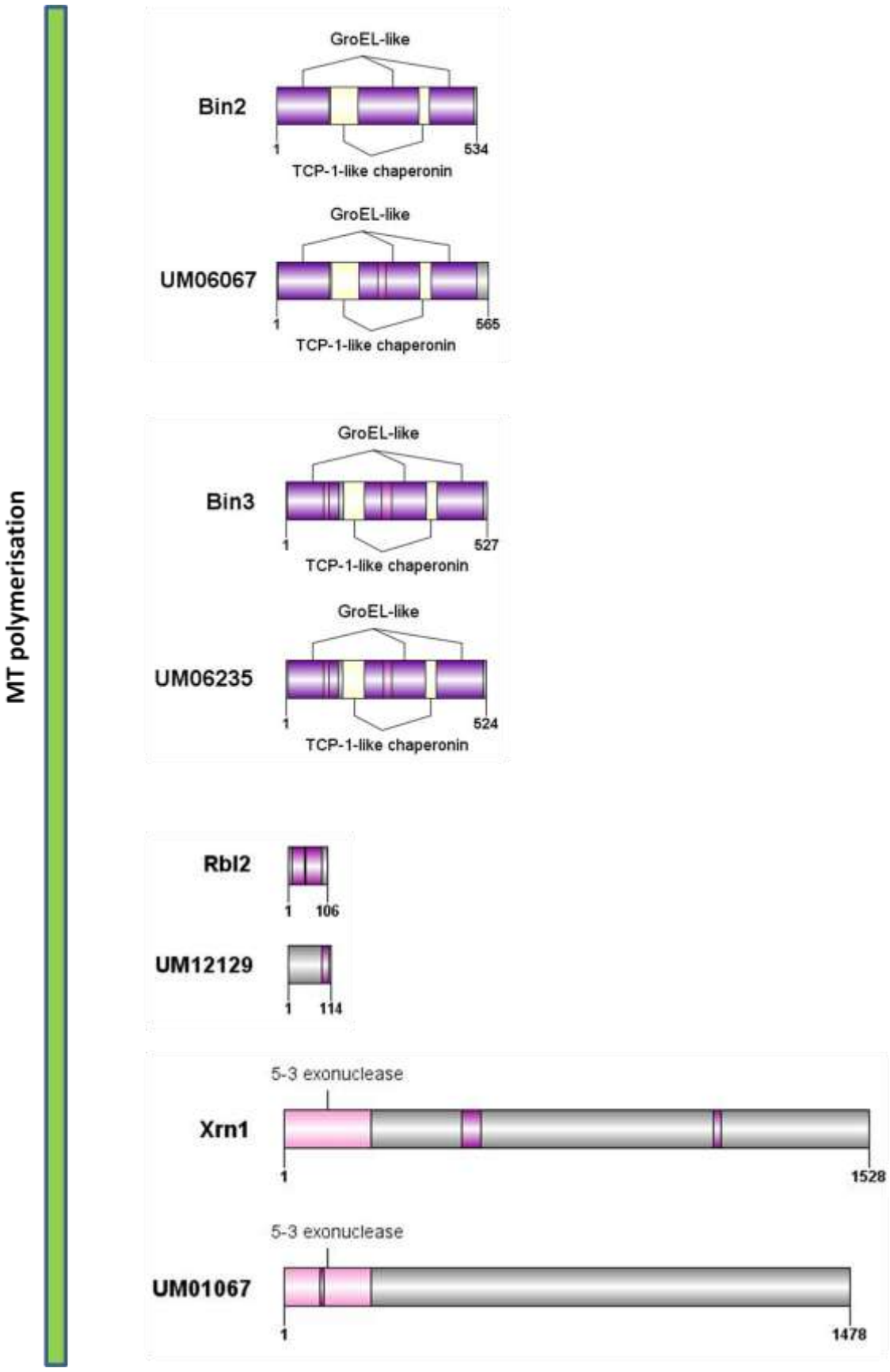
MT polymerisation
Bin2
GroEL-like
1
534
TCP-1-like chaperonin
UM06067
GroEL-like
1
565
TCP-1-like chaperonin
Bin3
GroEL-like
1
527
TCP-1-like chaperonin
UM06235
GroEL-like
1
524
TCP-1-like chaperonin
Rbl2
1
106
UM12129
1
114
Xrn1
5-3 exonuclease
1
1528
UM01067
5-3 exonuclease
1
1478

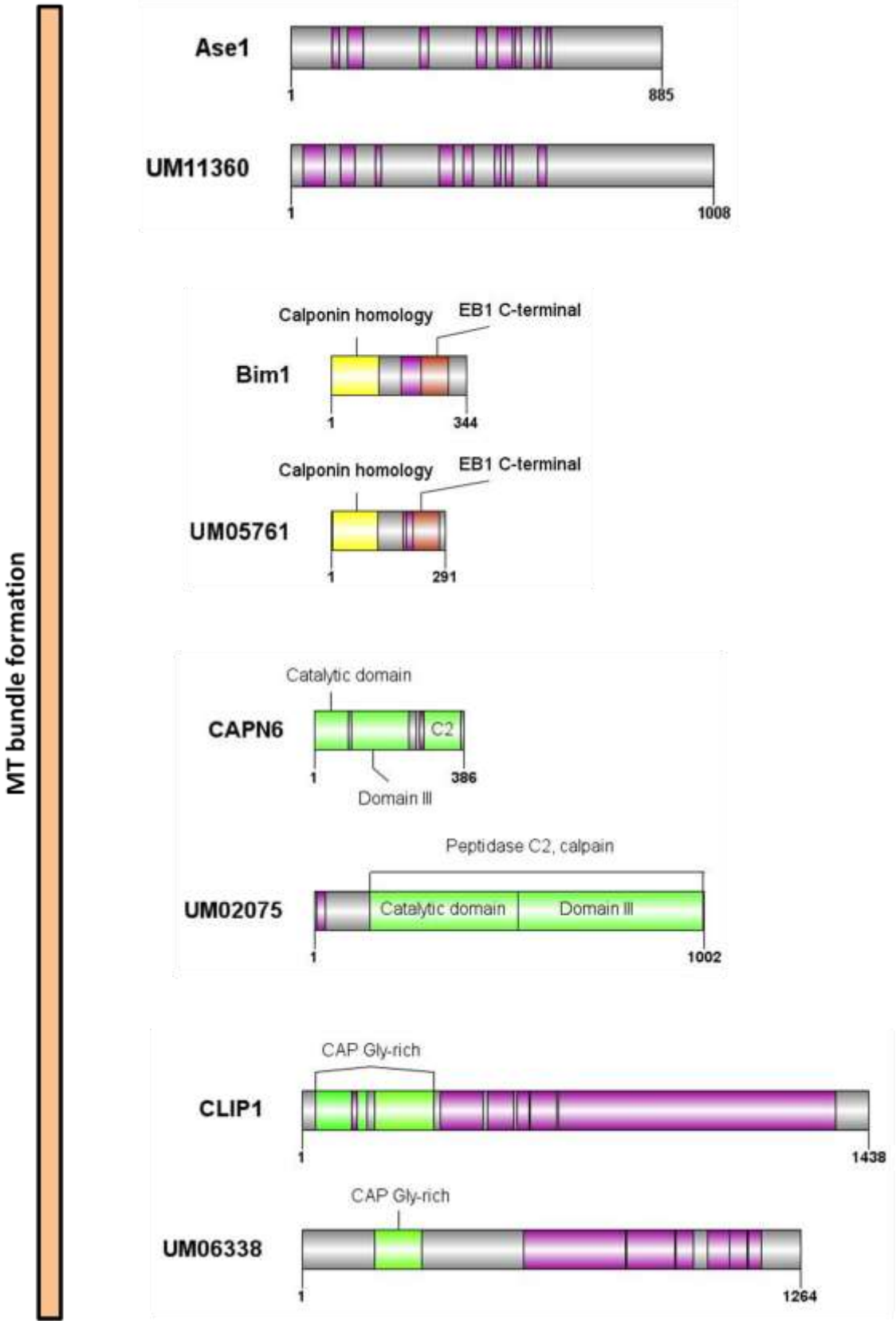
MT bundle formation
Ase1
1
885
UM11360
1
1008
Calponin homology
EB1 C-terminal
Bim1
1
344
Calponin homology
EB1 C-terminal
UM05761
1
291
Catalytic domain
CAPN6
C2
1
386
Domain III
Peptidase C2, calpain
UM02075
Catalytic domain
Domain III
1
1002
CAP Gly-rich
CLIP1
1
1438
CAP Gly-rich
UM06338
1
1264

MT bundle formation

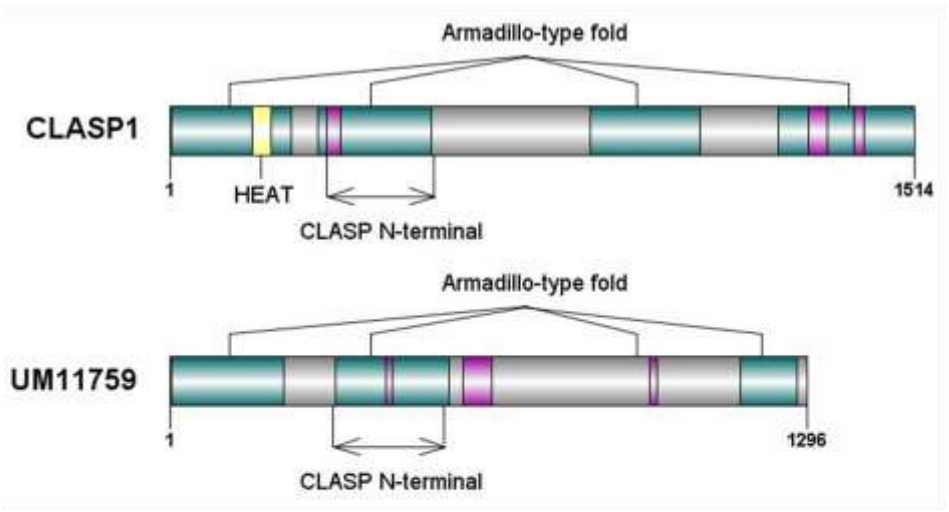

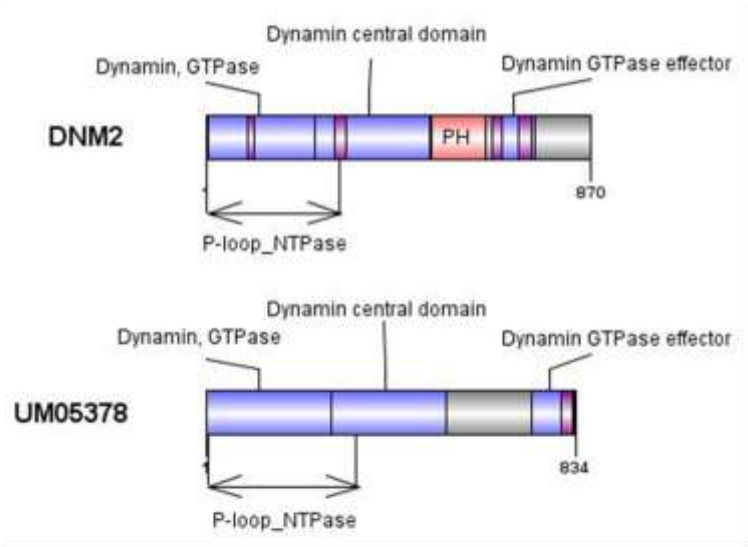

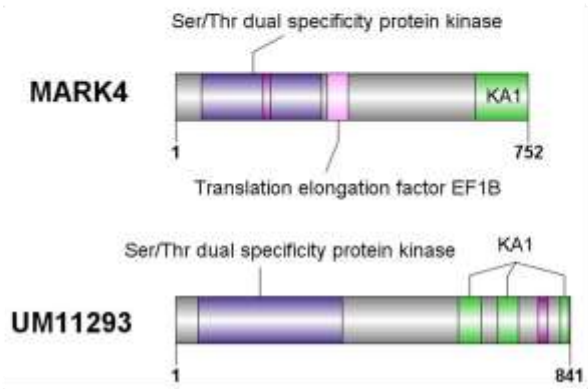

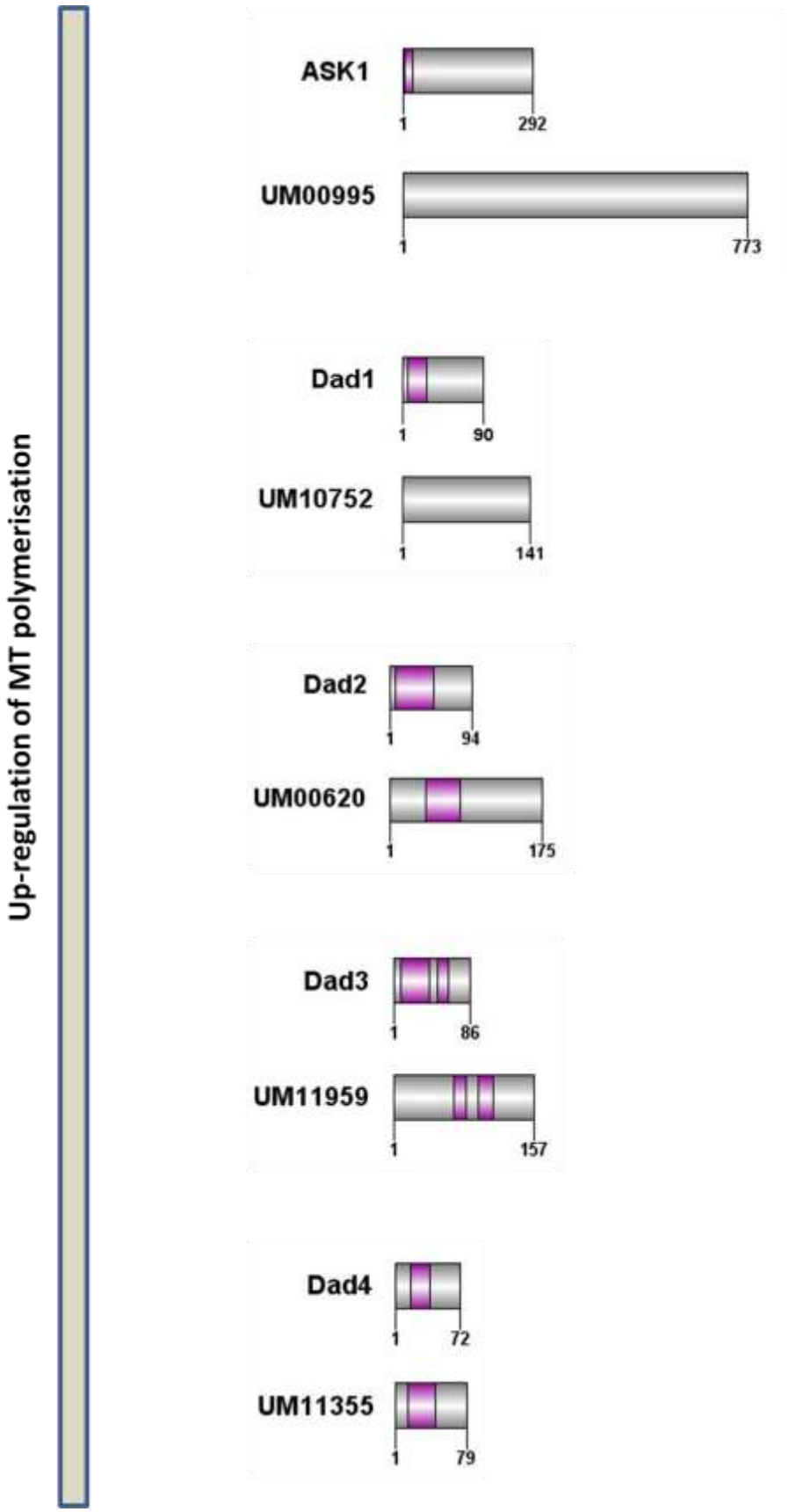
Up-regulation of MT polymerisation
ASK1
1
292
UM00995
1
773
Dad1
1
90
UM10752
1
141
Dad2
1
94
UM00620
1
175
Dad3
1
86
UM11959
1
157
Dad4
1
72
UM11355
1
79

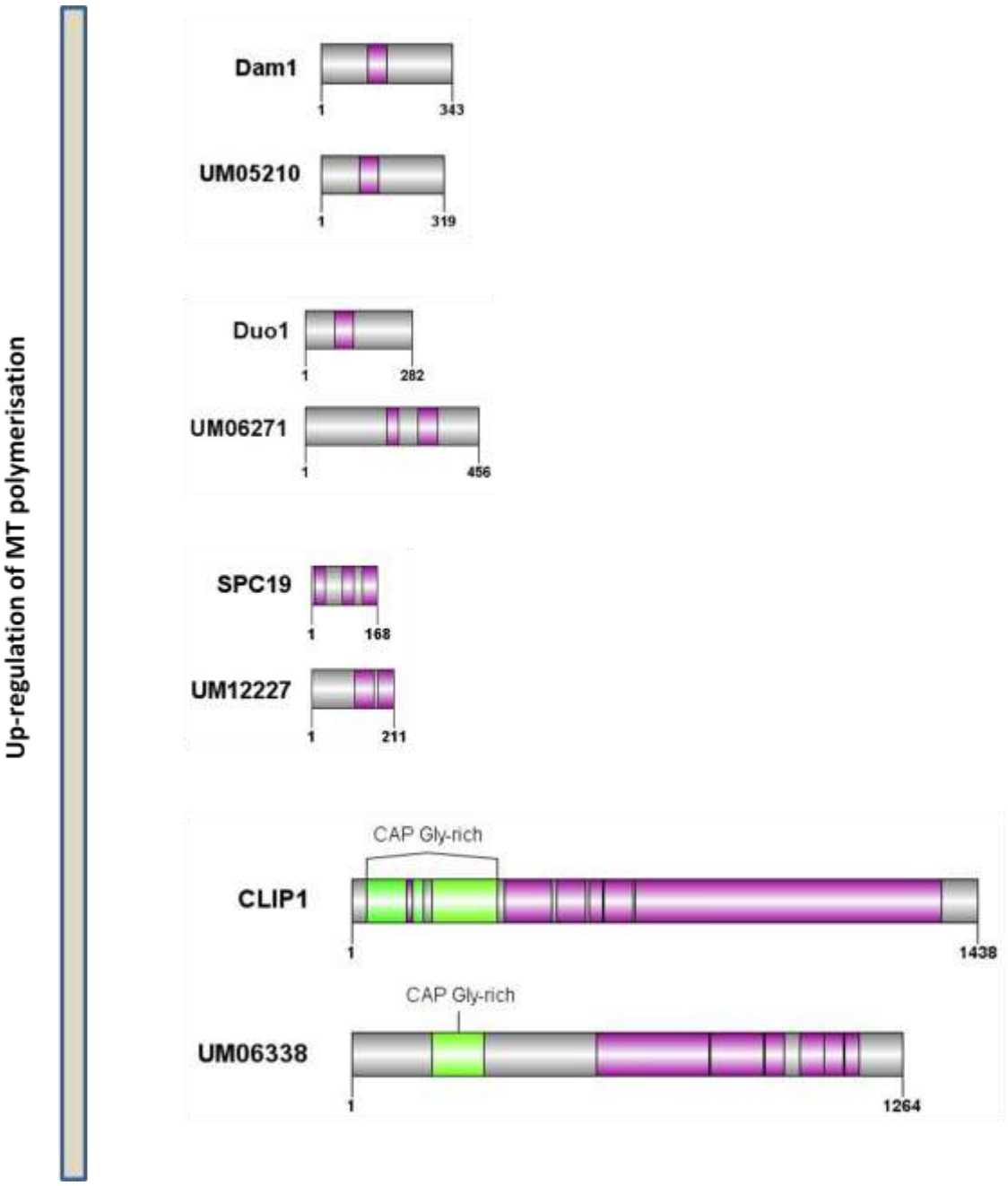
Up-regulation of MT polymerisation
Dam1
1
343
UM05210
1
319
Duo1
1
282
UM06271
1
456
SPC19
1
168
UM12227
1
211
CAP Gly-rich
CLIP1
1
1438
CAP Gly-rich
UM06338
1
1264

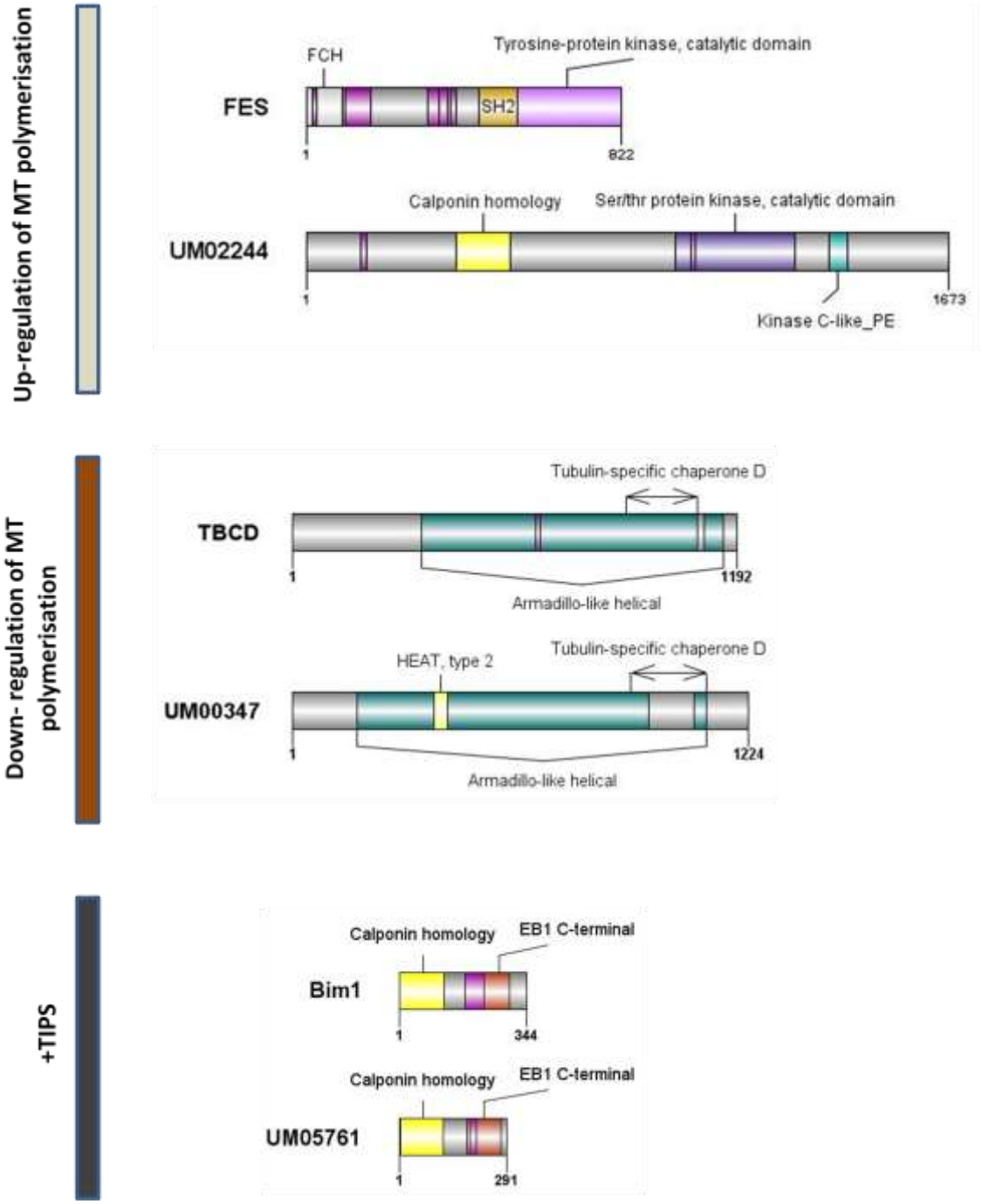
Up-regulation of MT polymerisation
FES
FCH
Tyrosine-protein kinase, catalytic domain
SH2
1
822
UM02244
Calponin homology
Ser/thr protein kinase, catalytic domain
1
1673
Kinase C-like_PE
Down- regulation of MT polymerisation
TBCD
Tubulin-specific chaperone D
1
1192
Armadillo-like helical
UM00347
HEAT, type 2
Tubulin-specific chaperone D
1
1224
Armadillo-like helical
+TIPS
Bim1
Calponin homology
EB1 C-terminal
1
344
UM05761
Calponin homology
EB1 C-terminal
1
291

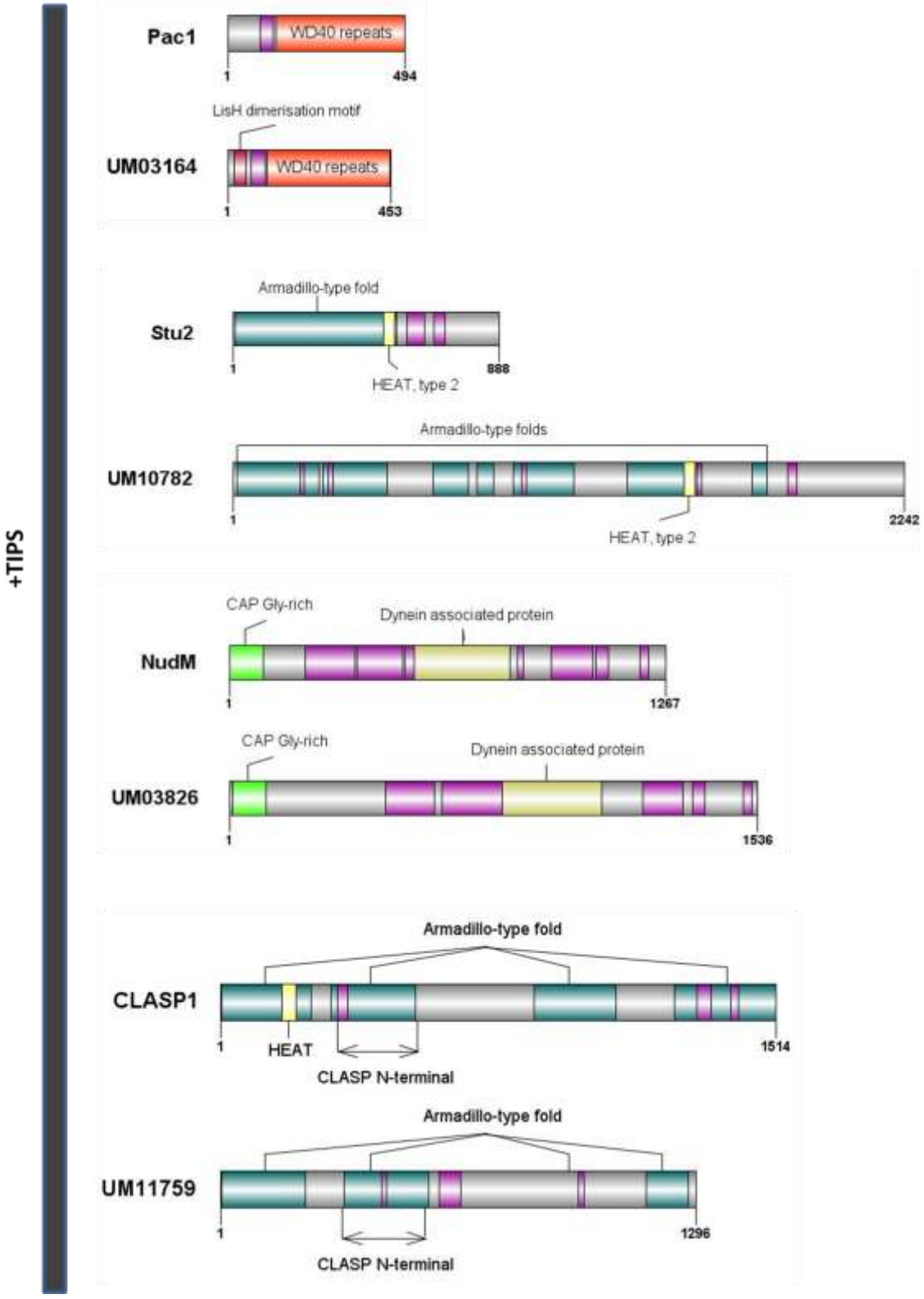
+TIPS
Pac1
WD40 repeats
1
494
LisH dimerisation motif
UM03164
WD40 repeats
1
453
Armadillo-type fold
Stu2
1
888
HEAT, type 2
Armadillo-type folds
UM10782
1
2242
HEAT, type 2
CAP Gly-rich
Dynein associated protein
NudM
1
1267
CAP Gly-rich
Dynein associated protein
UM03826
1
1536
Armadillo-type fold
CLASP1
1
HEAT
1514
CLASP N-terminal
Armadillo-type fold
UM11759
1
1296
CLASP N-terminal

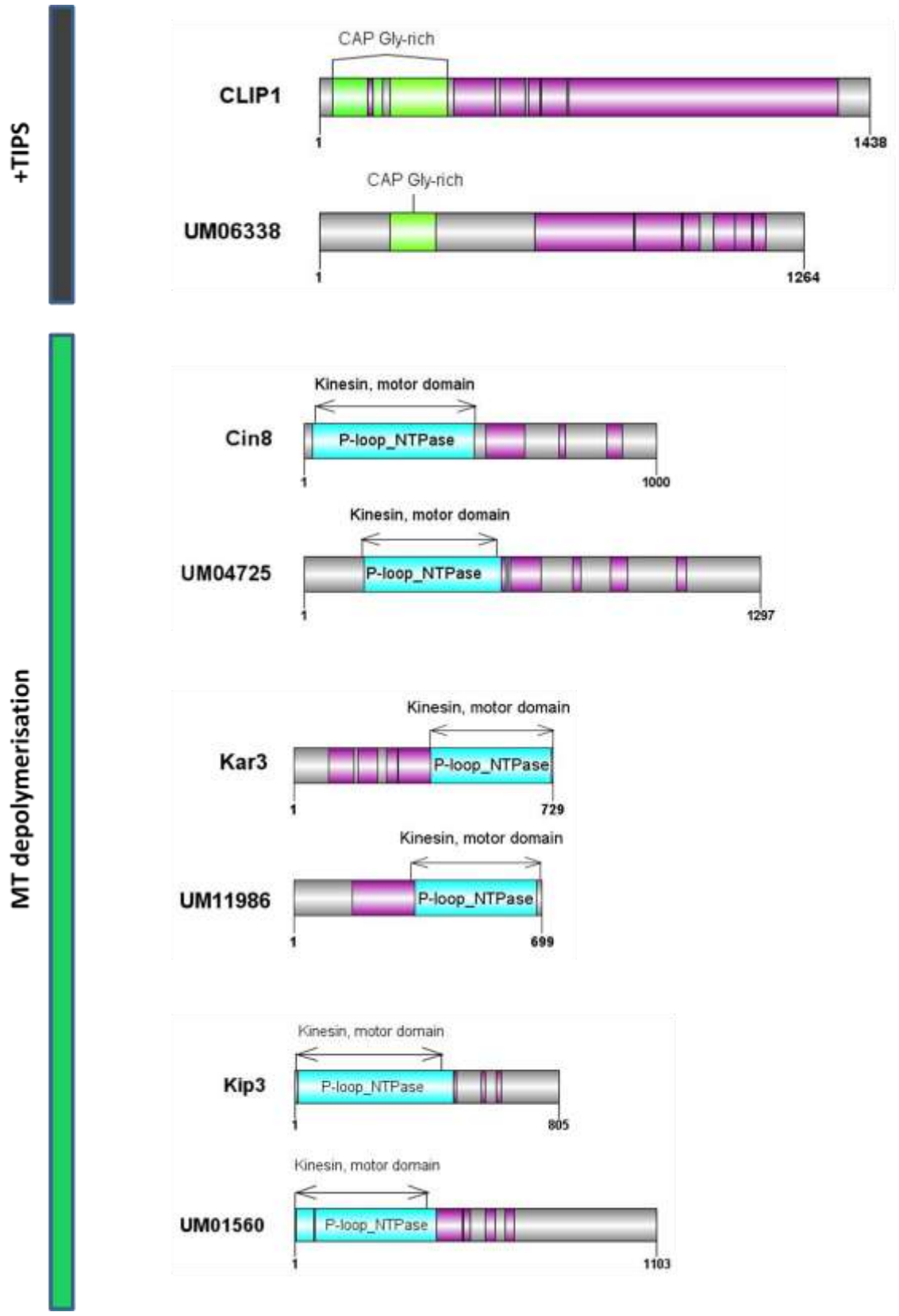
+TIPS
MT depolymerisation
CAP Gly-rich
CLIP1
1
1438
CAP Gly-rich
UM06338
1
1264
Kinesin, motor domain
Cin8
P-loop_NTPase
1
1000
Kinesin, motor domain
UM04725
P-loop_NTPase
1
1297
Kinesin, motor domain
Kar3
P-loop_NTPase
1
729
Kinesin, motor domain
UM11986
P-loop_NTPase
1
699
Kinesin, motor domain
Kip3
P-loop_NTPase
1
805
Kinesin, motor domain
UM01560
P-loop_NTPase
1
1103

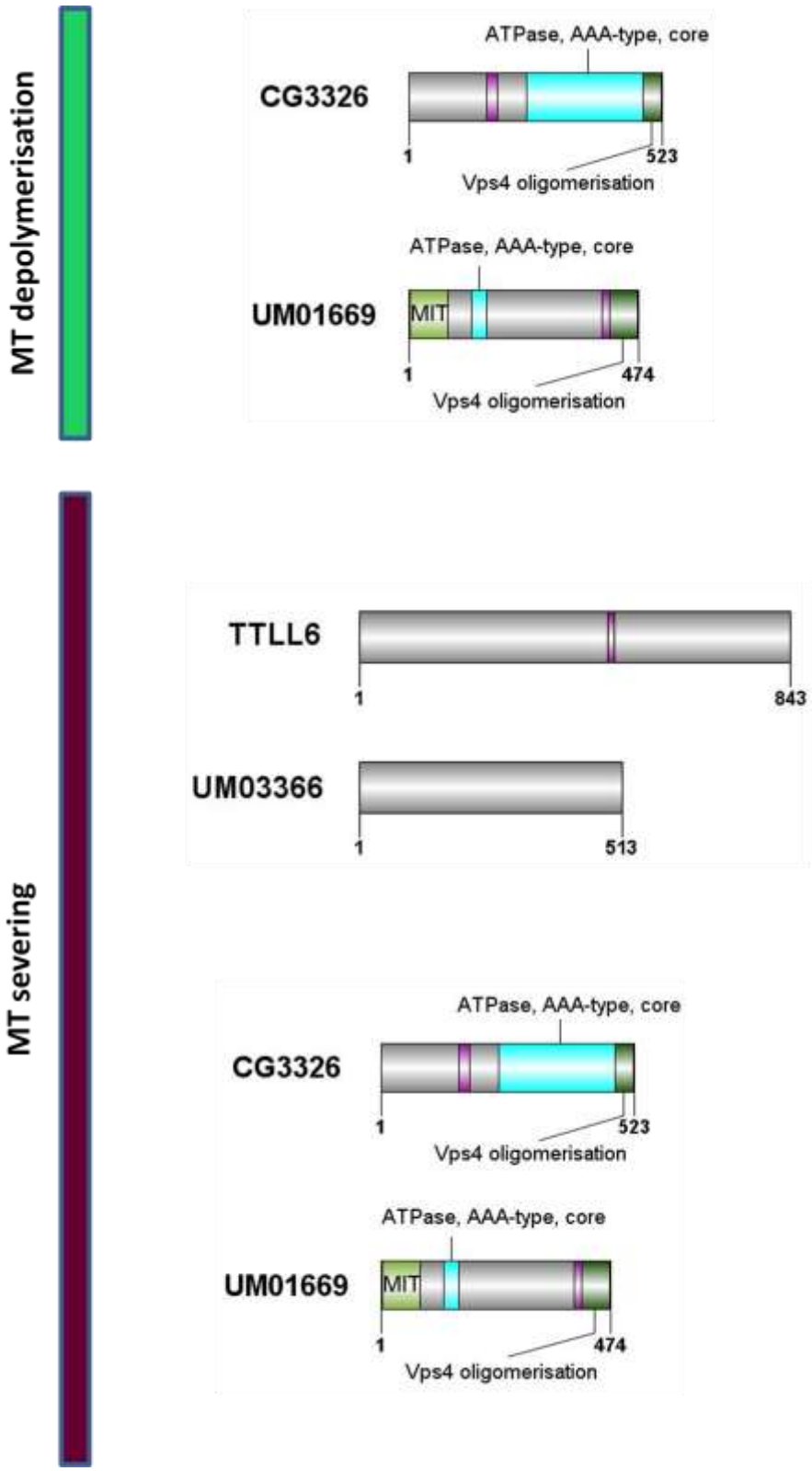
MT depolymerisation
ATPase, AAA-type, core
CG3326
1
523
Vps4 oligomerisation
ATPase, AAA-type, core
UM01669
MIT
1
474
Vps4 oligomerisation
MT severing
TTLL6
1
843
UM03366
1
513
ATPase, AAA-type, core
CG3326
1
523
Vps4 oligomerisation
ATPase, AAA-type, core
UM01669
MIT
1
474
Vps4 oligomerisation

Regulation of MT dynamics

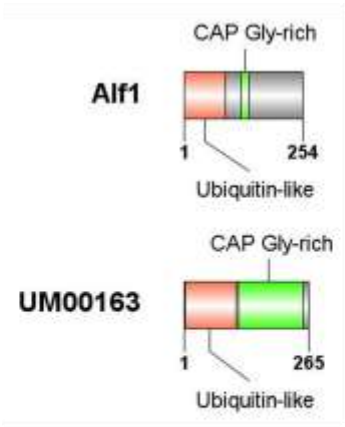

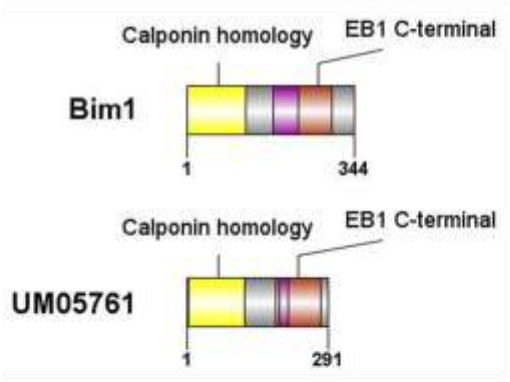

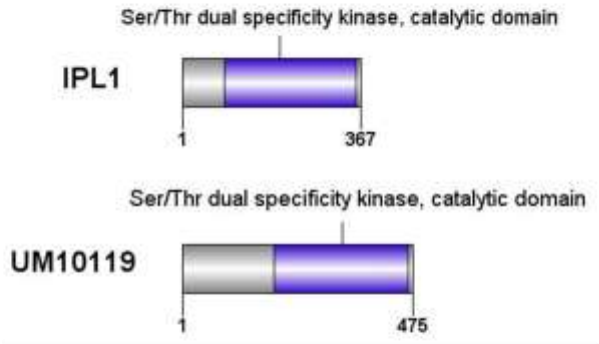

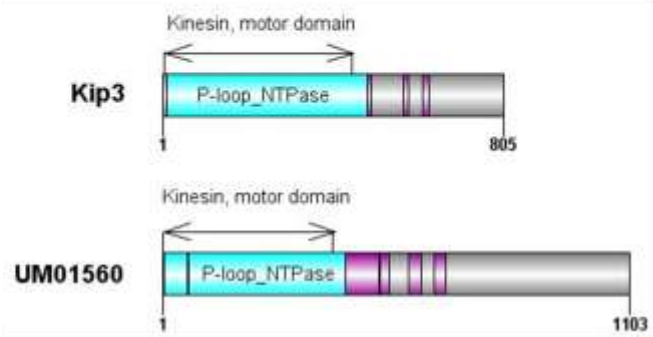

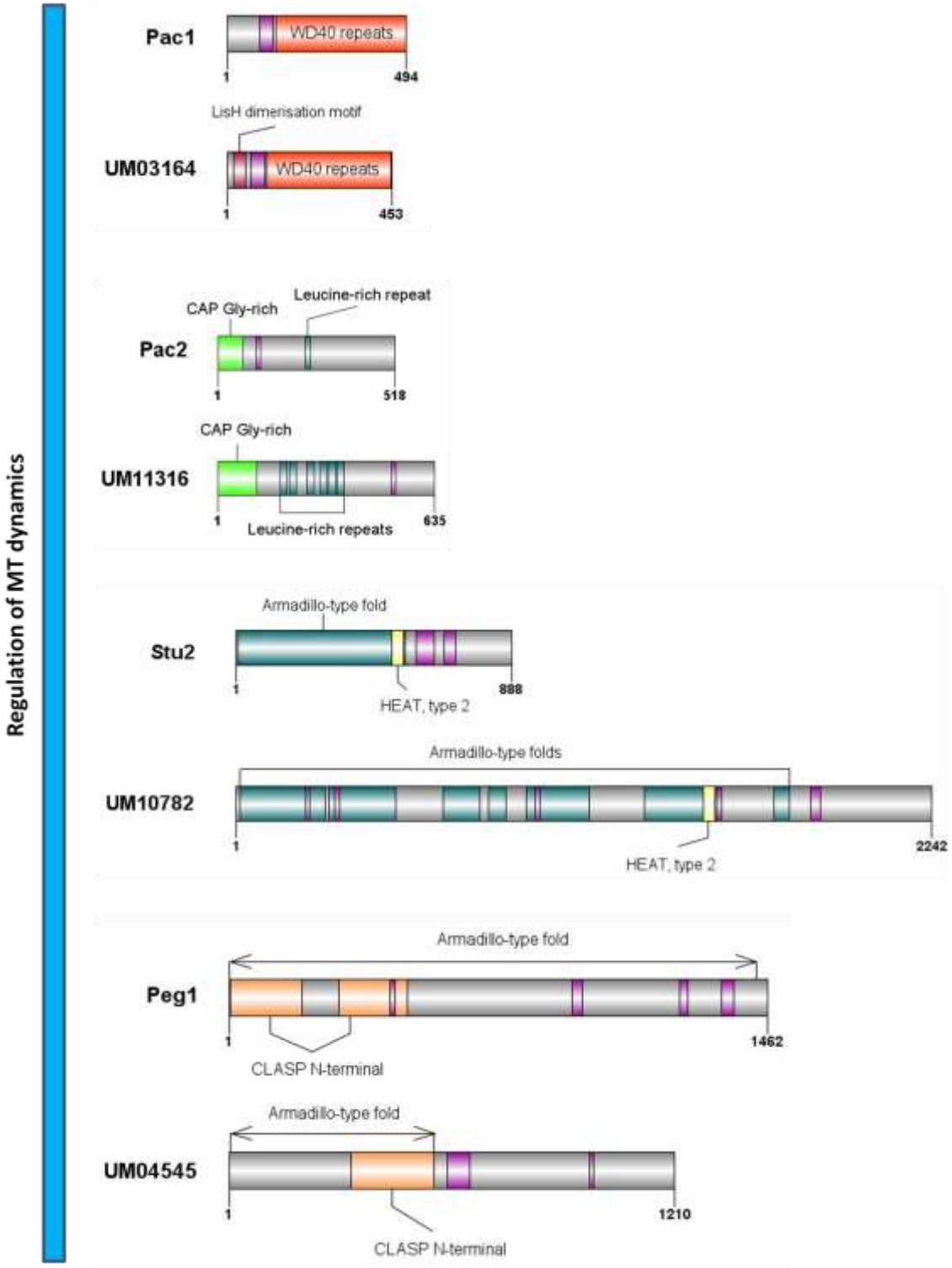
Regulation of MT dynamics
Pac1
WD40 repeats
1
494
LisH dimerisation motif
UM03164
WD40 repeats
1
453
CAP Gly-rich
Leucine-rich repeat
Pac2
1
518
CAP Gly-rich
UM11316
1
Leucine-rich repeats
635
Armadillo-type fold
Stu2
1
888
HEAT, type 2
Armadillo-type folds
UM10782
1
2242
HEAT, type 2
Armadillo-type fold
Peg1
1
1462
CLASP N-terminal
Armadillo-type fold
UM04545
1
1210
CLASP N-terminal

Regulation of MT dynamics

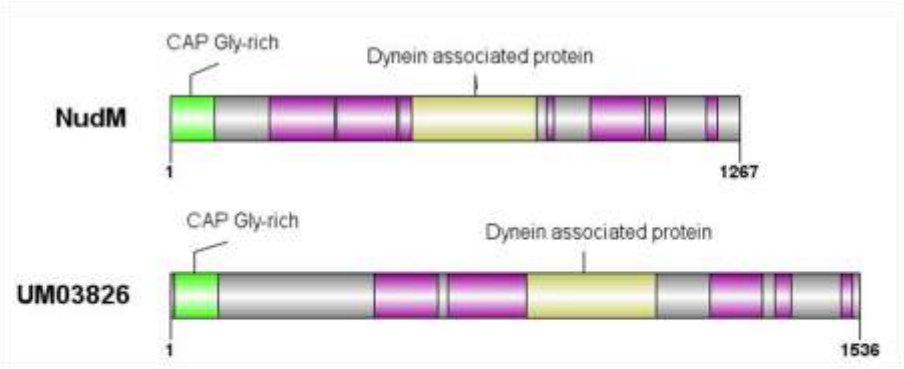

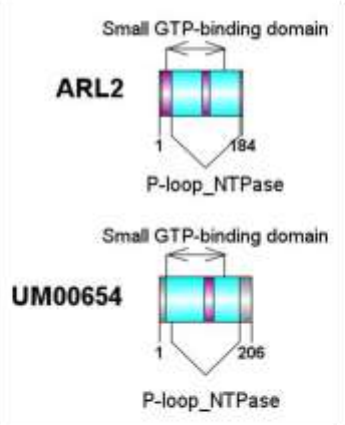

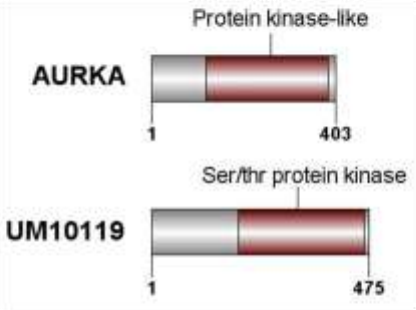

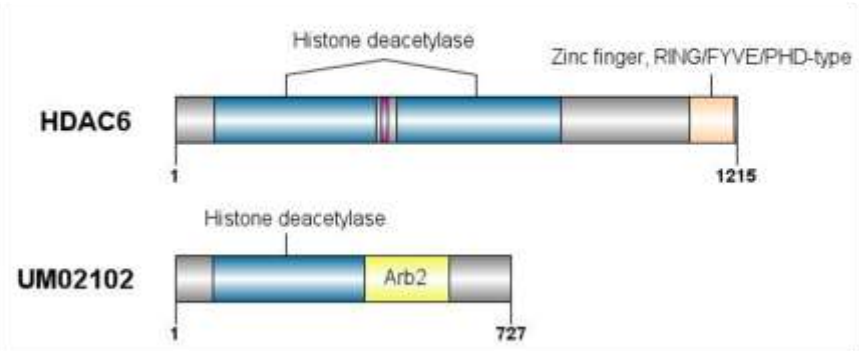

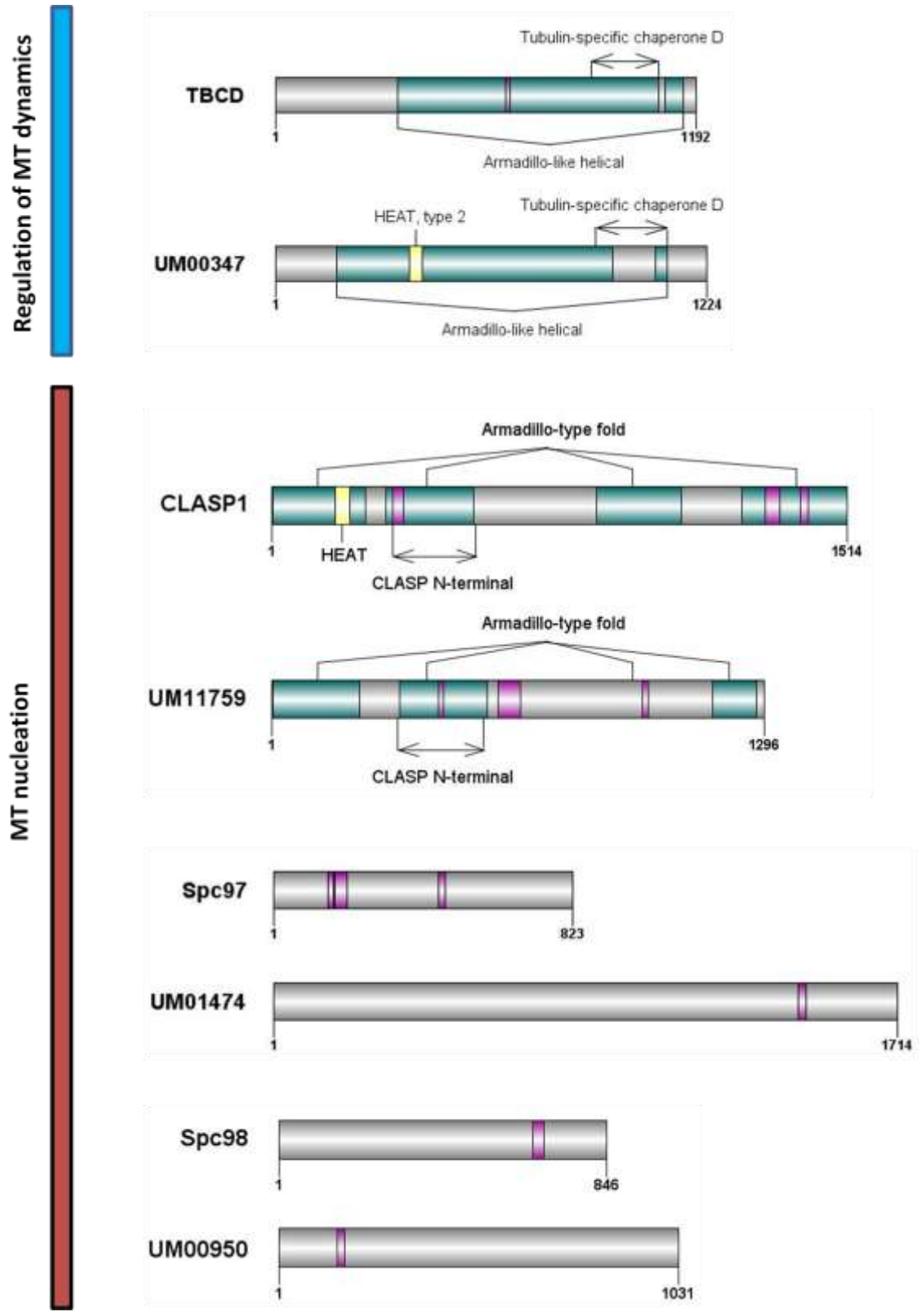
Regulation of MT dynamics
MT nucleation
TBCD
Tubulin-specific chaperone D
1
1192
Armadillo-like helical
UM00347
HEAT, type 2
Tubulin-specific chaperone D
1
1224
Armadillo-like helical
CLASP1
Armadillo-type fold
1
HEAT
1514
CLASP N-terminal
UM11759
Armadillo-type fold
1
1296
CLASP N-terminal
Spc97
1
823
UM01474
1
1714
Spc98
1
846
UM00950
1
1031

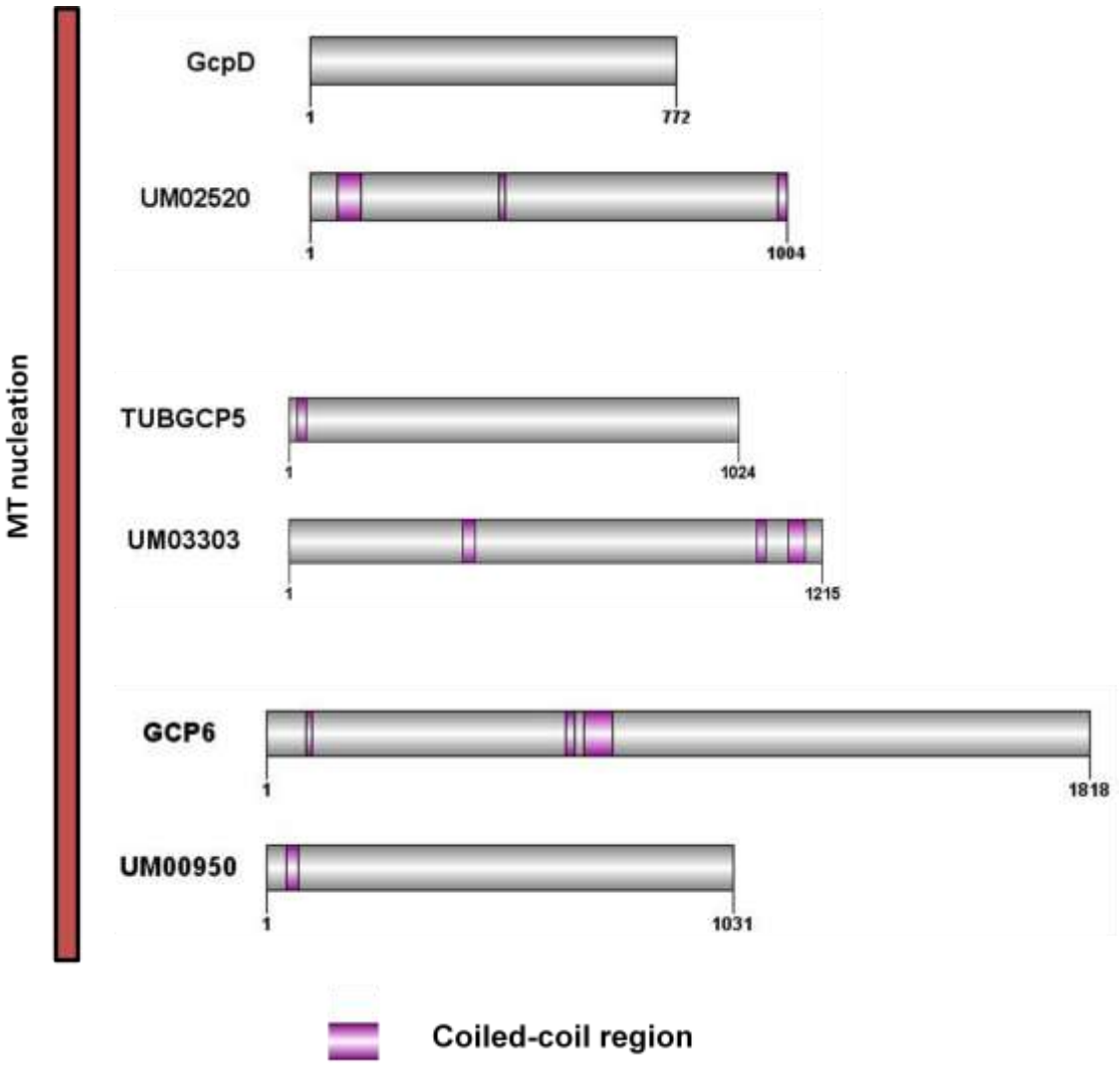

Appendix, Figure A1 Domain architecture of MAPs and their potential orthologues in *U. maydis*.

For each protein with a potential orthologue in *Ustilago*, I show their sequence architecture. All of the proteins were grouped according to their functions, found with the AmiGO database. In each cartoon, the upper structure is a known MAP from one of the selected species (*H. sapiens*, *D. melanogaster*, *A. nidulans*, *S. cerevisiae* or *S. pombe)*; the lower structure depicts the most probable *Ustilago* orthologue. The purple-coloured motif, present in most proteins, is a coiled-coil region. All domains detected by the InterPro online software (Hunter et al., 2012) were drawn on the protein structures. The numbers below each protein cartoon indicate protein length in amino acids. All cartoons were prepared using DOG 2.0 software.

SNPs found in mod mutants

mod1

Table A1 SNPs in mod1 mutant					
Position	**Reference**	**mod1**	**WT**	**Genes**	**Silent/non-silent/other**
1045234	G	A	G	um10881	Intron
1196775	C	T	C	um02440	Intron
1196907	T	C	T	um02440	Intron
229412	C	T	C	um02577	Intron
142754	C	T	C	um12304	intron
1399543	G	A	G	um15059	nonsense tgg (Trp)-> tgA (Stop);
675288	G	A	G	um02260	non-silent cgt (Arg) -> Tgt (Cys);
470528	C	T	C	um05036	non-silent atg (Met, start)-> atA (Ile);
1200051	G	A	G	um00424	non-silent cca (Pro) -> Tca (Ser);
1580418	G	A	G	um02018	non-silent cca (Pro)-> cTa (Leu);
276945	C	T	C	um05527	non-silent cca (Pro)-> cTa (Leu);
2413322	G	A	G	um12111	non-silent cca (Pro)-> Tca (Ser);
730853	G	A	G	um00274	non-silent ccc (Pro) -> cTc (Leu);
355045	C	T	C	um12159	non-silent ccc (Pro)-> cTc (Leu);
2413567	G	A	G	um12111	non-silent ccg (Pro)-> Tcg (Ser);
695068	G	A	G	um01040	non-silent cct (Pro) -> Tct (Ser);
611224	C	T	C	um15094	non-silent ctt (Leu)-> Ttt (Phe);
990673	G	A	G	um02371	non-silent gaa (Asp) -> Aaa (Lys);
293846	C	T	C	um05894	non-silent gag (Glu) -> Aag (Lys);
190247	C	T	C	um01499	non-silent gcc (Ala)-> gTc (Val);
1792979	C	T	C	um01414	non-silent gct (Ala) -> gTt (Val);
1276331	C	T	C	um00450	non-silent ggc (Gly)-> gAc (Asp);
393231	g	A	G	um03254	non-silent tca (Ser) -> tTa (Leu);
119997	C	T	C	um00048	non-silent tcc (Ser) -> tTc (Phe);
253923	C	T	C	um05340	non-silent tcg (Ser)-> tTg (Leu);
1439497	G	A	G	um00496	Promoter
1439498	G	A	G	um00496	Promoter

1923524	**C**	**T**	**C**	**um00656**	**Promoter**
184050	**C**	**T**	**C**	**um11843**	**Promoter**
533869	**C**	**T**	**C**	**um10307**	**Promoter**
722005	**C**	**T**	**C**	**um03049**	**Promoter**
118828	**C**	**T**	**C**	**um03166**	**Promoter**
363365	**G**	**A**	**G**	**um03762**	**Promoter**
177761	**C**	**T**	**C**	**um04544**	**Promoter**
463650	**C**	**T**	**C**	**um05402, um05403**	**Promoter**
91798	**C**	**T**	**C**	**um12321, um11595**	**Promoter**
1113777	C	T	C	um01171	silent aag -> aaA;
31344	C	T	C	um11963	silent acg -> acA;
526402	C	T	C	um05423	silent cag -> caA;
34326	C	T	C	um04318	silent ctc -> ctT;
354747	G	A	G	um11792	silent ctc -> ctT;
29811	G	A	G	um05806	silent ctg -> ctA;
273128	C	T	C	um05152	silent gag -> gaA;
28631	G	A	G	um02825	silent gag -> gaA;
77307	C	T	C	um05822	silent gtc -> gtT;
2413808	G	A	G	um12111	silent tcc -> tcT;
427214	G	A	G	um10294	silent tcc -> tcT;
534272	G	A	G	um00992	silent ttc -> ttT;
120027	C	T	C	um06014	silent atc -> atT;
309639	C	T	C	um06090	silent atc -> atT;

mod2

Table A2 SNPs in mod2 mutant					
Position	**Reference**	**mod2**	**WT**	**Genes**	**Silent/non-silent/other**
755958	**G**	**A**	**G**	**um11896**	**Intron**
1175536	**C**	**T**	**C**	**um00415**	**non-silent cca (Pro)-> Tca (Ser);**
233237	**C**	**T**	**C**	**um04371**	**non-silent ggt (Gly) -> Agt (Ser);**
900234	**C**	**T**	**C**	**um10099**	**non-silent tct (Ser) -> tTt (Phe);**
557298	**G**	**A**	**G**	**um00212**	**Promoter**
1219274	**G**	**A**	**G**	**um01206, um01207**	**Promoter**
853175	**C**	**T**	**C**	**um01714**	**Promoter**
894798	**G**	**A**	**G**	**um02279**	**Promoter**
67420	**G**	**A**	**G**	**um02835, um02836**	**Promoter**
600430	**C**	**T**	**C**	**um10837**	**Promoter**
911977	A	G	A	um02342	silent aca -> acG;
1550821	G	A	G	um02005	silent ccc -> ccT;
99523	G	A	G	um04127	silent ccg -> ccA;
355201	G	A	G	um03982	silent ctg -> Ttg;
561214	C	T	C	um05435	silent tcc -> tcT;

mod3

Table A3 SNPs in mod3 mutant					
Position	**Reference**	**mod3**	**WT**	**Genes**	**Silent/non-silent/other**
2310942	**C**	**T**	**C**	**um11202**	**Intron**
2310943	**C**	**T**	**C**	**um11202**	**Intron**
1586587	**T**	**C**	**T**	**um02021**	**Intron**
558407	**G**	**A**	**G**	**um10313**	**Intron**
106450	**G**	**A**	**G**	**um10386**	**nonsense cga (Arg) -> Tga (Stop);**
383867	**C**	**T**	**C**	**um06258**	**nonsense cga (Arg)-> Tga (Stop);**
720983, 720984	**c,c**	**T,T**	**c,c**	**um11009**	**non-silent ccc(Pro) -> TTc (Phe) ;**
37498	**G**	**A**	**G**	**um04319**	**non-silent ctc (Leu) -> Ttc (Phe);**
520505	**G**	**A**	**G**	**um04878**	**non-silent ctt (Leu) -> Ttt (Phe);**
1248300	C	T	C	um02456	silent aag -> aaA;
885208	G	A	G	um02331	silent ctc -> ctT;
514384	G	A	G	um11585	silent ctg -> Ttg;
541197	C	T	C	um11063	silent gcc -> gcT;
153265	G	A	G	um05486	silent ttc -> ttT;
178562	C	T	C		
178563	T	A	T		
395704	C	T	C		
424193	T	C	T		

mod4

Table A4 SNPs in mod4 mutant					
Position	**Reference**	**mod4**	**WT**	**Genes**	**Silent/non-silent/other**
1478512	**G**	**A**	**G**	**um01978**	**Intron**
197147	**G**	**A**	**G**	**um06043**	**nonsense cga (Arg) -> Tga (Stop);**
433677	**G**	**A**	**G**	**um02177**	**nonsense tgg (Trp)-> tgA (Stop);**
304445	**A**	**G**	**A**	**um01535**	**non-silent cag (Gln)-> cGg (Pro);**
140093	**G**	**A**	**G**	**um02859**	**non-silent cgc (Arg) -> Tgc (Cys);**
555809	**C**	**T**	**C**	**um03833**	**non-silent ctt (Leu)-> Ttt (Phe);**
749691	**C**	**T**	**C**	**um02733**	**non-silent gaa (Glu) -> Aaa (Lys);**
1340494	**C**	**T**	**C**	**um02487**	**non-silent tcc (Ser) -> tTc (Phe);**
691561	C	T	C	um00259	silent aag -> aaA;
334238	A	G	A	um04994	silent act -> acC;
118877	C	A	C	um00047	silent cgg -> cgT;
118829	G	A	G	um00047	silent ggc -> ggT;
600991	G	A	G	um15029	silent tga -> taa;
118828	A	G	A	um00047	silent ttg -> Ctg;
2003238	G	A	G	um00679	silent ttg -> ttA;
594936	G	A	G	um11103	silent atc -> atT;
1509478	G	A	G		
601197	G	A	G		

mod9

Table A5 SNPs in mod9 mutant					
Position	**Reference**	**mod9**	**WT**	**Genes**	**Silent/non-silent/other**
1209032	**C**	**T**	**C**	**um01868**	**non-silent ccc (Pro) -> Tcc (Ser);**
274102	**C**	**T**	**C**	**um05152**	**non-silent gaa (Glu) -> Aaa (Lys);**
340347	**C**	**T**	**C**	**um03238**	**non-silent gat (Asp) -> Aat (Asn);**
1248572	**C**	**T**	**C**	**um00442**	**Promoter**
2140369	**C**	**T**	**C**	**um00725**	**Promoter**
760280	**G**	**A**	**G**	**um10087**	**Promoter**
205920	**G**	**A**	**G**	**um01504**	**Promoter**
797916	G	A	G	**um03076**	**Promoter**
1857409	G	A	g	um00635	silent atc -> atT;
824658	C	T	C	um01085	silent atc -> atT;
924909	C	T	C	um01115	silent ctc -> ctT;
199166	G	A	G	um03927	silent ctc -> ctT;
1781283	G	A	G		
1435211	T	C	T		

Bibliography

Akhmanova, A., and Hoogenraad, C.C. (2005). Microtubule plus-end-tracking proteins: mechanisms and functions. Curr Opin Cell Biol *17*, 47-54.

Akhmanova, A., Hoogenraad, C.C., Drabek, K., Stepanova, T., Dortland, B., Verkerk, T., Vermeulen, W., Burgering, B.M., De Zeeuw, C.I., Grosveld, F.*, et al.* (2001). Clasps are CLIP-115 and -170 associating proteins involved in the regional regulation of microtubule dynamics in motile fibroblasts. Cell *104*, 923-935.

Akhmanova, A., and Steinmetz, M.O. (2008). Tracking the ends: a dynamic protein network controls the fate of microtubule tips. Nat Rev Mol Cell Biol *9*, 309-322.

Akhmanova, A., and Steinmetz, M.O. (2010). Microtubule +TIPs at a glance. J Cell Sci *123*, 3415-3419.

Al-Bassam, J., and Chang, F. (2011). Regulation of microtubule dynamics by TOG-domain proteins XMAP215/Dis1 and CLASP. Trends Cell Biol *21*, 604-614.

Alberts, B. (2008). Molecular biology of the cell, 5th ed. edn (New York, Garland Science ; [London : Taylor & Francis, distributor]).

Alberts, B., Wilson, J.H., and Hunt, T. (2008). Molecular biology of the cell, 5th ed., Reference ed. edn (New York, N.Y. ; Abingdon, Garland Science).

Allen, C., and Borisy, G.G. (1974). Structural polarity and directional growth of microtubules of *Chlamydomonas flagella*. J Mol Biol *90*, 381-402.

Allingham, J.S., Sproul, L.R., Rayment, I., and Gilbert, S.P. (2007). Vik1 modulates microtubule-Kar3 interactions through a motor domain that lacks an active site. Cell *128*, 1161-1172.

Altschul, S.F., Gish, W., Miller, W., Myers, E.W., and Lipman, D.J. (1990). Basic local alignment search tool. J Mol Biol *215*, 403-410.

Altschul, S.F., Madden, T.L., Schaffer, A.A., Zhang, J., Zhang, Z., Miller, W., and Lipman, D.J. (1997). Gapped BLAST and PSI-BLAST: a new generation of protein database search programs. Nucleic Acids Res *25*, 3389-3402.

Amos, L., and Klug, A. (1974). Arrangement of subunits in flagellar microtubules. J Cell Sci *14*, 523-549.

Archer, J.E., Magendantz, M., Vega, L.R., and Solomon, F. (1998). Formation and function of the Rbl2p-beta-tubulin complex. Mol Cell Biol *18*, 1757-1762.

Asthana, J., Kapoor, S., Mohan, R., and Panda, D. (2013). Inhibition of HDAC6 deacetylase activity increases its binding with microtubules and suppresses microtubule dynamic instability in MCF-7 cells. J Biol Chem *288*, 22516-22526.

Bakhoum, S.F., Thompson, S.L., Manning, A.L., and Compton, D.A. (2009). Genome stability is ensured by temporal control of kinetochore-microtubule dynamics. Nat Cell Biol *11*, 27-35.

Banuelos, S., Saraste, M., and Djinovic Carugo, K. (1998). Structural comparisons of calponin homology domains: implications for actin binding. Structure *6*, 1419-1431.

Banuett, F., and Herskowitz, I. (1996). Discrete developmental stages during teliospore formation in the corn smut fungus, *Ustilago maydis*. Development *122*, 2965-2976.

Banuett, F., Quintanilla, R.H., Jr., and Reynaga-Pena, C.G. (2008). The machinery for cell polarity, cell morphogenesis, and the cytoskeleton in the Basidiomycete fungus *Ustilago maydis*-a survey of the genome sequence. Fungal Genet Biol *45 Suppl 1*, S3-S14.

Basse, C.W. (2005). Dissecting defense-related and developmental transcriptional responses of maize during *Ustilago maydis* infection and subsequent tumor formation. Plant Physiol *138*, 1774-1784.

Bauer, R., Oberwinkler, F., and Vánky, K. (1997). Ultrastructural markers and systematics in smut fungi and allied taxa. Canadian Journal of Botany *75*, 1273-1314.

Bayley, P.M., Schilstra, M.J., and Martin, S.R. (1990). Microtubule dynamic instability: numerical simulation of microtubule transition properties using a Lateral Cap model. J Cell Sci *95 (Pt 1)*, 33-48.

Benanti, J.A., Matyskiela, M.E., Morgan, D.O., and Toczyski, D.P. (2009). Functionally distinct isoforms of Cik1 are differentially regulated by APC/C-mediated proteolysis. Mol Cell *33*, 581-590.

Berg, J.M., Tymoczko, J.L., and Stryer, L. (2002). Biochemistry, 5th ed. / Jeremy Berg, John Tymoczko, Lubert Stryer / web content by Neil D. Clarke. edn (New York, W. H. Freeman and Co. ; [Basingstoke : Palgrave] [distributor], 2001).

Bielska, E., Higuchi, Y., Schuster, M., Steinberg, N., Kilaru, S., Talbot, N.J., and Steinberg, G. (2014a). Long-distance endosome trafficking drives fungal effector production during plant infection. Nat Commun *5*, 5097.

Bielska, E., Schuster, M., Roger, Y., Berepiki, A., Soanes, D.M., Talbot, N.J., and Steinberg, G. (2014b). Hook is an adapter that coordinates kinesin-3 and dynein cargo attachment on early endosomes. J Cell Biol *204*, 989-1007.

Bielska, E.a., and Steinberg, G.d.s. (2013). The role of the tail of fungal kinesin-3 in binding to early endosomes and their role in plant pathogenicity (University of Exeter).

Blake-Hodek, K.A., Cassimeris, L., and Huffaker, T.C. (2010). Regulation of microtubule dynamics by Bim1 and Bik1, the budding yeast members of the

EB1 and CLIP-170 families of plus-end tracking proteins. Mol Biol Cell *21*, 2013-2023.

Bolker, M., Urban, M., and Kahmann, R. (1992). The a mating type locus of *U. maydis* specifies cell signaling components. Cell *68*, 441-450.

Borisy, G.G., Marcum, J.M., Olmsted, J.B., Murphy, D.B., and Johnson, K.A. (1975). Purification of tubulin and associated high molecular weight proteins from porcine brain and characterization of microtubule assembly *in vitro*. Ann N Y Acad Sci *253*, 107-132.

Borisy, G.G., and Taylor, E.W. (1967). The mechanism of action of colchicine. Colchicine binding to sea urchin eggs and the mitotic apparatus. J Cell Biol *34*, 535-548.

Bottin, A., Kamper, J., and Kahmann, R. (1996). Isolation of a carbon source-regulated gene from *Ustilago maydis.* Mol Gen Genet *253*, 342-352.

Boyle, J.S., and Lew, A.M. (1995). An inexpensive alternative to glassmilk for DNA purification. Trends Genet *11*, 8.

Brachmann, A., Weinzierl, G., Kamper, J., and Kahmann, R. (2001). Identification of genes in the bW/bE regulatory cascade in *Ustilago maydis*. Mol Microbiol *42*, 1047-1063.

Brouhard, G.J., Stear, J.H., Noetzel, T.L., Al-Bassam, J., Kinoshita, K., Harrison, S.C., Howard, J., and Hyman, A.A. (2008). XMAP215 is a processive microtubule polymerase. Cell *132*, 79-88.

Browning, H., Hayles, J., Mata, J., Aveline, L., Nurse, P., and McIntosh, J.R. (2000). Tea2p is a kinesin-like protein required to generate polarized growth in fission yeast. J Cell Biol *151*, 15-28.

Brunner, D., and Nurse, P. (2000). CLIP170-like tip1p spatially organizes microtubular dynamics in fission yeast. Cell *102*, 695-704.

Bu, W., and Su, L.K. (2003). Characterization of functional domains of human EB1 family proteins. J Biol Chem *278*, 49721-49731.

Bullitt, E., Rout, M.P., Kilmartin, J.V., and Akey, C.W. (1997). The yeast spindle pole body is assembled around a central crystal of Spc42p. Cell *89*, 1077-1086.

Busch, K.E., Hayles, J., Nurse, P., and Brunner, D. (2004). Tea2p kinesin is involved in spatial microtubule organization by transporting tip1p on microtubules. Dev Cell *6*, 831-843.

Buvelot, S., Tatsutani, S.Y., Vermaak, D., and Biggins, S. (2003). The budding yeast Ipl1/Aurora protein kinase regulates mitotic spindle disassembly. J Cell Biol *160*, 329-339.

Caldwell, C.M., and Kaplan, K.B. (2009). The role of APC in mitosis and in chromosome instability. Adv Exp Med Biol *656*, 51-64.

Camacho, C., Madden, T., and Ma, N., et al. (2008). BLAST Command Line Applications User Manual. BLAST® Help

Carbon, S., Ireland, A., Mungall, C.J., Shu, S., Marshall, B., and Lewis, S. (2009). AmiGO: online access to ontology and annotation data. Bioinformatics *25*, 288-289.

Carvalho, P., Gupta, M.L., Jr., Hoyt, M.A., and Pellman, D. (2004). Cell cycle control of kinesin-mediated transport of Bik1 (CLIP-170) regulates microtubule stability and dynein activation. Dev Cell *6*, 815-829.

Casselton, L.A., and Olesnicky, N.S. (1998). Molecular genetics of mating recognition in basidiomycete fungi. Microbiol Mol Biol Rev *62*, 55-70.

Cassimeris, L. (2002). The oncoprotein 18/stathmin family of microtubule destabilizers. Curr Opin Cell Biol *14*, 18-24.

Castresana, J., and Saraste, M. (1995). Does Vav bind to F-actin through a CH domain? FEBS Lett *374*, 149-151.

Caudron, F., Denarier, E., Thibout-Quintana, J.C., Brocard, J., Andrieux, A., and Fourest-Lieuvin, A. (2010). Mutation of Ser172 in yeast beta tubulin induces defects in microtubule dynamics and cell division. PLoS One *5*, e13553.

Cerqueira, G.C., Arnaud, M.B., Inglis, D.O., Skrzypek, M.S., Binkley, G., Simison, M., Miyasato, S.R., Binkley, J., Orvis, J., Shah, P.*, et al.* (2014). The *Aspergillus* Genome Database: multispecies curation and incorporation of RNA-Seq data to improve structural gene annotations. Nucleic Acids Res *42*, D705-710.

Chan, C.S., and Botstein, D. (1993). Isolation and characterization of chromosome-gain and increase-in-ploidy mutants in yeast. Genetics *135*, 677-691.

Charrasse, S., Schroeder, M., Gauthier-Rouviere, C., Ango, F., Cassimeris, L., Gard, D.L., and Larroque, C. (1998). The TOGp protein is a new human microtubule-associated protein homologous to the Xenopus XMAP215. J Cell Sci *111 (Pt 10)*, 1371-1383.

Cheeseman, I.M., Enquist-Newman, M., Muller-Reichert, T., Drubin, D.G., and Barnes, G. (2001). Mitotic spindle integrity and kinetochore function linked by the Duo1p/Dam1p complex. J Cell Biol *152*, 197-212.

Chen, J.S., Lu, L.X., Ohi, M.D., Creamer, K.M., English, C., Partridge, J.F., Ohi, R., and Gould, K.L. (2011). Cdk1 phosphorylation of the kinetochore protein Nsk1 prevents error-prone chromosome segregation. J Cell Biol *195*, 583-593.

Chen, P., Gao, R., Chen, S., Pu, L., Li, P., Huang, Y., and Lu, L. (2012). A pericentrin-related protein homolog in Aspergillus nidulans plays important roles in nucleus positioning and cell polarity by affecting microtubule organization. Eukaryot Cell *11*, 1520-1530.

Chen, X., Sullivan, D.S., and Huffaker, T.C. (1994). Two yeast genes with similarity to TCP-1 are required for microtubule and actin function *in vivo*. Proc Natl Acad Sci U S A *91*, 9111-9115.

Cheng, Z., Snustad, D.P., and Carter, J.V. (2001). Temporal and spatial expression patterns of TUB9, a beta-tubulin gene of *Arabidopsis thaliana*. Plant Mol Biol *47*, 389-398.

Cherry, J.M., Hong, E.L., Amundsen, C., Balakrishnan, R., Binkley, G., Chan, E.T., Christie, K.R., Costanzo, M.C., Dwight, S.S., Engel, S.R.*, et al.* (2012). Saccharomyces Genome Database: the genomics resource of budding yeast. Nucleic Acids Res *40*, 21.

Chikashige, Y., Tsutsumi, C., Yamane, M., Okamasa, K., Haraguchi, T., and Hiraoka, Y. (2006). Meiotic proteins bqt1 and bqt2 tether telomeres to form the bouquet arrangement of chromosomes. Cell *125*, 59-69.

Chiu, Y.H., Xiang, X., Dawe, A.L., and Morris, N.R. (1997). Deletion of nudC, a nuclear migration gene of *Aspergillus nidulans*, causes morphological and cell wall abnormalities and is lethal. Mol Biol Cell *8*, 1735-1749.

Ciani, L., Krylova, O., Smalley, M.J., Dale, T.C., and Salinas, P.C. (2004). A divergent canonical WNT-signaling pathway regulates microtubule dynamics: dishevelled signals locally to stabilize microtubules. J Cell Biol *164*, 243-253.

Coates, J.C. (2003). Armadillo repeat proteins: beyond the animal kingdom. Trends Cell Biol *13*, 463-471.

Collins, C.A., and Vallee, R.B. (1989). Preparation of microtubules from rat liver and testis: cytoplasmic dynein is a major microtubule associated protein. Cell Motil Cytoskeleton *14*, 491-500.

Cooper, G.M. (2000a). In The Cell: A Molecular Approach (Sunderland (MA): Sinauer Associates).

Cooper, G.M. (2000b). The cell : a molecular approach, 2nd edn (Washington, D.C.Sunderland, Mass., ASM Press ;Sinauer Associates).

Cottingham, F.R., Gheber, L., Miller, D.L., and Hoyt, M.A. (1999). Novel roles for *Saccharomyces cerevisiae* mitotic spindle motors. J Cell Biol *147*, 335-350.

Cui, H., Ghosh, S.K., and Jayaram, M. (2009). The selfish yeast plasmid uses the nuclear motor Kip1p but not Cin8p for its localization and equal segregation. J Cell Biol *185*, 251-264.

Cui, W., Sproul, L.R., Gustafson, S.M., Matthies, H.J., Gilbert, S.P., and Hawley, R.S. (2005). *Drosophila* Nod protein binds preferentially to the plus ends of microtubules and promotes microtubule polymerization *in vitro*. Mol Biol Cell *16*, 5400-5409.

Cuschieri, L., Miller, R., and Vogel, J. (2006). Gamma-tubulin is required for proper recruitment and assembly of Kar9-Bim1 complexes in budding yeast. Mol Biol Cell *17*, 4420-4434.

Daniels, M.J.E., Downie, J.A.E., and Osbourn, A.E.E. (1994). Advances in molecular genetics of plant-microbe interactions : 7th International symposium on molecular plant-microbe interactions : Papers. Vol 3 (Kluwer Academic).

de Forges, H., Bouissou, A., and Perez, F. (2012). Interplay between microtubule dynamics and intracellular organization. The International Journal of Biochemistry & Cell Biology *44*, 266-274.

Dehmelt, L., and Halpain, S. (2005). The MAP2/Tau family of microtubule-associated proteins. Genome Biol *6*, 204.

Desai, A., and Mitchison, T.J. (1997). Microtubule polymerization dynamics. Annu Rev Cell Dev Biol *13*, 83-117.

Djamei, A., and Kahmann, R. (2012). *Ustilago maydis*: dissecting the molecular interface between pathogen and plant. PLoS Pathog *8*, e1002955.

Djamei, A., Schipper, K., Rabe, F., Ghosh, A., Vincon, V., Kahnt, J., Osorio, S., Tohge, T., Fernie, A.R., Feussner, I.*, et al.* (2011). Metabolic priming by a secreted fungal effector. Nature *478*, 395-398.

Dobyns, W.B. (1987). Developmental aspects of lissencephaly and the lissencephaly syndromes. Birth Defects Orig Artic Ser *23*, 225-241.

Donaldson, M.E., and Saville, B.J. (2008). Bioinformatic identification of *Ustilago maydis* meiosis genes. Fungal Genet Biol *45 Suppl 1*, S47-53.

Dougherty, G.W., Adler, H.J., Rzadzinska, A., Gimona, M., Tomita, Y., Lattig, M.C., Merritt, R.C., Jr., and Kachar, B. (2005). CLAMP, a novel microtubule-associated protein with EB-type calponin homology. Cell Motil Cytoskeleton *62*, 141-156.

Drechsel, D.N., Hyman, A.A., Cobb, M.H., and Kirschner, M.W. (1992). Modulation of the dynamic instability of tubulin assembly by the microtubule-associated protein tau. Mol Biol Cell *3*, 1141-1154.

Dunsch, A.K., Linnane, E., Barr, F.A., and Gruneberg, U. (2011). The astrin-kinastrin/SKAP complex localizes to microtubule plus ends and facilitates chromosome alignment. J Cell Biol *192*, 959-968.

Dutcher, S.K. (2003). Long-lost relatives reappear: identification of new members of the tubulin superfamily. Curr Opin Microbiol *6*, 634-640.

Efimov, A., Kharitonov, A., Efimova, N., Loncarek, J., Miller, P.M., Andreyeva, N., Gleeson, P., Galjart, N., Maia, A.R., McLeod, I.X.*, et al.* (2007). Asymmetric CLASP-dependent nucleation of noncentrosomal microtubules at the trans-Golgi network. Dev Cell *12*, 917-930.

Egan, M.J., McClintock, M.A., and Reck-Peterson, S.L. (2012). Microtubule-based transport in filamentous fungi. Curr Opin Microbiol *15*, 637-645.

Elliott, S., Knop, M., Schlenstedt, G., and Schiebel, E. (1999). Spc29p is a component of the Spc110p subcomplex and is essential for spindle pole body duplication. Proc Natl Acad Sci U S A *96*, 6205-6210.

Endow, S.A., Kang, S.J., Satterwhite, L.L., Rose, M.D., Skeen, V.P., and Salmon, E.D. (1994). Yeast Kar3 is a minus-end microtubule motor protein that destabilizes microtubules preferentially at the minus ends. EMBO J *13*, 2708-2713.

Enquist-Newman, M., Cheeseman, I.M., Van Goor, D., Drubin, D.G., Meluh, P.B., and Barnes, G. (2001). Dad1p, third component of the Duo1p/Dam1p complex involved in kinetochore function and mitotic spindle integrity. Mol Biol Cell *12*, 2601-2613.

Erickson, H.P. (2000). Gamma-tubulin nucleation: template or protofilament? Nat Cell Biol *2*, E93-96.

Evans, K.J., Gomes, E.R., Reisenweber, S.M., Gundersen, G.G., and Lauring, B.P. (2005). Linking axonal degeneration to microtubule remodeling by Spastin-mediated microtubule severing. J Cell Biol *168*, 599-606.

Fabre-Jonca, N., Viard, I., French, L.E., and Masson, D. (1999). Upregulation and redistribution of E-MAP-115 (epithelial microtubule-associated protein of 115 kDa) in terminally differentiating keratinocytes is coincident with the formation of intercellular contacts. J Invest Dermatol *112*, 216-225.

Farkasovsky, M., and Kuntzel, H. (2001). Cortical Num1p interacts with the dynein intermediate chain Pac11p and cytoplasmic microtubules in budding yeast. J Cell Biol *152*, 251-262.

Feierbach, B., Nogales, E., Downing, K.H., and Stearns, T. (1999). Alf1p, a CLIP-170 domain-containing protein, is functionally and physically associated with alpha-tubulin. J Cell Biol *144*, 113-124.

Feldbrugge, M., Kamper, J., Steinberg, G., and Kahmann, R. (2004). Regulation of mating and pathogenic development in *Ustilago maydis*. Curr Opin Microbiol *7*, 666-672.

Fiechter, V., Cameroni, E., Cerutti, L., De Virgilio, C., Barral, Y., and Fankhauser, C. (2008). The evolutionary conserved BER1 gene is involved in microtubule stability in yeast. Curr Genet *53*, 107-115.

Finn, R.D., Clements, J., and Eddy, S.R. (2011). HMMER web server: interactive sequence similarity searching. Nucleic Acids Res *39*, W29-37.

Finn, R.D., Mistry, J., Schuster-Bockler, B., Griffiths-Jones, S., Hollich, V., Lassmann, T., Moxon, S., Marshall, M., Khanna, A., Durbin, R.*, et al.* (2006). Pfam: clans, web tools and services. Nucleic Acids Res *34*, D247-251.

Fletcher, D.A., and Mullins, R.D. (2010). Cell mechanics and the cytoskeleton. Nature *463*, 485-492.

Folker, E.S., Baker, B.M., and Goodson, H.V. (2005). Interactions between CLIP-170, tubulin, and microtubules: implications for the mechanism of Clip-170 plus-end tracking behavior. Mol Biol Cell *16*, 5373-5384.

Fong, K.W., Hau, S.Y., Kho, Y.S., Jia, Y., He, L., and Qi, R.Z. (2009). Interaction of CDK5RAP2 with EB1 to track growing microtubule tips and to regulate microtubule dynamics. Mol Biol Cell *20*, 3660-3670.

Fong, K.W., Leung, J.W., Li, Y., Wang, W., Feng, L., Ma, W., Liu, D., Songyang, Z., and Chen, J. (2013). MTR120/KIAA1383, a novel microtubule-associated protein, promotes microtubule stability and ensures cytokinesis. J Cell Sci *126*, 825-837.

Forman, M.S., Trojanowski, J.Q., and Lee, V.M. (2004). Neurodegenerative diseases: a decade of discoveries paves the way for therapeutic breakthroughs. Nat Med *10*, 1055-1063.

Fourest-Lieuvin, A., Peris, L., Gache, V., Garcia-Saez, I., Juillan-Binard, C., Lantez, V., and Job, D. (2006). Microtubule regulation in mitosis: tubulin phosphorylation by the cyclin-dependent kinase Cdk1. Mol Biol Cell *17*, 1041-1050.

Francisco, L., Wang, W., and Chan, C.S. (1994). Type 1 protein phosphatase acts in opposition to IpL1 protein kinase in regulating yeast chromosome segregation. Mol Cell Biol *14*, 4731-4740.

Franco, A., Meadows, J.C., and Millar, J.B. (2007). The Dam1/DASH complex is required for the retrieval of unclustered kinetochores in fission yeast. J Cell Sci *120*, 3345-3351.

Freedman, H., Luchko, T., Luduena, R.F., and Tuszynski, J.A. (2011). Molecular dynamics modeling of tubulin C-terminal tail interactions with the microtubule surface. Proteins *79*, 2968-2982.

Freitag, J., Lanver, D., Bohmer, C., Schink, K.O., Bolker, M., and Sandrock, B. (2011). Septation of infectious hyphae is critical for appressoria formation and virulence in the smut fungus *Ustilago maydis*. PLoS Pathog *7*, e1002044.

Fuchs, U., Hause, G., Schuchardt, I., and Steinberg, G. (2006). Endocytosis is essential for pathogenic development in the corn smut fungus *Ustilago maydis*. Plant Cell *18*, 2066-2081.

Fuchs, U., Manns, I., and Steinberg, G. (2005). Microtubules are dispensable for the initial pathogenic development but required for long-distance hyphal growth in the corn smut fungus *Ustilago maydis*. Mol Biol Cell *16*, 2746-2758.

Fujita, A., Vardy, L., Garcia, M.A., and Toda, T. (2002). A fourth component of the fission yeast gamma-tubulin complex, Alp16, is required for cytoplasmic microtubule integrity and becomes indispensable when gamma-tubulin function is compromised. Mol Biol Cell *13*, 2360-2373.

Fujiwara, T., Tanaka, K., Inoue, E., Kikyo, M., and Takai, Y. (1999). Bni1p regulates microtubule-dependent nuclear migration through the actin cytoskeleton in *Saccharomyces cerevisiae*. Mol Cell Biol *19*, 8016-8027.

Ganem, N.J., and Compton, D.A. (2004). The KinI kinesin Kif2a is required for bipolar spindle assembly through a functional relationship with MCAK. J Cell Biol *166*, 473-478.

Ganem, N.J., Upton, K., and Compton, D.A. (2005). Efficient mitosis in human cells lacking poleward microtubule flux. Curr Biol *15*, 1827-1832.

Gao, J., Sun, L., Huo, L., Liu, M., Li, D., and Zhou, J. (2010). CYLD regulates angiogenesis by mediating vascular endothelial cell migration. Blood *115*, 4130-4137.

Garcia-Muse, T., Steinberg, G., and Perez-Martin, J. (2003). Pheromone-induced G2 arrest in the phytopathogenic fungus *Ustilago maydis*. Eukaryot Cell *2*, 494-500.

García-Pedrajas, M.D., Baeza-Montañez, L., and Gold, S.E. (2010). Regulation of *Ustilago maydis* Dimorphism, Sporulation, and Pathogenic Development by a Transcription Factor with a Highly Conserved APSES Domain. Molecular Plant-Microbe Interactions *23*, 211-222.

Gard, D.L., and Kirschner, M.W. (1987). A microtubule-associated protein from *Xenopus* eggs that specifically promotes assembly at the plus-end. J Cell Biol *105*, 2203-2215.

Gardiner, J. (2013). The evolution and diversification of plant microtubule-associated proteins. Plant J *75*, 219-229.

Gardner, M.K., Charlebois, B.D., Janosi, I.M., Howard, J., Hunt, A.J., and Odde, D.J. (2011). Rapid microtubule self-assembly kinetics. Cell *146*, 582-592.

Gassmann, R., Essex, A., Hu, J.S., Maddox, P.S., Motegi, F., Sugimoto, A., O'Rourke, S.M., Bowerman, B., McLeod, I., Yates, J.R., 3rd*, et al.* (2008). A new mechanism controlling kinetochore-microtubule interactions revealed by comparison of two dynein-targeting components: SPDL-1 and the Rod/Zwilch/Zw10 complex. Genes Dev *22*, 2385-2399.

Geer, L.Y., Marchler-Bauer, A., Geer, R.C., Han, L., He, J., He, S., Liu, C., Shi, W., and Bryant, S.H. (2010). The NCBI BioSystems database. Nucleic Acids Res *38*, D492-496.

Geitmann, A., and Emons, A.M. (2000). The cytoskeleton in plant and fungal cell tip growth. J Microsc *198*, 218-245.

Gibbons, I.R. (1963). Studies on the Protein Components of Cilia from *Tetrahymena Pyriformis*. Proc Natl Acad Sci U S A *50*, 1002-1010.

Gibbons, I.R. (1965). Chemical dissection of cilia. Arch Biol (Liege) *76*, 317-352.

Gibbons, I.R., and Rowe, A.J. (1965). Dynein: A Protein with Adenosine Triphosphatase Activity from Cilia. Science *149*, 424-426.

Gillissen, B., Bergemann, J., Sandmann, C., Schroeer, B., Bolker, M., and Kahmann, R. (1992). A two-component regulatory system for self/non-self recognition in *Ustilago maydis*. Cell *68*, 647-657.

Gimona, M., Djinovic-Carugo, K., Kranewitter, W.J., and Winder, S.J. (2002). Functional plasticity of CH domains. FEBS Lett *513*, 98-106.

Goodwin, S.S., and Vale, R.D. (2010). Patronin regulates the microtubule network by protecting microtubule minus ends. Cell *143*, 263-274.

Goriounov, D., Leung, C.L., and Liem, R.K. (2003). Protein products of human Gas2-related genes on chromosomes 17 and 22 (hGAR17 and hGAR22) associate with both microfilaments and microtubules. J Cell Sci *116*, 1045-1058.

Goshima, G. (2011). Identification of a TPX2-like microtubule-associated protein in *Drosophila*. PLoS One *6*, e28120.

Goshima, G., Wollman, R., Goodwin, S.S., Zhang, N., Scholey, J.M., Vale, R.D., and Stuurman, N. (2007). Genes required for mitotic spindle assembly in *Drosophila* S2 cells. Science *316*, 417-421.

Goujon, M., McWilliam, H., Li, W., Valentin, F., Squizzato, S., Paern, J., and Lopez, R. (2010). A new bioinformatics analysis tools framework at EMBL-EBI. Nucleic Acids Res *38*, W695-699.

Grallert, A., Beuter, C., Craven, R.A., Bagley, S., Wilks, D., Fleig, U., and Hagan, I.M. (2006). S. pombe CLASP needs dynein, not EB1 or CLIP170, to induce microtubule instability and slows polymerization rates at cell tips in a dynein-dependent manner. Genes Dev *20*, 2421-2436.

Grintsevich, E.E., Galkin, V.E., Orlova, A., Ytterberg, A.J., Mikati, M.M., Kudryashov, D.S., Loo, J.A., Egelman, E.H., and Reisler, E. (2010). Mapping of drebrin binding site on F-actin. J Mol Biol *398*, 542-554.

Groves, M.R., Hanlon, N., Turowski, P., Hemmings, B.A., and Barford, D. (1999). The structure of the protein phosphatase 2A PR65/A subunit reveals the conformation of its 15 tandemly repeated HEAT motifs. Cell *96*, 99-110.

Grutzmann, K., Szafranski, K., Pohl, M., Voigt, K., Petzold, A., and Schuster, S. (2013). Fungal Alternative Splicing is Associated with Multicellular Complexity and Virulence: A Genome-Wide Multi-Species Study. DNA Res.

Gupta, M.L., Jr., Carvalho, P., Roof, D.M., and Pellman, D. (2006). Plus end-specific depolymerase activity of Kip3, a kinesin-8 protein, explains its role in positioning the yeast mitotic spindle. Nat Cell Biol *8*, 913-923.

Gupta, T., Marlow, F.L., Ferriola, D., Mackiewicz, K., Dapprich, J., Monos, D., and Mullins, M.C. (2010). Microtubule actin crosslinking factor 1 regulates the

Balbiani body and animal-vegetal polarity of the zebrafish oocyte. PLoS Genet *6*, e1001073.

Hanson, J., and Huxley, H.E. (1953). Structural basis of the cross-striations in muscle. Nature *172*, 530-532.

Hartman, J.J., Mahr, J., McNally, K., Okawa, K., Iwamatsu, A., Thomas, S., Cheesman, S., Heuser, J., Vale, R.D., and McNally, F.J. (1998). Katanin, a microtubule-severing protein, is a novel AAA ATPase that targets to the centrosome using a WD40-containing subunit. Cell *93*, 277-287.

Hartman, J.J., and Vale, R.D. (1999). Microtubule disassembly by ATP-dependent oligomerization of the AAA enzyme katanin. Science *286*, 782-785.

Hashimoto, T. (2013). Dissecting the cellular functions of plant microtubules using mutant tubulins. Cytoskeleton (Hoboken) *70*, 191-200.

Hatzfeld, M. (1999). The armadillo family of structural proteins. Int Rev Cytol *186*, 179-224.

Hayashi, I., and Ikura, M. (2003). Crystal structure of the amino-terminal microtubule-binding domain of end-binding protein 1 (EB1). J Biol Chem *278*, 36430-36434.

Hayashi, I., Wilde, A., Mal, T.K., and Ikura, M. (2005). Structural basis for the activation of microtubule assembly by the EB1 and p150Glued complex. Mol Cell *19*, 449-460.

Hazan, J., Fonknechten, N., Mavel, D., Paternotte, C., Samson, D., Artiguenave, F., Davoine, C.S., Cruaud, C., Durr, A., Wincker, P.*, et al.* (1999). Spastin, a new AAA protein, is altered in the most frequent form of autosomal dominant spastic paraplegia. Nat Genet *23*, 296-303.

Heath, I.B. (1995). The cytoskeleton. In The Growing Fungus (ed. N. A. R.Gow and G. M. Gadd), . London: Chapman & Hall., pp. 99-134.

Helmstaedt, K., Laubinger, K., Vosskuhl, K., Bayram, O., Busch, S., Hoppert, M., Valerius, O., Seiler, S., and Braus, G.H. (2008). The nuclear migration protein NUDF/LIS1 forms a complex with NUDC and BNFA at spindle pole bodies. Eukaryot Cell *7*, 1041-1052.

Hemetsberger, C., Herrberger, C., Zechmann, B., Hillmer, M., and Doehlemann, G. (2012). The *Ustilago maydis* effector Pep1 suppresses plant immunity by inhibition of host peroxidase activity. PLoS Pathog *8*, e1002684.

Hemetsberger, C.F. (2008). Entwicklung eines Mutantenscreens zur Identifikation von Komponenten des mikrotubuliabhängigen Langstreckentransports in Hyphen von *Ustilago maydis.* In Faculty of Biology (Marburg, Philipps-Universität Marburg), pp. 71.

Hirokawa, N., Niwa, S., and Tanaka, Y. (2010). Molecular motors in neurons: transport mechanisms and roles in brain function, development, and disease. Neuron *68*, 610-638.

Hlavanda, E., Klement, E., Kokai, E., Kovacs, J., Vincze, O., Tokesi, N., Orosz, F., Medzihradszky, K.F., Dombradi, V., and Ovadi, J. (2007). Phosphorylation blocks the activity of tubulin polymerization-promoting protein (TPPP): identification of sites targeted by different kinases. J Biol Chem *282*, 29531-29539.

Hlavanda, E., Kovacs, J., Olah, J., Orosz, F., Medzihradszky, K.F., and Ovadi, J. (2002). Brain-specific p25 protein binds to tubulin and microtubules and induces aberrant microtubule assemblies at substoichiometric concentrations. Biochemistry *41*, 8657-8664.

Ho, E.C., Cahill, M.J., and Saville, B.J. (2007). Gene discovery and transcript analyses in the corn smut pathogen Ustilago maydis: expressed sequence tag and genome sequence comparison. BMC Genomics *8*, 334.

Hoepfner, D., Schaerer, F., Brachat, A., Wach, A., and Philippsen, P. (2002). Reorientation of mispositioned spindles in short astral microtubule mutant

spc72Delta is dependent on spindle pole body outer plaque and Kar3 motor protein. Mol Biol Cell *13*, 1366-1380.

Hoffman, C.S., and Winston, F. (1987). A ten-minute DNA preparation from yeast efficiently releases autonomous plasmids for transformation of *Escherichia coli*. Gene *57*, 267-272.

Holliday, R. (1974). *Ustilago maydis*. In Handbook of genetics, R.C. King, ed. (New York, Plenum Press), pp. 575-595.

Holliday, R. (1975). Further evidence for an inducible recombination repair system in *Ustilago maydis.* Mutat Res *29*, 149-153.

Honnappa, S., Gouveia, S.M., Weisbrich, A., Damberger, F.F., Bhavesh, N.S., Jawhari, H., Grigoriev, I., van Rijssel, F.J., Buey, R.M., Lawera, A.*, et al.* (2009). An EB1-binding motif acts as a microtubule tip localization signal. Cell *138*, 366-376.

Hook, P., and Vallee, R.B. (2006). The dynein family at a glance. J Cell Sci *119*, 4369-4371.

Horesh, D., Sapir, T., Francis, F., Wolf, S.G., Caspi, M., Elbaum, M., Chelly, J., and Reiner, O. (1999). Doublecortin, a stabilizer of microtubules. Hum Mol Genet *8*, 1599-1610.

Horio, T. (2007). Role of microtubules in tip growth of fungi. J Plant Res *120*, 53-60.

Howard, J., and Hyman, A.A. (2007). Microtubule polymerases and depolymerases. Curr Opin Cell Biol *19*, 31-35.

Howell, B., Larsson, N., Gullberg, M., and Cassimeris, L. (1999). Dissociation of the tubulin-sequestering and microtubule catastrophe-promoting activities of oncoprotein 18/stathmin. Mol Biol Cell *10*, 105-118.

Hoyt, M.A., He, L., Loo, K.K., and Saunders, W.S. (1992). Two *Saccharomyces cerevisiae* kinesin-related gene products required for mitotic spindle assembly. J Cell Biol *118*, 109-120.

Hoyt, M.A., Macke, J.P., Roberts, B.T., and Geiser, J.R. (1997). Saccharomyces cerevisiae PAC2 functions with CIN1, 2 and 4 in a pathway leading to normal microtubule stability. Genetics *146*, 849-857.

Huang, Y., Wang, W., Yao, P., Wang, X., Liu, X., Zhuang, X., Yan, F., Zhou, J., Du, J., Ward, T.*, et al.* (2012). CENP-E kinesin interacts with SKAP protein to orchestrate accurate chromosome segregation in mitosis. J Biol Chem *287*, 1500-1509.

Huber, G., and Matus, A. (1984). Differences in the cellular distributions of two microtubule-associated proteins, MAP1 and MAP2, in rat brain. J Neurosci *4*, 151-160.

Hughes, J.R., Meireles, A.M., Fisher, K.H., Garcia, A., Antrobus, P.R., Wainman, A., Zitzmann, N., Deane, C., Ohkura, H., and Wakefield, J.G. (2008). A microtubule interactome: complexes with roles in cell cycle and mitosis. PLoS Biol *6*, e98.

Huisman, S.M., Bales, O.A., Bertrand, M., Smeets, M.F., Reed, S.I., and Segal, M. (2004). Differential contribution of Bud6p and Kar9p to microtubule capture and spindle orientation in S. cerevisiae. J Cell Biol *167*, 231-244.

Hung, L.Y., Chen, H.L., Chang, C.W., Li, B.R., and Tang, T.K. (2004). Identification of a novel microtubule-destabilizing motif in CPAP that binds to tubulin heterodimers and inhibits microtubule assembly. Mol Biol Cell *15*, 2697-2706.

Hung, L.Y., Tang, C.J., and Tang, T.K. (2000). Protein 4.1 R-135 interacts with a novel centrosomal protein (CPAP) which is associated with the gamma-tubulin complex. Mol Cell Biol *20*, 7813-7825.

Hunter, A.W., and Wordeman, L. (2000). How motor proteins influence microtubule polymerization dynamics. J Cell Sci *113 Pt 24*, 4379-4389.

Hunter, S., Jones, P., Mitchell, A., Apweiler, R., Attwood, T.K., Bateman, A., Bernard, T., Binns, D., Bork, P., Burge, S.*, et al.* (2012). InterPro in 2011: new developments in the family and domain prediction database. Nucleic Acids Res *40*, D306-312.

Hutton, M., Lendon, C.L., Rizzu, P., Baker, M., Froelich, S., Houlden, H., Pickering-Brown, S., Chakraverty, S., Isaacs, A., Grover, A.*, et al.* (1998). Association of missense and 5'-splice-site mutations in tau with the inherited dementia FTDP-17. Nature *393*, 702-705.

Huxley, H.E. (1953). X-ray analysis and the problem of muscle. Proc R Soc Lond B Biol Sci *141*, 59-62.

Huxley, H.E. (1957). The double array of filaments in cross-striated muscle. J Biophys Biochem Cytol *3*, 631-648.

Interthal, H., Bellocq, C., Bahler, J., Bashkirov, V.I., Edelstein, S., and Heyer, W.D. (1995). A role of Sep1 (= Kem1, Xrn1) as a microtubule-associated protein in *Saccharomyces cerevisiae*. EMBO J *14*, 1057-1066.

Irminger-Finger, I., and Mathis, N. (1998). Effect of microtubule-associated protein MHP1 on microtubule assembly and cell cycle progression in *Saccharomyces cerevisiae.* Cell Struct Funct *23*, 209-219.

Iyer, L.M., Koonin, E.V., and Aravind, L. (2003). Evolutionary connection between the catalytic subunits of DNA-dependent RNA polymerases and eukaryotic RNA-dependent RNA polymerases and the origin of RNA polymerases. BMC Struct Biol *3*, 1.

Jang, C.Y., Wong, J., Coppinger, J.A., Seki, A., Yates, J.R., 3rd, and Fang, G. (2008). DDA3 recruits microtubule depolymerase Kif2a to spindle poles and

controls spindle dynamics and mitotic chromosome movement. J Cell Biol *181*, 255-267.

Janke, C. (2014). The tubulin code: Molecular components, readout mechanisms, and functions. J Cell Biol *206*, 461-472.

Janke, C., and Bulinski, J.C. (2011). Post-translational regulation of the microtubule cytoskeleton: mechanisms and functions. Nat Rev Mol Cell Biol *12*, 773-786.

Jiang, K., and Akhmanova, A. (2011). Microtubule tip-interacting proteins: a view from both ends. Curr Opin Cell Biol *23*, 94-101.

Jiang, K., Hua, S., Mohan, R., Grigoriev, I., Yau, K.W., Liu, Q., Katrukha, E.A., Altelaar, A.F., Heck, A.J., Hoogenraad, C.C.*, et al.* (2014). Microtubule minus-end stabilization by polymerization-driven CAMSAP deposition. Dev Cell *28*, 295-309.

Johmura, Y., Soung, N.K., Park, J.E., Yu, L.R., Zhou, M., Bang, J.K., Kim, B.Y., Veenstra, T.D., Erikson, R.L., and Lee, K.S. (2011). Regulation of microtubule-based microtubule nucleation by mammalian polo-like kinase 1. Proc Natl Acad Sci U S A *108*, 11446-11451.

Kahmann, R., and Kämper, J. (2004). Ustilago maydis: how its biology relates to pathogenic development. New Phytologist *164*, 31-42.

Kahmann, R., Romeis, T., Bolker, M., and Kamper, J. (1995). Control of mating and development in *Ustilago maydis*. Curr Opin Genet Dev *5*, 559-564.

Kamper, J., Kahmann, R., Bolker, M., Ma, L.J., Brefort, T., Saville, B.J., Banuett, F., Kronstad, J.W., Gold, S.E., Muller, O.*, et al.* (2006). Insights from the genome of the biotrophic fungal plant pathogen *Ustilago maydis*. Nature *444*, 97-101.

Kang, J., Cheeseman, I.M., Kallstrom, G., Velmurugan, S., Barnes, G., and Chan, C.S. (2001). Functional cooperation of Dam1, Ipl1, and the inner centromere protein (INCENP)-related protein Sli15 during chromosome segregation. J Cell Biol *155*, 763-774.

Karpova, N., Bobinnec, Y., Fouix, S., Huitorel, P., and Debec, A. (2006). Jupiter, a new *Drosophila* protein associated with microtubules. Cell Motil Cytoskeleton *63*, 301-312.

Katayama, H., Zhou, H., Li, Q., Tatsuka, M., and Sen, S. (2001). Interaction and feedback regulation between STK15/BTAK/Aurora-A kinase and protein phosphatase 1 through mitotic cell division cycle. J Biol Chem *276*, 46219-46224.

Katoh, K., Asimenos, G., and Toh, H. (2009). Multiple alignment of DNA sequences with MAFFT. Methods Mol Biol *537*, 39-64.

Katoh, K., and Frith, M.C. (2012). Adding unaligned sequences into an existing alignment using MAFFT and LAST. Bioinformatics *28*, 3144-3146.

Katoh, K., Kuma, K., Toh, H., and Miyata, T. (2005). MAFFT version 5: improvement in accuracy of multiple sequence alignment. Nucleic Acids Res *33*, 511-518.

Katoh, K., Misawa, K., Kuma, K., and Miyata, T. (2002). MAFFT: a novel method for rapid multiple sequence alignment based on fast Fourier transform. Nucleic Acids Res *30*, 3059-3066.

Katoh, K., and Standley, D.M. (2013). MAFFT multiple sequence alignment software version 7: improvements in performance and usability. Mol Biol Evol *30*, 772-780.

Katoh, K., and Toh, H. (2007). PartTree: an algorithm to build an approximate tree from a large number of unaligned sequences. Bioinformatics *23*, 372-374.

Katoh, K., and Toh, H. (2008a). Improved accuracy of multiple ncRNA alignment by incorporating structural information into a MAFFT-based framework. BMC Bioinformatics *9*, 212.

Katoh, K., and Toh, H. (2008b). Recent developments in the MAFFT multiple sequence alignment program. Brief Bioinform *9*, 286-298.

Katoh, K., and Toh, H. (2010). Parallelization of the MAFFT multiple sequence alignment program. Bioinformatics *26*, 1899-1900.

Keates, R.A., and Hall, R.H. (1975). Tubulin requires an accessory protein for self assembly in microtubules. Nature *257*, 418-421.

Keating, T.J., Peloquin, J.G., Rodionov, V.I., Momcilovic, D., and Borisy, G.G. (1997). Microtubule release from the centrosome. Proc Natl Acad Sci U S A *94*, 5078-5083.

Kerres, A., Jakopec, V., Beuter, C., Karig, I., Pohlmann, J., Pidoux, A., Allshire, R., and Fleig, U. (2006). Fta2, an essential fission yeast kinetochore component, interacts closely with the conserved Mal2 protein. Mol Biol Cell *17*, 4167-4178.

Keskin, O., Durell, S.R., Bahar, I., Jernigan, R.L., and Covell, D.G. (2002). Relating molecular flexibility to function: a case study of tubulin. Biophys J *83*, 663-680.

Keyes, B.E., and Burke, D.J. (2009). Irc15 Is a microtubule-associated protein that regulates microtubule dynamics in *Saccharomyces cerevisiae*. Curr Biol *19*, 472-478.

Kilmartin, J.V. (1981). Purification of yeast tubulin by self-assembly in vitro. Biochemistry *20*, 3629-3633.

Kiris, E., Ventimiglia, D., and Feinstein, S.C. (2010). Quantitative analysis of MAP-mediated regulation of microtubule dynamic instability in vitro focus on Tau. Methods Cell Biol *95*, 481-503.

Kirk, K.E., and Morris, N.R. (1993). Either alpha-tubulin isogene product is sufficient for microtubule function during all stages of growth and differentiation in *Aspergillus nidulans*. Mol Cell Biol *13*, 4465-4476.

Kita, K., Wittmann, T., Nathke, I.S., and Waterman-Storer, C.M. (2006). Adenomatous polyposis coli on microtubule plus ends in cell extensions can promote microtubule net growth with or without EB1. Mol Biol Cell *17*, 2331-2345.

Kitamura, E., Tanaka, K., Komoto, S., Kitamura, Y., Antony, C., and Tanaka, T.U. (2010). Kinetochores generate microtubules with distal plus ends: their roles and limited lifetime in mitosis. Dev Cell *18*, 248-259.

Kitazawa, H., Iida, J., Uchida, A., Haino-Fukushima, K., Itoh, T.J., Hotani, H., Ookata, K., Murofushi, H., Bulinski, J.C., Kishimoto, T.*, et al.* (2000). Ser787 in the proline-rich region of human MAP4 is a critical phosphorylation site that reduces its activity to promote tubulin polymerization. Cell Struct Funct *25*, 33-39.

Kiyomitsu, T., Obuse, C., and Yanagida, M. (2007). Human Blinkin/AF15q14 is required for chromosome alignment and the mitotic checkpoint through direct interaction with Bub1 and BubR1. Dev Cell *13*, 663-676.

Kline-Smith, S.L., Khodjakov, A., Hergert, P., and Walczak, C.E. (2004). Depletion of centromeric MCAK leads to chromosome congression and segregation defects due to improper kinetochore attachments. Mol Biol Cell *15*, 1146-1159.

Kline-Smith, S.L., and Walczak, C.E. (2004). Mitotic spindle assembly and chromosome segregation: refocusing on microtubule dynamics. Mol Cell *15*, 317-327.

Knop, M., Pereira, G., Geissler, S., Grein, K., and Schiebel, E. (1997). The spindle pole body component Spc97p interacts with the gamma-tubulin of *Saccharomyces cerevisiae* and functions in microtubule organization and spindle pole body duplication. EMBO J *16*, 1550-1564.

Kollman, J.M., Polka, J.K., Zelter, A., Davis, T.N., and Agard, D.A. (2010). Microtubule nucleating gamma-TuSC assembles structures with 13-fold microtubule-like symmetry. Nature *466*, 879-882.

Kortazar, D., Fanarraga, M.L., Carranza, G., Bellido, J., Villegas, J.C., Avila, J., and Zabala, J.C. (2007). Role of cofactors B (TBCB) and E (TBCE) in tubulin heterodimer dissociation. Exp Cell Res *313*, 425-436.

Krapp, A., and Simanis, V. (2014). Dma1-dependent degradation of SIN proteins during meiosis in *Schizosaccharomyces pombe*. J Cell Sci *127*, 3149-3161.

Krissinel, E. (2007). On the relationship between sequence and structure similarities in proteomics. Bioinformatics *23*, 717-723.

Lacroix, B., van Dijk, J., Gold, N.D., Guizetti, J., Aldrian-Herrada, G., Rogowski, K., Gerlich, D.W., and Janke, C. (2010). Tubulin polyglutamylation stimulates spastin-mediated microtubule severing. J Cell Biol *189*, 945-954.

Laurent, C.E., Delfino, F.J., Cheng, H.Y., and Smithgall, T.E. (2004). The human c-Fes tyrosine kinase binds tubulin and microtubules through separate domains and promotes microtubule assembly. Mol Cell Biol *24*, 9351-9358.

Leandro-Garcia, L.J., Leskela, S., Landa, I., Montero-Conde, C., Lopez-Jimenez, E., Leton, R., Cascon, A., Robledo, M., and Rodriguez-Antona, C. (2010). Tumoral and tissue-specific expression of the major human beta-tubulin isotypes. Cytoskeleton (Hoboken) *67*, 214-223.

Lee, W.L., Oberle, J.R., and Cooper, J.A. (2003). The role of the lissencephaly protein Pac1 during nuclear migration in budding yeast. J Cell Biol *160*, 355-364.

Leipe, D.D., Koonin, E.V., and Aravind, L. (2004). STAND, a class of P-loop NTPases including animal and plant regulators of programmed cell death: multiple, complex domain architectures, unusual phyletic patterns, and evolution by horizontal gene transfer. J Mol Biol *343*, 1-28.

Lenz, J.H., Schuchardt, I., Straube, A., and Steinberg, G. (2006). A dynein loading zone for retrograde endosome motility at microtubule plus-ends. EMBO J *25*, 2275-2286.

Lewis, S.A., Ivanov, I.E., Lee, G.H., and Cowan, N.J. (1989). Organization of microtubules in dendrites and axons is determined by a short hydrophobic zipper in microtubule-associated proteins MAP2 and tau. Nature *342*, 498-505.

Li, D., and Roberts, R. (2001). WD-repeat proteins: structure characteristics, biological function, and their involvement in human diseases. Cell Mol Life Sci *58*, 2085-2097.

Li, H.H., Chiang, C.S., Huang, H.Y., and Liaw, G.J. (2009). mars and tousled-like kinase act in parallel to ensure chromosome fidelity in *Drosophila.* J Biomed Sci *16*, 51.

Li, J.M., Li, Y., and Elledge, S.J. (2005). Genetic analysis of the kinetochore DASH complex reveals an antagonistic relationship with the ras/protein kinase A pathway and a novel subunit required for Ask1 association. Mol Cell Biol *25*, 767-778.

Li, S., Finley, J., Liu, Z.J., Qiu, S.H., Chen, H., Luan, C.H., Carson, M., Tsao, J., Johnson, D., Lin, G.*, et al.* (2002a). Crystal structure of the cytoskeleton-associated protein glycine-rich (CAP-Gly) domain. J Biol Chem *277*, 48596-48601.

Li, Y., Bachant, J., Alcasabas, A.A., Wang, Y., Qin, J., and Elledge, S.J. (2002b). The mitotic spindle is required for loading of the DASH complex onto the kinetochore. Genes Dev *16*, 183-197.

Liakopoulos, D., Kusch, J., Grava, S., Vogel, J., and Barral, Y. (2003). Asymmetric loading of Kar9 onto spindle poles and microtubules ensures proper spindle alignment. Cell *112*, 561-574.

Ligon, L.A., Shelly, S.S., Tokito, M., and Holzbaur, E.L. (2003). The microtubule plus-end proteins EB1 and dynactin have differential effects on microtubule polymerization. Mol Biol Cell *14*, 1405-1417.

Lim, H.H., Zhang, T., and Surana, U. (2009). Regulation of centrosome separation in yeast and vertebrates: common threads. Trends Cell Biol *19*, 325-333.

Liu, S., Duan, Y., Ge, C., Chen, C., and Zhou, M. (2013). Functional analysis of the beta2 -tubulin gene of Fusarium graminearum and the beta-tubulin gene of Botrytis cinerea by homologous replacement. Pest Manag Sci *69*, 582-588.

Lopata, M.A., and Cleveland, D.W. (1987). In vivo microtubules are copolymers of available beta-tubulin isotypes: localization of each of six vertebrate beta-tubulin isotypes using polyclonal antibodies elicited by synthetic peptide antigens. J Cell Biol *105*, 1707-1720.

Lopus, M., Manatschal, C., Buey, R.M., Bjelic, S., Miller, H.P., Steinmetz, M.O., and Wilson, L. (2012). Cooperative stabilization of microtubule dynamics by EB1 and CLIP-170 involves displacement of stably bound P(i) at microtubule ends. Biochemistry *51*, 3021-3030.

Luduena, R.F. (1998). Multiple forms of tubulin: different gene products and covalent modifications. Int Rev Cytol *178*, 207-275.

Lupas, A., Van Dyke, M., and Stock, J. (1991). Predicting coiled coils from protein sequences. Science *252*, 1162-1164.

Maddox, P.S., Bloom, K.S., and Salmon, E.D. (2000). The polarity and dynamics of microtubule assembly in the budding yeast *Saccharomyces cerevisiae*. Nat Cell Biol *2*, 36-41.

Mahlert, M., Leveleki, L., Hlubek, A., Sandrock, B., and Bolker, M. (2006). Rac1 and Cdc42 regulate hyphal growth and cytokinesis in the dimorphic fungus *Ustilago maydis*. Mol Microbiol *59*, 567-578.

Mahlert, M., Vogler, C., Stelter, K., Hause, G., and Basse, C.W. (2009). The a2 mating-type-locus gene lga2 of *Ustilago maydis* interferes with mitochondrial dynamics and fusion, partially in dependence on a Dnm1-like fission component. J Cell Sci *122*, 2402-2412.

Maiato, H., Fairley, E.A., Rieder, C.L., Swedlow, J.R., Sunkel, C.E., and Earnshaw, W.C. (2003). Human CLASP1 is an outer kinetochore component that regulates spindle microtubule dynamics. Cell *113*, 891-904.

Maiato, H., Sampaio, P., and Sunkel, C.E. (2004). Microtubule-associated proteins and their essential roles during mitosis. Int Rev Cytol *241*, 53-153.

Mandelkow, E., and Mandelkow, E.M. (1995). Microtubules and microtubule-associated proteins. Curr Opin Cell Biol *7*, 72-81.

Manning, A.L., Ganem, N.J., Bakhoum, S.F., Wagenbach, M., Wordeman, L., and Compton, D.A. (2007). The kinesin-13 proteins Kif2a, Kif2b, and Kif2c/MCAK have distinct roles during mitosis in human cells. Mol Biol Cell *18*, 2970-2979.

Manning, B.D., Barrett, J.G., Wallace, J.A., Granok, H., and Snyder, M. (1999). Differential regulation of the Kar3p kinesin-related protein by two associated proteins, Cik1p and Vik1p. J Cell Biol *144*, 1219-1233.

Martin-Castellanos, C., Blanco, M., Rozalen, A.E., Perez-Hidalgo, L., Garcia, A.I., Conde, F., Mata, J., Ellermeier, C., Davis, L., San-Segundo, P.*, et al.* (2005). A large-scale screen in *S. pombe* identifies seven novel genes required for critical meiotic events. Curr Biol *15*, 2056-2062.

Martinez-Espinoza, A.D., Garcia-Pedrajas, M.D., and Gold, S.E. (2002). The Ustilaginales as plant pests and model systems. Fungal Genet Biol *35*, 1-20.

Masson, D., and Kreis, T.E. (1993). Identification and molecular characterization of E-MAP-115, a novel microtubule-associated protein predominantly expressed in epithelial cells. J Cell Biol *123*, 357-371.

Masson, D., and Kreis, T.E. (1995). Binding of E-MAP-115 to microtubules is regulated by cell cycle-dependent phosphorylation. J Cell Biol *131*, 1015-1024.

Mata, J., and Nurse, P. (1997). tea1 and the microtubular cytoskeleton are important for generating global spatial order within the fission yeast cell. Cell *89*, 939-949.

May, G.S. (1989). The highly divergent beta-tubulins of *Aspergillus nidulans* are functionally interchangeable. J Cell Biol *109*, 2267-2274.

May, G.S., Tsang, M.L., Smith, H., Fidel, S., and Morris, N.R. (1987). *Aspergillus nidulans* beta-tubulin genes are unusually divergent. Gene *55*, 231-243.

McKean, P.G., Vaughan, S., and Gull, K. (2001). The extended tubulin superfamily. J Cell Sci *114*, 2723-2733.

McNally, F.J., Okawa, K., Iwamatsu, A., and Vale, R.D. (1996). Katanin, the microtubule-severing ATPase, is concentrated at centrosomes. J Cell Sci *109 (Pt 3)*, 561-567.

McNally, F.J., and Thomas, S. (1998). Katanin is responsible for the M-phase microtubule-severing activity in *Xenopus* eggs. Mol Biol Cell *9*, 1847-1861.

McNally, F.J., and Vale, R.D. (1993). Identification of katanin, an ATPase that severs and disassembles stable microtubules. Cell *75*, 419-429.

McWilliam, H., Li, W., Uludag, M., Squizzato, S., Park, Y.M., Buso, N., Cowley, A.P., and Lopez, R. (2013). Analysis Tool Web Services from the EMBL-EBI. Nucleic Acids Res *41*, W597-600.

Meng, W., Mushika, Y., Ichii, T., and Takeichi, M. (2008). Anchorage of microtubule minus ends to adherens junctions regulates epithelial cell-cell contacts. Cell *135*, 948-959.

Milner-White, E.J., Coggins, J.R., and Anton, I.A. (1991). Evidence for an ancestral core structure in nucleotide-binding proteins with the type A motif. J Mol Biol *221*, 751-754.

Mimori-Kiyosue, Y., Grigoriev, I., Lansbergen, G., Sasaki, H., Matsui, C., Severin, F., Galjart, N., Grosveld, F., Vorobjev, I., Tsukita, S.*, et al.* (2005). CLASP1 and CLASP2 bind to EB1 and regulate microtubule plus-end dynamics at the cell cortex. J Cell Biol *168*, 141-153.

Mirzayan, C., Copeland, C.S., and Snyder, M. (1992). The NUF1 gene encodes an essential coiled-coil related protein that is a potential component of the yeast nucleoskeleton. J Cell Biol *116*, 1319-1332.

Mitchell, D.R. (2007). The evolution of eukaryotic cilia and flagella as motile and sensory organelles. Adv Exp Med Biol *607*, 130-140.

Mitchison, T., and Kirschner, M. (1984). Dynamic instability of microtubule growth. Nature *312*, 237-242.

Mocz, G., and Gibbons, I.R. (2001). Model for the motor component of dynein heavy chain based on homology to the AAA family of oligomeric ATPases. Structure *9*, 93-103.

Monnat, J., Ortega Perez, R., and Turian, G. (1997). Molecular cloning and expression studies of two divergent alpha-tubulin genes in *Neurospora crassa*. FEMS Microbiol Lett *150*, 33-41.

Moreno-Hagelsieb, G., and Latimer, K. (2008). Choosing BLAST options for better detection of orthologs as reciprocal best hits. Bioinformatics *24*, 319-324.

Morrell, J.L., Tomlin, G.C., Rajagopalan, S., Venkatram, S., Feoktistova, A.S., Tasto, J.J., Mehta, S., Jennings, J.L., Link, A., Balasubramanian, M.K.*, et al.* (2004). Sid4p-Cdc11p assembles the septation initiation network and its regulators at the *S. pombe* SPB. Curr Biol *14*, 579-584.

Mueller, A.N., Ziemann, S., Treitschke, S., Assmann, D., and Doehlemann, G. (2013). Compatibility in the *Ustilago maydis*-maize interaction requires inhibition of host cysteine proteases by the fungal effector Pit2. PLoS Pathog *9*, e1003177.

Munemitsu, S., Souza, B., Muller, O., Albert, I., Rubinfeld, B., and Polakis, P. (1994). The APC gene product associates with microtubules *in vivo* and promotes their assembly *in vitro*. Cancer Res *54*, 3676-3681.

Munsterkotter, M., and Steinberg, G. (2007). The fungus *Ustilago maydis* and humans share disease-related proteins that are not found in *Saccharomyces cerevisiae*. BMC Genomics *8*, 473.

Murphy, D.B., and Borisy, G.G. (1975). Association of high-molecular-weight proteins with microtubules and their role in microtubule assembly *in vitro*. Proc Natl Acad Sci U S A *72*, 2696-2700.

Murphy, D.B., Johnson, K.A., and Borisy, G.G. (1977). Role of tubulin-associated proteins in microtubule nucleation and elongation. J Mol Biol *117*, 33-52.

Murphy, S.M., Preble, A.M., Patel, U.K., O'Connell, K.L., Dias, D.P., Moritz, M., Agard, D., Stults, J.T., and Stearns, T. (2001). GCP5 and GCP6: two new members of the human gamma-tubulin complex. Mol Biol Cell *12*, 3340-3352.

Nakajima, Y., Tyers, R.G., Wong, C.C., Yates, J.R., 3rd, Drubin, D.G., and Barnes, G. (2009). Nbl1p: a Borealin/Dasra/CSC-1-like protein essential for Aurora/Ipl1 complex function and integrity in *Saccharomyces cerevisiae*. Mol Biol Cell *20*, 1772-1784.

Nakamura, M., Zhou, X.Z., and Lu, K.P. (2001). Critical role for the EB1 and APC interaction in the regulation of microtubule polymerization. Curr Biol *11*, 1062-1067.

Naz, F., Anjum, F., Islam, A., Ahmad, F., and Hassan, M.I. (2013). Microtubule affinity-regulating kinase 4: structure, function, and regulation. Cell Biochem Biophys *67*, 485-499.

Neer, E.J., Schmidt, C.J., Nambudripad, R., and Smith, T.F. (1994). The ancient regulatory-protein family of WD-repeat proteins. Nature *371*, 297-300.

Neuwald, A.F., Aravind, L., Spouge, J.L., and Koonin, E.V. (1999). AAA+: A class of chaperone-like ATPases associated with the assembly, operation, and disassembly of protein complexes. Genome Res *9*, 27-43.

Nguyen, T., Vinh, D.B., Crawford, D.K., and Davis, T.N. (1998). A genetic analysis of interactions with Spc110p reveals distinct functions of Spc97p and Spc98p, components of the yeast gamma-tubulin complex. Mol Biol Cell *9*, 2201-2216.

Nogales, E. (2000). Structural insights into microtubule function. Annu Rev Biochem *69*, 277-302.

Nogales, E. (2001). Structural insight into microtubule function. Annu Rev Biophys Biomol Struct *30*, 397-420.

Nogales, E., Whittaker, M., Milligan, R.A., and Downing, K.H. (1999). High-resolution model of the microtubule. Cell *96*, 79-88.

Nogales, E., Wolf, S.G., and Downing, K.H. (1998). Structure of the alpha beta tubulin dimer by electron crystallography. Nature *391*, 199-203.

Notredame, C., Higgins, D.G., and Heringa, J. (2000). T-Coffee: A novel method for fast and accurate multiple sequence alignment. J Mol Biol *302*, 205-217.

Oakley, B.R. (2004). Tubulins in *Aspergillus nidulans*. Fungal Genet Biol *41*, 420-427.

Ohkura, H., Garcia, M.A., and Toda, T. (2001). Dis1/TOG universal microtubule adaptors - one MAP for all? J Cell Sci *114*, 3805-3812.

Olah, J., Tokesi, N., Vincze, O., Horvath, I., Lehotzky, A., Erdei, A., Szajli, E., Medzihradszky, K.F., Orosz, F., Kovacs, G.G.*, et al.* (2006). Interaction of TPPP/p25 protein with glyceraldehyde-3-phosphate dehydrogenase and their co-localization in Lewy bodies. FEBS Lett *580*, 5807-5814.

Olmsted, J.B. (1986). Microtubule-associated proteins. Annu Rev Cell Biol *2*, 421-457.

Orban-Nemeth, Z., Simader, H., Badurek, S., Trancikova, A., and Propst, F. (2005). Microtubule-associated protein 1S, a short and ubiquitously expressed member of the microtubule-associated protein 1 family. J Biol Chem *280*, 2257-2265.

Page, B.D., Satterwhite, L.L., Rose, M.D., and Snyder, M. (1994). Localization of the Kar3 kinesin heavy chain-related protein requires the Cik1 interacting protein. J Cell Biol *124*, 507-519.

Page, B.D., and Snyder, M. (1992). CIK1: a developmentally regulated spindle pole body-associated protein important for microtubule functions in *Saccharomyces cerevisiae*. Genes Dev *6*, 1414-1429.

Pardo, M., and Nurse, P. (2005). The nuclear rim protein Amo1 is required for proper microtubule cytoskeleton organisation in fission yeast. J Cell Sci *118*, 1705-1714.

Pereira, G., and Schiebel, E. (2001). The role of the yeast spindle pole body and the mammalian centrosome in regulating late mitotic events. Curr Opin Cell Biol *13*, 762-769.

Pierre, P., Pepperkok, R., and Kreis, T.E. (1994). Molecular characterization of two functional domains of CLIP-170 in vivo. J Cell Sci *107 (Pt 7)*, 1909-1920.

Pot, I., Knockleby, J., Aneliunas, V., Nguyen, T., Ah-Kye, S., Liszt, G., Snyder, M., Hieter, P., and Vogel, J. (2005). Spindle checkpoint maintenance requires Ame1 and Okp1. Cell Cycle *4*, 1448-1456.

Poulton, J.S., Mu, F.W., Roberts, D.M., and Peifer, M. (2013). APC2 and Axin promote mitotic fidelity by facilitating centrosome separation and cytoskeletal regulation. Development *140*, 4226-4236.

Pruyne, D., Legesse-Miller, A., Gao, L., Dong, Y., and Bretscher, A. (2004). Mechanisms of polarized growth and organelle segregation in yeast. Annu Rev Cell Dev Biol *20*, 559-591.

Pryer, N.K., Walker, R.A., Skeen, V.P., Bourns, B.D., Soboeiro, M.F., and Salmon, E.D. (1992). Brain microtubule-associated proteins modulate microtubule dynamic instability *in vitro*. Real-time observations using video microscopy. J Cell Sci *103 (Pt 4)*, 965-976.

Puhalla, J.E. (1970). Genetic studies of the b incompatability locus of *Ustilago maydis*. Genetics Research *16*, 229-232.

Qureshi, H.Y., and Paudel, H.K. (2011). Parkinsonian neurotoxin 1-methyl-4-phenyl-1,2,3,6-tetrahydropyridine (MPTP) and alpha-synuclein mutations promote Tau protein phosphorylation at Ser262 and destabilize microtubule cytoskeleton *in vitro*. J Biol Chem *286*, 5055-5068.

Rapley, J., Nicolas, M., Groen, A., Regue, L., Bertran, M.T., Caelles, C., Avruch, J., and Roig, J. (2008). The NIMA-family kinase Nek6 phosphorylates the kinesin Eg5 at a novel site necessary for mitotic spindle formation. J Cell Sci *121*, 3912-3921.

Raymond, C.K., Mugford, V.R., and Sexson, S.L. (1999). Plasmid topologies that enhance the transformation efficiency of yeast. Biotechniques *27*, 892-894, 896.

Raymond, C.K., Sims, E.H., and Olson, M.V. (2002). Linker-mediated recombinational subcloning of large DNA fragments using yeast. Genome Res *12*, 190-197.

Raynaud-Messina, B., and Merdes, A. (2007). Gamma-tubulin complexes and microtubule organization. Curr Opin Cell Biol *19*, 24-30.

Ren, J., Wen, L., Gao, X., Jin, C., Xue, Y., and Yao, X. (2009a). DOG 1.0: illustrator of protein domain structures. Cell Res *19*, 271-273.

Ren, J., Wen, L., Gao, X., Jin, C., Xue, Y., and Yao, X. (2009b). DOG 1.0: illustrator of protein domain structures. Cell Res *19*, 271-273.

Rice, P., Longden, I., and Bleasby, A. (2000). EMBOSS: the European Molecular Biology Open Software Suite. Trends Genet *16*, 276-277.

Risler, T. (2009). CytoskeletonCytoskeleton and Cell Motility. In Encyclopedia of Complexity and Systems Science (Springer), pp. 1738-1774.

Risler, T. (2011). Cytoskeleton and Cell Motility. In ArXiv e-prints.

Rizk, R.S., Discipio, K.A., Proudfoot, K.G., and Gupta, M.L., Jr. (2014). The kinesin-8 Kip3 scales anaphase spindle length by suppression of midzone microtubule polymerization. J Cell Biol *204*, 965-975.

Robertson, A.S., Allwood, E.G., Smith, A.P., Gardiner, F.C., Costa, R., Winder, S.J., and Ayscough, K.R. (2009). The WASP homologue Las17 activates the novel actin-regulatory activity of Ysc84 to promote endocytosis in yeast. Mol Biol Cell *20*, 1618-1628.

Robson, G.D., West, P.v., Gadd, G.M., and British Mycological Society. (2007). Exploitation of fungi : Symposium of the British Mycological Society held at the University of Manchester, September 2005 (Cambridge, UK ; New York, Cambridge University Press).

Roll-Mecak, A., and McNally, F.J. (2010). Microtubule-severing enzymes. Curr Opin Cell Biol *22*, 96-103.

Rout, M.P., and Kilmartin, J.V. (1990). Components of the yeast spindle and spindle pole body. J Cell Biol *111*, 1913-1927.

Ruchaud, S., Carmena, M., and Earnshaw, W.C. (2007). The chromosomal passenger complex: one for all and all for one. Cell *131*, 230-231.

Ruiz-Herrera, J., Ortiz-Castellanos, L., Martinez, A.I., Leon-Ramirez, C., and Sentandreu, R. (2008). Analysis of the proteins involved in the structure and synthesis of the cell wall of *Ustilago maydis*. Fungal Genet Biol *45 Suppl 1*, S71-76.

Saadi, I., Alkuraya, F.S., Gisselbrecht, S.S., Goessling, W., Cavallesco, R., Turbe-Doan, A., Petrin, A.L., Harris, J., Siddiqui, U., Grix, A.W., Jr.*, et al.* (2011). Deficiency of the cytoskeletal protein SPECC1L leads to oblique facial clefting. Am J Hum Genet *89*, 44-55.

Sahab, Z.J., Kirilyuk, A., Zhang, L., Khamis, Z.I., Pompach, P., Sung, Y., and Byers, S.W. (2012). Analysis of tubulin alpha-1A/1B C-terminal tail post-

translational poly-glutamylation reveals novel modification sites. J Proteome Res *11*, 1913-1923.

Saito, K., Kigawa, T., Koshiba, S., Sato, K., Matsuo, Y., Sakamoto, A., Takagi, T., Shirouzu, M., Yabuki, T., Nunokawa, E.*, et al.* (2004). The CAP-Gly domain of CYLD associates with the proline-rich sequence in NEMO/IKKgamma. Structure *12*, 1719-1728.

Saitou, N., and Nei, M. (1987). The neighbor-joining method: a new method for reconstructing phylogenetic trees. Mol Biol Evol *4*, 406-425.

Salinas, P.C. (2007). Modulation of the microtubule cytoskeleton: a role for a divergent canonical Wnt pathway. Trends Cell Biol *17*, 333-342.

Salinas, S., Carazo-Salas, R.E., Proukakis, C., Cooper, J.M., Weston, A.E., Schiavo, G., and Warner, T.T. (2005). Human spastin has multiple microtubule-related functions. J Neurochem *95*, 1411-1420.

Sambrook, J., Fritsch, E.F., and Maniatis, T. (1989). Molecular cloning : a laboratory manual, 2nd ed. edn (Cold Spring Harbor, N.Y., Cold Spring Harbor Laboratory).

Samejima, I., Lourenco, P.C., Snaith, H.A., and Sawin, K.E. (2005). Fission yeast mto2p regulates microtubule nucleation by the centrosomin-related protein mto1p. Mol Biol Cell *16*, 3040-3051.

Samora, C.P., Mogessie, B., Conway, L., Ross, J.L., Straube, A., and McAinsh, A.D. (2011). MAP4 and CLASP1 operate as a safety mechanism to maintain a stable spindle position in mitosis. Nat Cell Biol *13*, 1040-1050.

Saraste, M., Sibbald, P.R., and Wittinghofer, A. (1990). The P-loop--a common motif in ATP- and GTP-binding proteins. Trends Biochem Sci *15*, 430-434.

Sasai, K., Katayama, H., Stenoien, D.L., Fujii, S., Honda, R., Kimura, M., Okano, Y., Tatsuka, M., Suzuki, F., Nigg, E.A.*, et al.* (2004). Aurora-C kinase is

a novel chromosomal passenger protein that can complement Aurora-B kinase function in mitotic cells. Cell Motil Cytoskeleton *59*, 249-263.

Sato, M., Vardy, L., Angel Garcia, M., Koonrugsa, N., and Toda, T. (2004). Interdependency of fission yeast Alp14/TOG and coiled coil protein Alp7 in microtubule localization and bipolar spindle formation. Mol Biol Cell *15*, 1609-1622.

Saunders, W., Hornack, D., Lengyel, V., and Deng, C. (1997). The *Saccharomyces cerevisiae* kinesin-related motor Kar3p acts at preanaphase spindle poles to limit the number and length of cytoplasmic microtubules. J Cell Biol *137*, 417-431.

Saunders, W.S., Koshland, D., Eshel, D., Gibbons, I.R., and Hoyt, M.A. (1995). *Saccharomyces cerevisiae* kinesin- and dynein-related proteins required for anaphase chromosome segregation. J Cell Biol *128*, 617-624.

Sawin, K.E., Lourenco, P.C., and Snaith, H.A. (2004). Microtubule nucleation at non-spindle pole body microtubule-organizing centers requires fission yeast centrosomin-related protein mod20p. Curr Biol *14*, 763-775.

Scheel, J., Pierre, P., Rickard, J.E., Diamantopoulos, G.S., Valetti, C., van der Goot, F.G., Haner, M., Aebi, U., and Kreis, T.E. (1999). Purification and analysis of authentic CLIP-170 and recombinant fragments. J Biol Chem *274*, 25883-25891.

Schilling, L., Matei, A., Redkar, A., Walbot, V., and Doehlemann, G. (2014). Virulence of the maize smut *Ustilago maydis* is shaped by organ-specific effectors. Molecular Plant Pathology *15*, 780-789.

Schliwa, M., and Woehlke, G. (2003). Molecular motors. Nature *422*, 759-765.
Schmitt, M.E., Brown, T.A., and Trumpower, B.L. (1990). A rapid and simple method for preparation of RNA from *Saccharomyces cerevisiae*. Nucleic Acids Res *18*, 3091-3092.

Schroer, T.A. (2004). Dynactin. Annu Rev Cell Dev Biol *20*, 759-779.

Schuchardt, I., Assmann, D., Thines, E., Schuberth, C., and Steinberg, G. (2005). Myosin-V, Kinesin-1, and Kinesin-3 cooperate in hyphal growth of the fungus *Ustilago maydis*. Mol Biol Cell *16*, 5191-5201.

Schulz, B., Banuett, F., Dahl, M., Schlesinger, R., Schafer, W., Martin, T., Herskowitz, I., and Kahmann, R. (1990). The b alleles of *U. maydis*, whose combinations program pathogenic development, code for polypeptides containing a homeodomain-related motif. Cell *60*, 295-306.

Schuster, M., Lipowsky, R., Assmann, M.A., Lenz, P., and Steinberg, G. (2011). Transient binding of dynein controls bidirectional long-range motility of early endosomes. Proc Natl Acad Sci U S A *108*, 3618-3623.

Schuyler, S.C., Liu, J.Y., and Pellman, D. (2003). The molecular function of Ase1p: evidence for a MAP-dependent midzone-specific spindle matrix. Microtubule-associated proteins. J Cell Biol *160*, 517-528.

Schuyler, S.C., and Pellman, D. (2001). Microtubule "plus-end-tracking proteins": The end is just the beginning. Cell *105*, 421-424.

Siller, K.H., and Doe, C.Q. (2009). Spindle orientation during asymmetric cell division. Nat Cell Biol *11*, 365-374.

Simeonov, D.R., Kenny, K., Seo, L., Moyer, A., Allen, J., and Paluh, J.L. (2009). Distinct Kinesin-14 mitotic mechanisms in spindle bipolarity. Cell Cycle *8*, 3571-3583.

Sirajuddin, M., Rice, L.M., and Vale, R.D. (2014). Regulation of microtubule motors by tubulin isotypes and post-translational modifications. Nat Cell Biol *16*, 335-344.

Slep, K.C., and Vale, R.D. (2007). Structural basis of microtubule plus end tracking by XMAP215, CLIP-170, and EB1. Mol Cell *27*, 976-991.

Sloboda, R.D., Rudolph, S.A., Rosenbaum, J.L., and Greengard, P. (1975). Cyclic AMP-dependent endogenous phosphorylation of a microtubule-associated protein. Proc Natl Acad Sci U S A *72*, 177-181.

Smith, T.F., Gaitatzes, C., Saxena, K., and Neer, E.J. (1999). The WD repeat: a common architecture for diverse functions. Trends Biochem Sci *24*, 181-185.

Snaith, H.A., and Sawin, K.E. (2003). Fission yeast mod5p regulates polarized growth through anchoring of tea1p at cell tips. Nature *423*, 647-651.

Snell, V., and Nurse, P. (1994). Genetic analysis of cell morphogenesis in fission yeast--a role for casein kinase II in the establishment of polarized growth. EMBO J *13*, 2066-2074.

Snetselaar, and Mims (1993). Infection of maize stigmas by *Ustilago maydis*: light and electron microscopy. . Phytopathology 83: 843–850.

Snetselaar, and Mims (1994). Light and electron microscopy of *Ustilago maydis* hyphae in maize. Mycol Res 347–355.

Solomon, F., Magendantz, M., and Salzman, A. (1979). Identification with cellular microtubules of one of the co-assembling microtubule-associated proteins. Cell *18*, 431-438.

Sonnhammer, E.L., Eddy, S.R., Birney, E., Bateman, A., and Durbin, R. (1998). Pfam: multiple sequence alignments and HMM-profiles of protein domains. Nucleic Acids Res *26*, 320-322.

Spang, A., Courtney, I., Grein, K., Matzner, M., and Schiebel, E. (1995). The Cdc31p-binding protein Kar1p is a component of the half bridge of the yeast spindle pole body. J Cell Biol *128*, 863-877.

Spellig, T., Bolker, M., Lottspeich, F., Frank, R.W., and Kahmann, R. (1994). Pheromones trigger filamentous growth in *Ustilago maydis*. EMBO J *13*, 1620-1627.

Sproul, L.R., Anderson, D.J., Mackey, A.T., Saunders, W.S., and Gilbert, S.P. (2005). Cik1 targets the minus-end kinesin depolymerase kar3 to microtubule plus ends. Curr Biol *15*, 1420-1427.

St Pierre, S.E., Ponting, L., Stefancsik, R., and McQuilton, P. (2014). FlyBase 102--advanced approaches to interrogating FlyBase. Nucleic Acids Res *42*, D780-788.

Steinberg, G. (2007a). On the move: endosomes in fungal growth and pathogenicity. Nat Rev Microbiol *5*, 309-316.

Steinberg, G. (2007b). Preparing the way: fungal motors in microtubule organization. Trends Microbiol *15*, 14-21.

Steinberg, G. (2007c). Tracks for traffic: microtubules in the plant pathogen *Ustilago maydis.* New Phytol *174*, 721-733.

Steinberg, G., and Perez-Martin, J. (2008). Ustilago maydis, a new fungal model system for cell biology. Trends Cell Biol *18*, 61-67.

Steinberg, G., Wedlich-Soldner, R., Brill, M., and Schulz, I. (2001). Microtubules in the fungal pathogen *Ustilago maydis* are highly dynamic and determine cell polarity. J Cell Sci *114*, 609-622.

Straube, A., Brill, M., Oakley, B.R., Horio, T., and Steinberg, G. (2003). Microtubule organization requires cell cycle-dependent nucleation at dispersed cytoplasmic sites: polar and perinuclear microtubule organizing centers in the plant pathogen Ustilago maydis. Mol Biol Cell *14*, 642-657.

Sullivan, K.F., Havercroft, J.C., Machlin, P.S., and Cleveland, D.W. (1986). Sequence and expression of the chicken beta 5- and beta 4-tubulin genes define a pair of divergent beta-tubulins with complementary patterns of expression. Mol Cell Biol *6*, 4409-4418.

Surrey, T., Nedelec, F., Leibler, S., and Karsenti, E. (2001). Physical properties determining self-organization of motors and microtubules. Science *292*, 1167-1171.

Sweet, T.J., Boyer, B., Hu, W., Baker, K.E., and Coller, J. (2007). Microtubule disruption stimulates P-body formation. RNA *13*, 493-502.

Takeshita, N., and Fischer, R. (2011). On the role of microtubules, cell end markers, and septal microtubule organizing centres on site selection for polar growth in *Aspergillus nidulans*. Fungal Biol *115*, 506-517.

Takeshita, N., Higashitsuji, Y., Konzack, S., and Fischer, R. (2008). Apical sterol-rich membranes are essential for localizing cell end markers that determine growth directionality in the filamentous fungus *Aspergillus nidulans*. Mol Biol Cell *19*, 339-351.

Takeshita, N., Mania, D., Herrero, S., Ishitsuka, Y., Nienhaus, G.U., Podolski, M., Howard, J., and Fischer, R. (2013). The cell-end marker TeaA and the microtubule polymerase AlpA contribute to microtubule guidance at the hyphal tip cortex of *Aspergillus nidulans* to provide polarity maintenance. J Cell Sci *126*, 5400-5411.

Tamura, K., Stecher, G., Peterson, D., Filipski, A., and Kumar, S. (2013). MEGA6: Molecular Evolutionary Genetics Analysis version 6.0. Mol Biol Evol *30*, 2725-2729.

Tanenbaum, M.E., Macurek, L., van der Vaart, B., Galli, M., Akhmanova, A., and Medema, R.H. (2011). A complex of Kif18b and MCAK promotes microtubule depolymerization and is negatively regulated by Aurora kinases. Curr Biol *21*, 1356-1365.

Tang, N.H., Okada, N., Fong, C.S., Arai, K., Sato, M., and Toda, T. (2014). Targeting Alp7/TACC to the spindle pole body is essential for mitotic spindle assembly in fission yeast. FEBS Lett *588*, 2814-2821.

Thakur, J., and Sanyal, K. (2011). The essentiality of the fungus-specific Dam1 complex is correlated with a one-kinetochore-one-microtubule interaction present throughout the cell cycle, independent of the nature of a centromere. Eukaryot Cell *10*, 1295-1305.

Thein, K.H., Kleylein-Sohn, J., Nigg, E.A., and Gruneberg, U. (2007). Astrin is required for the maintenance of sister chromatid cohesion and centrosome integrity. J Cell Biol *178*, 345-354.

Thompson, H.M., Skop, A.R., Euteneuer, U., Meyer, B.J., and McNiven, M.A. (2002). The large GTPase dynamin associates with the spindle midzone and is required for cytokinesis. Curr Biol *12*, 2111-2117.

Thompson, J.D., Gibson, T.J., Plewniak, F., Jeanmougin, F., and Higgins, D.G. (1997). The CLUSTAL_X windows interface: flexible strategies for multiple sequence alignment aided by quality analysis tools. Nucleic Acids Res *25*, 4876-4882.

Thompson, J.D., Higgins, D.G., and Gibson, T.J. (1994). CLUSTAL W: improving the sensitivity of progressive multiple sequence alignment through sequence weighting, position-specific gap penalties and weight matrix choice. Nucleic Acids Res *22*, 4673-4680.

Tian, G., Thomas, S., and Cowan, N.J. (2010). Effect of TBCD and its regulatory interactor Arl2 on tubulin and microtubule integrity. Cytoskeleton (Hoboken) *67*, 706-714.

Tonami, K., Kurihara, Y., Aburatani, H., Uchijima, Y., Asano, T., and Kurihara, H. (2007). Calpain 6 is involved in microtubule stabilization and cytoskeletal organization. Mol Cell Biol *27*, 2548-2561.

Torres, J.Z., Summers, M.K., Peterson, D., Brauer, M.J., Lee, J., Senese, S., Gholkar, A.A., Lo, Y.C., Lei, X., Jung, K.*, et al.* (2011). The STARD9/Kif16a kinesin associates with mitotic microtubules and regulates spindle pole assembly. Cell *147*, 1309-1323.

Toya, M., Terasawa, M., Nagata, K., Iida, Y., and Sugimoto, A. (2011). A kinase-independent role for Aurora A in the assembly of mitotic spindle microtubules in *Caenorhabditis elegans* embryos. Nat Cell Biol *13*, 708-714.

Trieselmann, N., and Wilde, A. (2002). Ran localizes around the microtubule spindle in vivo during mitosis in Drosophila embryos. Curr Biol *12*, 1124-1129.

Trokter, M., Mucke, N., and Surrey, T. (2012). Reconstitution of the human cytoplasmic dynein complex. Proc Natl Acad Sci U S A *109*, 20895-20900.

Tsuchihara, K., Lapin, V., Bakal, C., Okada, H., Brown, L., Hirota-Tsuchihara, M., Zaugg, K., Ho, A., Itie-Youten, A., Harris-Brandts, M.*, et al.* (2005). Ckap2 regulates aneuploidy, cell cycling, and cell death in a p53-dependent manner. Cancer Res *65*, 6685-6691.

Tsukuda, T., Carleton, S., Fotheringham, S., and Holloman, W.K. (1988). Isolation and characterization of an autonomously replicating sequence from *Ustilago maydis*. Mol Cell Biol *8*, 3703-3709.

Tuszynski, J.A., Carpenter, E.J., Huzil, J.T., Malinski, W., Luchko, T., and Luduena, R.F. (2006). The evolution of the structure of tubulin and its potential consequences for the role and function of microtubules in cells and embryos. Int J Dev Biol *50*, 341-358.

Uehara, R., Nozawa, R.S., Tomioka, A., Petry, S., Vale, R.D., Obuse, C., and Goshima, G. (2009). The augmin complex plays a critical role in spindle microtubule generation for mitotic progression and cytokinesis in human cells. Proc Natl Acad Sci U S A *106*, 6998-7003.

van der Vaart, B., Manatschal, C., Grigoriev, I., Olieric, V., Gouveia, S.M., Bjelic, S., Demmers, J., Vorobjev, I., Hoogenraad, C.C., Steinmetz, M.O.*, et al.* (2011). SLAIN2 links microtubule plus end-tracking proteins and controls microtubule growth in interphase. J Cell Biol *193*, 1083-1099.

van der Voorn, L., and Ploegh, H.L. (1992). The WD-40 repeat. FEBS Lett *307*, 131-134.

van Nocker, S., and Ludwig, P. (2003). The WD-repeat protein superfamily in *Arabidopsis:* conservation and divergence in structure and function. BMC Genomics *4*, 50.

Venkatram, S., Jennings, J.L., Link, A., and Gould, K.L. (2005). Mto2p, a novel fission yeast protein required for cytoplasmic microtubule organization and anchoring of the cytokinetic actin ring. Mol Biol Cell *16*, 3052-3063.

Verde, F., Mata, J., and Nurse, P. (1995). Fission yeast cell morphogenesis: identification of new genes and analysis of their role during the cell cycle. J Cell Biol *131*, 1529-1538.

Vetter, I.R., and Wittinghofer, A. (1999). Nucleoside triphosphate-binding proteins: different scaffolds to achieve phosphoryl transfer. Q Rev Biophys *32*, 1-56.

Wade, R.H. (2009). On and around microtubules: an overview. Mol Biotechnol *43*, 177-191.

Wahl, R., Wippel, K., Goos, S., Kamper, J., and Sauer, N. (2010). A novel high-affinity sucrose transporter is required for virulence of the plant pathogen *Ustilago maydis*. PLoS Biol *8*, e1000303.

Wakefield, J.G., Bonaccorsi, S., and Gatti, M. (2001). The drosophila protein asp is involved in microtubule organization during spindle formation and cytokinesis. J Cell Biol *153*, 637-648.

Wang, Y., Zhang, X., Zhang, H., Lu, Y., Huang, H., Dong, X., Chen, J., Dong, J., Yang, X., Hang, H.*, et al.* (2012). Coiled-coil networking shapes cell molecular machinery. Mol Biol Cell *23*, 3911-3922.

Wedlich-Soldner, R., Bolker, M., Kahmann, R., and Steinberg, G. (2000). A putative endosomal t-SNARE links exo- and endocytosis in the phytopathogenic fungus *Ustilago maydis*. EMBO J *19*, 1974-1986.

Wedlich-Soldner, R., Straube, A., Friedrich, M.W., and Steinberg, G. (2002). A balance of KIF1A-like kinesin and dynein organizes early endosomes in the fungus *Ustilago maydis*. EMBO J *21*, 2946-2957.

Weingarten, M.D., Lockwood, A.H., Hwo, S.Y., and Kirschner, M.W. (1975). A protein factor essential for microtubule assembly. Proc Natl Acad Sci U S A *72*, 1858-1862.

Weisenberg, R.C., Borisy, G.G., and Taylor, E.W. (1968). The colchicine-binding protein of mammalian brain and its relation to microtubules. Biochemistry *7*, 4466-4479.

Weisshaar, B., Doll, T., and Matus, A. (1992). Reorganisation of the microtubular cytoskeleton by embryonic microtubule-associated protein 2 (MAP2c). Development *116*, 1151-1161.

Welburn, J.P., Grishchuk, E.L., Backer, C.B., Wilson-Kubalek, E.M., Yates, J.R., 3rd, and Cheeseman, I.M. (2009). The human kinetochore Ska1 complex facilitates microtubule depolymerization-coupled motility. Dev Cell *16*, 374-385.

Westermann, S., Avila-Sakar, A., Wang, H.W., Niederstrasser, H., Wong, J., Drubin, D.G., Nogales, E., and Barnes, G. (2005). Formation of a dynamic kinetochore- microtubule interface through assembly of the Dam1 ring complex. Mol Cell *17*, 277-290.

Wiese, C., and Zheng, Y. (2006). Microtubule nucleation: gamma-tubulin and beyond. J Cell Sci *119*, 4143-4153.

Wood, V., Harris, M.A., McDowall, M.D., Rutherford, K., Vaughan, B.W., Staines, D.M., Aslett, M., Lock, A., Bahler, J., Kersey, P.J.*, et al.* (2012).

PomBase: a comprehensive online resource for fission yeast. Nucleic Acids Res *40*, 28.

Wootton, J.C., and Federhen, S. (1996). Analysis of compositionally biased regions in sequence databases. Methods Enzymol *266*, 554-571.

Worth, D.C., Daly, C.N., Geraldo, S., Oozeer, F., and Gordon-Weeks, P.R. (2013). Drebrin contains a cryptic F-actin-bundling activity regulated by Cdk5 phosphorylation. J Cell Biol *202*, 793-806.

Wu, C., Singaram, V., and McKim, K.S. (2008). mei-38 is required for chromosome segregation during meiosis in *Drosophila* females. Genetics *180*, 61-72.

Xiang, X., Osmani, A.H., Osmani, S.A., Xin, M., and Morris, N.R. (1995). NudF, a nuclear migration gene in *Aspergillus nidulans*, is similar to the human LIS-1 gene required for neuronal migration. Mol Biol Cell *6*, 297-310.

Xiong, Y., and Oakley, B.R. (2009). *In vivo* analysis of the functions of gamma-tubulin-complex proteins. J Cell Sci *122*, 4218-4227.

Yamashita, A., Sato, M., Fujita, A., Yamamoto, M., and Toda, T. (2005). The roles of fission yeast ase1 in mitotic cell division, meiotic nuclear oscillation, and cytokinesis checkpoint signaling. Mol Biol Cell *16*, 1378-1395.

Yang, G., Cameron, L.A., Maddox, P.S., Salmon, E.D., and Danuser, G. (2008). Regional variation of microtubule flux reveals microtubule organization in the metaphase meiotic spindle. J Cell Biol *182*, 631-639.

Yang, H., Ganguly, A., and Cabral, F. (2010). Inhibition of cell migration and cell division correlates with distinct effects of microtubule inhibiting drugs. J Biol Chem *285*, 32242-32250.

Yao, X., Zhang, J., Zhou, H., Wang, E., and Xiang, X. (2012). *In vivo* roles of the basic domain of dynactin p150 in microtubule plus-end tracking and dynein function. Traffic *13*, 375-387.

Yenjerla, M., Lopus, M., and Wilson, L. (2010). Analysis of dynamic instability of steady-state microtubules *in vitro* by video-enhanced differential interference contrast microscopy with an appendix by Emin Oroudjev. Methods Cell Biol *95*, 189-206.

Yoshida, H., and Goedert, M. (2012). Phosphorylation of microtubule-associated protein tau by AMPK-related kinases. J Neurochem *120*, 165-176.

Yoshikawa, M., Yang, G., Kawaguchi, K., and Komatsu, S. (2003). Expression analyses of beta-tubulin isotype genes in rice. Plant Cell Physiol *44*, 1202-1207.

Zdobnov, E.M., and Apweiler, R. (2001). InterProScan--an integration platform for the signature-recognition methods in InterPro. Bioinformatics *17*, 847-848.

Zhang, D., Rogers, G.C., Buster, D.W., and Sharp, D.J. (2007). Three microtubule severing enzymes contribute to the "Pacman-flux" machinery that moves chromosomes. J Cell Biol *177*, 231-242.

Zhang, G., Breuer, M., Forster, A., Egger-Adam, D., and Wodarz, A. (2009a). Mars, a *Drosophila* protein related to vertebrate HURP, is required for the attachment of centrosomes to the mitotic spindle during syncytial nuclear divisions. J Cell Sci *122*, 535-545.

Zhang, J., Yao, X., Fischer, L., Abenza, J.F., Penalva, M.A., and Xiang, X. (2011). The p25 subunit of the dynactin complex is required for dynein-early endosome interaction. J Cell Biol *193*, 1245-1255.

Zhang, X., Liu, D., Lv, S., Wang, H., Zhong, X., Liu, B., Wang, B., Liao, J., Li, J., Pfeifer, G.P.*, et al.* (2009b). CDK5RAP2 is required for spindle checkpoint function. Cell Cycle *8*, 1206-1216.

Zhao, Z., Liu, H., Luo, Y., Zhou, S., An, L., Wang, C., Jin, Q., Zhou, M., and Xu, J.R. (2014). Molecular evolution and functional divergence of tubulin superfamily in the fungal tree of life. Sci Rep *4*, 6746.

Zheng, L., Schwartz, C., Wee, L., and Oliferenko, S. (2006). The fission yeast transforming acidic coiled coil-related protein Mia1p/Alp7p is required for formation and maintenance of persistent microtubule-organizing centers at the nuclear envelope. Mol Biol Cell *17*, 2212-2222.

Zimmerman, S., and Chang, F. (2005). Effects of {gamma}-tubulin complex proteins on microtubule nucleation and catastrophe in fission yeast. Mol Biol Cell *16*, 2719-2733.

Zimmerman, S., Tran, P.T., Daga, R.R., Niwa, O., and Chang, F. (2004). Rsp1p, a J domain protein required for disassembly and assembly of microtubule organizing centers during the fission yeast cell cycle. Dev Cell *6*, 497-509.